NBS SPECIAL PUBLICATION
332

Spectrum Formation in Stars With Steady-State Extended Atmospheres

U.S. DEPARTMENT OF COMMERCE
National Bureau of Standards

ITED STATES DEPARTMENT OF COMMERCE Maurice H. Stans, *Secretary*
NATIONAL BUREAU OF STANDARDS Lewis M. Branscomb, *Director*

Spectrum Formation in Stars With Steady-State Extended Atmospheres

Proceedings of the International Astronomical Union Colloquium No. 2, Commission 36

Munich, Germany, April 16-19, 1969

Edited by

H. G. Groth and P. Wellmann

Universitäts-Sternwarte München
Institut für Astronomie und Astrophysik
München, Germany

U. S. National Bureau of Standards, Special Publication 332

Nat. Bur. Stand. (U.S.), Spec. Publ. 332, 342 pages (August 1970)
CODEN: XNBSA

Issued August 1970

GENERAL ABSTRACT

Commission 36 of the International Astronomical Union sponsored a symposium on Spectrum Formation in Extended Stellar Atmospheres held 16 - 19 April, 1969. The host was the Observatory of the University of Munich. A major problem is the definition of what is meant by an extended stellar atmosphere. There are intuitive notions in the literature, but the question of specific definitions in various kinds of objects was discussed. Questions of what specifically cause the anomalous extent were largely bypassed. Attention focused mainly on the type spectrum to be expected in various situations. The spectral features to be expected in both static and dynamic atmospheres, including and excluding departures from LTE, were discussed. The symposium was divided into four sections: A. Type of Problems Which Exist; B. Theoretical Methods for Handling Non-LTE Problems; C. Chromospheres and Coronae of Stars; D. Summary. This volume contains the mms of the formal papers that were presented plus an edited and abridged version of the discussions following each paper.

Key words: extended atmospheres; non-LTE; chromospheres; coronae; non-classical atmospheres.

Foreword

The planning of this colloquium on Extended Stellar Atmospheres was carried out by Dr. A. B. Underhill, President of Commission 36, and the Organizing Committee of Commission 36, comprised of Drs. K. H. Böhm, R. Cayrel, J. T. Jefferies, V. V. Ivanov, R. N. Thomas, and S. Ueno in close collaboration with Drs. P. Wellmann and H. Groth whose kind invitation gave rise to the idea. This colloquium is one of a series that have been sponsored by Commission 36 on problems in stellar atmospheres. The aim of these colloquia has been to hold a working session among a number of people vitally interested in the problem, and to provide an inexpensive and readily accessible volume of the proceedings, which can be used by all interested in the subject, especially students and young researchers. A number of United States federal laboratories having strong programs in astronomy have been hosts to these colloquia and editors-publishers of the proceedings. These include the National Bureau of Standards through the Joint Institute for Laboratory Astrophysics, the Smithsonian Astrophysical Observatory, and now the Goddard Space Flight Center. These proceedings, published by NBS for JILA, follow the approach explored with the publication of the proceedings of the Symposium on Wolf-Rayet Stars, hosted by JILA in 1968. Dr. R. N. Thomas, aided by Alice Levine, of the JILA staff have provided the link between the formal editors, Drs. Wellmann and Groth, and the NBS publications group, under Betty L. Oberholtzer. The typescript was prepared by Breta Triolo.

Lewis M. Branscomb, *Director*

CONTENTS

PREFACE

This colloquium was one of similar colloquia of Commission 36 held in the past few years. The president of Commission 36, Professor A. B. Underhill, planned this colloquium, while the staff members of the Universitäts-Sternwarte München were responsible for the local organization. There was an urgent need to discuss problems connected with the structure of extended atmospheres and line formation in these atmospheres.

Each session of the colloquium had one or two introductory papers followed by discussion. The number of contributed papers was limited.

There was no case where the chairman was forced to cut off the discussion because of lack of time, but there was an important criticism by J. C. Pecker and R. N. Thomas: "This colloquium has absolutely no point, if it is so formal that no one ventures to say anything except the older people who think they know what they are doing anyway. It is very important that the younger people take part in the discussion."

When compiling these proceedings we have tried to report the discussion remarks as far as possible, when they were relevant to the problem. The paper by G. Rybicki arrived only as the manuscript of this conference was going to press. We were forced to omit the discussion of this paper from the proceedings because the discussion could not be understood without the paper.

We are very grateful to Anne B. Underhill for the decision to hold this colloquium at Munich. We thank all participants of the conference for coming to our institute.

H. G. Groth
P. Wellmann

PARTICIPANTS

R. C. ALTROCK, Sacramento Peak Observatory, Sunspot, New Mexico 88349
R. G. ATHAY, High Altitude Observatory, Boulder, Colorado, 80302
K. H. BÖHM, Department of Astronomy, University of Washington, Seattle, Washington 98105
R. C. CANFIELD, Sterrewacht Sonnenborgh, Servaas Bolwerk 13, Utrecht, Netherlands
F. CAPUTO, Laboratorio di Astrofisica, Casella Postale 67, 00044 Frascati (Roma), Italia
T. R. CARSON, University Observatory, Buchanan Gardens, St. Andrews, Scotalnd, U.K.
J. M. le CONTEL, Observatoire de Paris, 61 Avenue de l'Observ. Paris 14^{e}, France
Y. CUNY, Observatoire de Paris, Section d'Astrophysique, 92 Meudon, France
A. M. DELPLACE, Observatoire de Meudon, Meudon 92, France
S. DUMONT, Observatoire de Meudon, 92 Meudon, France
G. H. ELST, Sterrewacht, Ringlaan 3, Brussel 18, Belgium
H. GEROLA, Universidad de Buenos Aires, Facultad de Ciencias Exactas y Naturales, Depto de Fisica, Buenos Aires, Argentina
N. GÖKDOGAN, University Obs. Astronomi Kürsüsü, Beyazit, Istanbul, Turkey
G. GONCZI, Laboratoire d'Astrophysique, Faculte des Sciences, Av. Valrose, 06 Nice, France
I. P. GRANT, Atlas Computer Laboratory, Chilton, Didcot Berkshire, England
H. G. GROTH, Universitäts-Sternwarte München, 8 München 80, Scheinerstr.1, Germany
A. G. HEARN, Culham Laboratory, Abingdon, Berkshire, England
R. HERMAN, 7 bis rue Trudon, 92 Antony, France
T. HIRAYAMA, Tokyo Astr. Obs. Univ. of Tokyo, Mitaka, Tokyo, Japan
R. W. HILLENDAHL, Lockheed Palo Alto Research Laboratories 3251 Hanover Street, Palo Alto, California 94304
M. HOTINLI, University Obs. Astronomi Kürsüsü, Beyazit, Istanbul, Turkey
L. HOUZIAUX, Department d'Astrophysique, Faculté des Sciences, Plaine de Nimy, Mons, Belgium
D. G. HUMMER, JILA, University of Colorado, Boulder, Colorado 80302
K. HUNGER, Institut für theoretische Physik, Technische Univ. Berlin, 1 Berlin 10, Ernst-Reuter-Platz, Germany

G. E. HUNT, Atlas Computer Laboratory, Chilton, Didcot, Berkshire, England
W. KALKOFEN, Harvard and Smithsonian Observatories, Cambridge, Massachusetts 02138
H. LAMERS, Sterrewacht Sonnenborgh, Servaas Bolwerk 13, Utrecht, Netherlands
A. MARTINI, Laboratorio di Astrofisica, Casella Postale 67, 00044 Frascati, Italy
CHR. MAGNAN, Institut d'Astrophysique, 98 bis BD Arago, Paris (14e), France
D. H. MENZEL, Harvard College Observatory, Cambridge, Massachusetts 02138
D. MUGGLESTONE, Department of Theoretical Physics, University of Queensland, Australia
L. NEVEN, Sterrewacht, Ringlaan 3, Brussel 18, Belgium
H. NUSSBAUMER, Physics Department, University College, Gower Street, London W.C.1., England
D. E. OSTERBROCK, Department of Astronomy, University of Wisconsin, Madison, Wisconsin
N. PANAGIA, Laboratorio di Astrofisica, Casella Postale 67, 00044 Frascati, Italy
J. C. PECKER, Observatoire de Meudon, Place Jules Janssen, 92 Meudon, France
A. PETON, Observatoire de Meudon, Meudon 92, France
E. PEYTREMANN, Observatoire de Geneve, 1290 Sauverny, Switzerland
F. PRADERIE, Observatoire de Meudon, 92 Meudon, France
L. PUPPI, Laboratorio di Astrofisica, Casella Postale 67, 00044 Frascati, Italy
F. QUERCI, Observatoire de l'Université Toulouse, 1. Avenue Camille, Flammarion
M. RUDKJÖBING, Ole Romer Observatory, 800 Aarhus C, Denmark
G. RYBICKI, Smithsonian Astrophysical Observatory, 60 Garden Street, Cambridge, Massachusetts 02138
A. SKUMANICH, High Altitude Observatory, Boulder, Colorado 80302
D. W. STIBBS, University Observatory, Buchanan Gardens, St. Andrews, Fife, Scotland
P. SWINGS, Institut d'Astrophysique, Cointe Sclessin, Belgique
R. N. THOMAS, JILA, University of Colorado, Boulder, Colorado 80302
A. B. UNDERHILL, Sterrewacht, Servaas Bolwerk 13, Utrecht, Netherlands
R. VIOTTI, Laboratorio di Astrofisica, Casella Postale 67, 00044 Frascati, Italy
P. WELLMANN, Universitäts-Sternwarte München 8 München 80, Scheinerstr.1, Germany

LOCAL PARTICIPANTS

R. Born	USW
H. Donecker	USW
S. Drapatz	MPI
F. Forster	USW
K. Friedrich	USW
M. Gumtau	USW
R. Häfner	USW
R. Herbst	USW
W. Kegel	Garching, Institut Plasmaphysik
H. U. Keller	MPI
K. Kolbe	USW
H. Kohnert	USW
K. Metz	USW
F. Meyer	MPI
E. Meyer-Hofmeister	MPI
G. Oleownik	USW
H. Pfennig	MPI
G. Pöllitsch	USW
R. Rickert	USW
F. Schmeidler	USW
H. Schmid	USW
R. Schoembs	USW
K. v. Sengbusch	MPI
M. Stix	MPI
H. C. Thomas	MPI
E. Trefftz	MPI
Ch. Wellmann	USW
B. Wolf	USW

USW = University Observatory of Munich
MPI = Max Planck Institut for Astrophysics Munich

PART A

TYPE OF PROBLEMS THAT EXIST

Chairmen: P. Swings, P. Wellmann

DEFINITION OF THE TYPES OF PROBLEMS THAT EXIST IN STEADY-STATE EXTENDED ATMOSPHERES

by

Anne B. Underhill*

Astronomical Institute
Utrecht, Netherlands

ABSTRACT

In section 1 practical details concerning the equivalence of observational and theoretical descriptions of stellar spectra are reviewed, particularly the difficulty of identifying the observed reference level (continuum) with the theoretical continuum in the case when many lines are present. In this connection thought must be given to how integrals over frequency should be normalised and evaluated because the effective continuous absorption coefficient does not remain constant over the range from 0 to ∞. The choice of spectroscopic details by which to determine T_{eff}, log g and abundances requires careful consideration.

In section 2 the factors by which an extended atmosphere are recognized are summarized and the question is posed do all stars have extended atmospheres. Another question requiring an answer is whether the concepts microturbulence and macroturbulence are physically real concepts or whether they are merely fitting parameters to make a simple LTE theory account for the observed spectra of supergiants in which rather wide lines occur and many multiplets show rather steep gradients. In section 3 the types of line sensitive to non-LTE conditions are described. These are resonance lines, lines arising from metastable levels, subordinate lines for which the upper level is sufficiently separated from the continuum and other levels that this upper level is chiefly populated by radiative processes from the ground or other low lying levels and lines which go

*Now at NASA Goddard Space Flight Center.

into emission in low density atmospheres as a result of optical-pumping (fluorescent) processes. Such lines should not be used for abundance determinations by means of LTE theory though this is frequently done.

Theoretical considerations are discussed in Section 4 where first the problem of the two-level atom is sketched and then the problem is generalised to a many-level atom. The parameter λ which gives the probability that a photon is lost from the line by de-excitation processes other than spontaneous emission is defined and it is pointed out that non-LTE physics has the effect of adding a scattering term to the expression for the source function. One example is given of the effect of changing the line source function from the Planck function to a form suitable for isotropic coherent scattering. The line becomes deeper and wider for the same number of atoms. Interpretational problems in stellar spectra are discussed in section 5. It is noted that many lines in main-sequence early type spectra show the effects of departures from LTE. These effects are shown to a conspicuous degree by the spectra of shell stars. The example of He I 5876 in 10 Lacertae, O9V, is discussed and the implication for interpreting the He I lines in all B type main-sequence stars are touched upon. Helium-weak and helium-strong spectra probably indicate variations in density of the outer atmosphere rather than true abundance differences. The spectra of supergiants are also considered and it is pointed out that the Ia supergiants of type B may be hydrogen-poor.

Finally in section 6 the problem of choosing simplified physical representations of line forming when non-LTE physics must be used is discussed. Some relevant points concerning the observed spectral lines used for spectral classification are illustrated by means of partial energy-level diagrams.

Key words: interpretation of stellar spectra, extended atmospheres, line formation.

I. INTRODUCTION

This colloquium is concerned with finding a physical and mathematical description of how the stellar spectrum is formed in an atmosphere that is "extended" but in a steady state. We first need to

decide what are the important physical characteristics implied by the word "extended." Secondly a definition of "steady state" should be agreed upon, and thirdly some description should be given of what is meant by spectrum. The spectrum of a star comprises strong absorption lines, weak absorption lines, and continuous spectrum as well as emission lines; each of these characteristic parts of a stellar spectrum has properties determined by the interaction of each atom, ion, or molecule with the radiation field to produce the stellar spectrum.

The ideas we use and the words by which these ideas are transmitted are in many cases rather vague and contradictory. Something of value will have been accomplished at this colloquium if we are able to make our ideas and the words used to describe them more precise. Even more will have been accomplished if we are able to see how existing methods of analysis can be used, and to define rather sharply the physical as well as the mathematical aspects of our problems. In what follows I am going to speak as a stellar spectroscopist anxious to obtain information about the physical conditions in stellar atmospheres from a quantitative study of the parts of the stellar spectrum available to me. The standard way of proceeding is to compare observed spectroscopic observations with theoretical predictions resulting from an explicitly defined physical and mathematical model. If agreement is found then one says the parameters of the model are characteristic of that part of the stellar atmosphere involved in forming the part of the spectrum under consideration. If no agreement is found then the model must be changed.

One must consider carefully the meaning of the word "agreement" used in this context. Clearly the variation with wavelength of any predicted intensity distribution which is the same as the observed spectral distribution within the uncertainties of the measurements must be considered to offer a possible solution to our problem. A choice between several (at first glance possible) models can be made by using a well thought-out selection of spectral details for the comparison.

With stars one observes the total radiation field from the part of the star facing the observer; thus the variation of an intensity distribution with wavelength corresponds to the variation of the theoretical quantity F_ν with wavelength. Furthermore because of practical difficulties the observed intensity distributions are not given in absolute energy units but are expressed as relative inten-

sities. In the case of line profiles, the observed intensities are expressed as fractions of the intensity that would have been available if no line was present. The reference level of intensity is known as the continuum; it is found by drawing a smooth curve through the intensity level of parts of the spectrum where no absorption lines appear to be. When one interprets the observed variation with wavelength of the intensity in the continuous spectrum, which means comparing intensities over a range of several thousand angstroms, the intensity at some particular wavelength is chosen as reference point.

It is important to keep these practical definitions in mind when comparing theoretical and observed spectra because often what seems to be an obvious theoretical level of reference is not what is in practice used. For instance the simple concept of a continuous spectrum and a few superimposed absorption lines is useful only when the lines are too few in number to obscure the trend of the continuous spectrum with wavelength. This is so over much of the normally observed spectral range for O and B stars. In these cases it appears to be straightforward to compare observed and predicted spectra of early type stars. However, if one considers the far ultraviolet spectral range for OB stars, $912\text{Å} < \lambda < 1900\text{Å}$, the spectra are full of strong lines and the definition of a theoretical continuum that corresponds to the observed datum line selected as the continuous spectrum may be difficult. This problem is familiar to those who attempt to interpret the spectra of stars of types F and later in the spectral region $\lambda < 5000\text{Å}$.

Because the observed quantity is a relative variation of intensity with wavelength, one theoretical parameter of interest is $(\ell_\nu + \kappa_\nu)/\kappa_o$ where ℓ_ν represents the total absorption coefficient due to all possible lines and κ_ν represents the absorption coefficient due to all possible sources of continuous absorption at frequency ν. Here κ_o is the total absorption coefficient due to continuous sources of opacity at the reference frequency ν_o. In all theoretical studies of line formation done to date it has been assumed that one may replace κ_ν by κ_o, whatever the value $\nu - \nu_o$. With non-coherent processes the appropriate expressions for the emergent intensity contain integrals over ν from 0 to ∞ with $(\ell_\nu + \kappa_\nu)$ as a varying parameter. When these expressions are evaluated (typical expressions are the kernel functions of Avrett and of Hummer) use is made of the fact that the variation with ν of ℓ_ν is given

by a function which is normalised over the range 0 to ∞. However in this range κ_ν is also normalised and the shape function varies from zero to a maximum value to zero again. With non-coherent processes, which indeed are what occur in stellar atmospheres, the transport of radiation at different frequencies rather far from the line center depends quite sensitively on what sort of exchanges may take place in the wings of the lines. It may be a minor point, but it seems to me that we might consider whether in some of the lines it is reasonable to replace $\ell_\nu + \kappa_\nu$ by $\ell_\nu + \kappa_o$, that is, to assume that we can write the total absorption as $\ell_o(\phi_\nu + \beta)$ where β is a constant which is κ_o/ℓ_o and ϕ_ν is a normalised shape function. The rate of change of κ_ν with ν might be closely the same as that of ℓ_ν over an important part of the range and furthermore both quantities may have comparable values over part of the range. Whether such considerations are important depends upon the ratio of ℓ_ν to κ_ν at the line center. If this ratio is large, ℓ_ν and κ_ν will not attain comparable values until $\nu - \nu_o$ is large. Then the difference between κ_ν and κ_o may be significant and an asymmetry might occur between the two sides of the line profile as it is defined observationally. These considerations should be held in mind when deciding upon the appropriate quadrature formula for the frequency integrals, a point which will certainly come to discussion later in the conference.

The parameters that are sought to describe the stellar atmosphere are factors such as the temperature, pressure, and density as functions of depth in the atmosphere and the composition of the atmosphere. The parameters that describe the star are effective temperature and surface gravity. In principle these can be found by studying spectral features that are sensitive to the temperature distribution in the stellar atmosphere and to the density distribution so long as the temperature distribution is determined by the total radiative flux passing through the atmosphere and the pressure structure is determined by the need to maintain hydrostatic equilibrium against the acceleration of gravity. It is by no means obvious which spectral features are most suited for these purposes at each spectral type though the well known spectroscopic type and luminosity criteria serve as an empirical starting selection.

A star with an extended atmosphere usually refers to a supergiant or a shell star. However this concept requires more detailed consideration which will be given below. So far as the words "steady

state" are concerned, the intent is to restrict the discussion to stars having atmospheres in which spectroscopic changes do not occur, or occur so slowly that the process of change does not need to be considered. We have arbitrarily excluded from discussion rapidly changing, evolving situations. Furthermore in the case of pulsating variables we are not seeking at this time to find the cause of the observed regular changes in light and spectrum so much as to find out what sets of physical variables correspond to the various recurring sets of spectroscopic phenomena. This problem has a known solution if one may assume that the physical variables and the observable spectroscopic details are bound together as though thermodynamic equilibrium existed at each place in the atmosphere. However, the values of temperature, pressure and density found in this way are not consistent with the hypothesis of local thermodynamic equilibrium. Furthermore the motion of the atmosphere may have a significant effect on the line shapes and strengths.

II. FACTORS BY WHICH AN EXTENDED ATMOSPHERE IS RECOGNISED

The concept "an extended atmosphere" grew up empirically as a result of comparing details in the spectral type, thus effective temperature, and interpreting the differences in spectrum in terms of LTE theories applied to a single layer of gas open to interstellar space and irradiated from below by the flux emerging from the rather dense layer known as the photosphere. The gas pressure in supergiant reversing layers was found to be approximately 100 times less than that in main sequence reversing layers. Simple geometric considerations indicate that the reversing layer of a supergiant has a considerably greater size than that of a main sequence star of the same effective temperature. Hence the origin of the term "extended."

Many of the extra absorption lines, which appear in the spectra of some B type main sequence stars and lead to the classification of these stars as shell stars, are very like lines in the spectra of A or late B type supergiants. From this observed fact has come the idea that the atmospheres of shell stars have even greater extension and lower density than the atmospheres of supergiants.

The conclusion that the pressure is lower in a

supergiant atmosphere than in a main sequence atmosphere comes from the facts that in supergiant spectra the Stark-broadened wings are not strikingly present for H or He I lines and the forbidden He I lines do not appear. Also the lines in the second spectra of the metals are stronger in supergiant spectra relative to the lines from the first spectra of the metals than is the case for main sequence stars of about the same temperature. Further differences between absorption lines in supergiant spectra and those in main sequence stars are that in supergiants the lines have rather wide, steep-sided profiles and that when the spectra are compared multiplet by multiplet it is seen that the supergiant lines, in spite of their greater equivalent width appear to lie on the Doppler part of the curve of growth rather than on the transition part where many of the lines in main sequence spectra lie. This effect is known as the gradient effect; it was interpreted by Struve and Elvey[1] in terms of microturbulence. When Struve[2] noticed that the profiles of the strong lines in supergiant spectra were wider than could be accounted for by the velocity fields deduced from curves of growth and the hypothesis of microturbulence, the concept "macro-turbulence" was introduced to account for the extra width. These attempts to reconcile a simple LTE theory of line formation with what is observed in the case of stars having extended atmospheres have lead to the introduction of physical concepts that are difficult to justify in detail. It is time to ask whether the observed phenomena--steep gradients and rather wide lines in supergiant spectra--should not be interpreted in terms of an improved and more realistic theory of line formation.

In the case of shell stars, absorption lines of the second spectra of the metals very like those in supergiant spectra may be found but the hydrogen lines have much deeper cores, in some cases going nearly to zero intensity, and emission wings are seen for the first few members of the Balmer series. The strong lines of Fe II also often have emission wings. In some stars the relative intensities of the He I lines from the levels 2^3S, 2^1S, 2^3P and 2^1P are not the same as for main sequence stars, the lines from 2^3S and 2^1S being stronger than normally expected according to the observed strengths of lines from 2^3P and 2^1P. Struve and Wurm[3] named such changes in relative line strengths dilution effects and they showed that the relative populations would change in a low density gas in which the radiation

density was reduced from its thermal equilibrium value in such a way that the atoms tend to accumulate in the metastable levels. Consequently whenever the lines arising from metastable levels are seen to be unusually strong in a stellar spectrum, one speaks of an extended atmosphere. The theory of Struve and Wurm is a simple version of the type of theory one must consider when it is not appropriate to assume LTE.

In summary, the qualitative characteristics of a stellar spectrum that lead to the inference of the presence of an extended atmosphere are (1) broad, steep-sided absorption lines, (2) little or no Stark broadening of the H and He I lines and the absence of [He I] lines, (3) a steep gradient in multiplets of strong lines, and (4) exceptionally great relative strength of absorption lines arising from metastable levels. In an extended atmosphere the density is sufficiently low that one cannot assume that collisional processes will establish LTE level populations.

A phenomenological description of these ideas coupled with pertinent references to the details seen in stellar spectra has been given by Struve.[4] He asked nearly the same questions as those facing us now.

1. Why do some stars possess tenuous outer atmospheres or shells while other stars, apparently of identical physical characteristics, do not have such shells?

2. What is the origin of a shell and how is it supported in apparent violation of the laws of mechanics?

3. How can we account for the remarkable tendency of nearly all shells to vary either periodically or, more often, in an irregular manner?

4. Why do some shells expand while others are stationary?

The first question should be modified to enquire whether all stars have extended atmospheres and to ask what factors make these extended atmospheres visible in the normally accessible spectral region. It is essential to define accurately criteria that are sensitive to the presence of a tenuous outer atmosphere. The low density of particles in an extended atmosphere surrounding a star and the departure of the radiation field from the black-body distribution appropriate to the electron temperature make it necessary to abandon the hypothesis of LTE. We would like to have a calibration of the strength and shape of suitable lines in terms of the density,

electron temperature, and size of the extended atmosphere. Another relevant factor will be the velocity field in the line of sight. An extended atmosphere can be detected only if spectral lines of adequate sensitivity to the conditions in an extended atmosphere happen to fall in the spectral region under study. Observation has already shown that extended atmospheres of widely different properties exist around many stars. The corona of the sun is an example of an extended atmosphere that can be detected only by very special observations, whereas the extended atmospheres of Wolf-Rayet stars can be detected by simple low-dispersion observations. All stars may possess extended atmospheres in the general sense; we should like to find out what spectroscopic phenomena at each spectral type give the clearest evidence of the presence of the extended atmosphere and of its physical properties. The complementary question (what spectroscopic details in a stellar spectrum can be interpreted reliably in terms of simple LTE theories of spectrum formation?) is also not without interest. Such features can be used with the existing methods of analysis to obtain an estimate of the physical conditions and the abundances of the elements in the parts of the stellar atmosphere where the density is high enough that LTE is a reasonable hypothesis.

III. THE TYPES OF SPECTRAL LINE SENSITIVE TO NON-LTE CONDITIONS

Spectral classification and the recognition of stars with extended atmospheres is based on the apparent relative strengths of selected absorption lines. These relative strengths are chiefly determined by the central intensities of the lines; the width of the line and the exact shape of the profile are less important factors. The central intensity of a strong line is determined by the value of the source function at the edge of the atmosphere. In the case of a two-level atom one can write

$$S_\nu \propto n_2 n_1 \qquad (1)$$

where n_2 is the population of the upper level and n_1 is the population of the lower level. In the case of a normal atmosphere the balance of radiative and

collisional processes results in certain values of n_2/n_1 through the atmosphere, thus in a certain central intensity for the line. If in an extended atmosphere, owing to the lower density and the changed radiation field, the ratio n_2/n_1 is reduced, a deeper line will result and the line will be said to have become stronger. If the ratio n_2/n_1 is increased strongly, the line may appear in emission. Lines that go into emission are those for which the upper level can be populated by absorption of line radiation generated in an intrinsically strong line such as Lyman α of H or He II 303. In the literature of the 1930's and 1940's this process was called fluorescence. Its occurrence is a sure indication that non-LTE effects are important in at least part of the stellar atmosphere. (In this discussion it is implicitly assumed that the continuous absorption is small with respect to that in the line center and that it remains essentially unchanged by changes in the density of the atmosphere.)

However, it is not sufficient to focus attention on the changes in population of only one level; the change in source function is brought about by the relative change of n_2 to n_1. The populations of levels 1 and 2 can vary at different rates under different circumstances. The type of variation depends explicitly upon the spectroscopic description of levels 1 and 2 and the sizes of the collision and radiative cross sections between these levels and all other levels in the atom or ion including the continuum and doubly excited states lying above the primary ionization limit. All such doubly excited states do not autoionize with high probability.

The types of line which will be sensitive to non-LTE conditions are (1) resonance lines, (2) lines arising from metastable levels, (3) subordinate lines for which the upper level is sufficiently separated from the continuum and other levels that this upper level is chiefly populated by radiative processes from the ground or other low lying levels, and (4) lines that go into emission in low density atmospheres as a result of the optical pumping (fluorescent) processes mentioned above. Resonance lines are sensitive to non-LTE conditions because the spontaneous transition probabilities from neighbouring levels into the ground level are large for permitted dipole transitions whereas often the energy differences from the ground level to neighbouring levels are sufficiently great that the probability of collision-induced transitions is small when electrons having energies corresponding to tempera-

tures of 10,000 to 20,000 degrees are considered. Electron temperatures of this size are expected in the atmospheres of A and B stars. Somewhat similar arguments hold for metastable levels, although it may happen, as with He I, that the lowest metastable level is within easy "collision distance" of the continuum. In that case, when the density is not too low, the population of the metastable level may approach its thermal equilibrium value for the local electron temperature because the level is strongly coupled through collisions to the continuum.

Lines sensitive to non-LTE conditions include many of the lines that are used for classifying stars of types A, B, O and Wolf-Rayet. Some examples are the Balmer lines of hydrogen; the He I lines from 2^3S, 2^1S, 2^3P and 2^1P; the He II lines from n = 3 and n = 4; C III 4647, 50, 51 and 5696; C IV 5801, 12; N III 4634, 40, 41; N IV 3478, 82, 84 and 4057; N V 4603, 19; O 17771, 74, 75; Ca II H and K; Mg II 4481; Si II 4128, 30 and 4200; Si III 4552, 68, 74 and Si IV 4088 and 4116. In the cooler stars and in shell stars, strong lines arising from the metastable levels of the ground configuration of Cr II, Mn II, Fe II, and Ni II influence strongly our classification of stars. In each case both the lower and the upper level of the line are sufficiently isolated that radiative processes as well as collisional processes are important in establishing the population ratio n_2/n_1. In a few cases (for example $H\alpha$, He II 4686, C III 5696, and N III 4634, 40, 41) particular radiative processes are known to generate emission lines by causing an overpopulation of the upper level of the line. In other cases the ratio n_2/n_1 decreases in extended atmospheres relative to its value in normal atmospheres with the result that deeper (stronger) than normal absorption lines are seen. Most of these changes are due to the decreased density. An increased density in the atmosphere (more collisions) forces the population ratios towards the LTE values. The intensities of none of the above lines should be interpreted in terms of abundance without first making some investigation of the effects of non-LTE and how the relevant level populations depend on the density, temperature, and the available geometric path length.

That the level populations of H and He are sensitive to non-LTE conditions in those parts of the atmosphere where the strong lines are formed, that is in regions where the electron density is less than 10^{13}, has been shown by Strom and Kalkofen,[5,6] Kalkofen and Strom,[7] Kalkofen,[8] by Mihalas[9,10]

and by Mihalas and Stone.[11] Most of these studies are concerned with the continuous spectrum of early type stars. The effects on the line spectrum have not been investigated in detail. Hearn (in press) has studied some effects of non-LTE conditions on the strengths of the He I lines. All of these investigations lead to the inference that the strengths of the classification lines are very sensitive to the density in the atmosphere. The sensitivity to temperature changes is much less. These facts are used empirically for recognising supergiants and shell stars. The calculations referred to were made with models believed to represent main sequence stars. It is clear that non-LTE effects are important for understanding the meaning of the spectral classification of main sequence A, B, and O stars as well as that of supergiants.

IV. THEORETICAL CONSIDERATIONS

In the case of an atom with two bound levels only and no continuum, the equation of transfer within the line can be written for plane parallel layers as

$$\frac{\mu dI_\nu(\tau,\mu)}{\phi_\nu d\tau} = I_\nu(\tau,\mu) - S(\tau) \qquad (2)$$

with

$$S(\tau) = [1 - \lambda(\tau)] \int_0^\infty \phi_\nu(\tau) J_\nu(\tau) d\nu + \lambda(\tau)\, B_\nu(\tau). \qquad (3)$$

Here τ is the optical depth at the center of the line, $\phi_\nu(\tau)$ is a normalised shape function for the line, $B_\nu(\tau)$ is the Planck function and μ, I_ν and J_ν have their usual meaning. The quantity $\lambda(\tau)$ is the relative probability that a line photon is lost to the line as a result of collisional de-excitation,

$$\lambda(\tau) = n_e C_{21} / (A_{21} + n_e C_{21}), \qquad (4)$$

where C_{21} is the cross section for collisional de-excitation, n_e is the electron density at level and A_{21} is the Einstein probability for spontaneous

emission. Since both n_e and C_{21} depend upon the electron temperature at level τ, λ is a function of τ.

In the case of many-level atoms, re-emission at frequencies within the line may occur because of spontaneous emission and from the energy field associated with the electrons. This possibility can be taken into account formally by writing the source function in line frequencies as

$$S(\tau) = [1 - \lambda(\tau)] \int_0^\infty \phi_\nu(\tau)\, J_\nu(\tau) d\nu + \lambda^* B_\nu(\tau), \quad (5)$$

where

$$\lambda(\tau) = (n_e C_{21} + \sum_k A_{2k} + D)/(A_{21} + n_e C_{21} + \sum_k A_{2k} + D) \quad (6)$$

and λ^* is suitably defined. In equation (6) D represents all possible transitions from level 2 that are generated by the radiation field and all collisional transitions except from level 2 to level 1. No general rules can be given for defining λ^*; it represents photons that are emitted at line frequencies as a result of the original line photons going into the energy of the electron gas on one of the alternative routes out of level 2. The index k in equation (6) refers to all levels below level 2 into which the atom can decay be spontaneous emission except level 1. For the lines used to classify stellar spectra k is a small integer, usually less than four.

Other terms can be added to equations (2) and (5) to take account of sources of continuous absorption and blending lines. Once the source function is known, the emergent flux from the plane parallel layers can be found as the Φ - transform for the case $\tau = 0$.

The well known difficulties of this transfer problem arise because equation (2) is an integro-differential equation owing to the occurrence of the quantity

$$J_\nu(\tau) = \frac{1}{2} \int_{-1}^{+1} I_\nu(\tau, \mu)\, d\mu \quad (7)$$

in equation (5) and because λ and λ^* depend on the radiation field as does τ which depends on the popu-

lation of the lower level on the line, $n_1(z)$. We have

$$\tau(z) = - \int_z^\infty n_1(z)\ \alpha_o\ dz \qquad (8)$$

where α_o is the atomic absorption coefficient at the center of the line. The level populations are related to the radiation field and to each other by the demand that a steady state exist. The quantity λ may be defined to be independent of the radiation field by neglecting transitions out of level 2 generated by the radiation field. In the case of some extended atmospheres, photo-excitation processes and photo-ionizations may be neglected. Then the problem becomes simpler.

One advantage of writing the source function in the form of equation (5) is that one sees that there is a "scattering term"--the first term--and a term from all other processes. When collisional de-excitation is much more important for the upper level than spontaneous emission, $\lambda \to 1$ and the source function becomes identical with the Planck function. Then the equation of transfer has the simple form which is used in all LTE studies. One reason why LTE calculations usually are unsuitable for resonance lines, for lines arising from metastable levels, and for subordinate lines from low-lying levels is that for these lines λ may be significantly different from unity over much of the atmosphere owing to the low density in the line-forming regions and the diluted radiation field.

Finally it should be noted that if the scattering term in the source function dominates, i.e., λ and λ^* are both small, a deeper and stronger line will result for the same number of atoms than is found when λ and λ^* are large. A simple example is shown in Figure 1 where the calculated profile of Si III 4552 is displayed for the case that the re-emission in line frequencies is according to Kirchhoff's law (thin line) and when it is given by coherent, isotropic scattering (thick line). The model atmosphere used (Guillaume[13]) is a line-blanketed model of approximate type B1.5V, having T_{eff} = 23 255°K and log g = 4.0. The line absorption coefficient corresponds to thermal Doppler broadening and a damping coefficient 10 times the classical damping constant; the fractional abundance by weight of silicon is 1.206×10^{-3}. This example is merely an illustration of the very significant changes in

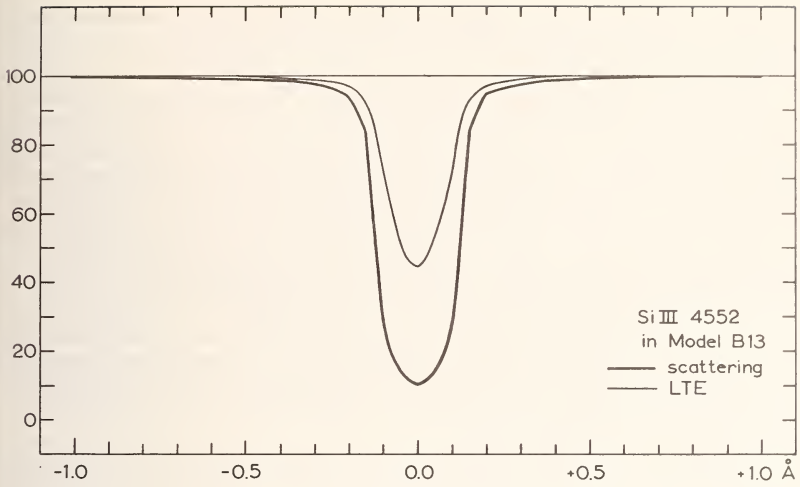

Figure 1. Predicted profiles of Si III 4552 in a line-blanketed model of type B1.5V for the cases (a) that the line is formed by coherent, isotropic scattering (thick line) and (b) that the line is formed in LTE (thin line).

line shape and depth which can occur as the source function varies owing to changes in λ and λ^*. In the example the level populations were calculated according to the Saha and Boltzmann laws. An optical depth of 1.0 in the center of the line has been reached when τ, the characteristic optical depth in which the model is defined, is 0.01. The electron density at the level $\tau = 0.01$ is 5.0×10^{13}.

V. INTERPRETATION PROBLEMS IN STELLAR SPECTRA

Main-sequence Stars

Model atmospheres in radiative and hydrostatic equilibrium can be constructed that give a continuous spectrum very like what is observed for B and early A type main sequence stars. The most satisfactory models include absorption in the strongest lines as a source of opacity as well as absorption in the continua of H^-, H, He and He^+ and electron scattering. What may be termed the classical method for computing model atmospheres adopts the hypothesis of LTE in order to simplify predicting the spectrum. More

elegant methods of finding the continuous spectrum that allows for non-LTE have been developed by Kalkofen, Mihalas and Strom and by Feautrier[14] but so far as B stars are concerned, the difference of the predicted continuous spectrum in the normally observed spectral range from that of a classical main sequence model is too little to be detected using the presently available observational material (cf. Mihalas[15]). The classical models have been used, with an LTE theory of line formation, to predict the equivalent widths and profiles of absorption lines in the spectrum and to find abundances of the elements. The method is to choose those abundances that give a best overall fit between the predicted equivalent widths and the observed values. The technique is familiar and no detailed comments on this procedure are necessary here.

This type of analysis is a somewhat more sophisticated way to find abundances than simple curve-of-growth analysis in that account is taken of the variation of pressure and temperature with depth in the atmosphere. However, because the hypothesis of LTE is used, the chief free parameter that remains by which to obtain a fit between observed and predicted equivalent widths is the abundance. No attempt is made to compare computed and observed profiles. A further fitting parameter that is used with lines on the flat part of the curve of growth is microturbulence.

Sets of abundances in a number of B and early A type stars have been found by model-atmosphere and curve-of-growth studies. The observed fact that about ten percent of the main sequence stars between types A5 and B3 have absorption line spectra that differ from each other and from the spectra of most stars having the same distribution of energy in the continuous spectrum over the range 3500 to 6700Å leads to differing sets of abundances. Ingenious attempts have been made to explain these anomalous abundances in terms of nucleogenesis in the center of the star and/or spallation on the surface of the star. However, the whole chain of reasoning is not very satisfactory and it is time to consider seriously whether we do not have anomalous atmospheres rather than anomalous abundances; an idea put forward by the author in 1964 (Underhill[16]). By anomalous atmospheres it is meant that the process of line formation, in the case of the lines that lead to deviating abundances, is not an LTE process as has been assumed. That classical model atmospheres and the LTE theory of line formation are not truly

satisfactory for explaining many details in the observed spectra of normal sharp-lined main sequence stars can be demonstrated by comparing observed and predicted line profiles (Underhill[17,18]). It is easy to show that the radiation in the profiles of all strong and moderately strong lines in O and B type spectra comes from such high levels in the atmosphere that the density is too low to ensure that LTE be established as a result of collisions for the lines that are studied.

It is chastening to note that in the peculiar main sequence stars the so-called anomalous abundances have usually been estimated from lines of the types listed in Section 3 as being particularly sensitive to departures from LTE. The H, He I, O I, and Si III spectra as well as the second spectra of the metals and of the rare earths contain metastable levels. The occurrence of these levels affects the populations of all the lower levels of the relevant atom or ion while closely coupled to the metastable levels. The abundances of Li, Be, Ca, Sr, and Ba are usually estimated from resonance lines. The ionization balance of P II $\rightleftarrows$ P III is particularly sensitive to collisions with He I atoms in the metastable 2^3S state (Underhill[19]), while Ba II can be ionized efficiently by Lα quanta. Furthermore, LTE theories of line formation and the use of the best available gf values for Si II lines do not give a satisfactory understanding of the strengths of the Si II lines in what are usually called normal stars (Underhill[20]). The reason for the observed discrepancies in the Si II spectrum is not understood at present. Clearly many problems remain in the interpretation of the lines from apparently sharp-lined main sequence stars. Any abundance anomalies of less than a factor 100 should be scrutinized carefully to see if they do not reflect departures from LTE rather than true abundance anomalies.

Mention has been made of normal stars. These are stars with spectra like the spectra of most of the spectral classification standard stars. It is going too far to assume without proof that normal also means that the stronger lines, that is the classification lines, can be interpreted correctly by means of the hypothesis of LTE.

The ad hoc fitting parameter microturbulence may well be an indication that in the case of the stronger lines $\lambda < 1$ and consequently a scattering term must be added to the source function. Such a term gives stronger lines for a given number of atoms than does a purely LTE source function. Con-

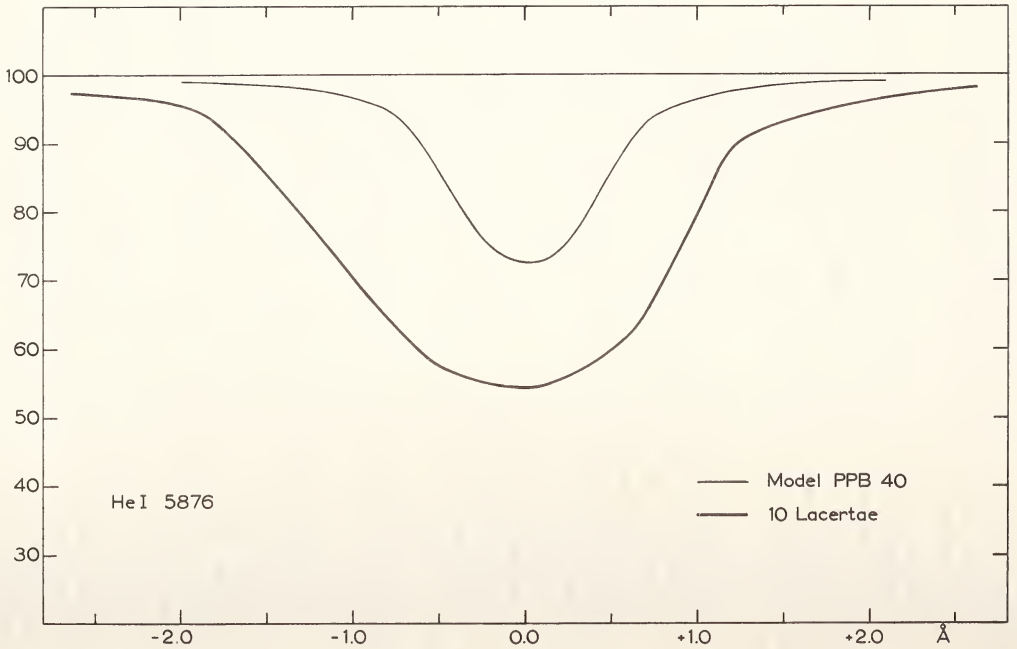

Figure 2. Predicted profile of He I 5876 in a line-blanketed O type model compared with the observed profile for 10 Lacertae, O9V.

cern regarding the interpretation of microturbulence has been expressed by Menzel[21] and by Jefferies and Thomas.[22]

An extreme example of what sort of discrepancies occur between observed profiles and profiles predicted assuming LTE is shown in Figure 2 where the predicted profile for He I 5876 obtained with a line-blanketed model which should represent 10 Lacertae, O9V, well (Underhill[17]) is compared with the observed profile. This observed profile is from only one IIIM spectrogram, 30 Å/mm at 5876Å, obtained at the Dominion Astrophysical Observatory, thus it is somewhat uncertain, but the uncertainties are not greater than ± 5 percent, particularly in the center of the line. Observational error is not the source of the discrepancy. The predicted profile has been found assuming that the line profile is given by the Voigt function with thermal Doppler broadening and a damping constant 100 times the classical damping constant. Such a value for the damping constant is close to what a more exact representation of the Stark effect of the $2^3P^0 - 3^3D$ line of He I will give. The predicted equivalent width is 0.344Å which is comparable with the value predicted by Mihalas[23] using the correct Stark broadening theory and a model of similar pressure-temperature structure. The equivalent width of the observed profile in Figure 2 is 1.14Å; Traving[24] has found 1.23Å and Mihalas[25] gives 0.90Å. No reasonable changes in the model nor adjustments of the line absorption coefficient will compensate for this discrepancy. It is necessary to use a theory of line formation that takes into account the fact that $\lambda \neq 1$ for He I 5876 in the outer layers of an O type star. The electron density is less than 1.7×10^{14} in the layers of model PPB40 which are important for forming the parts of the profile between ± 1.0Å.

Another indication that changes of the density in the atmosphere (thus changes of the significance of non-LTE physics for the strength of the He I absorption lines in B type main sequence stars) rather than gross changes in the helium abundance may be the explanation of "helium-weak" and "helium-strong" B stars of the same colour is afforded by the spectroscopic changes of HD 125823. Bidelman[26] noted that when the He I lines changed strength the rest of the spectrum remained essentially unchanged. This was confirmed by Thackeray.[27] The changes are more precisely described by Jaschek, Jaschek, Morgan, and Slettebak[28] who find that the variations in the spectrum of HD 125823 can be represented as an

oscillation between MK types B2V and B7IV. On high dispersion spectrograms the Si II and Si III lines are sensibly unchanged in intensity throughout the variations.

Another observational confirmation of the different sensitivity of lines seen in late B type spectra to non-LTE physics is the variation observed by Struve and Swings[29] and by Struve[30] of the strengths of the Ti II, Mn II, Fe II and Ni II lines in the spectrum of Pleione. Most of these lines are used with unjustified confidence in LTE theories of line formation to deduce anomalous abundances in main sequence stars. The spectra of shell stars show to an enhanced degree the line intensity changes that have been mentioned above as indicating that non-LTE physics should be used. In addition the geometrical arrangement of the extended atmosphere affects the profiles that are observed.

Supergiants

The chief differences between the spectra of supergiants and those of main sequence stars having about the same intensity distribution in the continuous spectrum are that in supergiants (1) the Stark broadening of the H and He lines is greatly reduced, (2) all other lines are stronger and wider, and (3) multiplets generally show a greater gradient. Since the electron pressure is lower in the atmospheres of supergiants than in the atmospheres of main sequence stars, there is even less reason to believe that the hypothesis of LTE will be adequate for a theory of line formation.

Similar discrepancies between LTE theory and observation occur as have been noted for the main sequence stars. Simple LTE analysis of the equivalent widths of lines in the spectra of B type supergiants (for example Unsöld,[31] Voigt[32]) has always lead to a somewhat larger abundance of helium relative to hydrogen than is found for the main sequence B stars. This result is at least partly due to the fact that the observable lines of the He I spectrum are not in LTE in supergiant atmospheres and departures from LTE tend to make the He I lines deeper.

The hydrogen lines in B type supergiants do not look like the lines predicted using LTE theory and classical model atmospheres. Some example of the discrepancies that occur are shown in Figure 3 which displays profiles taken from the observations of van Helden,[33] Lamers,[34] and Smit[35] of Hγ in β

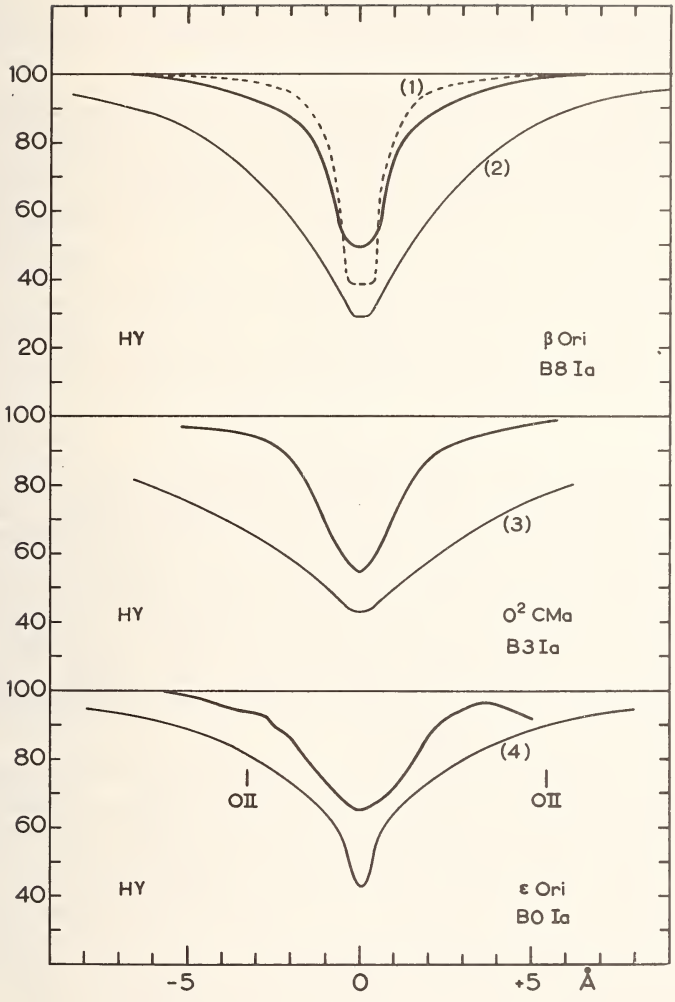

Figure 3. Observed Hλ profiles in B type supergiants compared with Hλ profiles predicted by Mihalas. Profile (1) is from a model with T_{eff} = 10,080°, log g = 1.0; profile (2) from a model with T_{eff} = 10,080°, log g = 2.0; profile (3) from a model with T_{eff} = 14,000°, log g = 3.5; profile (4) from a model with T_{eff} = 24,000°, log g = 3.5. The wavelength unit indicated is one angstrom.

Orionis, B8Ia, o^2 Canis Majoris, B3Ia, and ε Orionis, B0Ia, compared with profiles computed by Mihalas.[23] Mihalas used the best available LTE theory and a normal hydrogen-helium composition. The theoretical profiles are from unblanketed models with the following characteristics:

Profile	T_{eff}(°K)	log g
1	10 080	1.0
2	10 080	2.0
3	14 000	3.5
4	24 000	3.5

These models have the lowest values of log g of each group computed at each effective temperature. It is generally considered that log g in B type supergiant atmospheres is of the order of 2.0 although at effective temperatures near 24,000°K the condition of hydrostatic equilibrium cannot be met for log g smaller than about 3.0. If the effective temperatures of the selected supergiants are higher than the values listed above, say by 2000°, the predicted profiles for the same value of log g will be a few percent (< 5) less deep.

The observed profiles of Hγ do not have wings like the predicted Stark-broadened wings. From consideration of the fit in the wings alone one would postulate that the electron densities in the atmosphere are like those given by a model with log g of the order of 1.5 or less. However, the Balmer series of hydrogen breaks off at n = 25 in β Orionis, at n = 24 o^2 Canis Majoris and at n = 21 in ε Orionis. These values indicate electron densities of the order of 5.8×10^{12} to 2.3×10^{13}. The Mihalas model with T_{eff} = 10,080°K and log g = 2.0 has electron densities of this order in its outer layers while the model with log g = 1.0 has electron densities between 10^{10} and 10^{12}. Consequently one concludes that log g in the atmospheres of the B type supergiants of luminosity class Ia is probably not smaller than 2.0. The apparent fit of computed profile (1) with the observed profile for β Orionis must be fortuitous.

It is clear that the observed Hγ profiles are

less deep than the predicted LTE profiles over their whole range. (An extrapolation to lower log g must be made in the case of the two high temperature models.). The computed equivalent widths are too large. Another indication that the profiles do not have the Stark wings which are expected is that the break off of the Balmer series is sharp in each of these supergiants. The wings of the last members of the Balmer series do not merge noticeably. Struve and Chun[36] have noticed that the He I lines in the spectrum of 55 Cygni, B3Ia, give evidence of Stark broadening indicating that the electron density is not particularly low in the atmosphere of this supergiant.

The discrepancies in the centers of the hydrogen lines are as interesting as the lack of Stark wings. In each case the line is less deep by 10 to 20 percent of the continuum than what is predicted. In the center of a very strong line the central intensity is proportional to the ratio of the source function at the edge of the atmosphere to the source function at the depth where the continuous spectrum is formed. The predicted profiles displayed in Figure 3 have been computed using LTE theory, thus the computed residual intensity at the center of Hγ represents approximately the ratio of the Planck function at the edge of the atmosphere to the Planck function at the depth where the continuum is formed. The predicted central depths are a representation of the adopted temperature law in the atmosphere. The work of Kalkofen, of Strom and Mihalas using main sequence models indicates that the hydrogen atom will not behave in the atmospheres of supergiants as if it were in LTE, for the density is too low to maintain Saha-Boltzmann populations in all levels. Consequently the source function in the center of Hγ at the outer edge of the atmopshere may be reduced significantly from its LTE value. In any case, the LTE value is the maximum value which can be attained. Let us postulate that the source function in the continuous spectrum, which in an atmosphere of normal composition is dominantly due to absorption in the Paschen continuum of hydrogen, is not significantly changed from its LTE value when more correct non-LTE calculations are made. It follows that acknowledging that LTE is not valid in supergiant atmospheres leads us to expect even deeper Hγ profiles than have been predicted, provided that we do not change the temperature structure of the atmosphere greatly. Thus allowing for departures from LTE will not resolve the discrepancy found for Hγ.

Motion of the atmosphere such as rotation of

the star or large scale random motions in the atmosphere will not resolve the problem either, because although one may obtain a shallower profile in this way, the equivalent width is not reduced. The observed discrepancy is not only one of shape of profile, but also one of equivalent width.

Another possible solution is to introduce a rising temperatute in the outermost parts of the model. Such an ad hoc procedure would require rejection of the condition that the transfer of energy through the atmosphere is regulated only by the condition that radiative equilibrium exist. The fact that emission is observed at Hα in the Ia supergiants is, perhaps, an encouragement for proceeding in this manner, but care would be required not to destroy the rather satisfactory interpretation of the colours of B type supergiants provided by models with a temperature that decreases outwards. Furthermore it should be noted that lines of Na I and Fe II are visible in the spectrum of β Orionis while the spectra of o^2 Canis Majoris and ε Orionis do not contain lines suggesting significantly higher levels of excitation than are seen in B3 and B0 main sequence stars respectively. Another objection against adding to the model a high temperature outer layer in which the core of Hγ is formed is that at a short distance from the line center, say 5Å, one would be outside the Hγ line absorption coefficient of this layer and thus would be able to see through to the cooler "normal" atmosphere. According to the LTE predictions one should then see the extended Stark-broadened wings of the Hγ profile formed in the normal reversing layer. Such wings are not seen. The ad hoc solution of adding a hot layer to the model seems unsatisfactory, but it must be admitted that no details have been worked out.

A more promising solution to the problem of the weak hydrogen lines in B type supergiants of luminosity class Ia is to postulate that these atmospheres are hydrogen-poor (Underhill[37]). If the abundance of hydrogen is so small that hydrogen is no longer the chief source of opacity in the region 3650 - 7000Å, then the strengths of the Balmer lines should reflect the hydrogen abundance, cf. the calculations of Böhm-Vitense.[38] Strong Stark-broadened wings will not be seen because the low abundance of hydrogen prevents the wings from attaining observable depths at distances from the line center great enough that Stark effect dominates the shape of the line absorption coefficient. The rather steep-sided deep cores may still be due to the effect of departures from LTE.

If the atmospheres of the B type supergiants are hydrogen-poor, but perhaps not quite so poor as the helium stars like HD 124448, the chief source of opacity in the region 3650-7000Å will be absorption from the n = 3 levels of He I. These continuous absorption coefficients vary as ν^{-3}, thus no significant difference in UBV colour is expected between model atmospheres of normal, hydrogen-rich composition and those of hydrogen-poor composition. The temperature-pressure structure may well be different since the opacity in the region 504 - 912Å will differ greatly between hydrogen-rich and hydrogen-poor atmospheres.

The model-atmosphere calculations and line-profile predictions for hydrogen-poor stars with effective temperatures of 12,900°, 9,900° and 7350°K and log g = 2.0 and 4.5 presented by Böhm-Vitense[38] point in the direction of the conclusions sketched above. The value of the suggestion that the Ia supergiants of type B are hydrogen-poor cannot be fully assessed until more models such as those of Böhm-Vitense are available at a greater range of temperature and gravity and until an improved theory for predicting line profiles which takes into account the major effects of departures from LTE is developed. Some models for hydrogen-poor stars in the needed range of T_{eff} and log g have been computed by Klinglesmith[39] but they are not generally available.

The results of Böhm-Vitense indicate that hydrogen profiles of the observed shape can be obtained by reducing the hydrogen abundance in the atmospheres of the Ia supergiants of type B by a factor of at least 1000. If the atmosphere is hydrogen-poor, presumably the whole star is hydrogen-poor. To reach such a state would require mixing the outer parts of the star with the core in which hydrogen had been depleted as the result of nuclear reactions. The hydrogen lines in the spectra of the Ib supergiants of type B are stronger than those of the Ia supergiants. It may be that the Ib supergiants are hydrogen-rich stars at the beginning of their departure from the main sequence while the Ia supergiants are much further evolved.

VI. THE CHOICE OF SIMPLIFIED PHYSICAL REPRESENTATIONS OF LINE FORMING IN NON-LTE

The full problem of line formation in a stellar

atmosphere when the hypothesis of LTE cannot be made is too complex to be solved in the most general manner, for it involves the simultaneous solution of coupled transfer equations in all frequencies of interest and the equations of statistical equilibrium. Furthermore the atmosphere must be taken to consist of at least three species of atom: hydrogen, helium and the atom under consideration in several stages of ionization. This last requirement occurs because in some spectra the observed line intensities are affected by energy coincidences between the observed energy levels and radiations such as Lyman α of hydrogen or of He^+ or because collisions with abundant excited atoms such as metastable helium atoms can cause particularly strong ionization or excitation of certain species. Furthermore hydrogen and helium serve as the chief sources of continuous opacity.

A first simplification may be obtained by postulating that all the levels down to some particular energy below the primary ionization limit have LTE populations with respect to the population of the ion. This step is justified because the higher levels are relatively close together in energy and if the electron density is not very low, Boltzmann populations will be set up as a result of collisions. The chief problem is to decide how far down LTE populations extend. The populations of all levels below the selected level must be calculated using the equations of statistical equilibrium. The number of terms in these equations can be reduced by a judicious selection of the significant processes causing transitions between the various energy states of the atom or ion.

If the spectral lines under study occur between levels that have excitation energies so high that at the local electron densities LTE populations prevail, then adopting the LTE theory of line formation is probably a fairly good approximation. However, most of the significant lines in early type spectra do not fall into this class and the energy-level diagram of the atom or ion must be studied together with estimates of the radiative and collision transition probabilities to see what processes are important in establishing the level populations and the effective value of λ.

Some examples of the distribution of levels in essentially one-electron spectra are shown in Figure 4. The ordinate is excitation potential/ionization potential; the ionization potential of each atom or ion is given. Metastable levels are indicated by

an M. More levels occur above the levels which have been drawn. The transitions that give the characteristic absorption lines observed in stellar spectra are indicated. Two types of transitions are observed: (1) resonance lines (Li, Ca^+, Ba^+), and (2) subordinate lines from the second, third, or fourth lowest level (H, C^{+3}, N^{+4}, Si^{+3}, Mg^+).

Clearly resonance lines are particularly sensitive to non-LTE physics since they are formed between levels that are well isolated from all other levels. In the case of Ca^+ and Ba^+ metastable levels occur between the levels of the resonance lines, and the whole set of low lying levels makes an isolated group.

In the case of the subordinate lines, in each case the lower level is sufficiently isolated that non-LTE physics is important in determining its population. Whether the population of the upper level is seriously affected by departures from LTE or not is something that requires detailed investigation in each case. The transitions indicated in Figure 4 are Hα, Li I 6708, C IV 5801, 12, N V 4603, 20, Si IV 4088, 4116, Mg II 4481, Ca II 3933, 68 and Ba II 4554, 4934.

In the case of essentially two-electron spectra somewhat similar patterns emerge. Some partial energy-level diagrams are shown in Figure 5. More levels occur above the levels that are shown. In the case of the light elements the intersystem transitions are rather weak and the sets of energy levels of different multiplicity are pretty well independent of each other. In the heavier elements, for instance Ga^+, the intersystem radiative transitions are fairly strong. In spectra from ions and atoms like those shown in Figure 5 the presence of metastable levels will play a considerable role in establishing the

---

→

Figure 4 (pp. 30-31). Scaled diagrams of the lowest energy levels of some effectively one-electron spectra. The ordinate is excitation potential/ionization potential. The ionization potential is given above each column. The transition that gives the characteristic lines observed for each atom or ion in stellar spectra is indicated. Metastable levels are marked by an M.

→

Figure 5 (pp. 32-33). Scaled diagrams of the lowest energy levels of some effectively two-electron spectra. Ordinate and notation as in Figure 4.

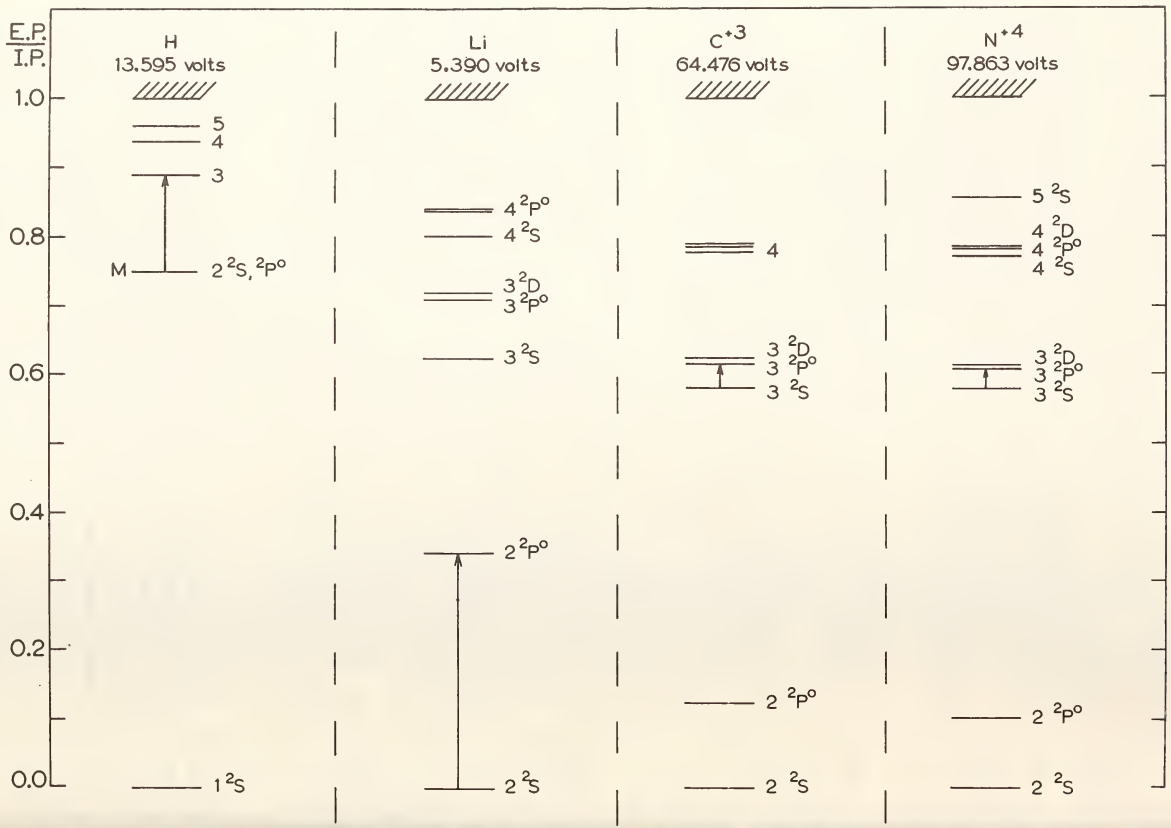
E.P.
I.P.
1.0
0.8
0.6
0.4
0.2
0.0
H
13.595 volts
5
4
3
M
2 ²S, ²P°
1 ²S
Li
5.390 volts
4 ²P°
4 ²S
3 ²D
3 ²P°
3 ²S
2 ²P°
2 ²S
C⁺³
64.476 volts
4
3 ²D
3 ²P°
3 ²S
2 ²P°
2 ²S
N⁺⁴
97.863 volts
5 ²S
4 ²D
4 ²P°
4 ²S
3 ²D
3 ²P°
3 ²S
2 ²P°
2 ²S

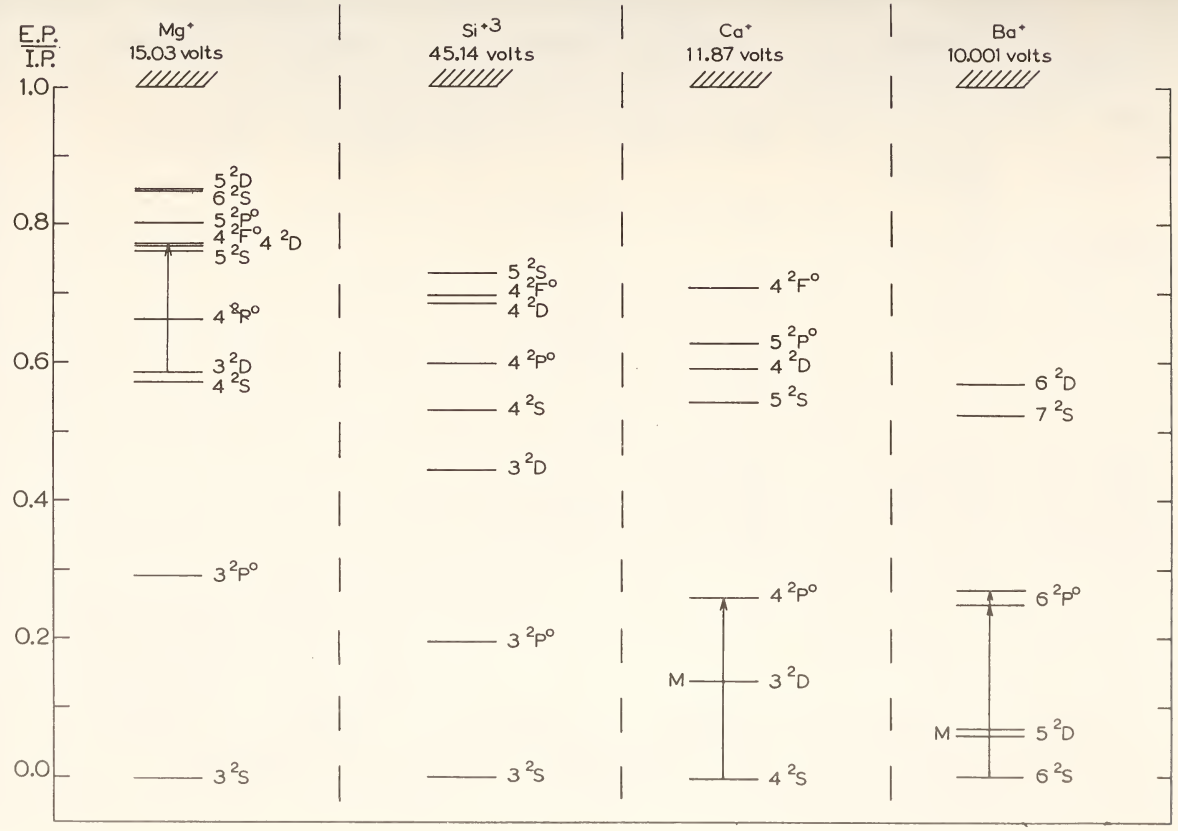
E.P.
I.P.
1.0
0.8
0.6
0.4
0.2
0.0
Mg+
15.03 volts
5 2D
6 2S
5 2P°
4 2F°
4 2D
5 2S
4 2P°
3 2D
4 2S
3 2P°
3 2S
Si+3
45.14 volts
5 2S
4 2F°
4 2D
4 2P°
4 2S
3 2D
3 2P°
3 2S
Ca+
11.87 volts
4 2F°
5 2P°
4 2D
5 2S
4 2P°
M
3 2D
4 2S
Ba+
10.001 volts
6 2D
7 2S
6 2P°
M
5 2D
6 2S

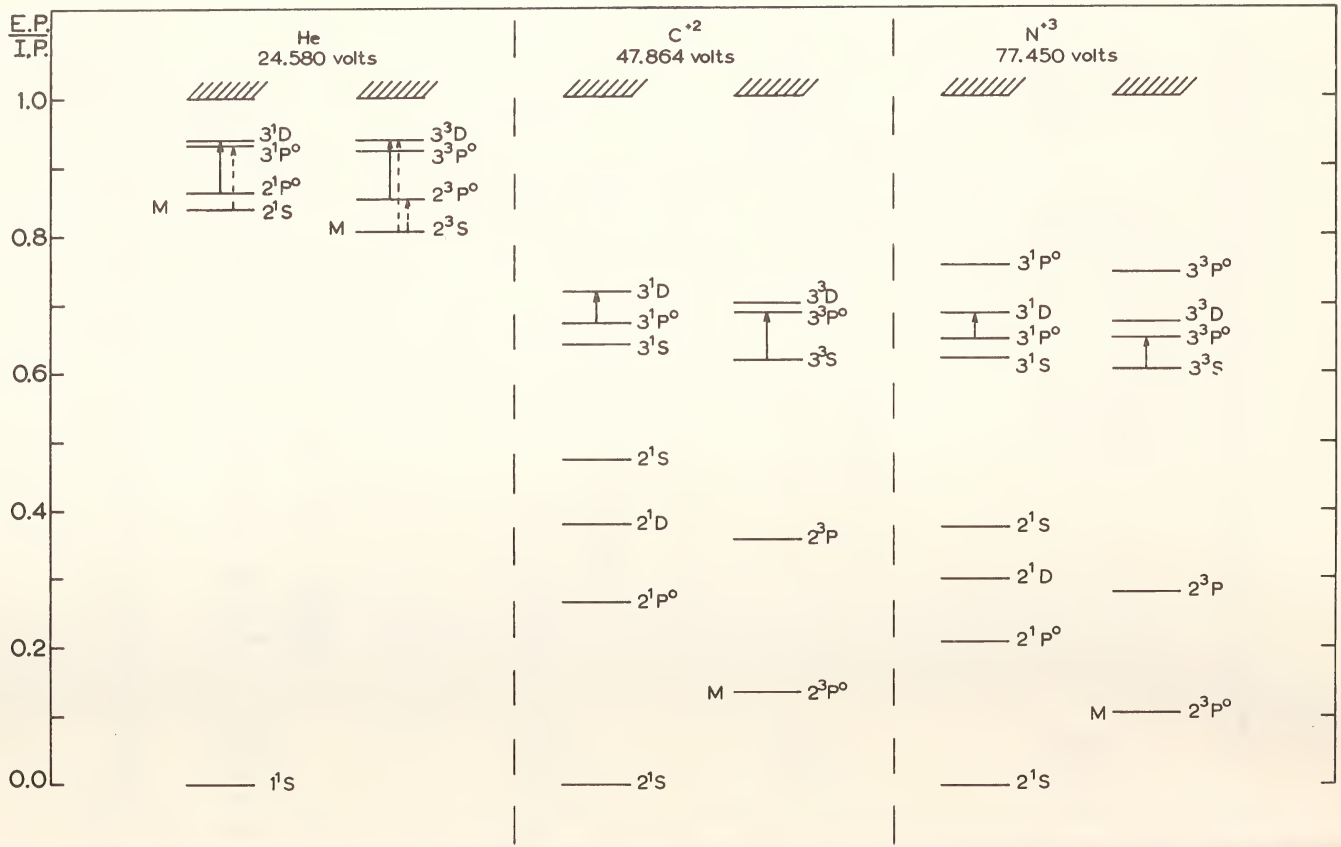
E.P.
I.P.
1.0
0.8
0.6
0.4
0.2
0.0
He
24.580 volts
3¹D
3¹P°
2¹P°
M
2¹S
3³D
3³P°
2³P°
M
2³S
1¹S
C⁺²
47.864 volts
3¹D
3¹P°
3¹S
2¹S
2¹D
2¹P°
3³D
3³P°
3³S
2³P
M
2³P°
2¹S
N⁺³
77.450 volts
3¹P°
3¹D
3¹P°
3¹S
2¹S
2¹D
2¹P°
3³P°
3³D
3³P°
3³S
2³P
M
2³P°
2¹S

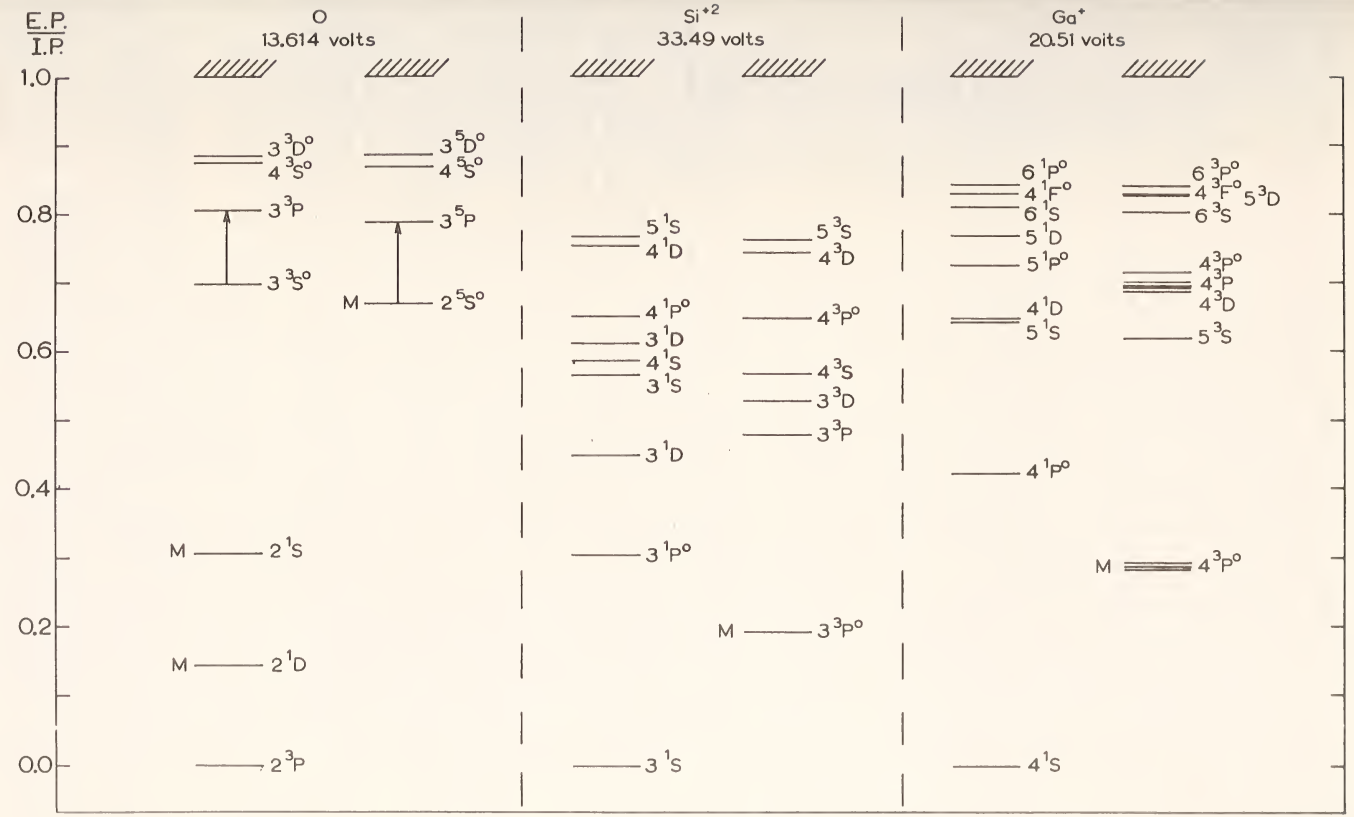
E.P.
I.P.
1.0
0.8
0.6
0.4
0.2
0.0
O
13.614 volts
3 3D°
4 3S°
3 3P
3 3S°
3 5D°
4 5S°
3 5P
M
2 5S°
M
2 1S
M
2 1D
2 3P
Si+2
33.49 volts
5 1S
4 1D
4 1P°
3 1D
4 1S
3 1S
3 1D
3 1P°
5 3S
4 3D
4 3P°
4 3S
3 3D
3 3P
M
3 3P°
3 1S
Ga+
20.51 volts
6 1P°
4 1F°
6 1S
5 1D
5 1P°
4 1D
5 1S
4 1P°
4 1S
6 3P°
4 3F° 5 3D
6 3S
4 3P°
4 3P
4 3D
5 3S
M
4 3P°

level populations. No resonance lines are observed from spectra of this sort. The chief subordinate transitions of He I are shown as well as C III 5696 (3^1P^0 - 3^1D) and 4647, 50, 51 (3^3S - 3^3P^0); N IV 4057 (3^1P^0 - 3^1D) and 3478, 82, 84 (3^3S - 3^3P^0); O I 8446 (3^3S^0 - 3^3P) and 7771, 4, 5 (2^5S^0 - 3^5P); Si III 4552, 68, 74 (4^3S - 4^3P^0) and Ga II 4251 etc. (4^3D - 4^3P^0). The chief absorption lines of Ga II which are observed (Bidelman and Corliss[40]) come from the 4^3D levels.

It is quite clear that the chief lines that are observed in the spectra of He and the ions shown in Figure 5 come from levels sufficiently isolated that one cannot assume that the level populations are in the Saha-Boltzmann ratios and that $\lambda \equiv 1$ for lines like those shown. Adoption of LTE methods of analysis to estimate the populations of the upper and lower levels of triplet lines (quintet in the case of O I) may be justified to some extent because it appears quite possible that the triplet levels are rather tightly bound to the continuum by collisions. The difficulty arises in relating these populations to the total abundance of the element and the populations of the singlet levels (singlet and triplet levels for O I). Because of the rather large energy gaps in the lower part of the energy level diagram, the populations of the lower singlet levels are most likely not in LTE at electron densities of the order of 10^{13} - 10^{14} which are the electron densities found in the atmospheres of main sequence stars.

The 3^1P^0 - 3^1D transitions of C III and N IV appear selectively in emission in Of stars and have flat-topped profiles in Wolf-Rayet stars. The 3^1D level is believed to be selectively populated by a radiative process in the case of C III and by a collisional process in the case of N IV.

No procedure can be given here for how to solve for the desired level populations and line intensities. However the data displayed in Figures 4 and 5 should make it clear that the full non-LTE problem must be solved and that it is not necessary to consider anything like an infinite number of levels or of transitions between these levels.

One question that remains is how significant are transport problems for determining the radiation field that enters into the equations of statistical equilibrium which determine the level populations. One way of advancing with the problem might be to simplify considerably the transfer problem in most radiative transitions and just retain a full transport representation for the line in question and for

one or two related lines. If there is a differential field of motion in the atmosphere such that over a geometric length corresponding to unit optical depth in the line the Doppler shift places the relevant line radiation outside the extent of the line absorption coefficient, the transfer problem can be simplified. Then the atmosphere, or at least well defined parts of it, can be treated as if optically thin. Such a manipulation is done, for instance, in order to estimate the line shapes to be expected from a spherically expanding atmosphere. However if the radiation field is completely separated from the populations of the energy levels, the strengths of the observed spectral lines can tell nothing about the physical processes going on or the abundances of the elements.

VII. SUMMARY

The interpretational problems posed by the spectra of main sequence stars, shell stars, and supergiants of types A5 and earlier have been reviewed. It is indicated that the hypothesis of LTE is untenable for the interpretation of most lines that are characteristic for the classification of these stars. A sketch has been given of how an improved theory might be developed. Particular problems that are encountered are listed in the abstract. A significant result of these yet qualitative considerations is the realisation that the atmospheres of the Ia supergiants of type B may be hydrogen-poor. In no other way can one obtain weak hydrogen lines such as are observed and still maintain electron densities of sufficient magnitude to cause the Balmer series to break off between n = 21 and n = 25.

ACKNOWLEDGMENTS

I am indebted to the Kitt Peak National Observatory for the privilege of obtaining the high dispersion spectra of B type supergiants which spurred this investigation and to R. C. P. van Helden, H. J. Lamers, and A. B. M. Smit of the Utrecht Observatory for deriving line profiles from these spectra. The theoretical considerations given

here have benefited greatly from many discussions with A. G. Hearn who spent three months at the Utrecht Observatory on a fellowship from the Netherlands Organization for the Advancement of Pure Research.

REFERENCES

1. O. Struve and C. T. Elvey, *Astrophys. J.* 79, 409 (1934).
2. O. Struve, *Astrophys. J.* 104, 138 (1946).
3. O. Struve and K, Wurm, *Astrophys. J.* 88, 84 (1938).
4. O. Struve, *Astrophys. J.* 95, 134 (1942).
5. S. E. Strom and W. Kalkofen, *Astrophys. J.* 144, 76 (1966).
6. S. E. Strom and W. Kalkofen, *Astrophys. J.* 149, 191 (1967).
7. W. Kalkofen and S. E. Strom, *J. Quant. Spectrosc. and Rad. Transfer.* 6, 653 (1966).
8. W. Kalkofen, *Astrophys. J.* 151, 317 (1968).
9. D. Mihalas, *Astrophys. J.* 149, 169 (1967).
10. D. Mihalas, *Astrophys. J.* 150, 909 (1967).
11. D. Mihalas and M. E. Stone, *Astrophys. J.* 151, 293 (1968).
12. A. G. Hearn, *Mon. Not. Roy. Astron. Soc.* (in press).
13. C. Guillaume, *Bull. Astron. Inst. Netherlands* 18, 175 (1966).
14. P. Feautrier, *Ann. Ap.* 31, 257 (1968).
15. D. Mihalas, *Astrophys. J.* 153, 317 (1968).
16. A. B. Underhill, *Proc. I. A. U. Symp. No. 26* (ed. Hubenet) Academic Press, London (1966) p. 118.
17. A. B. Underhill, *Bull. Astron. Inst. Netherlands* 19, 500 (1968).
18. A. B. Underhill, *Vistas in Astronomy* (in press).
19. A. B. Underhill, *Bull. Astron. Inst. Netherlands* 19, 537 (1968).
20. A. B. Underhill, *Astrophys. J.* 151, 765 (1968).
21. D. H. Menzel, *Pop. Astron.* 47, 66 (1939).
22. J. T. Jefferies and R. N. Thomas, *Astrophys. J.* 127, 667 (1958).
23. D. Mihalas, *Astrophys. J. Supp.* 9, 321 (1965).
24. G. Traving, *Z. Astrophys.* 41, 215 (1957).
25. D. Mihalas, *Astrophys. J.* 140, 885 (1964).
26. W. P. Bidelman, *Astron. J.* 70, 667 (1965).

27. A. D. Thackeray, *Mon. Not. Astron. Soc. S. Africa* 25, 7 (1966).
28. C. Jaschek, M. Jaschek, W. W. Morgan and A. Slettebak, *Astrophys. J.* 153, L 87 (1968).
29. O. Struve and P. Swings, *Astrophys. J.* 97, 426 (1943).
30. O. Struve, *Astrophys. J.* 99, 205 (1944).
31. A. Unsöld, *Z. Astrophys.* 23, 100 (1944).
32. H. H. Voigt, *Z. Astrophys.* 31, 48 (1952).
33. R. C. P. van Helden, unpublished material kindly communicated.
34. H. J. Lamers, in preparation.
35. A. B. M. Smit, *Astron. and Astrophys.* (in press).
36. O. Struve and H. Chun, *Astrophys. J.* 107, 109 (1948).
37. A. B. Underhill, *Astron. and Ap.* 1, (1969).
38. E. Böhm-Vitense, *Astrophys. J.* 150, 483 (1967).
39. D. A. Klinglesmith, *Astron. J.* 72, 808 (1967).
40. W. P. Bidelman and C. H. Corliss, *Astrophys. J.* 135, 968 (1962).

DEFINITION OF THE PHYSICAL PROBLEMS CONNECTED WITH EXTENDED ATMOSPHERES

by

R. N. Thomas

*Joint Institute for Laboratory Astrophysics**
Boulder, Colorado

ABSTRACT

The necessity of carefully defining the phenomenological basis for classification of atmospheres as being "extended" is emphasized, and four alternative bases for such classification are suggested (1) the necessity to include curvature terms; (2) the presence of an ejected shell surrounding a central star; (3) an observational discrepancy between predicted and observed density gradient; (4) an anomaly between predicted and observed phenomena in stars with "dynamic" atmospheres such as cepheids. A number of physical problems connected with the presence of an extended stellar atmosphere are then categorized according to these alternative bases.

Key words: extended stellar atmosphere, classical atmosphere model.

The general subject of this conference is "spectrum formation in stars with extended steady-state atmospheres." The theme of this first day is "definitions of the problems that exist." Because we use the term "extended atmosphere," we imply that these stars differ from the usual kind of star, which have atmospheres that are "nonextended." But we must recognize that most of our experience and physical intuition rests on our experience with these ordi-

*Of the National Bureau of Standards and the University of Colorado.

nary, nonextended atmospheres. There is the very real possibility that we may assess erroneously some problem on an extended atmosphere by applying an intuition that was developed in the study of non-extended atmospheres. So at the beginning of this first day I think we must be very explicit, even pedantic, in defining the terms we use to describe both the general subject and the problems that we think exist.

On this basis, I am not quite satisfied with the definitions Anne Underhill used, and the implications of some of her terms, because it seems to me that her approach is indeed wholly intuitive. For example, her most explicit definition is: "A star with an extended stellar atmosphere usually means a super-giant or a shell star." She then defines each of these stellar types in terms of certain spectral features, which we think we can interpret. But most of this interpretive process rests on our experience as to how these spectral features would be produced in ordinary, nonextended atmospheres. Again, Anne states: "We assume T_{eff} is the same for main sequence and supergiant stars. Then a spectral difference between these two classes reflects a pressure difference in the atmospheres, which implies a difference in radius, thus an atmospheric extension." and "We have certain types of lines in main sequence stars, and certain types in supergiants; some stars combine features of each--these we call shell stars."

There are strong implications in these definitions, but we are so accustomed to making them, when discussing ordinary stars, that we gloss over them. The balance of Anne's talk, logically enough, is devoted to a discussion of these spectral features and her reasons for thinking that our conventional, classical atmosphere [CA] models cannot describe them.

I myself think that there are many features that cannot be interpreted by the classical atmosphere models in stars whose atmospheres are neither "supergiant" nor "shell." Some of these features may arise because some parts of the atmosphere are more "extended" than the classical atmosphere model predicts. Other features may be anomalous on the basis of the classical atmosphere model, yet their appearance may have nothing to do with atmospheric extension.

So I would prefer to have a definition of an extended stellar atmosphere that is more directly tied to a pictorial, geometrical notion of "atmospheric extent." There are several possibilities

for setting up such a definition, and I think we should consider them all. During this symposium we can use these categories as a reference frame. Perhaps we will find one particular category is preferable; perhaps we will find none are very satisfactory. I will outline my suggested alternatives; you may object and change them as you like.

A. DEFINITION OF AN EXTENDED ATMOSPHERE

We have several possibilities for this definition: one conceptual, from an a priori standpoint, within the framework of our ordinary models; one based on some circumstance that produced a configuration of an "unusual" type but to which we try to apply our "usual" thinking; one based on observations that directly contradict what we would expect from our "usual" models; and one based on some configuration we expect to occur but which we expect to lie outside the scheme of our "usual" models. I will summarize these, then ask which we might adopt.

For reference, first recall that the classical atmosphere (CA) is defined by: RE (radiative equilibrium) or CE (convective equilibrium); HE (hydrostatic equilibrium); and LTE (local thermodynamic equilibrium). Then we have four alternative classification schemes, each based on some distinction between the category and some property of the CA.

1. Distinction between an atmosphere where curvature terms need be included and an atmosphere where they need not be included. Other than this difference, we could hold to the CA model, if such a CA model could give an extended atmosphere.

Note that this was essentially the type of atmosphere considered by Kosirev, Chandrasekhar, and others during the 1930's when they were trying to find the change in the spectral distribution of emergent radiation due to the effects of extent and curvature. Note that they did not apply the CA assumptions literally, but adopted arbitrary density distributions to get the atmospheric extent; but they did retain, at least implicitly, the "physics" of the CA model.

It may be that to get such an atmosphere under CA, we need to go to small values of $g_{eff} = (g_{dynamical} - g_{radiative})$, and problems of stability arise. But this is the direction of approach.

2. A distinction based on the presence of an "ejected" atmosphere or shell surrounding a central star and atmosphere where the configuration is considered to be now steady, or at least quasi-steady, but where there is no pretense that the configuration occurred as a CA evolution, just that a CA model, only slightly fudged, may now describe it.

A variety of objects could possibly be placed in this category: shell stars of all sorts; various nebulae including planetary nebulae, T Tauri shells, etc.

3. The wholly observational distinction between the predicted extent of a star with given g and T_{eff} and its "observed " extent. Then, assuming the parameters necessary to compute the CA model--g and T_{eff}—are reasonably accurate, the essential question is how does one specify the "observed extent." (We bypass for the moment the question of the implication on the model of the "microturbulent" parameter required for stellar spectral fit to the CA models).

The question of specifying the "observed extent" obviously underlies this whole possibility for defining extended stellar atmospheres. There are a number of possibilities for defining the observed extent:

(a) Direct approach.

"Tangential" observations, i.e., eclipse studies, that directly measure extent. Solar studies are obvious. Studies of stars like 31 Cyg, ζ Aur, and V444 Cyg give direct evidence of atmospheric extent.

(b) Indirect studies of "extent" parameters.

Studies of spectral features that appear to imply large geometrical extent: (1) "dilution" effects; (2) observation of an abnormally large number of Balmer lines; (3) some forbidden line effects (These last two are a combination of low-density and large geometrical extent phenomena.); and (4) interpretation of emission lines as coming from an extended stellar atmosphere.

(c) Indirect studies based on the predicted effect of other parameters.

Micro- and macro-turbulence values that are comparable to the compression-disturbance velocity in the atmosphere would be expected to distend the atmosphere.

Excitation effects that suggest anomalously high excitation, hence higher electron temperature, suggest greater atmospheric extent. (Note

that some of these effects were what led to studies trying to find a UV excess in an extended atmosphere.)

Some years ago, the sun would have been included as the classical example of this type. After all, people thought that there was absolutely nothing in the non-eclipse spectrum to imply anything "anomalous." But now, with hindsight, we recognize that there are many things in the visual disk spectrum that suggest the following classification: e.g., the H and K line profiles, the λ10830 He line, the presence of the solar granulation.

4. Distinction between the "normal" CA models that we expect most stars to satisfy and whatever models are required to describe pulsating stars, ejecting stars, and other dynamically unstable stars which do, however, exhibit at least a quasi-steady-state configuration.

While we know what we mean by stars that exhibit an overall divergence from the strict CA model, we do not know in detail which these are. For example, we would now include the solar chromosphere-corona in the class of such atmospheres that the CA model will not satisfy, but several years ago we would not have done so. Further, the sun as a whole is thought, by most people, to satisfy the CA, and it is often argued that the chromosphere-corona are an essentially unimportant part of the solar atmosphere. (With which viewpoint some of us would take issue.)

It is often argued that at each phase of the cepheid pulsation the atmospheric configuration can be mimicked by a CA model with the proper choice of T_{eff} and g_{eff}.

It is sometimes argued that supergiant atmospheres satisfy the CA model. Other people disagree. The current satellite observations of their far UV spectrum show large mass outflow, and almost certainly a chromosphere-coronal phenomenon.

Despite the problem of identifying the stars, or the parts of the stellar atmosphere that might satisfy the distinction of being in the extended stellar atmosphere class, all seem to agree that the effect of a momentum input or a mechanical energy dissipation or both is to make the atmosphere more extended than it would be in the CA model. But in any event, a basic point is that the CA assumptions are violated. Thus in discussing an extended stellar atmosphere, we must carefully decide which of the above criteria we adopt in defining an extended stellar atmosphere (ESA).

B. SUMMARY OF THE PHYSICAL PROBLEMS CONNECTED WITH THE IDEA OF AN ESA

Clearly, the problems we will list and emphasize depends upon which definition of an ESA we adopt. Let us consider some of these problems according to the various alternatives given above:

1. "Curvature" criterion

(a) The main question is, Under what conditions can a CA model give an ESA?

(b) The second question is, What structural difference comes from such an ESA model?

1. What difference does it make in a $T_e(\tau)$ model?
2. What difference does it make in the predicted spectrum: I (λ, continuum); line profiles. We should consider this problem according to LTE, to be wholly consistent.
3. What difference does such a model induce, in the expectation of non-LTE effects? Since such effects come wholly from inhomogeneity induced by the boundary, and the "kind" of boundary behavior changes with these curvature terms, it is an important question.

2. "Ejected" atmosphere or shell

(a) A major problem is to deduce the geometric distribution of the ejected material. One approach is to try to follow in detail the distribution of matter to be expected from a nova outburst, checking the inferred distribution, based on some sort of calculations, against the spectrum that should be produced by such a distribution. Another approach is to assume various degrees of "connectedness" of the distribution of material, and determine the "stratification" spectrum.

(b) It is equally important to ask whether the CA model or a simple modification can be applied. Clearly, here the non-LTE aspects associated with "dilute" radiation are important, but it is also important to ask whether such things as RE, HE, etc., can be taken over. So it comes down to asking what kinds of steady-state equilibrium can be stable for such configurations, taking into

account various kinds of interaction with the "parent" star--radiation, continuous small-scale mass ejection, etc.

(c) There are also many problems connected with predicting the spectrum from such an ESA. Again, these are connected with Session II of this symposium.

3. *"Observational discrepancy" with prediction of CA model*

(a) We made the point above that the primary problem is one of inferring parameters that either support or negate the CA predictions. Again the problem can be broken down:

1. Eclipse studies. Just as there was no real understanding of the implications of solar eclipse studies on the specific details of the outer solar atmosphere until a complete non-LTE diagnostics was developed, so there exists the same situation for eclipse studies of 31 Cyg, etc. Mainly, we have curve-of-growth studies. We need to see what is needed, in terms of data available, and develop the diagnostic methods.
2. Non-eclipse studies. Many of these studies are simply spectral studies and spectroscopic diagnostics, and thus come under Session II. Some of these studies are of the physical implication type and resemble solar studies, where, e.g. "observed" supersonic turbulence required high T_e. Thus we ask for studies of the physical consistency between the simultaneous "inferred" presence of various parameters. It is sometimes difficult to separate the above point and this point, just as in the solar problem, and they must be studied together. E.G., does an inferred supersonic turbulence imply a faulty diagnostics or a faulty inference on T_e?

(b) Emission lines: general approach. While this is logically part of the spectroscopic studies it should be broadened in implication to be mentioned separately. Basically the question we ask about emission lines is whether their presence can be interpreted to

imply: (1) simply an extended atmosphere, and "classical" grad T_e, (2) the presence of a "specialized" mechanism, such as the Schuster mechanism, and again essentially a "classical" atmosphere, (3) the presence of a chromosphere-corona, thus mechanical energy supply, and definite departure from RE.

Thus the presence of emission lines is a class by itself when discussing spectroscopic diagnostics. It is also a bridge to alternative(4).

4. "A priori" rejection of CA models

The foremost problem is a conceptual one: What are the parameters that fix the state of the atmosphere of such a star? There may, of course, be several cases. But overall, the big difference between a classical aerodynamical situation and a classical stellar atmospheric configuration is the coupling of velocity field to internal degrees of freedom. In the aerodynamic case, coupling is through T_e (electron temperature), whose value is fixed by the kinetic temperature, whose value is fixed by the dynamical flow problem directly. In the stellar case, the coupling is through the radiation field, whose value is indirectly affected by the velocity field. The question is, In such cases as this model type 4 distinction between ESA and "normal" atmospheres, does this situation change with respect to the static case? The "classical" arguments on cepheids, etc., would say it does not change: you give g_{eff} and T_{eff} at each phase, with g_{eff} being the thing fixed by the dynamical problem--but the radiation field still fixes the local value of T_e, and the internal degrees of freedom, and so the spectral properties. Thus the atmospheric extent would arise from dynamical properties, not from increased T_e due to mechanical energy dissipation, in this "classical," RE, cepheid picture. The CA would not apply in its entirety, of course, only in this modified version.

But it is also possible that mechanical energy dissipation must also be included. In this case, we must determine the effect on T_e, and the coupling to internal degrees of freedom. In this case, the basic question posed is: How do you really describe the dependence of the local value of T_e on the quantity and quality of the radiation field and the local mechanical energy dissipation?

DISCUSSION

Pecker: It should be noted that, even in steady state, we should write time-dependent equilibrium equations. At a given location in the atmosphere conditions are fluctuating; they are steady only in a statistical way. Depending on the relaxation time of the medium, as compared with the characteristic time of fluctuations, it may be necessary to solve the time-dependent equations before integration over the time. The result could be different from the solution of time-independent equilibrium equations.

A. B. Underhill made a guess of "what lines are sensitive to non-LTE conditions." She proposes three categories. This seems to me very dangerous. As soon as we suspect that non-LTE physics is necessary, we have to investigate, in each particular case, whether LTE might be used as a sufficiently good approximation.

The Balmer lines should be added to the list. The studies by Feautrier, for example, show that b_1, b_2 are far from equilibrium.

In the case of the hydrogen lines in supergiants even a non-LTE theory does not solve all problems. A. B. Underhill mentions that we could consider a smaller hydrogen abundance to reconcile observations and theory (i.e. β Ori and others). But what about departures from hydrostatic and radiative equilibrium? These could give rise to an increase in temperature and variations of g_{eff} in the outer layers of the atmosphere and should be seriously considered.

Underhill: If the temperature increases with height in an atmosphere, you may find emission components in some lines or indications for higher excitation temperature in the lines. But the spectra of B-type supergiants seem to indicate that there is a very low excitation temperature.

Menzel: Are there some similarities to the solar chromosphere?

Underhill: It is very difficult to observe chromospheric effects in the light integrated over the disk, even in the case of the sun.

Pecker: If the lines show low excitation temperature, you can only say that there is no increase of the source-function. It is wrong to conclude there is no increase of excitation temperature.

Underhill: There is no known mechanism for heating a chromosphere, for hydrogen and helium are already completely ionized in the outermost layers.

Kalkofen: The model calculations by Mihalas and Feautrier do show an increase of temperature in the UV.

Underhill: An increase of 2000° for an average of 20,000° K is too small to show conspicuous effects.

Menzel: I disagree with the statement that the assumption of LTE gives only absorption lines. Strictly, if the temperature of the gas equals that of the photosphere, the spectrum will contain neither absorption nor emission lines. If the photospheric temperature is greater, we obtain absorption lines; if the temperature of the gas is greater, the lines appear in emission.

I am not implying that departures from LTE do not exist. Cyclic transitions, perhaps involving metastable levels, must cause such departures. However, they may not be as great as certain non-LTE theories seem to require. Such neglected phenomena as non-static atmospheres, flares, "star spots," magnetic fields, atmospheres with non-uniform temperatures and dynamical flow can produce what appear to be significant spectral anomalies, as interpreted by conventional theories.

Most proponents of non-LTE theories of stellar atmospheres attribute the supposed spectral anomalies to the interaction of the radiation and collision fields, a source function differing from that of Planck radiation for a given temperature, or non-Maxwellian distribution of velocities of colliding electrons, plus the interactions and resonances--real or fancied--between different atomic constituents.

We don't have to go very far to see that this model simply does not work. The sun is an excellent example, as I first demonstrated about 40 years ago, not from any model but from the observations alone.

I have always insisted that observations are fundamental. Models are important, but they must be subservient to the observations rather than to traditional or classical concepts of how stellar atmospheres should be constructed.

Just look at the sun! The normal Fraunhofer spectrum is consistent--at least roughly-- with that from a gas at a temperature of about 5000°K. The chromosphere, a layer of gas contiguous to the reversing layer, contains strong lines of ionized metals, of helium, and of ionized helium. In the old days-- and by "old days" I mean the very ancient pre-DHM era, which no one here other than I can recall--some astrophysicists claimed that the chro-

mospheric spectrum was entirely in accord with the existing theory. They pointed qualitatively to the Saha formula and naively suggested that low pressure was responsible for the presence of ionized helium in the chromosphere, a fact that I later showed could be explained only on the basis of high temperature.

Miss Underhill calls attention to many lines she doesn't "like," because they "behave anomalously." Anomalously, that is, according to her models. But I think we need to postulate the existence of truly distended atmospheres--stellar coronas, if you will. In such regions we shall expect to find numerous "anomalous" conditions, such as shock waves, magneto-hydrodynamic flow, and atmospheric irregularities. No wonder the spectra seem to be anomalous. But the fault lies in our models, not in the stars.

Underhill: What I don't like is calculating those lines with LTE-theories. I do like those lines because they do give us a clue to what is going on in particular processes. I cannot agree with Dr. Menzel that it may be possible to heat the extended atmospheres in layer sections, giving each section a temperature and then going on with LTE calculations. The critical lines do come from levels so widely separated that you cannot justify Saha-Boltzmann relations. The reason is that in early type stars the particle densities are too low (of the order of 10^{12}-10^{14}) even in main sequence stars. Saha-Boltzmann relations are reasonably valid if the particle density is of the order of 10^{16}.

The difference between the atmospheres of early type stars and the sun is, that in early type stars the density of the photosphere is comparable with the density of the solar chromosphere. In extended atmospheres the densities must be even lower.

Wellmann: It seems that the lack of adequate mathematical methods to treat the NLTE case is a severe handicap for the explanation of many observations related to stars ranging in type from the supergiants with minor deviations from LTE to extreme NLTE-objects like planetary nebulae, as well as certain Be stars, WR stars, and novae. The complete problem is to solve the (infinite) system of linear equations N_i = const together with the transfer equations for the radiation densities u_{ik}. It might be possible to introduce new special functions adapted to this task. This is a challenge to the theoreticians.

Underhill: It should be possible to reduce the infinite system to only a few equations by neglecting many transitions for physical reasons or by tying the

higher levels to the continuum. In addition it might not be too bad to assume black-body radiation density for the secondary lines and restrict the transfer problem to one or two lines. How to proceed is a question to be answered by the theoreticians.

Wellman: I should like to point out that the formation of emission lines might be strongly influenced by the velocity distribution in the atmosphere.

Hillendahl: In calculations recently completed for supergiant atmospheres the line shapes (core depth, width, wings and equivalent width) were found to be quite sensitive to the velocity distribution in the atmosphere. Because of this sensitivity it is difficult to see how one can draw conclusions about the importance of non-LTE unless the velocity dependence has been taken into account.

Thomas: Let's be sure that questions on symbiosis are not questions of the method of description rather than physical facts. Since Menzel's work in the 1930's it is clear that the sun is a symbiotic object in the above sense: T = 3400° for NaD-lines, 25000° for He II. But recent work using non-LTE and non-radiative equilibrium has shown that this "apparent" symbiosis is not symbiosis at all; it is just a deficiency in our methods.

Pecker: If there are objects between the supergiants and the stars with large shells, i.e. planetary nebuale, it is not a priori necessary that we find the same mechanism. The only reason for intermediate objects could come from stellar evolution.

Wellman: The gap is filled by novae in different states and by Be stars of different types.

Rybicki: The question of the appearance of emission lines is a question of the behaviour of the source function. Independent of LTE or non-LTE conditions it is the projected area that gives rise to emission lines. So it is important to consider the geometric structure.

Thomas: The point is not whether an extended atmosphere can produce an emission line only by geometry--but whether an observed emission line implies such a geometrical origin uniquely. It is possible to have an intrinsic emission line in a non-extended atmosphere.

Rybicki: If you are going to obtain the mechanism of emission from the observations you must be sure what kind of mechanism you mean. In the case of supergiants you cannot get an emission line, if you do not have an increase in the source function.

Groth: A. B. Underhill postulated that the

atmospheres of some B-type supergiants of luminosity class Ia are hydrogen-poor. Our studies of supergiants (α Cyg A2 Ia, ϕ Cas FO Ia) show that the atmospheres of these stars do have normal hydrogen abundances. The Balmer series of hydrogen breaks off at n = 32-34, as one would expect for supergiants of low electron density. Using an LTE model with variable microturbulence, I found excellent agreement between calculated and observed hydrogen lines (H_γ-H_{10}) for α Cyg.

Estimates show, that the luminosity of α Cyg is very high, M_{bol} being of the order of -8^m. ϕ Cas is one of the most luminous stars of our galaxy ($M_{bol} = -8^m.9$). We don't yet have a model calculation of its atmosphere, but the appearance of hydrogen lines is quite normal. The high luminosities of α Cyg and ϕ Cas imply that these stars are evolved stars, probably further evolved, than the B type Ia supergiants. The mass of α Cyg and ϕ Cas can be estimated to be 30-40 solar masses.

Hillendahl: In the calculations mentioned above it is unnecessary to assume a turbulent velocity. The dispersion in atmospheric velocities, which occur as a result of hydrodynamic motion, fulfills the role of the turbulent velocity.

Houziaux: To fit the Balmer line profiles you introduced a change in He/H abundance. Did you find an influence on the shape of the continuum?

Underhill: I used the schematic models by Böhm-Vitense, who has only calculated the continuum. Line calculations have not been done.

Groth: At Munich we are working on the analysis of spectra of a number of supergiants (Ia, Ib) with spectral types A and F. In two cases (α Cyg, η Leo) we already have model calculations.

The observed equivalent widths of metallic lines cannot be explained, if we assume an LTE model with constant microturbulence. The abundances of weak and strong lines, even within one multiplet, differ by a factor of 10-100. If we introduce an increasing microturbulence with decreasing optical depth we get excellent agreement for the abundances of weak and strong lines.

Using a curve-of-growth analysis, we find for all supergiants a damping parameter log 2α of the order of -1 to -1.5. We know that there is only one effective damping process for low density atmospheres, namely radiation damping which should give log 2α approximately -2.5 to -3.0. Again there is a discrepancy by a factor of 10 to 100 between observed and predicted damping constants, which can be ex-

plained by the variation of microturbulence.

Underhill: Do you have spectra of high dispersion, so that you can compare the predicted turbulent velocities with the line profile?

Groth: Normally it is impossible for supergiants to prove the predicted microturbulence by the profiles. In all stars studied the shape of the profile is due to rotation or macroturbulence with a Doppler width larger than that of microturbulence.

Menzel: The departures from LTE must not be very large. If you assume changes in atmospheric structure, it is possible to fit the observations using only very small deviations from LTE.

Mugglestone: Does the dependence of microturbulence on optical depth change the line core or the wings?

Groth: The central depth of the lines becomes smaller and the wings get broader, as in the case of higher damping, if you assume that the equivalent width is the same as in the case of constant turbulence velocity.

Hillendahl: Using the microturbulence in the calculation of line profiles does mean that you introduce an additional parameter. I propose to take another free parameter. Using a linear velocity distribution you get the gradient of velocities as a new parameter. I believe that you will find the same result as before.

Groth: It is possible that a velocity gradient in the atmosphere could give similar line profiles to those which you get with microturbulence depending on optical depth. But a velocity gradient must give rise to differential displacements of lines, which are formed in different optical depths.

Pecker: Describing a velocity field by a given number of parameters is an ambigious procedure, as long as one does not define the shape of the function. For instance the functions

(a) $\xi = \xi_1 \qquad o \leq \tau < \tau_\ell$

$\xi = \xi_2 \qquad \tau_\ell \leq \tau < \infty$ (step function)

(b) and $\xi = a+b\tau$ new line have a completely different shape and are not equivalent.

If one tries to represent a solar line at the center of the disk, one can get a fit either using (a) or (b). This has been shown clearly by Roddier and Gonczi for lines of SrI.

Underhill: To get a good fit of the observations, it is necessary to use as many lines as possible. It is important to use lines of different excitation and ionization potential to find unique solution.

Hillendahl: My proposal to use a linear velocity distribution comes from the result of calculations for supergiants type Ia where I got this result.

Thomas: Do you know the mechanism producing the velocity field?

Hillendahl: The velocity field is produced by a rarefaction wave, which is excited by a shock front. (Detailed description of the processes in Hillendahl's paper.)

Pecker: D. H. Menzel has rightly attracted attention to the fact that improvement of fitting the observations by theory can be done either by working on non-LTE analysis with a classical model, or by using LTE and an improved model (i.e. an improved T_e and n_e distribution).

I do not challenge this fact. Actually a given set of observations can be accounted for by a variety of situations. This means there are indeterminacies in the problem. One must realize that the several discrepancies we have are not necessarily of the same nature. If we consider the theory of line formation, we do know the physics well, the main difficulty being either numerical or bad knowledge of physical parameters. I cannot say anything about the models. We don't know the physics of heating processes, or the effects of gravity waves etc. Therefore in a first approximation one should always use NLTE analysis for which the physics is unambiguous. The next step in learning more about the physical mechanism involved in the departures from radiative and hydrostatic equilibrium must be the comparison between the observations and the result of theoretical non-LTE treatment.

Böhm: In the case of plane-parallel atmospheres the progress of the non-LTE theory has been very large. Recently we have made NLTE calculations for spherical atmospheres. We found these calculations to be very complicated, so that they can be done only in extreme cases, i.e. planetary nebulae.

Hummer: It is possible to do non-LTE calculations in spherical geometry. If the velocity gradients are very large, then this becomes fairly simple. This has been worked out by J. Castor at JILA and has been applied to He II in Wolf-Rayet stars. Work on small or zero gradient has been performed by

Mathis at Wisconsin and Skumanich at Boulder.

Pecker: I agree that non-LTE problems can be handled mathematically for plane-parallel and spherical atmospheres, but the main problem is to understand the physics of extended atmospheres.

Thomas: The physical principles for non-LTE atmospheres are well known. It is important to use them in the right way.

Böhm: I am not sure that the physics is so simple if you take a large number of coupled terms.

EXTENDED ATMOSPHERES OF PLANETARY NUCLEI

by

K. H. Böhm and J. Cassinelli

University of Washington
Seattle

ABSTRACT

Exploratory calculations on nongray, hydrostatic-equilibrium model envelopes for central stars of planetary nebulae of high temperature and possibly near the instability limit are reported. It is conjectured that these may be related to Wolf-Rayet type nuclei; it appears possible to obtain an OV absorption, and OVI emission, spectrum even in an LTE calculation.

Key words: nongray, central stars of planetary nebulae, Wolf-Rayet nuclei, instability limit.

There are a number of theoretical and empirical arguments that indicate that central stars of planetary nebulae in the range 5.5×10^4 °K < T_{eff} < 9.0×10^4 °K have extended atmospheres (in the sense that curvature effects become very important).

From a theoretical point of view we must realize that:

(1) Because of the high effective temperature of these objects, the scale height

$$H = RT/\mu g \qquad (1)$$

tends to be rather large; and

(2) The objects in the temperature range quoted are fairly close to the instability limit due to ra-

diation pressure effects (Harman and Seaton 1964) as defined by

$$|g| = |g_{rad}| = \frac{\pi}{c} \int_0^\infty \{\kappa_\nu + \sigma_{e\ell}\} F_\nu d_\nu \approx \frac{\sigma T_{eff}}{c} \sigma_{e\ell} \quad (2)$$

with g = surface gravity of the star, g_{rad} = radiative acceleration, κ_ν = monochromatic absorption coefficient, $\sigma_{e\ell}$ = electron scattering coefficient. This fact leads to a rather low effective surface gravity in these stars which in turn leads to an additional considerable increase of the scale heights. As pointed out earlier (Böhm 1969), one gets hydrostatic atmospheres with a thickness larger than one stellar radius if one approaches the instability limit (2) to a point where

$$|g_{rad}| \approx 0.9 \times |g| \quad . \quad (3)$$

In such an atmosphere curvature effects become very important. This point will be discussed below.

From an empirical point of view it is important to note (O'Dell 1968) that central stars showing Wolf-Rayet spectra occur practically only on the part of the Harman-Seaton sequence that lies close to the instability limit.*

Since Wolf-Rayet spectra can be formed only in a rather extended atmosphere (or envelope) we may also conclude that the observational evidence indicates that stars in this region of the T_{eff}-g-plane have extended envelopes. One might even hope that a thorough study of atmospheres in the indicated range of T_{eff}- and g-values will eventually lead to a the-

---

* In view of the considerable uncertainties in the empirical determination of T_{eff} and g, it is difficult to be absolutely certain about a statement like this (Cf. diagram no. 7 in Böhm 1968). However, the evidence given by O'Dell (1968) certainly shows that the above statement at least does not contradict the present observational evidence.

oretical understanding of the Wolf-Rayet phenomenon.**

(A study of planetary nuclei has one great advantage as compared to the investigation of WR field stars: We know T_{eff} and g before we start the study.)

The problem of constructing model envelopes for central stars is being approached in three steps:

(1) in order to get some basic orientation, Böhm (1969) calculated some nongrey hydrostatic models near the instability limit using a plane-parallel approximation. Of course these results can be considered at best only as a qualitative approximation. However, even these crude calculations offer some interesting insight. They show the very strong dependence of the geometrical thickness of the atmosphere and also of the energy distribution of the surface flux $F_\nu(0)$ on g (Böhm 1969). In this connection it is also instructive to see how strongly the density stratification is changed by a rather small change in the surface gravity. This is illustrated by Figure 1.

(2) J. Cassinelli is trying to construct hydrostatic nongrey model envelopes for these objects taking into account curvature effects. He showed that a generalization of Lucy's (1964) temperature connection procedure is possible though the setting up of a relation between the zero-order moment J_ν and the second-order moment K_ν of the intensity $I_\nu(\mu)$ offers some difficulties in the spherically symmetric case. As in the plane-parallel case the determination of the monochromatic J_ν for a given $B_\nu(\tau_\nu,r)$ has to be carried out for every frequency between two successive temperature correction steps. This can be accomplished e.g. by the application of Carlson's S_n method (Cf. Carlson and Lathrop 1968). It is obvious that the determination of nongrey model envelopes is a laborious task (even if one makes the drastic simplification of assuming LTE). It is therefore important to ask whether the effort is worthwhile and what one may hope to accomplish. We do hope that a detailed study of these envelopes will eventually lead to an understanding of central star

---

** As J. Schmid-Burgk (1968) has pointed out stars close to the instability limit (2) (but not yet in the actual instability region) easily generate a "strong stellar wind." This would make the mass loss of these Wolf-Rayet stars understandable.

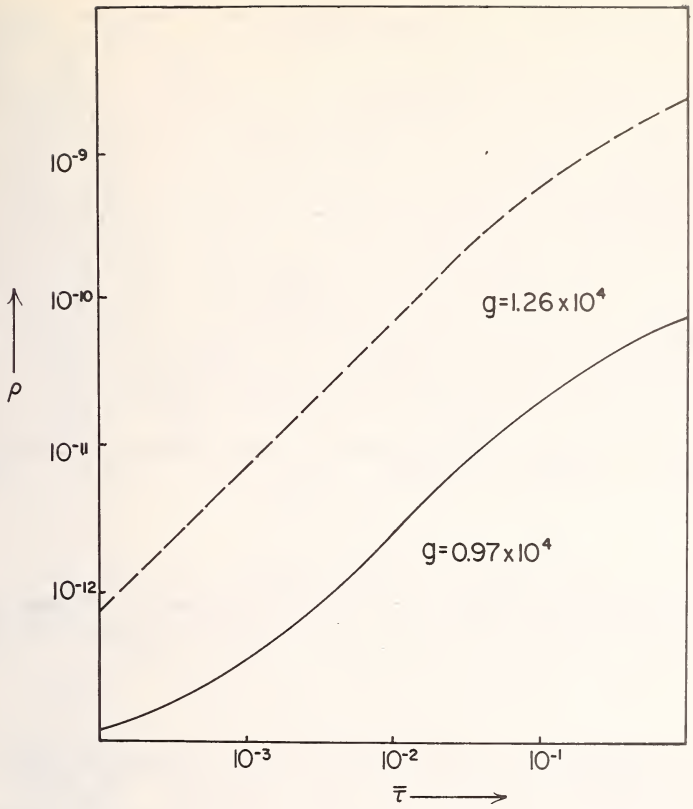

Figure 1. The density stratification $\rho(\bar{\tau})$ for the models with $T_{eff} = 6.3 \times 10^4$ °K, $g = 1.26 \times 10^4$ cm sec^{-2} and $T_{eff} = 6.3 \times 10^4$ °K, $g = 0.97 \times 10^4$ cm sec^{-2}.

spectra showing emission lines. Preliminary calculations indicate that it might, for instance, be possible to understand why certain central stars, especially of the type NGC 246 (see Greenstein and Minkowski 1964), show OVI lines in emission while the OV lines appear in absorption. Figure 2 shows that with a simple LTE assumption for the model with $T_{eff} = 6.3 \times 10^4$, $g = 0.97 \times 10^4$ cm sec^{-2} we can get a situation where in the outer very extended part of the atmosphere ($\tau < 3 \times 10^{-3}$) the oxygen exists mostly in the form of OVI whereas in deeper layers down to $\tau = 0.45$ the OV dominates. It is obvious that such an extended atmosphere could give rise to an OVI emission spectrum (because the OVI exists in an "extended envelope" that is optically thin in the continuous radiation) and an OV absorption spectrum.

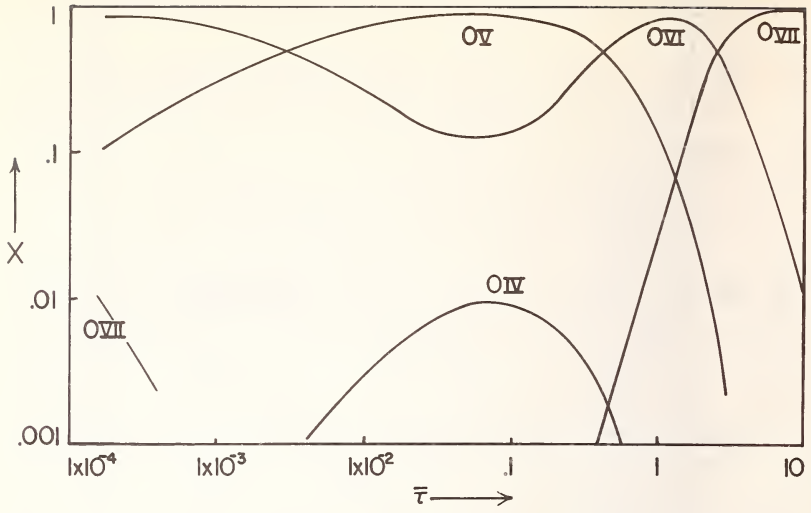

Figure 2. The ratio x of the number of ions in a given ionization stage to the total number of oxygen ions as a function of τ for the envelope model with $T_{eff} = 6.3 \times 10^4$ °K, $g = 0.97 \times 10^4$ cm sec^{-2}.

Whether this model could explain the observed spectrum in detail has not yet been checked. We felt such a detailed check would be worthwhile only after a really self-consistent spherically symmetric radiative equilibrium model has been constructed.

(3) For the reasons indicated above it is obvious that stellar envelopes with a continuous outflow of matter and not in hydrostatic equilibrium should be investigated. Such a study is being carried out by J. Schmid-Burgk. However, in this case the combined hydrodynamics--radiative transfer problem becomes so complex that one has to restrict oneself to a grey approximation of the radiative transfer problem. Curvature effects have been included in this treatment.

We feel that the two lines of approach described under (2) and (3) should be followed simultaneously in order to learn something about the nongrey radiative transfer and the hydrodynamic aspects of the problem. One may hope, of course, that eventually we shall be able to treat the whole problem combining the hydrodynamics and a realistic treatment of the nongrey radiative transfer problem.

REFERENCES

Böhm, K. H. 1968, *I.A.U. Symposium No. 34 "Planetary Nebulae,"* eds. D. R. Osterbrock and C. R. O'Dell, Dordrecht: D. Reidel Publ. Co., p. 297.

Böhm, K. H. 1969, *Astron. and Astrophys.* 1, 180.

Carlson, B. G., and Lathrop, K. D. 1968, *Computing Methods in Reactor Physics*, eds. H. Greenspan, C. N. Kelber, D. Okrent, New York: Gordon and Breach , p. 167.

Harman, R. J., and Seaton, M. J. 1964, *Ap. J.* 149, 824.

O'Dell, C. R. 1968, *I.A.U. Symposium No. 34 "Planetary Nebulae,"* eds. D. E. Osterbrock and C. R. O'Dell, Dordrecht: D. Reidel Publ. Co., p. 361.

Schmid-Burgk, J. 1968, unpublished.

DISCUSSION

Böhm: I would like to ask whether there are better methods to solve the nongrey spherical problem.

Hummer: There are papers by Mathis and Skumanich who treat these problems.

Rybicki: Perhaps the method of Feautrier can be generalized to solve the spherical problem.

Thomas: Are the shells you have calculated close to the instability limit?

Böhm: The observations show a very large scatter, so that it is not possible to find a clear decision. O'Dell, using new observations, does believe that for all planetary nebulae with central stars that are of the WR type, the shells are close to the limit of instability; but I think the scattering in absolute magnitude ($\Delta M = 1^{m}.5$) is too large for one to make this conclusion. Some of the central stars at the lower end of the sequence are Of stars.

Hummer: The nebulae that are connected with Of stars are very large in general. The calculated Zanstra temperatures do not correspond with the observed Of spectra.

Underhill: Some years ago I estimated roughly the temperatures of WR stars. I concluded from these temperatures that the difference between WC and WR stars is not due to differences in abundance but it is differences in excitation.

Wellman: I have tried to solve the transfer problem in spherical atmospheres by using the follow-

ing procedure: The radiation is split up in two parts, (1) the radiation that is coming directly from the star, and (2) the diffuse radiation of the shell. If you integrate each part independently, you get a simple solution of the problem.

Böhm: That is the same procedure we followed, but we feel uncertain about it. In the nongrey case the radiation in different frequencies is coupled, and we should solve the general transport equation.

THE N IV λ5820 MULTIPLET IN WN STARS

by

H. Nussbaumer*

Department of Physics
University College
London

ABSTRACT

Evaluating transition probabilities of N IV 2p3d $^3P^0$ to 2s4s ^3S and 2p3p ^3P and an emission feature at λ7410 it is shown that a disputed emission at λ5810 in WN stars may not be attributed to N IV.

Key words: HD 192163 WN6, N IV transition probabilities.

The interpretation of stellar spectra assumes the knowledge of atomic data, energy differences for identification, oscillator strengths and cross sections for explaining the spectral intensities.

A group under the direction of M. J. Seaton at University College, London, has completed programs for the calculation of atomic structures, oscillator strengths and collision cross sections for complex atoms. The atomic structure program is essentially based on the work of Condon and Shortley (1935) but the inclusion of configuration interaction is built in as an essential feature. I shall apply some of our first results to solve a puzzle in the spectra of Wolf-Rayet WN stars. If any of you have some particularly pressing needs for oscillator strengths or collision cross sections we shall do our best to provide them.

---

*On an E.S.R.O. Fellowship.

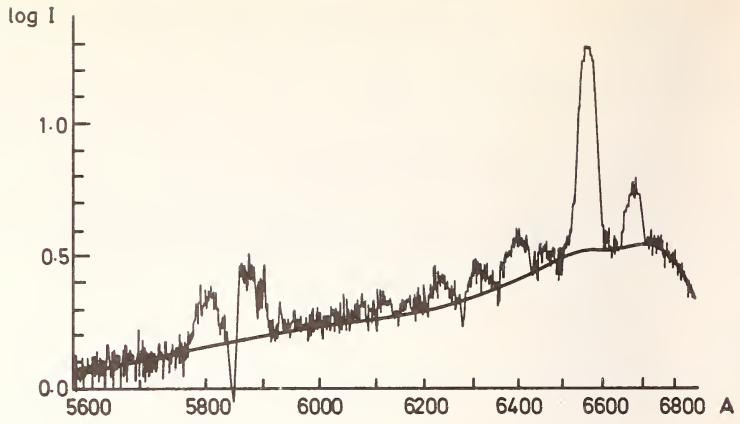

Log I tracing of the spectrum of H.D. 192 163 WN 6

Figure 1.

Figure 1 shows part of the spectrum of HD 192163 WN6, taken by Underhill (1959). The emission feature at λ5810 is usually attributed to C IV. But the case in favor of the attribution to N IV $2p3p\,^3P\text{-}2p3d\,^3P^0$ has again been argued by Hiltner and Schild (1966); this transition gives a line centered at λ5820. Laboratory investigations of N IV by Hallin (1966) have failed to produce that line. Figure 2 shows the allowed transitions from $2p3d\,^3P^0$ with the corresponding transition probabilities. They are from Table 3 of Nussbaumer (1969) where gf values for all the transitions between the 34 lowest levels of N IV have been calculated. The level $2p3d\,^3P^0$ will be depopulated mainly to $2p^2\ ^3P$. But in an extended atmosphere that radiation might be reabsorbed and the relative intensities of $2p^2\ ^3P\text{-}2p3d\,^3P^0$ λ298 and $2p3p\,^3P\text{-}2p3d\,^3P^0$ λ5820 need therefore not be the same in laboratory experiments and in astronomical observations. For this reason the absence of N IV λ5820 in the laboratory cannot be invoked to ban that line from the Wolf-Rayet spectrum.

Figure 2 shows that at λ7413 there is a line with a transition probability three times higher than for N IV λ5820. Swings and Jose (1950) find a faint emission feature at λ7410 of intensity 1 against an intensity of 20 for Hα λ6563. They attribute λ7410 to N III $2s2p3s\,^4P^0\text{-}2s^2\ 4s\ ^2S$. But even if we attribute that emission to the two-elec-

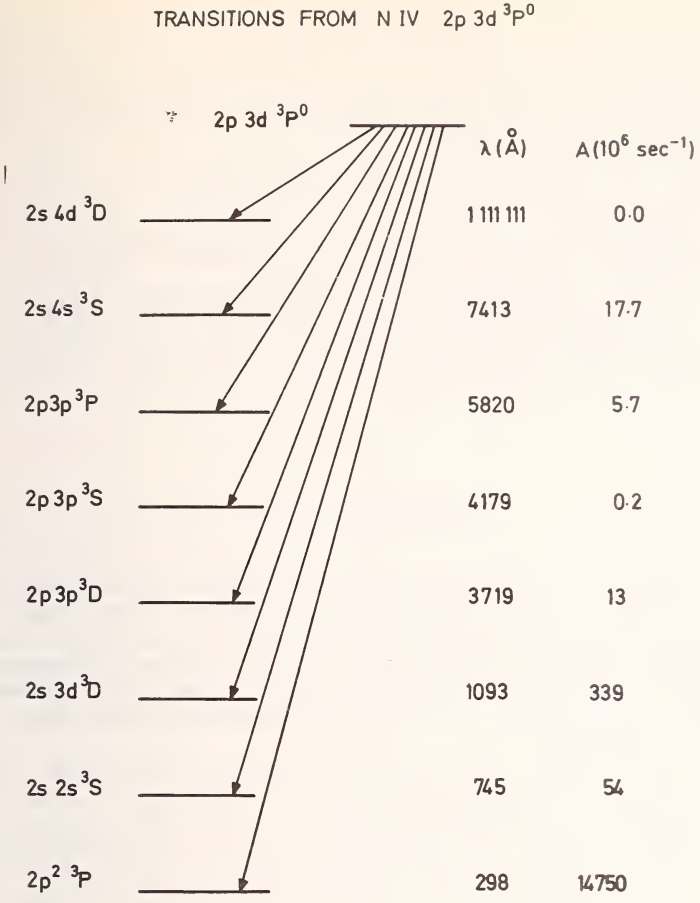

Figure 2.

tron transition 2s4s ^{3}S-2p3d $^3P^0$ it is obvious from the data of Figure 2 that the emission at λ5810 is far too strong to be attributed to N IV 2p3p ^{3}P-2p3d $^3P^0$. I think these arguments based on transitions from a common upper level will finally dispose of the temptation to attribute the emission feature at λ5810 to N IV.

The transition 2s4s ^{3}S-2p3d $^3P^0$ is an example of a two-electron jump; such transitions are naturally accommodated in our approach based on the idea of configuration interaction.

REFERENCES

Condon, E. U., and Shortley, G. H. 1935, *The Theory of Atomic Spectra* (Cambridge: Cambridge University Press).

Hallin, R. 1966, *Ark. Fys.*, 32, 201-211.

Hiltner, W. A., and Schild, R. E. 1966, *Ap. J.*, 143, 770-773.

Nussbaumer, H. 1969, Mon. Not. R. astr. Soc., 145, 141-150.

Swings, P., and Jose, P. D. 1950, *Ap. J.*, 111, 513-529.

Underhill, A. B. 1959, *Pub. Dom. Ap. Obs. Victoria*, 11, 209-234.

DISCUSSION

Trefftz: We have made the same calculation and it would be interesting to compare the results. For Si II we were able to compare our values with those of other authors and we found very large differences for weak and strong lines. The result does depend on the number of transitions, which are included in the calculations.

Nussbaumer: In our calculation all known transitions are included.

Wellmann: May I remind you, that Dr. Nussbaumer asked to know which transition probabilities of astrophysical interest should be calculated. I would like to remind you that the exact calculations of collision cross sections for forbidden lines by Seaton and his group were very important for the determination of electron densities and temperatures in diffuse nebulae. They should be continued.

Underhill: Observations show that the N IV line at λ6200A, which should be much stronger than the λ5820A line, is only a very weak feature. This also leads to the conclusion that the observed emission at λ5810 is not due to N IV.

Swings: Could you calculate gf-values for Fe II lines?

Nussbaumer: I am not sure because Fe II is a very complicated ion.

A SELF-CONSISTENT MODEL ATMOSPHERE PROGRAM WITH APPLICATIONS TO SOLAR 0I RESONANCE LINES

by

R. Grant Athay and Richard C. Canfield*

High Altitude Observatory
National Center for Atmospheric Research
Boulder, Colorado

ABSTRACT

Profiles and total intensities are computed for solar 0I resonance lines at λ1302 and λ1305 using a model atmosphere program that includes non-LTE effects in both hydrogen and oxygen and that includes microturbulence both as a line broadening mechanism and as a contribution to the gas pressure. Good agreement is obtained between computed and observed intensities. The computed profiles appear to have too much self-reversal.

Key words: resonance lines, non-LTE line formation, solar UV lines.

I. INTRODUCTION

The development of adequate methods for computing profiles and intensities of strong stellar lines where non-LTE (local thermodynamic equilibrium) effects are of overriding importance has provided a powerful new means for studying the outer envelopes of extended stellar atmospheres. In principle, at least, such studies are capable of yielding thermodynamic models and the statistical characteristics of the fluid motions at the depths where the lines are formed. In practice, we are barely beginning

*Currently at Utrecht Observatory.

to make use of such methods, partly because we are still developing the diagnostic techniques and partly because we still lack adequate data.

The solar chromosphere provides an excellent proving ground for the development of the diagnostic methods of the non-LTE approach to line formation. Although the thermodynamic and hydrodynamic state of the chromosphere are known only approximately, a few properties of the chromosphere and its adjacent layers are known with relatively high precision. Eclipse data, for example, provide spatially averaged values of the quantity $\langle n_e n_p T^{-3/2} \rangle$, where n_e = electron density, n_p = proton density, and T = electron temperature, that are accurate to about a factor of two in the height range 500 km to 2500 km above the solar limb. It is not known exactly what the "average" refers to, but present evidence indicates that at depths near 500 km the chromosphere is not grossly inhomogeneous. Thus, one may assume that the eclipse value of $\langle n_e n_p T^{-3/2} \rangle$, a quantity we shall subsequently denote by EPT, is representative of the mean chromosphere near 500 km. Above about 1000 km the chromosphere is evidently dominated by inhomogeneities (such as spicules) and the value of EPT is not representative of the mean chromosphere. Below 500 km EPT is not well known.

The known values of EPT near 500 km provide very useful checks on model atmosphere calculations. Additional valuable boundary conditions are provided by photospheric models and coronal models, which are reasonably well known. It seems well established, for example, that in the low corona the electron density is of the order 3×10^8 cm^{-3} and the electron temperature is of the order of 2×10^6 °K. Assuming that $n_p = n_e$, we find that the gas pressure in the low corona is approximately 0.2 dyne cm^{-2}. The gas pressure at a continuum (λ5000) optical depth, τ_o, of 10^{-5}, which corresponds to a geometrical height of about 500 km above the limb, is of the order of 2×10^2 dyne cm^{-2}. Thus, the gas pressure decreases by a factor of only about 10^3 between a height of 500 km in the chromosphere and the base of the corona. Within this same interval T increases from about 6000°K to 2×10^6°K.

In addition to the stronger Fraunhofer lines that are formed in the chromosphere, profiles are available for the Lyman-α and Lyman-β lines of hydrogen and for the C II line at λ1336 (Berger and Bruner[1]) and the OI lines at λ1302 and λ1305 (Bruner and Rense[2]). The OI lines are of interest in that they are formed in the middle chromosphere where the

quantity EPT is reasonably well known.

Oxygen and hydrogen have similar ionization potentials and similar excitation potentials for their respective resonance lines. This leads to the result that the two atomic species ionize at the same depths in the atmosphere. The ionization of hydrogen largely determines both the mean molecular weight in the atmosphere and the electron density and therefore critically influences the model atmosphere. In addition, part of the ionization of 0I is produced by the Lyman continuum radiation of hydrogen. It is necessary, therefore, to solve the ionization equilibrium and Lyman continuum radiative transfer problems for hydrogen in order to compute profiles of the 0I lines.

II. CONSTRUCTION OF SELF-CONSISTENT MODEL CHROMOSPHERES

We propose to compute a model chromosphere using a minimum number of arbitrary parameters, i.e., we maximize the constraints on the model. The constraints exercised are the following:

1. The quantity $n_e n_p T^{-3/2}$ = EPT given by the model must agree within a factor of two with eclipse values derived by Henze[3] in the height range 500-1000 km, and it must not exceed the eclipse values at heights above 1000 km.
2. The gas pressure in the chromosphere must exceed 0.2 dyne cm^{-2}.
3. At height zero, i.e., at the limb as defined by a tangential continuum opacity of unity at $\lambda 5000$, we adopt T = 4600° and a hydrogen density, n_H of 1.6×10^{16}.
4. We assume that the hydrostatic equation

$$dp = - \rho g \, dh \tag{1}$$

is valid and that

$$p = nkT + \frac{1}{3} \zeta^2 \Sigma n_i m_i \quad , \tag{2}$$

where ζ is the microturbulent velocity and n_i and m_i are the number density and mass of particles of type i. The other symbols have their usual meaning. We

adopt a helium:hydrogen number density ratio of 1:10.

5. We require that the flux in the Lyman continuum produced by the model chromosphere be within fifty percent of the value reported by Noyes and Kalkofen[4].

With these constraints there is very little freedom in the temperature model, but there is essentially complete freedom in $\zeta(\tau)$.

Equation (2) may be rewritten in the form

$$p = nkT\ F \tag{3}$$

where

$$F = 1 + \frac{\zeta^2 \sum_i n_i m_i}{3nkT} \quad . \tag{4}$$

Also, we may write

$$\rho = 1.4\ n_H m_H \quad , \tag{5}$$

$$n = 1.1\ n_H + n_e \quad , \tag{6}$$

and

$$I = \frac{n_H}{n_H + n_e} \quad , \tag{7}$$

where n_H is the number of neutral hydrogen atoms plus protons and m_H is the hydrogen mass. Equations (1) and (3) then yield

$$d\ell n\ (1.1\ n_H + n_e) = -\ d\ell n\ T - \frac{1.4\ m_H\ g\ I}{k\ F\ T\ (1+0.1I)}\ dh \quad . \tag{8}$$

The ionization parameter I has limits $0.5 \leq I \leq 1$ and can be determined for a given model atmosphere only by solving the radiative transfer equations for the Lyman continuum. The transfer solutions depend upon n_e and n_H as well as T_e. Thus, we must proceed iteratively to find a self-consistent solution. We start by assuming T(h), F(h) and I(h). We then solve equation (8) to obtain preliminary

values of $n_H(h)$ and $n_e(h)$. We use these initial values, denoted by $n_H(1)$ and $n_e(1)$ to obtain initial values of all collision and recombination rates and initial values of τ in the Lyman continuum. Since τ depends upon n_1, the ground state population, and n_1 depends upon τ through the transfer equation, the transfer equation must be solved iteratively with n_1 to obtain consistent values of $n_1(1)$ and τ. The converged values of $n_1(1)$ are then combined with $n_H(1)$ to give $n_e(1')$ and $I(2)$. From $I(2)$ we obtain $n_H(2)$ and $n_e(2)$ from equation (8) and repeat the iteration on τ and n_1. This double iterative procedure is continued until final convergence is achieved for τ, n_H, n_1 and n_e.

For an arbitrary choice of $T(h)$ and $F(h)$, we do not satisfy the constraints (1), (2) and (5). Hence, for a given $F(h)$, we must adjust $T(h)$ until the constraints are satisfied. Each change in either $T(h)$ or $F(h)$ requires a new iterative solution for n_H, n_1 and n_e.

We have constructed by this technique twelve self-consistent model atmospheres. Most of the ionization of hydrogen occurs in the regions where Lyman continuum transfer is important and where the Lyman lines are in radiative detailed balance. Hence, it is not essential to consider the transfer problem in the Lyman lines. Furthermore, most of the ionizations in hydrogen occur from the n_2 level, which is populated mainly from the n_1 level, and a fairly accurate solution is obtained using a model atom with two bound energy levels plus a continuum.

III. LYMAN CONTINUUM TRANSFER SOLUTIONS

In treating the Lyman continuum problem we make the following simplifying assumptions: (1) There is no opacity other than Lyman continuum opacity from $\lambda 912$ to approximately $\lambda 450$. (2) Stimulated emissions may be ignored. (3) Lyman-α is in radiative detailed balance, and we ignore bound levels above n=2. (4) The scattering is non-coherent.

It is convenient to work with the b_n parameters rather than energy level populations. The Lyman continuum source function for the problem we are considering is

$$S_\nu = \frac{2h\nu^3}{c^2} \frac{e^{-h\nu/kt}}{b_1} . \qquad (9)$$

The only unknown in this equation is b_1 . We could, therefore, formulate the problem in such a way as to solve for b_1^{-1} or the product of b_1^{-1} and any known function. For convenience, we define a dimensionless frequency parameter y such that

$$y = \frac{\nu}{\nu_1} \tag{10}$$

where ν_1 is the frequency at the Lyman limit. We may then write

$$S_y = y^3 \exp - [h\nu_1(y-1)/kT]\ S_1, \tag{11}$$

where

$$S_1 = \frac{2h\nu_1^3}{c^2}\ \frac{e^{-h\nu_1/kT}}{b_1} \quad . \tag{12}$$

This divides S_y into two factors, one frequency dependent and one frequency independent. We shall formulate the transfer equation to solve for the frequency independent term, S_1.

It follows from the equations of statistical equilibrium and from the frequency dependence of the photoionization cross section for hydrogen that

$$S = \frac{\frac{e^{-h\nu_1/kT}}{E_1}\int_1^\infty \frac{J_y}{y^4}\,dy + \varepsilon^* B_1}{1 + \varepsilon^\dagger} \quad , \tag{13}$$

where

$$E_1 = \int_{\nu_1}^{\infty} \frac{e^{-h\nu/kT}}{\nu}\,d\nu \ , \tag{14}$$

J_y = mean intensity,

B_1 = Planck function at y = 1 ,

$$\varepsilon^* = \varepsilon + \frac{R_{12}\, R_{2C}}{W_C A_{C1} R_{22}} \quad , \tag{15}$$

$$\varepsilon^\dagger = \varepsilon + \frac{R_{21}\, R_{C2}}{W_C A_{C1} R_{22}} \quad , \tag{16}$$

$$\varepsilon = \frac{C_{C1}}{A_{C1}} = \frac{\text{collisional recombination rate}}{\text{radiative recombination rate}} \quad ,$$

$$R_{ij} = W_i P_{ij} = \tilde{\omega}_i e^{-h\nu_i/kT} P_{ij} \quad ,$$

$\tilde{\omega}_i$ = statistical weight of level i,

$h\nu_i$ = energy of level i measured from the ground state,

P_{ij} = transition rate i to j,

P_{ii} = sum of all rates out of level i.

We write the transfer equation in the flux derivative form

$$\frac{dH_y}{d\tau_y} = J_y - S_y \tag{17}$$

and eliminate the term in J_y from equations (17) and (13). From equation (17), we have

$$\frac{e^{-h\nu_1/kT}}{E_1} \int_1^\infty \frac{J_y}{y^4}\, dy = \frac{e^{-h\nu_1/kT}}{E_1} \int_1^\infty \frac{1}{y^4} \frac{dH_y}{d\tau_y}\, dy + S_1 \quad . \tag{18}$$

It follows from equation (13) that

$$S_1 = \frac{\varepsilon^* B_1}{\varepsilon^\dagger} + \frac{e^{-h\nu_1/kT}}{\varepsilon^\dagger E_1} \int_1^\infty \frac{1}{y^4} \frac{dH_y}{d\tau_y} \, dy \ . \tag{19}$$

In symbolic form, equation (17) gives

$$\frac{dH_y}{d\tau_y} = J_y - S_y = (\Lambda - I)S_y \quad , \tag{20}$$

where Λ is the mean intensity operator and I is the unit operator. Using equation (11), we may rewrite equation (20) as

$$\frac{dH_y}{d\tau_y} = y^3 \left\{ (\Lambda - I) \exp - \left[h\nu_1 (y-1)/kT \right] \right\} S_1 \tag{21}$$

$$= y^3 \, \Phi \, (y,\tau) \, S_1 \ . \tag{22}$$

Thus, we have finally

$$S_1 = \frac{\varepsilon^* B_1}{\varepsilon^\dagger} + \frac{e^{-h\nu_1/kT}}{\varepsilon^\dagger E_1} \int_1^\infty y^{-1} \, \Phi \, (y,\tau) S_1 \, dy \ . \tag{23}$$

This equation is solved by the method of Athay and Skumanich[5] by writing

$$S_1 = (1 - \alpha)^{-1} \frac{\varepsilon^* B_1}{\varepsilon^\dagger} \quad , \tag{24}$$

where α is a matrix operator defined by

$$\alpha = \frac{e^{-h\nu_1/kT}}{\varepsilon^\dagger E_1} \int_1^\infty y^{-1} \, \Phi \, (y,\tau) \, dy. \tag{25}$$

The y and τ spaces are discretized into 9 points in y between y = 1 and y = 2 and 42 points in τ. We have tried increasing the number of y points and increasing the range in y to y = 3. Neither change produces significant changes in S_1.

The iterative process of solving equations (8) and (25) to obtain self-consistent solutions for a given T(h) and F(h) generally requires 13 iterations. The complete program requires approximately 3 minutes on a CDC 6600. The solutions appear to be very stable even when large gradients in T(h) and F(h) are introduced.

The assumption that Lyman-α is in detailed balance is not necessary of course. The problem could be solved by including transfer solutions in Lyman-α, but trial calculations showed that this greatly increases the number of iterations required and did not result in any important changes in the model atmosphere for the region of interest for the 0I lines.

IV. CHARACTERISTICS OF MODELS

Constraint (1) from Section II effectively fixes T(h) between 500 and 1000 km subject somewhat to the assumed form of F(h). However, it follows from equation (4) that the ratio of ζ to the mean thermal velocity of hydrogen atoms is given by

$$\frac{\zeta}{V(H)} = 1.04\ (F-1)^{1/2}\ (1.1 + \frac{n_e}{n_H})^{1/2} \quad . \qquad (26)$$

Thus, if $n_e/n_H \ll 1$, $\zeta/V(H) = .5$ for $F \approx 1.2$ and $\zeta/V(H) = .75$ for $F \approx 1.5$. In the low chromosphere ζ is a few km/sec at most, and F is therefore close to unity. In the mid-chromosphere even if we want $\zeta \approx 10$ km/sec, which is larger than required for the 0I lines, we need only $F \approx 1.5$. In practice, therefore, we cannot change F(h) very much without introducing unreasonable values of ζ.

Between heights of zero and 500 km we have adopted a rather arbitrary model for T(h) and we have set F = 1. The T(h) model has a slow rise in T to 4700°K at 200 km followed by a more rapid rise to 5200°K at 400 km and $\approx$ 5600°K at 500 km. The

value of T at 500 km is dictated by the eclipse value of $n_e\ n_p\ T^{-3/2}$ at that height. It would make little difference to the model at 500 km and higher if, for example, we decreased T to 4000°K at 200 km followed by a rapid rise to $\approx$ 5600°K at 500 km. This would effectively change the density scale height by about 20 percent for one scale height and would result in a small density decrease at 500 km. The constraints we have set on the model do not, therefore, lead to any practical restrictions on the temperature minimum region.

Between 500 km and 1000 km constraint (1) imposes a gradual rise in T to $\approx$ 6200° at 1000 km (cf. Athay[6]). If T is constant in this height interval the computed values of EPT decreases much too rapidly with height. If T increases only somewhat more rapidly than indicated EPT increases with height.

The reason for the strong sensitivity to T in the height interval 500-1000 km results from the fact that hydrogen is still only partially ionized. In fact at 1000 km hydrogen is only about 2 percent ionized. The ionization does not reach the 50 percent level until T reaches about 8000°K. This again means that constraint (1) limits the kinds of models that may be considered. A rapid increase of T with height cannot be permitted in a model of the mean chromosphere at depths where T $\lesssim$ 8000° without introducing an increase in EPT with height, which is unacceptable.

At 1000 km the gas pressure in the chromosphere is approximately 7 dyne cm^{-2}. Therefore, constraint (2) becomes very important in determining the nature of the model at heights above 1000 km. The gas pressure cannot fall by more than a factor of 40 before the coronal temperature rise occurs, and a sharp temperature rise cannot occur until T $\gtrsim$ 8000°. This requires that T continue to rise rather gradually until it reaches about 8000°.

We have somewhat arbitrarily adopted a T(h) distribution above 1000 km that gives $d \log_{10} T/dh \approx 10^{-9}$ cm^{-1} up to T $\approx$ 7200°. This is the same gradient that exists between 500 and 1000 km, and is about the maximum gradient allowed by EPT. The value T = 7200° is reached at approximately 1600 km and the gas pressure has decreased to about 0.5 dyne cm^{-2}. If we continued increasing T at this same rate, the gas pressure would reach 0.2 dyne cm^{-2} before T reached 8000°. It is necessary, therefore, to steepen the gradient in T between 7200° and 8000°. Hydrogen is sufficiently ionized at 7200° to permit

a steepening of the temperature gradient without making EPT too large. The larger T becomes the more the gradient may be steepened.

Restrictions on d $\log_{10}$ T/dh are also imposed by constraint (5) - the observed Lyman continuum intensity. The type of model under consideration tends to give too much flux in the Lyman continuum. Steepening the temperature gradient between T = 7500° and T = 10000° reduces the Lyman continuum flux to within the limits set by constraint (5).

A model that satisfies all of the constraints in Section II is given in Table 1. It is possible to construct a family of such models with different assumed values for F(h). Such models differ from one another primarily in the height at which the sharp temperature rise occurs. The differences amount to only a few hundred kilometers, however, even for relatively large changes in ζ.

A total of 12 models were tested by comparing computed and observed profiles for the 0I lines. Each of the 12 models gave Lyman continuum intensities within a few percent of the observed values and each gave total intensities in the 0I lines that agreed within a factor of two with the intensities observed by Hinteregger[7]. The model in Table 1 gave the best agreement with the 0I profiles. Details of the oxygen calculations are discussed in the following sections.

V. OXYGEN TRANSFER SOLUTIONS

Source functions for the resonance lines of 0I are computed using the technique described by Athay and Canfield[8] for the Mg b and Na D lines. The 0I transitions occur between $2p^4\ ^3P$ and $3s^3S^o$. There appears to be no interlocking transitions of importance other than transitions to and from the continuum. This conclusion was reached after trial calculations that included $3s^5S^0$, $3p^5P^o$ and $3p^3P$ levels showed that the source functions for the resonance triplet were essentially the same as when these levels were omitted.

Both ionization and recombination occur mainly from and to the ground state, $2p^4\ ^3P$. Also, the ground state serves as the primary source of electrons for the $3s^3S^o$ level. This accounts for the lack of important interlocking levels.

Photoionization rates from the $2p^4\ ^3P$ level are computed using the Lyman continuum intensities computed for the model atmosphere and photoionization

TABLE 1

MODEL CHROMOSPHERE

Height (km)	T	log n_H	log n_p	log n_e	log n_2	b_1	b_2	log P	F	ζ (km/sec)
0	4600	16.20	10.56	12.20	5.61	.24	.24	4.04	1.0	0
200	4700	15.42	10.73	11.49	5.06	.30	.30	3.28	1.0	0
400	5200	14.62	11.20	11.32	5.32	.73	.73	2.52	1.0	0
550	5700	14.08	11.42	11.45	5.65	1.5	1.5	2.00	1.0	0
700	5900	13.63	11.36	11.36	5.50	2.0	2.0	1.59	1.1	3.5
1000	6250	12.84	11.23	11.23	5.20	3.1	3.1	.83	1.15	4.5
1200	6500	12.38	11.14	11.14	5.04	4.0	4.0	.40	1.2	5.3
1500	7000	11.74	11.08	11.08	4.89	6.4	6.7	-.23	1.3	7.1
17 0	7600	11.23	10.88	10.88	4.49	22	11	-.57	1.3	8.0
1935	8400	10.97	10.66	10.66	4.04	260	21	-.70	1.3	8.6
1975	9250	10.87	10.59	10.59	3.92	1900	40	-.82	1.3	9.1
1983	10400	10.79	10.59	10.59	3.98	1.1×10^4	97	-.82	1.3	10
1998	14900	10.54	10.52	10.52	4.00	1.7×10^5	700	-.82	1.3	13
2007	20200	10.40	10.40	10.40	3.65	6.6×10^5	1800	-.82	1.3	15

cross sections measured by Cairnes and Samson[9]. For the $3s\,^3S^o$ photoionization rates we use a cross section equal to $.19\pi a_o^2\ (\nu_o/\nu)^3$ obtained from the Burgess and Seaton[10] quantum defect method together with quantum defects computed by Peach[11]. We use a solar radiation temperature of 5350° to give the mean intensity for photoionization.

Transition probabilities for the resonance triplet are obtained from Σ gf = .19 as given by Parkes, Keyser, and Kaufman[12]. Electron collisional excitation cross sections, Q_{ij}, are not well known for 0I. We adopt a mean value of $Q = .1\pi a_o^2$ for each of the resonance transitions (cf. Stauffer and McDowell[13]). However, we vary this Q to ascertain its effect upon the 0I lines. For transitions between J substates of $2p^4\ ^3P$ we use $Q = 10\pi a_o^2$. Collisional ionization rates are unimportant. However, we use $Q = .15\pi a_o^2$ for ionizations from $2p^4\ ^3P$ and $Q = 7.5\pi a_o^2$ for ionizations from $3s\ ^3S^o$.

The source functions for the triplet are evaluated iteratively. Stimulated emissions are ignored and the scattering is assumed to be non-coherent. We adopt an oxygen abundance of 6×10^{-4}.

The three members of the 0I triplet appear to be of about equal intensity, .01 ergs cm^{-2} sec^{-1} at the orbit of earth (Hinteregger[7]). Assuming that the intensity is relatively uniform across the solar disk, we find a flux at the center of the solar disk of approximately 35 ergs cm^{-2} sec^{-1} $ster^{-1}$.

Computed intensities of the 0I lines are sensitive to the model atmosphere, to the oxygen abundance, to the gf values, and to line broadening parameters. However, they are not particularly sensitive to the collisional excitation cross section. For example, an increase in Q by a factor of four for each of the triplet lines increases the line intensity by a factor of approximately 1.5 only (see Table 2).

The chromosphere is effectively thick in the 0I triplet and the line intensities are proportional to the product of the degradation length, τ_{deg}, and the mean source term for photon generation $\langle\varepsilon^*B\rangle$ in the layer $0 \leq \tau \leq \tau_{deg}$. An increase in the collisional excitation cross section increases ε^* and decreases τ_{deg}. The two effects nearly cancel.

The line broadening parameters affect τ_{deg}, and hence the line intensities. We have used a Voigt profile with both radiation and collision damping. Since the cross section for collision damping is not accurately known, we pick a value for the collision damping half width that gives best agreement with

TABLE 2

LINE FLUXES (ergs sec^{-1} cm^{-2} $ster^{-1}$) AND RATIOS OF PEAK INTENSITY TO CENTRAL INTENSITY FOR λ1302 AND λ1305

line		λ1302		λ1305	
Q	VW	Flux	Peak:Center	Flux	Peak:Center
	1	17	2.6	16	2.3
.1	3	24	2.7	22	2.2
	10	39	3.1	37	2.7
	1	25	2.2	23	2.1
.4	10	60	2.5	56	2.2
	30	41	2.4	40	2.6

the observed profile. The adopted form for the half width in angstroms is $6.4 \times 10^{-21} n_H$ (VW) where the parameter VW may take on different values. The value of VW affects the intensity of the line as well as its profile. Intensities of the λ1302 and λ1305 members of the multiplet are given in Table 2 as a function of VW and the electron excitation cross section Q. The intensities would be influenced also by changes in the gf values.

The shapes of the wings of the lines depend upon the damping parameters and can be fitted reasonably well by adjusting VW. The shapes of the Doppler cores of the lines depend upon both the magnitude and gradient of ζ. In general, the computed profiles show strong self reversal whereas the observed profiles show weak self-reversal. The amount of self-reversal in the computed profiles decreases as $d\zeta/dh$ is increased. However, it does not appear to be possible to obtain complete agreement between observed and computed profiles without excessively large values of $d\zeta/dh$. The self-reversal is not markedly sensitive to either the collision damping or the collisional excitation cross section as evidenced by the ratios of peak intensity to central intensity given in Table 2.

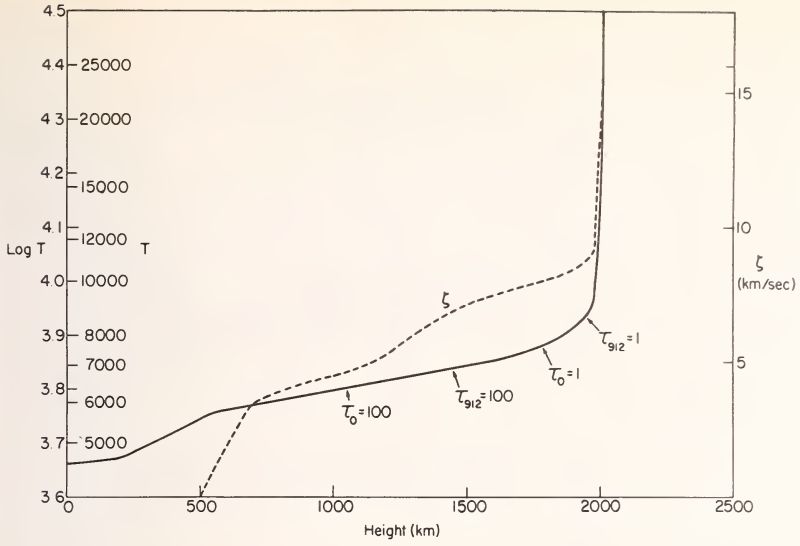

Figure 1. A temperature model deduced from the constraints in Section IV and a $\zeta(h)$ model that gives best agreement with the position of peak intensity and the ratio of peak intensity to central intensity in the 0I lines. The optical depth at the center of λ1305 is indicated by τ_0, and the optical depth at the head of the Lyman continuum is indicated by τ_{912}.

Figure 1 exhibits $\zeta(h)$ and $T(h)$ from Table 1. Figure 2 exhibits the λ1305 profile computed from the model in Table 1 for three values of VW together with an observed profile. The observed profile shown is reduced from observations by Bruner and Rense[2]. Improved observations have been made with increased spectral resolution and are in process of reduction at the time of this writing. It does not appear that the improved profiles will differ greatly from the one shown. The source function for the λ1305 line and the non-LTE departure coefficients for the ground state, b_1, and the 3s $^3S^o$ level, b_3, are shown in Figure 3. A more complete tabulation of the 0I calculations is given in Table 3. The adopted collision cross section between different J states in the ground level is sufficiently large to give relative populations that conform very nearly to a Boltzmann distribution.

Although the computed and observed profiles do not show good agreement near line center there are several possible explanations. The sharp emission

TABLE 3

OXYGEN CALCULATIONS

Height (km)	τ_o(1305)	S(1305)	S(1302)	log n ($2p^4\ ^3P$,J=1)	log n ($3s\ ^3S^o$)	b ($2p^4\ ^3P$,J=1)	b ($3s\ ^3S^o$)
0	1×10^5	1.4×10^{-11}	1.4×10^{-11}	11.91	1.80	.27	.43
200	3.2×10^4	3.0	3.0	11.43	1.65	.32	.65
400	6.1×10^3	31	30	10.63	1.75	.88	1.26
550	8.2×10^2	82	82	9.74	1.40	2.2	1.33
700	5.0×10^2	89	89	9.47	1.14	2.5	1.20
1000	1.5×10^2	91	90	8.94	.65	3.4	.80
1200	79	86	86	8.77	.45	3.6	.57
1500	19	58	64	8.30	-.16	4.6	.24
1770	6.0	32	35	7.77	-.96	6.9	.089
1935	1.6	18	19	7.40	-1.60	14	.043
1975	.41	12	11	6.97	-2.22	80	.050
1983	.067	9.0	8.4	6.83	-2.48	790	.11
1998	.013	13	13	6.56	-2.56	9.8×10^4	.84
2007	.0043	35×10^{-11}	35×10^{-11}	6.34	-2.37	1.7×10^6	5.6

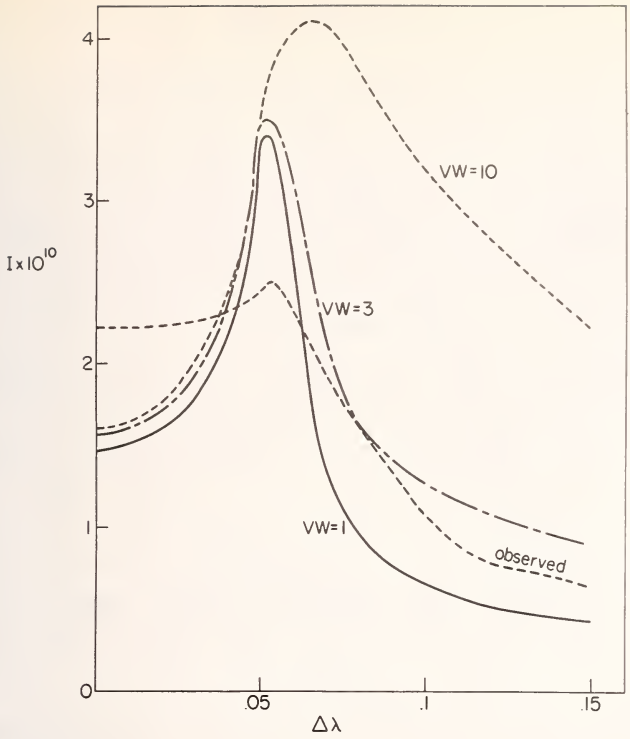

Figure 2. Comparison of observed λ1305 profile (preliminary reduction, see text for explanation) and computed profiles for VW = 1, 3 and 10.

peak in the computed profiles at the edge of the Doppler core has a width of the same order as the instrumental resolution and is perhaps partially "lost" in the observed profile. Also, macroturbulence and atmospheric inhomogenieties may substantially alter the "average" profile observed with low spatial resolution.

The tendency for non-LTE source functions to give central intensities that are somewhat lower than observed appears to be a common difficulty. In computations of Mg II and Ca II profiles (Athay and Skumanich[14]) and Na D profiles (Athay and Canfield[8]) it has been necessary to resort to rather large values of $d\zeta/dh$ in order to obtain central intensities as large as those observed. Broadly speaking, the values of ζ in Table 1 and Figure 1 are consistent with values obtained from the Ca II and Na D lines. The 0I lines are formed

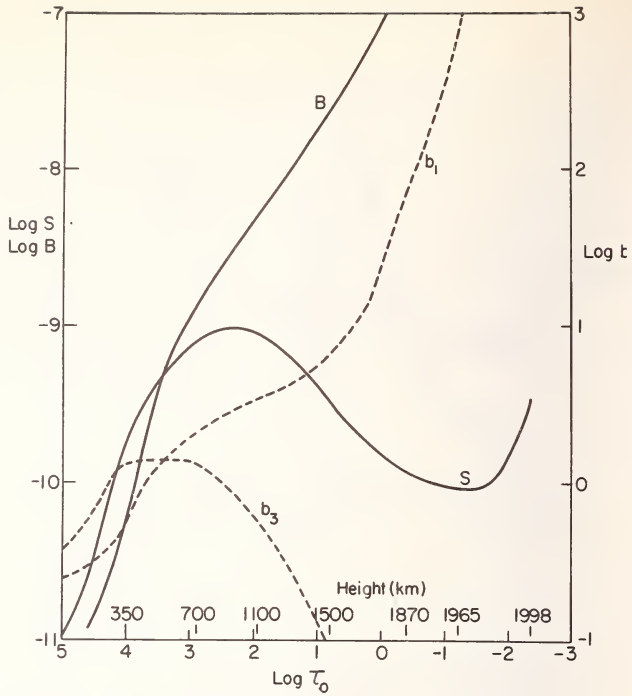

Figure 3. Source function and non-LTE departure coefficients for λ1305. Source functions for the other two members of the triplet are closely equal to the λ1305 source function (see Table 3).

somewhat higher than the Ca II lines, but the Doppler cores of these lines are strongly overlapped in their depths of formation. It should be possible to combine analyses of the Na D, Ca II, Mg II, and 0I lines to obtain a single $\zeta(h)$ model provided the concept of a spherically symmetric chromosphere has a valid meaning in this context at the depths where the lines are formed. Additional help will come from analysis of C II profiles recently observed by Berger and Bruner[1].

The authors are indebted to W. Frye for most of the programming and computing and especially to W. A. Rense and E. Bruner for allowing them the use of the 0I profiles prior to publication.

REFERENCES

1. R. A. Berger and E. C. Bruner, Jr. 1969, *Ap. J.* 155, L115.
2. E. C. Bruner, Jr., and W. A. Rense 1969, *Ap. J.*, in press.
3. W. B. Henze 1968, Thesis, Univ. of Colorado, Boulder (also Solar Physics, in press).
4. R. W. Noyes and W. Kalkofen 1969, Paper presented at Solar Physics Meeting of AAS, Pasadena.
5. R. G. Athay and A. Skumanich 1967, *Ann. d'Ap.* 30, 669.
6. R. G. Athay 1969, *Solar Physics*, in press.
7. H. E. Hinteregger 1965, *The Solar Spectrum*, Ed. C. de Jager (Reidel: Dordrecht), 179.
8. R. G. Athay and R. C. Canfield 1969, *Ap. J.* 156, 000.
9. R. B. Cairnes and J. A. R. Samson 1965, *Phys. Rev.* 139, A1403.
10. A. Burgess and M. Seaton, 1960 *M.N.* 120, 121.
11. G. Peach 1962, *M.N.* 124, 371.
12. D. A. Parkes, L. F. Keyser and F. Kaufman 1967, *Ap. J.* 149, 217.
13. A. D. Stauffer and M. R. C. McDowell 1966, *Proc. Phys. Soc. Lon.* 89, 289.
14. R. G. Athay and A. Skumanich 1968, *Solar Physics* 3, 181.

DISCUSSION

Thomas: You find a very steep temperature rise for $\tau_{912} = 1$. How is the fit of other observation such as the Balmer and Paschen jump? Can you explain the observed helium lines? Also, I worry at your neglect of Hα in solving the LyC transfer problem. Including it, as I did in the chromosphere book we wrote, will raise b_1, b_2, T_e, dT_e/dh if that solution is a guide.

Athay: If I change the microturbulence and the pressure gradient I shall get the increase of temperature at smaller heights and the observations fit very well. The helium lines can be explained if you take an asymmetric atmosphere.

Mugglestone: Are your results very sensitive to the dependence of microturbulence with height?

Athay: The increase of turbulence has different effects. It makes the line broader, increases the

central intensity, and it decreases the intensity of the emission. The observed relation of emission to absorption is 2:1.

Underhill: The resolution of the observed spectra is low, of the order of 20 or 5A.

Athay: There are new observations with a resolution of 0.015A (Bruner and Rense Ap. J. 157, 417, 1969). But even with this resolution you cannot observe the reversal in the line center with sufficient accuracy. We do find similar problems with reversal in the line centers for Lyα, Ca II K and Na I D lines.

Kalkofen: What about Lyβ?

Athay: Lyβ is very weak. The Ly-continuum is strong, approximately 10 times the intensity of Lyα; Lyβ has only 1% of the intensity of Lyα.

Kalkofen: Did you test your theory with observed lines of high excitation and with the observed center to limb variations?

Athay: We find agreement within a few percent with the observed limb darkening and limb brightening.

Wellmann: If one observes OI lines in stellar spectra and can do a temperature determination with these lines, can you say in which layer the lines are formed?

Athay: No.

PART B

THEORETICAL METHODS FOR HANDLING NON-LTE PROBLEMS

Chairmen: R. N. Thomas, A. G. Hearn

THEORETICAL METHODS OF TREATING LINE FORMATION PROBLEMS IN STEADY-STATE EXTENDED ATMOSPHERES

by

George B. Rybicki

Smithsonian Astrophysical Observatory
Cambridge, Massachusetts

ABSTRACT

Theoretical methods applicable to the study of line formation in steady-state extended atmospheres are reviewed. The formal solution of the transfer equation is considered, as well as numerical and analytical methods of determining the source function. Topics discussed include: the local frequency transformation, geometrical effects, and the case of large velocity gradients. A new plane-parallel approximation for spherically symmetric moving atmospheres is given that takes account of transverse velocity gradients.

Key words: spectral line formation, spherical geometry, radiative transfer, stellar atmospheres, moving atmospheres.

INTRODUCTION

Methods of handling line formation problems have advanced markedly in recent years for atmospheres that are static and for which the plane-parallel approximation is reasonably valid. However, two major difficulties may arise when extended atmospheres are considered: first, the geometrical extension may be so large that the plane-parallel approximation is no longer valid; and second, macroscopic velocity fields may need to be taken into account. While only the first of these is strictly implied by the term "extended atmosphere," the second is included because so many of the

astronomical examples of extended atmospheres have such macroscopic velocity fields.

In this paper the theoretical work relating to these two difficulties will be reviewed. In doing so primary consideration has been given to work in the spirit of the modern approach (see, e.g. Jefferies, 1968) to line formation, in which the equations of statistical equilibrium are solved in conjunction with the transfer equations. Many of the results of the early work that depend on the assumption of coherent scattering, for example, must be viewed with suspicion for the problem of line formation. However, many of the methods and techniques developed in these papers are relevant, and it has been the intention here to extract such useful information whenever possible.

After introducing the basic equations, the formal solution of the transfer equation will be discussed. Then analytical and numerical methods of determining the source function will be considered, including Sobolev's theory of moving atmospheres.

One new result presented here is a formulation of the plane-parallel approximation for moving atmospheres having spherical symmetry that takes account of transverse velocity gradients.

BASIC EQUATIONS

The line formation problem is defined by the simultaneous solution of the equations of statistical equilibrium and the transfer equations for the atom or ion under consideration. The assumption of complete redistribution is usually made to account for the noncoherent nature of the scattering. While this assumption has proved of great utility in static, plane-parallel atmospheres, there are reasons to believe that it may not be as good when large velocity gradients are present. This is because the mechanism of trapping radiation, which usually produces isotropic, frequency independent intensities in the line core, will not operate so effectively, since radiation can escape more readily and because of the anisotropy introduced by non-uniform expansion. The only work relating to this point is Magnan's (1968). He found only fairly small errors due to the complete redistribution assumption in an atmosphere with velocities of the same order as

the Doppler velocity. However, the question deserves further investigation under a variety of conditions before any final conclusions can be drawn. In this paper complete redistribution will be assumed, and the modifications necessary to treat Doppler redistribution will merely be indicated.

The effect of extended geometry on the equations of statistical equilibrium is simply to make all quantities depend on a general spatial point $\underset{\sim}{r}$, instead of the simple height or optical depth variable of the plane-parallel case. The transfer equations must be similarly modified by considering specific intensities which are functions of position $\underset{\sim}{r}$, frequency ν, and direction defined by a unit vector $\underset{\sim}{\ell}$. In geometries having certain symmetries, such as spherical symmetry, the equations may depend on fewer variables, of course, and in the limit of a thin spherically symmetric shell, the plane-parallel equations are recovered. With few exceptions (e.g., Bappu and Menzel, 1954) all of the work done on the problem of extended geometries has assumed spherical symmetry. In cases where Sobolev's theory of moving atmospheres is applicable it is not strictly bound by any particular assumption on the geometry, but in the actual applications of this theory spherical or plane-parallel geometry have been used.

The primary effect of velocity gradients is the Doppler shift of the radiation field as seen in a local frame of reference moving with the material at any point. This manifests itself in those terms in the equations accounting for the interaction between matter and radiation, namely, in the emission and absorption coefficients. For complete redistribution, where the source function is frequency independent, the modification to the usual equations is simply to replace the absorption profile $\phi(\underset{\sim}{r},\nu)$ by $\phi(\underset{\sim}{r},\underset{\sim}{\ell},\nu) = \phi(\underset{\sim}{r},\nu - \frac{\nu_o}{c}\,\underset{\sim}{\ell}\cdot\underset{\sim}{v}(\underset{\sim}{r}))$, where ν_o is the line center frequency, $\underset{\sim}{v}(\underset{\sim}{r})$ is the velocity of the material at point $\underset{\sim}{r}$, and c is the velocity of light. This correctly describes the Doppler effect to lowest order in v/c. For the radiation field this effect is important because it can radically change optical depth relations along a ray, as the absorption at any point depends sensitively on any displacement of the profile. Similarly the matter can be brought to quite different states of excitation by motion which causes it to absorb far more or far less in any transition, as it absorbs in different parts of the highly frequency-dependent radiation field.

A secondary effect of velocity fields is to add streaming terms to the statistical equilibrium equations, which describe the changes to the populations from convective transport of material. Although this might be an important effect in some physical situations, it would not seem that it will be so for any stars discussed here. This may be seen by considering an extreme physical example with velocities on the order of 10^3 km s^{-1} and a characteristic length of 10^6 km, which are typical for some Wolf-Rayet stars. This leads to an effective rate coefficient or order 10^{-3} s^{-1} which is very small compared with other typical rate coefficients entering the statistical equilibrium equations. Therefore this effect will be neglected here.

The equations of statistical equilibrium are statements that the populations $n_i(\underset{\sim}{r})$ at a point corresponding to the various relevant levels of excitation energy E_i are independent of time

$$0 = \sum_j (n_j \Gamma_{ji} - n_i \Gamma_{ij}) \quad . \tag{1}$$

Typically i ranges from 1 to N for N bound levels, with the addition of values for adjacent stages of ionization.

The rate coefficients Γ_{ij} may be separated into rate coefficients due to radiation and to collision with other particles (probably mainly electrons, but perhaps high energy protons or alpha particles may contribute)

$$\Gamma_{ij} = R_{ij} + C_{ij} \quad , \tag{2}$$

For the radiative transitions between bound levels,

$$R_{ij} = A_{ij} + B_{ij} \bar{J}_{ij} \quad ,$$

$$E_i > E_j$$

$$R_{ji} = B_{ji} \bar{J}_{ij} \quad , \tag{3}$$

where the A's and B's are the Milne form of the Einstein coefficients and

$$\bar{J}_{ij} = \frac{1}{4\pi} \int_0^\infty d\nu \int d\underset{\sim}{\ell}\, \phi(\underset{\sim}{r}, \nu - \frac{\nu_{ij}}{c}\, \underset{\sim}{\ell}\cdot\underset{\sim}{v}(\underset{\sim}{r}))\; I_\nu(\underset{\sim}{r}, \underset{\sim}{\ell}) \quad . (4)$$

Here $I_\nu(\underset{\sim}{r}, \underset{\sim}{\ell})$ is the specific intensity of radiation at frequency ν at point $\underset{\sim}{r}$ in direction $\underset{\sim}{\ell}$. The normalized profile function is defined by

$$\phi(\underset{\sim}{r}, \nu) = k_\nu^{(\ell)}(\underset{\sim}{r}) / k_\ell(\underset{\sim}{r}) \quad , \qquad (5)$$

where $k_\nu^{(\ell)}$ is the line opacity for the transition $i \to j$, in the rest frame of the material, and where the integrated line opacity k_ℓ is

$$k_\ell(\underset{\sim}{r}) = \int_0^\infty k_\nu^{(\ell)}(\underset{\sim}{r})\, d\nu \quad . \qquad (6)$$

Thus

$$\int_0^\infty (\underset{\sim}{r}, \nu)\, d\nu = 1 \quad . \qquad (7)$$

The line center frequency ν_{ij} is computed from

$$h\nu_{ij} = E_i - E_j \qquad (8)$$

h being Planck's constant.

The appearance of the velocity field in the profile function in Eq. (4) is responsible for the velocity effects associated with the equations of statistical equilibrium. It should be noted that the profile function cannot now be taken outside of the angular integration, as in the static case.

The equation of transfer for radiation in the line transition i→j is

$$\underset{\sim}{\ell} \cdot \frac{\partial}{\partial \underset{\sim}{r}} I_\nu(\underset{\sim}{r},\underset{\sim}{\ell}) = k_\ell(\underset{\sim}{r})\ \phi(\underset{\sim}{r},\nu - \frac{\nu_{ij}}{c}\ \underset{\sim}{\ell}\cdot\underset{\sim}{v}(\underset{\sim}{r}))\left[- I_\nu(\underset{\sim}{r},\underset{\sim}{\ell}) + S(\underset{\sim}{r})\right] + k_c(\underset{\sim}{r})\left[- I_\nu(\underset{\sim}{r},\underset{\sim}{\ell}) + B_c(\underset{\sim}{r})\right] \quad , \tag{9}$$

where

$$S(\underset{\sim}{r}) = \frac{2h\nu_{ij}^3}{c^2}\left(\frac{g_i n_j(\underset{\sim}{r})}{g_j n_i(\underset{\sim}{r})} - 1\right)^{-1} \tag{10}$$

is the line source function and g_i is the statistical weight of level i. The line opacity k_ℓ is given by

$$k_\ell(\underset{\sim}{r}) = \frac{h\nu_{ij}}{4\pi}\left(n_j B_{ji} - n_i B_{ij}\right) \quad . \tag{11}$$

The boundary conditions are usually given by specifying the incident intensities on all boundaries of the region, or, in some cases, certain linear relations (reflection conditions) relating incident and emergent intensities.

In writing Eq. (9) continuum absorption has been taken into account by means of the continuum source function B_c and the continuum opacity k_c. Also, complete redistribution has been assumed in this equation. In order to account for Doppler redistribution properly, the absorption and emission of a number $n_i(\underset{\sim}{r},\underset{\sim}{w})d\underset{\sim}{w}$ of particles in level i in velocity range $d\underset{\sim}{w}$ would have to be considered, rather than simply the total number in each level. This would also necessitate writing a more complete equation of statistical equilibrium for $n_i(\underset{\sim}{r},\underset{\sim}{w})$. Another way to take Doppler redistribution into account is by use of redistribution functions (Hummer, 1962, 1968) although this method assumes that the velocity distribution of the lower level is known to be Maxwellian, and that stimulated emissions are

negligible; these assumptions will certainly apply to resonance lines of high excitation potential, but perhaps not necessarily for other lines. The relationship between non-Maxwellian velocity distributions of the excited levels and Doppler redistribution has been emphasized by Oxenius (1965).

It is somewhat more convenient to work in terms of a normalized frequency variable defined by

$$x = \frac{\nu - \nu_{ij}}{\Delta_{ij}} \quad , \tag{12}$$

where

$$\Delta_{ij} = \frac{\nu_{ij} \bar{v}_{th}}{c} \quad , \tag{13}$$

and where $\bar{v}_{th}$ is a typical Doppler velocity characterizing the atmosphere, given by

$$\bar{v}_{th} = \left[\frac{2kT_{kin}}{m} \right]^{1/2} \quad . \tag{14}$$

Here $\bar{T}_{kin}$ is a typical kinetic temperature, which may include contributions from "microturbulence." For Doppler profiles the profile function then becomes

$$\phi(\underset{\sim}{r}, x) = \frac{1}{\sqrt{\pi}\ \delta(r)}\ e^{-x^2/\delta^2(r)} \quad , \tag{15}$$

where

$$\delta(r) = \frac{v_{th}(\underset{\sim}{r})}{\bar{v}_{th}}$$

and

$$v_{th}(\underset{\sim}{r}) = \left[\frac{2kT_{kin}(\underset{\sim}{r})}{m} \right]^{1/2} \tag{17}$$

is the Doppler velocity characterizing the profile at the point r. A dimensionless variable u(r) is also

defined in units of $\bar{v}_{th}$ by

$$\underset{\sim}{u}(\underset{\sim}{r}) = \frac{\underset{\sim}{v}(\underset{\sim}{r})}{\bar{v}_{th}} \tag{18}$$

With these variables Eqs. (4) and (9) become

$$\bar{J}_{ij}(\underset{\sim}{r}) = \frac{1}{4\pi} \int_{-\infty}^{\infty} dx \int d\underset{\sim}{\ell}\, \phi(\underset{\sim}{r}, x - \underset{\sim}{\ell}\cdot\underset{\sim}{u}(\underset{\sim}{r})) I_x(\underset{\sim}{r}, \underset{\sim}{\ell}) \tag{19}$$

$$\underset{\sim}{\ell}\cdot\frac{\partial}{\partial \underset{\sim}{r}} I_x(\underset{\sim}{r}, \underset{\sim}{\ell}) = k_\ell(\underset{\sim}{r})\ \phi(\underset{\sim}{r}, x - \underset{\sim}{\ell}\cdot\underset{\sim}{u}(\underset{\sim}{r}))\left[-I_x + S\right]$$

$$+ k_c(\underset{\sim}{r})\left[-I_x + B_c\right] \tag{20}$$

while in Eqs. (5), (6), and (7) the variable ν is replaced by x. Finally in Eq. (11) an additional factor of Δ_{ij}^{-1} appears on the right-hand side. The range of the variable x may be taken as $-\infty$ to $+\infty$ with inconsequential error.

The advantage of these dimensionless variables is that material velocities of the order of the typical thermal velocity correspond to $|u| \sim 1$, and it is in these cases that velocity effects begin to be important.

THE FORMAL SOLUTION

Since the pioneering work of Beals (1931) many investigators have assumed various structures for extended atmospheres, including the specification of the source function, and then have computed the emergent flux using the formal solution of the transfer equation. Such calculations avoid the difficult problems of actually determining the source function as a consistent result of the specification of the fundamental atmospheric parameters. Despite their possible inconsistencies, however, the importance of these calculations for the development of the subject should not be underestimated. It is probably fair to say that the present-day conception of extended stellar atmo-

spheres is largely based upon such calculations, or upon intuition based upon knowledge of the formal solution. It is not yet possible to solve for the source function including all those effects that are known or suspected to be important, so the calculations based on the formal solution are still likely to be important for some time. In any case such calculations will be necessary as a final step in a more detailed calculation and in some cases the primary effects of velocity fields are to be found in this step. For example, the redshift found by Hummer and Rybicki (1968) for an expanding atmosphere is, as pointed out by them, solely due to the change in optical depth relations in various parts of the line, and not to any substantial change in the source function from the static case.

The formal solution of the transfer equation is well-known (see, e.g., Chandrasekhar (1934). Write Eq. (20) as

$$\frac{\partial I_x(\xi)}{\partial \xi} = \kappa_x(\xi)[-I_x+\mathcal{J}_x] \tag{21}$$

where ξ measures path length along a ray from some convenient point, and where

$$\kappa_x(\xi) = k_\ell(\xi)\ \phi(\xi,x) + k_c(\xi)$$

$$\mathcal{J}_x(\xi) = \frac{k_\ell(\xi)\ \phi(\xi,x)\ S(\xi) + k_c(\xi)\ B_c(\xi)}{k_\ell(\xi)\ \phi(\xi,x) + K_c(\xi)} \tag{22}$$

All quantities are expressed as functions of ξ along the ray. Then the formal solution is

$$I_x(\xi) = I_x(0)\ e^{-\int_0^\xi \kappa_x(\xi')d\xi'} + \int_0^\xi \kappa_x(\xi')\ _x(\xi')\ e^{-\int_{\xi'}^\xi \kappa_x(\xi'')d\xi''}\ d\xi' \tag{23}$$

The intensity at a given point is then expressed as a quadrature involving the total opacity κ_x, the total source function $\mathcal{J}_x$, and a value of intensity at another point on the ray $I_x(0)$, which is known if $\xi = 0$ is a boundary point and $I_x(0)$ is known incident boundary condition. In some cases the zero point can be taken so that the exponential factor multiplying $I_x(0)$ is essentially zero, and the value of $I_x(0)$ is not needed.

For a given set of values for the function κ_x and $\mathcal{J}_x$ the emergent intensity along any ray can be computed. A convenient measure of the emergent flux which would be received by a distant observer over the area of a projected disk of the atmosphere. This quantity might be called the specific luminosity of the star in that direction and at the given frequency; in cases where the star radiates isotropically it is simply the total luminosity per unit frequency range divided by 4π. The actual flux at the point of observation is proportional to the specific luminosity, the factor being the inverse square of the observation distance. The observed shape of the spectrum at any distance from the star is correctly given by the specific luminosity as a function of frequency.

The introduction of any symmetries, such as spherical symmetry, will simplify the problem considerably. In plane-parallel geometry the formal solution is given by Eq. (23) except all quantities depend on the depth variable z alone, so that ξ becomes z and $d\xi$ becomes dz/μ, and similarly for the various primed variables. In spherically symmetric geometry all quantities in Eq. (23) depend on the radius r alone, but the relationship between ξ and r is much more complex. It is sometimes convenient in this case to use a new variable p which represents the distance of closest approach of the ray to the center of spherical symmetry, and to express all quantities in terms of r and p rather than r and μ. This latter procedure was first introduced by Chandrasekhar (1934). It is also possible to use ξ and p as the basic variables and this has essentially been done by Castor and Van Blerkom (1970). These two choices of variables are useful because the transfer equation can be written in terms of a single partial derivative, rather than the two of the r,μ representation. This is already clear from Eq. (21).

Another kind of simplification arises for stars with large velocity gradients. For each

frequency the radiation in a spectral line originates in relatively localized regions that lie very close to the so-called surfaces of constant radial velocity defined by $x = \underset{\sim}{\ell} \cdot \underset{\sim}{u} = u_\ell$ where u_ℓ is the component of velocity along the line of sight. For any given velocity field these surfaces can be determined; then assuming that the continuum opacity is small, the only region where any emission in the line can take place at frequency x is very near the appropriate surface. The line source function S can be assumed to be constant over this region and the intensity along the ray is equal to

$$I_x(\xi) = I_x(0)\, e^{-\tau_x} + S(1-e^{-\tau_x}) \quad , \qquad (24)$$

where τ_x is the optical thickness of the region along the ray. The computation of τ_x will be postponed until the following section when local frequency variables are introduced. When more than one such surface is cut by a single ray corresponding formulas can be similarly derived. For example, when two surfaces are involved,

$$I_x(\xi) = I_x(0)\, e^{-(\tau_x+\tau_x')} + S\, e^{-\tau_x'}(1-e^{-\tau_x}) + S'(1-e^{-\tau'x}) \quad . \qquad (25)$$

Here the ray starts at $\xi = 0$, first cuts the surface corresponding to the unprimed quantities, and then cuts the surface with the primed quantities. For further details of such calculations see Rublev (1961, 1964), Lyong (1967), and Castor (1970).

ANALYTICAL METHODS FOR DETERMINING THE SOURCE FUNCTION

While most methods for actually determining the source function are numerical ones, there are some topics of an analytical nature that are relevant to the line formation problem beyond the simple consid-

erations of the formal solution. Among these are the local frequency transformation, special geometries, the infinite medium with constant velocity gradient, and Sobolev's theory of moving atmospheres. These will be discussed in this section and the numerical methods in the next.

a. Local Frequency Transformation

Milne (1930) introduced a transformation to a new frequency variable x' related to x by

$$x' = x - \underset{\sim}{u}(\underset{\sim}{r}) \cdot \underset{\sim}{\ell} \quad . \tag{26}$$

Originally this transformation was formulated in the plane-parallel case; Eq. (26) is the generalization to arbitrary geometry. Clearly x' is the frequency seen in a frame of reference moving with the local material at the point $\underset{\sim}{r}$ when radiation travelling in direction $\underset{\sim}{\ell}$ has frequency x in the stationary frame.

If intensities and other variables are written as functions of x' instead of x then the transfer equation becomes

$$\underset{\sim}{\ell} \cdot \frac{\partial I_{x'}}{\partial \underset{\sim}{r}} - Q(\underset{\sim}{r},\underset{\sim}{\ell}) \frac{\partial I_{x'}}{\partial x'} =$$

$$= k_{\ell}(\underset{\sim}{r})\,\phi(\underset{\sim}{r},x')\left[-I_{x'}+S\right] + \left[k_c(\underset{\sim}{r}) - I_{x'} + B_c\right] \tag{27}$$

where Q is the following quadratic form in the components of the vector $\underset{\sim}{\ell}$:

$$Q(\underset{\sim}{r},\underset{\sim}{\ell}) = \sum_{\alpha\beta} \frac{\partial u_\alpha}{\partial r_\beta} \ell_\alpha \ell_\beta = \sum_{\alpha\beta} G_{\alpha\beta} \ell_\alpha \ell_\beta \tag{28}$$

Here α and β are tensor indices ranging from 1 to 3, which label the components of the corresponding vectors. Since the antisymmetric part of $G_{\alpha\beta}$ does not contribute to Q, it may be defined as

$$G_{\alpha\beta}(\underset{\sim}{r}) = \frac{1}{2}\left(\frac{\partial u_\alpha}{\partial r_\beta} + \frac{\partial u_\beta}{\partial r_\alpha}\right) = G_{\beta\alpha}(\underset{\sim}{r}) \quad . \tag{29}$$

This may be recognized as the rate of strain tensor of fluid dynamics. There are several special forms for $\underset{\sim}{u}$, $G_{\alpha\beta}$, and Q corresponding to cases of various symmetries:

1. Plane-parallel symmetry

Let $\alpha=3$ be the index for the direction normal to the planes of symmetry. Then

$$\begin{aligned} u_1 = u_2 = 0 \quad ; \quad u_3 &\equiv u(z) \\ G_{33} &= u'(z) \\ Q &= \mu^2 u'(z) \quad . \end{aligned} \tag{30}$$

2. Spherical symmetry

Let the indices take the values r, θ, and ϕ, corresponding to the radial, polar, and azimuthal directions at the given point. Then

$$\begin{aligned} u_\theta = u_\phi = 0 \quad ; \quad u_r &\equiv u(r) \\ G_{\theta\theta} = G_{\phi\phi} = u(r)/r \quad ; \quad G_{rr} &= u'(r) \\ Q &= \mu^2 u'(r) + (1-\mu^2)u(r)/r \quad . \end{aligned} \tag{31}$$

Note that here and in the preceding the values of $G_{\alpha\beta}$ not given are zero, and that μ is the usual direction cosine of the ray.

There are two special cases that frequently occur in the spherical case. When u(r) is constant there results $Q = (1-\mu^2)u/r$, and when u(r) is proportional to r (uniform expansion) there results $Q = u'$.

One advantage of such a transformation is that absorption and emission in the local frame are usually close to being isotropic, so that the vari-

ation of intensity with angle can be expected to be smoother at fixed x' than at fixed x. For example, consider a rapidly moving region, $|\underset{\sim}{u}|>>1$. As the direction of a ray is varied slightly the absorption in the region can vary tremendously when the right condition of line of sight velocity is met for the particular frequency x. This leads to rapidly varying functions of angle, which are hard to handle numerically.

The local frequency transformation makes obvious the fact that only velocity gradients affect the line formation problem, since only gradients appear in Q. This is also quite obvious on physical grounds, but some of the implications are quite deep. If the opacities and profile function are independent of position $\underset{\sim}{r}$, and if $Q(\underset{\sim}{r},\underset{\sim}{\ell})$ is likewise independent of $\underset{\sim}{r}$, then Eq. (27) is a integro-differential equation with spatial translational invariance. It is therefore susceptible to a host of techniques of solution more or less familiar in the static case, but now referring to a constant velocity gradient. This fact forms the basis of Sobolev's analytical solution, to be discussed later in this section.

The problem left in the last section, that of computing the value of τ_x in Eq. (25), will now be completed. It is given by

$$\tau_x = \int_0^{\xi} k_{\ell}(\underset{\sim}{r})\ \phi(\underset{\sim}{r},x-\underset{\sim}{u}(\underset{\sim}{r}))d\xi' \quad ,$$

where $\underset{\sim}{r} = \underset{\sim}{r}(\xi')$ along the ray and where k_c is assumed negligible. Changing the variable of integration to the local frequency variable gives

$$\tau_x = \frac{k_{\ell}(\underset{\sim}{r}_o)}{|Q(\underset{\sim}{r}_o,\underset{\sim}{\ell})|} \int \phi(\underset{\sim}{r}_o,x')dx' \quad ,$$

where the value $\underset{\sim}{r} = \underset{\sim}{r}_o$, the position of the surface of constant velocity, has been inserted in those functions that are slowly varying over the range in which the integrand is not negligible. These functions have further been taken from under the integral. The origin of the factor in the denominator is the transformation of differentials,

$$\frac{d\xi'}{dx'} = \left(\frac{dx'}{d\xi'}\right)^{-1} \quad , \qquad (32)$$

and

$$\frac{dx'}{d\xi'} = - \sum_{\alpha\beta} \frac{\partial u_{\ell}(\underset{\sim}{r})}{\partial r_{\beta}} \frac{\partial r_{\beta}}{\partial \xi'} \ell_{\alpha} \quad , \qquad (33)$$

noting that

$$\ell_{\beta} = \frac{\partial r_{\beta}}{\partial \xi'} \quad . \qquad (34)$$

The absolute value is to account for the correct ordering of the limits of integration, making the lower limit smaller than the upper limit. From the normalization of ϕ it follows that

$$\tau_x = \frac{k_{\ell}(\underset{\sim}{r}_o)}{|Q(\underset{\sim}{r}_o, \underset{\sim}{\ell})|} \quad , \qquad (35)$$

since the range of integration for large velocity gradients is essentially over the entire line.

There are further uses of the local frequency transformation, one of which will appear presently. It will merely be pointed out here that, in such a local frequency description, redistribution functions can be used in their static form, rather than having to take the macroscopic motions directly into account in the redistribution functions themselves.

b. Special Geometries

The two special geometries of interest are the plane-parallel (pp) and spherically symmetric (ss) ones. The directional derivatives for these two cases are

$$\underset{\sim}{\ell} \cdot \frac{\partial I_x}{\partial \underset{\sim}{r}} = \mu \frac{\partial I_x}{\partial r} \qquad \text{(pp)} \qquad (36)$$

and

$$\underset{\sim}{\ell} \cdot \frac{\partial I_x}{\partial \underset{\sim}{r}} = \mu \frac{\partial I_x}{\partial r} + \frac{1-\mu^2}{r} \frac{\partial I_x}{\partial \mu} \qquad \text{(ss)} \qquad (37)$$

in terms of the frequency x. In terms of the local (l) frequency variable $x' = x - \mu u(r)$ they are

$$\underset{\sim}{\ell} \cdot \frac{\partial I_x}{\partial \underset{\sim}{r}} = \mu \frac{\partial I_{x'}}{\partial r} - \mu^2 u'(r) \frac{\partial I_{x'}}{\partial x'} \quad \text{(lpp)} \qquad (38)$$

$$\underset{\sim}{\ell} \cdot \frac{\partial I_x}{\partial \underset{\sim}{r}} = \mu \frac{\partial I_{x'}}{\partial r} + \frac{1-\mu^2}{r} \frac{\partial I_{x'}}{\partial \mu} +$$

$$- \left[\mu^2 u'(r) + (1-\mu^2)\frac{u(r)}{r}\right] \frac{\partial I_{x'}}{\partial x'} \quad \text{(lss)} \quad . \qquad (39)$$

An interesting fact emerges from these expressions. The plane-parallel equations are usually obtained by dropping the term involving the partial derivative with respect to μ, as in Eqs. (36) and (37), the argument being that this term is of order of the ratio of a mean free path to the radius of curvature of a layer. By the same argument the corresponding term in Eq. (39) may be dropped, but this still leaves an extra term involving u/r when compared to Eq. (38). This term cannot be dropped on any reasonable grounds since in extended atmospheres it is on the same order as the term in u'(r), which is clearly not negligible since it accounts for all the velocity gradient effects. Thus a paradox has appeared: Making the plane-parallel approximation first and performing the local frequency transformation second does not give the same results as these operations performed in the reverse order.

We feel that the reason for this paradox is that the derivative $\partial I_x/\partial\mu$ at constant x is not small and cannot be dropped, while the derivative $\partial I_{x'}/\partial\mu$ at constant x' is small and can be dropped. This point was discussed in the preceding subsection. As a consequence Eq. (36) is probably not the best formulation of the plane-parallel approximation for moving spherically symmetric atmospheres. A more correct formulation (c) in local frequency variables would be

$$\underset{\sim}{\ell} \cdot \frac{\partial I_{x'}}{\partial \underset{\sim}{r}} = \mu \frac{\partial I_{x'}}{\partial r} +$$

$$- \left[\mu^2 u'(r) + (1-\mu^2) \frac{u(r)}{r}\right] \frac{\partial I_{x'}}{\partial x'} \quad \text{(clpp)} \quad (40)$$

rather than Eq. (38).

In order to understand why this new plane-parallel approximation differs from the usual one, it is useful to distinguish between two types of spherical divergence effects: First, there is the usual divergence of the rays, which may be neglected for cases where the thickness of the layer in question is much smaller than the mean free path. Second, there is the divergence of the velocities, which may be quite important because of the extreme sensitivity of the absorption coefficient to slight shifts in frequency. The terms corresponding to divergence of the velocities have been retained in this new formulation while the terms corresponding to the divergence of the rays have been dropped. It is interesting to note that precisely the same arguments have been used by McCrea and Mitra (1936) for including Doppler shifts in the moving atmosphere equations while dropping aberration effects, even though these are of the same order in $\underset{\sim}{v}/c$.

This idea may be illustrated by some examples giving some further physical insight. Suppose first of all that $u(r)$ is proportional to r, the velocity field for a uniformly expanding atmosphere. The local velocity field as viewed from a local frame of reference moving with the material at any point is isotropic; in fact it appears to be a uniform expansion away from that point. This simple fact is correctly represented by Eq. (40) where the coefficient of $\partial I_{x'}/\partial x'$ is independent of μ, while in Eq. (38) it is proportional to μ^2, implying a strong directional effect. Another case of interest is that of constant outflow, $u(r) = \text{const}$; the term in Eq. (38) now vanishes, which implies the absence of any velocity effects. This is clearly not so, however, since there is a transverse velocity gradient in this case, which, for example, makes it easier for photons to escape the atmosphere along a tangent. These examples show the superiority of Eq. (40) over Eq. (38).

It remains to write the corrected formula in terms of the variable x,

$$\underset{\sim}{\ell} \cdot \frac{\partial I_x}{\partial \underset{\sim}{r}} = \mu \frac{\partial I_x}{\partial r} - (1-\mu^2)\frac{u(r)}{r} \frac{\partial I_x}{\partial x} \quad \text{(cpp)}. \tag{41}$$

There would not seem to be any particular advantage in using Eq. (41) over Eq. (40) since a derivative with respect to frequency still appears. However, this derivative can be eliminated by performing a different sort of frequency transformation to a frequency x" defined by

$$x'' = x + \left(\frac{1}{\mu} - \mu\right) \int \frac{u(r)}{r} \, dr \quad , \tag{42}$$

where any indefinite integral can be chosen. Then

$$\underset{\sim}{\ell} \cdot \frac{\partial I_x}{\partial \underset{\sim}{r}} = \mu \frac{\partial I_{x''}}{\partial r} \quad \text{(ppp)} \quad , \tag{43}$$

which is exactly in plane-parallel form, but in terms of the new frequency variable. This will be called the pseudo-plane-parallel formulation (ppp), and may be of particular use for methods, such as those using integral equations, where frequency derivatives cannot be easily handled.

It is interesting to write the (ppp) equation in full for the case of a uniform expansion. Taking

$$\int \frac{u}{r} \, dr = u$$

for this case yields

$$\mu \frac{\partial I_{x''}}{\partial r} = k_\ell(r) \, \phi\left(r, x'' - \frac{u(r)}{\mu}\right)\left[- I_{x''} + S\right] +$$

$$+ k_c(r) \left[- I_{x''} + B_c\right] \quad . \tag{44}$$

This would be precisely the usual plane-parallel equation, except that in the argument of the profile function u is divided, rather than multiplied by μ.

c. Infinite Medium With Constant Velocity Gradient

Sobolev (1957) showed that in an infinite plane-parallel medium with a constant velocity gradient the solution for the source function of a two-level atom with no continuum could be reduced to the solution of the integral equation (in a notation which differs from Sobolev's)

$$S(\tau) = (1-\varepsilon) \int_{-\infty}^{\infty} K(|\tau-\tau'|)S(\tau')d\tau' + \varepsilon B(\tau) \quad . \quad (45)$$

Here ε is a constant, the ratio of the collisional de-excitation rate to the total de-excitation rate, and the kernel function K is defined by

$$K(\tau) =$$

$$= \frac{1}{2} \int_{-\infty}^{\infty} dx \int_{0}^{1} \frac{d\mu}{\mu} \phi(x)\phi(x + \gamma\mu\tau) \exp\left\{ - \int_{0}^{\tau} \phi(x + \gamma\mu z)dz \right\}. \quad (46)$$

The variable τ is an equivalent integrated line optical depth, defined for a medium at rest. The velocity gradient is a constant and is defined by

$$\gamma = \frac{\partial u}{\partial \tau} \quad . \quad (47)$$

The factor A that appears in Sobolev's paper is to be taken as unity here because of the use of integrated line absorption to define the optical depth scale rather than the line center absorption that Sobolev uses. The function $B(\tau)$ is the Planck function at the local electron temperature and at the line frequency.

The translational invariance of the problem is clear, since the kernel function of this integral equation is a function of the difference $|\tau - \tau'|$ alone. Such integral equations have been extensively studied, but usually in the static case. Much is known about the solutions of such equations and how they depend on ε and on $B(\tau)$.

A very useful physical picture is obtained by regarding the quantity $S(\tau)$ in this equation as the probability of emission of a single photon, rather than as the average number of such emissions. Then $\varepsilon B(\tau)$ gives the probability density of creation of a photon at the point τ, $K(\tau)$ gives the single-step distribution function for the free propagation distance of the photon before absorption, and ε is the probability that an absorption will be followed by the destruction of the photon. A very useful concept associated with this probabilistic viewpoint is that of thermalization length, an average distance traveled by the photon between its creation and its destruction (see Rybicki and Hummer, 1969). By use of the concept of thermalization length much can be said about the solution $S(\tau)$ without actually solving the entire problem, and it is instructive to do so in the present simple case of a moving atmosphere.

There is a very important physical distinction between the usual static case of thermalization and the present one, however, which is due to a change in the normalization of the kernel function. Ordinarily the normalization would be

$$\int_{-\infty}^{\infty} K(|\tau|)d\tau = 1 \qquad \text{(static case)} \tag{48}$$

since any photon eventually is absorbed somewhere. But in the present case this is to be replaced by

$$\int_{-\infty}^{\infty} K(|\tau|)d\tau = 1 - \beta \tag{49}$$

with $0<\beta<1$. This implies that a photon need not be absorbed, but can escape the medium entirely with escape probability β. This is an entirely new phenomenon which might be called intrinsic escape,

since it does not depend on the presence of boundaries, but rather on the rapidly decreasing opacity seen by a photon as it becomes further and further removed into the line wings by virtue of the Doppler shift of the material. This opacity decreases rapidly enough so that the optical thickness in the direction of a velocity gradient is bounded no matter how long the geometrical path length is.

From Eq. (46) it follows that

$$\beta = |\gamma| \int_0^1 \left[1 - \exp\left(-\frac{1}{|\gamma|\mu^2}\right)\right] \mu^2 d\mu \qquad (50)$$

For details of this reduction the reader is referred to Sobolev (1957).

In spite of this normalization the equations can again be brought to the form

$$S(\tau) = (1 - \bar{\varepsilon}) \int_{-\infty}^{\infty} \bar{K}(|\tau-\tau'|) S(\tau') d\tau' + \bar{\varepsilon}\, \bar{B}(\tau) \qquad (51)$$

where the kernel $\bar{K}$ is now normalized,

$$\int_{-\infty}^{\infty} \bar{K}(|\tau|) d\tau = 1 \qquad (52)$$

This is accomplished by the definitions

$$\bar{K}(\tau) = \frac{1}{1 - \beta} K(\tau)$$

$$\bar{\varepsilon} = 1 - (1-\beta)(1-\varepsilon) = \varepsilon + \beta - \varepsilon\beta$$

$$\bar{B}(\tau) = \frac{\varepsilon}{\bar{\varepsilon}} B(\tau) \qquad (53)$$

Since Eq. (51) is now in the usual form, the thermalization length may be discussed. First of all, it should be noted that when $\beta >> \varepsilon$ the value of $\bar{\varepsilon}$ is insensitive to ε, and in fact $\bar{\varepsilon} \sim \beta$. This means that the mechanism of loss of photons by

intrinsic escape dominates the loss by collisional de-excitation, and therefore the thermalization process will be determined by β rather than ε when $\beta >> \varepsilon$. Secondly, it should be noted that the kernel $\bar{K}(\tau)$ is very much more sharply cut off for large values of τ than in the static case, at least for Doppler profiles. This is because it is precisely those photons which would have traveled a long distance in the static case that now escape and do not appear in the distribution $\bar{K}(\tau)$ at all. The actual cutoff of the kernel can be roughly estimated to be at distances of the order of $\tau \sim 1/\gamma$, since this is roughly the scale over which the profile shifts through its own width, and photons that travel to larger distances will escape completely.

Rybicki and Hummer (1969) have shown that when the distribution of single flights is sharply cut off, the thermalization length Λ is of the coherent type, and is of the order of the width of the kernel times $(\bar{\varepsilon})^{-1/2}$, that is, $\Lambda \sim \gamma^{-1}(\bar{\varepsilon})^{-1/2}$. When properties vary slowly on the scale of the thermalization length an approximate solution to Eq. (51) may be obtained by removing $S(\tau)$ from under the integral. Then

$$S(\tau) = \bar{B}(\tau) \quad , \tag{54}$$

or, when $\beta >> \varepsilon$,

$$S(\tau) = \frac{\varepsilon B(\tau)}{\beta} \quad . \tag{55}$$

The source function is in this case simply determined by the creation rate $\varepsilon\, B(\tau)$ and the escape probability β.

It is important to note that for Eq. (55) to be valid it is not necessary to have very large gradients, $\gamma >> 1$. For example, a fairly small γ can still lead to a β satisfying $\beta >> \varepsilon$, thus the sole requirement is one concerning thermalization length and the scale of variation of properties L. For small γ it follows that $\beta \sim \gamma/3$ (see Sobolev 1957), and $\beta >> \varepsilon$ implies $\bar{\varepsilon} \sim \beta$, so that the thermalization length is $\Lambda \sim \gamma^{-3/2}$. The condition of validity is simply $\Lambda >> L$, and if L is sufficiently large this can be met for arbitrarily small γ.

The reason that so much space has been given here to the discussion of Eqs. (45) and (51) from

the point of view of thermalization theory is that, within the framework of the simplifying assumptions made, it has been possible to derive solution (55), which is identical with the one found in Sobolev's theory of moving atmospheres. Furthermore (and most importantly) it has been possible to fix conditions of validity of this solution, which relate the magnitude of the velocity gradient to scales of variation of the physical parameters. In particular, it has been pointed out that this solution may be valid for "small" gradients, whereas Sobolev's theory of moving atmospheres has often been regarded only as a "large" gradient theory. These considerations will be useful in the following discussion.

Castor (1970) also discusses the validity of Sobolev's theory by deriving diffusion-like corrections and estimating their magnitude. This is roughly analogous to the above procedure, since the use of the coherent type of thermalization length is essentially a diffusion theory result. However, the criterion Castor obtains is that the typical mean thermal velocities must be small in comparison to typical macroscopic velocities. By estimating the macroscopic velocity as the gradient times a scale length we may put this into the form $L \gg \gamma^{-1}$, which is a less restrictive condition than the one obtained here. This point needs further investigation.

d. Sobolev's Theory of Moving Atmospheres

In general, velocity gradients present great difficulties in the problem of line formation. However, the remarkable theory of moving atmospheres developed by Sobolev (1947, 1957) demonstrates that velocity gradients are actually a simplifying feature when they are of sufficient magnitude. In favorable cases an entire coupled multi-level transfer problem, a formidable problem even in the static case, can be reduced to a set of algebraic equations for the populations at each point in the atmosphere. A brief discussion of Sobolev's theory will now be given to show how the concept of escape probability can be extended to multi-level problems. The continuum opacity k_C will be assumed negligible in the neighborhood of each line.

The basic idea of the theory is as follows: consider a region of the atmosphere in which the properties are more or less homogeneous, and which is sufficiently large in the sense to be discussed below. In the static case the radiative transition rate between any two levels, say i to j, is exactly the same as the rate in the reverse transition, j to i. This is because any transition leading to the emission of a photon will in turn produce the reverse transition when that photon is absorbed somewhere else in the same region. The two transition rates averaged over the region must then be equal, and if the conditions are homogeneous the equality applies also at a single point. The condition on the size of the homogeneous region can be seen to be that every photon emitted in the region must also be absorbed there, to a good approximation.

When there is a velocity gradient a photon can escape the atmosphere entirely, and in this case the downward radiative transition rate will exceed the upward rate. The difference in these two rates is simply $n_i A_i \beta_{ji}$, where β_{ji} is the probability of escape of the photon due to the Doppler shift of the profile.

The escape probability β_{ji} can be easily found by assuming a constant velocity gradient over the region of interest. Suppose a photon is emitted at frequency x and direction $\underset{\sim}{\ell}$ at a certain point. It is convenient to use a frame of reference such that this point is at rest at the origin. The velocity field is then

$$u_\alpha(\underset{\sim}{r}) = \sum_\beta \frac{\partial u_\alpha}{\partial r_\beta} r_\beta \tag{56}$$

The total optical thickness of the medium from the origin in the direction $\underset{\sim}{\ell}$ at frequency x is

$$\tau_x(\underset{\sim}{\ell}) = k_{ij} \int_0^\infty \phi(x - \underset{\sim}{u}(\xi\underset{\sim}{\ell})\cdot\underset{\sim}{\ell})\, d\xi \tag{57}$$

Setting $x' = x - \underset{\sim}{u}(\xi\underset{\sim}{\ell})\cdot\underset{\sim}{\ell} = x - \xi Q(\underset{\sim}{\ell})$, there results

$$\tau_x(\underset{\sim}{\ell}) = \frac{k_{ij}}{|Q(\underset{\sim}{\ell})|} \int_{-\infty}^{x} \phi(x')dx' \tag{58}$$

The integrated line opacity for the transition i to j is denoted by k_{ij}.

The probability of escape in a frequency range dx about x and in an angular range $d\underset{\sim}{\ell}$ about $\underset{\sim}{\ell}$ is

$$\frac{1}{4\pi} d\underset{\sim}{\ell}\, \phi(x)\, dx \exp\left[-\tau_x(\underset{\sim}{\ell})\right] . \qquad (59)$$

The net probability of escape is thus

$$\beta_{ji} = \frac{1}{4\pi} \int d\underset{\sim}{\ell} \int_{-\infty}^{\infty} dx\, \phi(x) \exp\left[-\frac{k_{ij}}{|Q|} \int_{-\infty}^{x} \phi(x')dx'\right].$$

Changing the variable of integration from x to

$$t = \int_{-\infty}^{x} \phi(x')dx'$$

yields the final result

$$\beta_{ji} = \frac{1}{4\pi} \int d\underset{\sim}{\ell}\, \frac{|Q(\underset{\sim}{\ell})|}{k_{ij}} \left[1 - \exp\left(-\frac{k_{ij}}{Q(\underset{\sim}{\ell})}\right)\right] . \qquad (60)$$

The escape probability is therefore independent of the profile function under the assumption of complete redistribution. The restriction to rectangular profiles in the original work of Sobolev (1947) is unnecessary, as pointed out by Sobolev (1957).

The expression (60) is the generalization of the escape probability formula for arbitrary velocity gradients. Substituting in the appropriate Q for plane-parallel geometry, namely Eq. (30), the expression (50) is again obtained, since $u'(z)/k = \partial u/\partial\tau = \gamma$. Similarly Eq. (31) for spherical geometry

leads to the formula

$$\beta_{ji}(r) = \frac{1}{k_{ij}} \int_0^1 \left| \mu^2 u'(r) + (1-\mu^2) u(r)/r \right| \cdot \left[1 - \exp\left(\frac{-k_{ij}}{\left| \mu^2 u'(r) + (1-\mu^2) u(r)/r \right|} \right) \right] d\mu \quad . (61)$$

An equivalent formula was derived by Castor (1970). For the special case of uniform expansion, $u' = u/r = \text{const.}$, and the corresponding formula is

$$\beta_{ji} = \frac{u'}{k_{ij}} \left[1 - \exp\left(- \frac{k_{ij}}{u'} \right) \right] \quad . \qquad (62)$$

The determination of the escape probability for each transition depends on local parameters in the atmosphere, namely the integrated line opacity and the velocity gradient. The equations of statistical equilibrium can be written in terms of net radiative rates, which are simply related to the escape probabilities, as shown above. It follows that an entire multi-level problem can be reduced to an algebraic set of equations, which can be solved locally at each point in the atmosphere, without regard for conditions at other points. This uncoupling of the various parts of the atmosphere is due to the Doppler shift between material at separated points, which causes them to absorb and emit in quite different parts of the spectrum.

As an example of such a formulation of a multi-level problem, consider the case of an atom in the dilute radiation field ρ_{ic} of a star. The statistical equilibrium equations are

$$n_i \left(\sum_{k=1}^{i-1} A_{ik} \beta_{ki} + B_{ic} \rho_{ic} \right) = \sum_{k=i+1}^{\infty} n_k A_{ki} \beta_{ik} + n_e n^+ C_i(T_e) \quad , \qquad (63)$$

where all collisional processes except recombination have been neglected. The local physical parameters fix all the constants in this equation, which may then be solved for the n_i. For details see Sobolev (1947).

A more recent and more sophisticated example of the formulation and solution of multi-level problems using Sobolev's method is given by Castor and Van Blerkom (1970), who solve a 30-level He atom in spherical geometry. Collision processes are included and the effects of continuous absorption are taken into account approximately.

An important area for future investigation is the determination of criteria for the validity of Sobolev's theory. The crucial question seems to be, as in the simplified two-level case, how small a scale of variation of the physical parameters is allowable while still maintaining the local homogeneity that is necessary for the use of the escape probability concept. Possible approaches are to extend the two-level thermalization arguments or Castor's diffusion correction terms to the multi-level case.

NUMERICAL METHODS

Most numerical calculations have treated the effects of velocity gradients for two-level atoms in plane-parallel geometries. These calculations have been exploratory in nature, to discover effects rather than to obtain accurate solutions to a physical problem. This seems to be appropriate at the present stage of development of the subject.

Kulander (1964, 1968) assumed an atmosphere which consisted of several layers in which all physical properties were constant. This allowed a semi-analytic approach to be taken, since the solution for the discrete ordinate intensities in each layer was a linear combination of elementary exponential functions. Boundary conditions at the interface between two layers were simply that all intensity components must be continuous. In this way Kulander was able to solve for the source function and the emergent intensities for many different cases. This work showed that the source function was generally discontinuous across the boundary between layers and sometimes large increases in source function near the surface could be obtained in this way. These increases simply

mean that the radiation field near the boundary is quite weak in the line core for material at rest, but as the material moves it can absorb the more intense radiation in the line wings. Examples were shown where emission features could actually result from these increases in source function. In general, line profiles are now much more complex and, of course, asymmetrical.

Kulander (1967) also developed a numerical method of solution using differential equations, which is directly applicable to media with continuous variation of properties. However, it would seem that this method must be unstable for large optical thicknesses for reasons given by Hummer and Rybicki (1967) in their discussion of the fundamental matrix method. The method of slabs, on the other hand, can be used for arbitrarily thick atmospheres, including semi-infinite ones, if not too many slabs are taken. When large numbers of slabs are taken in order to model a continuous distribution of properties then the choice of a stable method of solving the relevant equations becomes important. The number of frequency and angular components that can be treated poses another limitation of the method. Kulander used a single-point angle quadrature, which is roughly equivalent to the Eddington approximation. Numerical problems would probably limit the total number of frequency components to perhaps 100. Up to 13 components were used by Kulander (1967).

It should perhaps be mentioned here that the methods used by Abyankhar (1964a,b; 1965) are closely related to the above slab method, but they have been formulated in terms of coherent scattering so that the details are not directly relevant here.

Hummer and Rybicki (1968) have used a differential equation method based on an extension of the Riccati method (Rybicki and Hummer, 1967), which is applicable to continuous variation of properties. Using this method they show how a uniformly expanding atmosphere can produce a red-shifted emission line. The reason for this shift is simply an optical depth effect, the actual change in the source function due to the motion being irrelevant. The emission and absorption of the material closest to the observer is shifted to the violet and therefore optical depth unity on the violet side of the line occurs much closer to the surface, where the excitation is smaller. This reduces the intensity of the violet emission, and the line appears red-shifted.

The small step size which must be used in the numerical integration to avoid multiscale instabil-

ities limits the use of the Riccati method to atmospheres having optical depths perhaps of a few hundred (Rybicki and Hummer, 1967). There is a way of treating semi-infinite atmospheres if variation of properties is confined to a layer near the surface, again of no more than a few hundred optical depths in thickness. The Riccati method is also limited by the number of discrete ordinates in angle and frequency that can be reasonably handled, no more than perhaps 60 components in one hemisphere.

Another method which no doubt can be employed to advantage in this problem is that of Feautrier (1964) which should avoid the difficulties of the Riccati method as far as the multiscale instability is concerned.

One modification of the method is necessary if the usual form of the equations in the method is not to be changed, namely, the quantities J and F must now be defined by

$$J(\tau,\mu,x) = \frac{1}{2}\,[I(\tau,\mu,x) + I(\tau,-\mu,-x)]$$

$$F(\tau,\mu,x) = \frac{1}{2}\,[I(\tau,\mu,x) - I(\tau,-\mu,-x)] \quad . \quad (64)$$

Changing the sign of x, as well as that of μ, takes advantage of the symmetry of the profile function $\phi(\tau,\mu,x)$ under the joint interchanges $\mu \to -\mu$ and $x \to -x$.

The methods employing integral equations that have been used in the static case can be modified to include velocity gradients, as Kalkofen (1970) has shown. One advantage of this method is that a much larger number of angle and frequency points can be taken than in the above methods, since the computation time increases linearly rather than quadratically or cubically with the number of components chosen. This advantage may be very important for cases of large velocity gradients.

Calculations of line formation have been performed by Mathis (1968) and Magnan (1968) in spherical geometries. Mathis used an iteration scheme to solve for the source function and emergent intensities for a uniformly expanding, spherically symmetric atmosphere and he found a red-shifted emission line of the same type as the plane-parallel calculation of Hummer and Rybicki (1968). Since his method appears to be equivalent to Λ - iteration

in the plane-parallel case, its rate of convergence will be slow when the mean number of scatterings is large.

Magnan (1968) used a Monte Carlo method for a spherically symmetric atmosphere with a constant velocity of outflow. This macroscopic velocity was the same order of magnitude as the thermal velocity. He treated several cases, which included effects of dipole scattering and of various boundary conditions. A very interesting and important comparison is that between the calculations made with and without the assumption of complete redistribution. The difference between the emergent profiles for these two cases is that the complete redistribution profile seems more smoothed-out than the exact calculation, but the differences are quite small. It would be unwise, however, to generalize about the adequacy of the assumption of complete redistribution from this calculation, since the physical case is not a severe one, the macroscopic velocity not being very large in comparison to thermal velocities.

An outstanding advantage of the Monte Carlo method is the ease of formulation in complex situations, which derives from the functional matching of a probabilistic numerical method to a basically probabilistic physical process. However, as is well known, there is a heavy penalty in that the accuracy of the calculation grows as the square root of the computation time so that the method is only useful when the time to calculate one "event" is very small. This requires that the mean number of scatterings be small. In a calculation such as Magnan's the advantages are clear, since the case is not severe and the aims are limited. The range of problems for which the method is useful has yet to be determined.

It might be pointed out that the effects found by Magnan are entirely due to the transverse velocity gradient, which no plane-parallel calculation, as presently formulated, accounts for properly. Therefore, there is no plane-parallel calculation that can be compared with this one in order to determine the effect of spherical geometry. By use of the improved plane-parallel approximation given in this paper such a comparison would be possible.

ACKNOWLEDGMENTS

The author wishes to express his thanks to

D. G. Hummer and W. Kalkofen for several helpful discussions, and to J. Castor for sending manuscripts prior to publication.

REFERENCES

Abyankar, K. C. 1964a, *Ap. J.*, 140, 1353.
Abyankar, K. D. 1964b, *Ap. J.*, 140, 1368.
Abyankar, K. D. 1965, *Ap. J.*, 141, 1056.
Bappu, and Menzel, D. J. 1954, *Ap. J.*, 119, 508.
Beals, C. S. 1931, *Monthly Notices Roy. Astron. Soc.*, 91, 966.
Castor, J. I. 1970, *Monthly Notices Roy. Astron. Soc.* (to be published).
Castor, J. I., and Van Blerkom, D. 1970 (to be published).
Chandrasekhar, S. 1934, *Monthly Notices Roy. Astron. Soc.*, 94, 522.
Feautrier, P. 1964, *Compt. Rend. Acad. Sci. Paris* 258, 3189.
Hummer, D. G. 1962, *Monthly Notices Roy. Astron. Soc.*, 125, 21.
Hummer, D. G. 1968, *Monthly Notices Roy. Astron. Soc.*, 141, 479.
Hummer, D. G., and Rybicki, G. B. 1967, in *Methods of Computational Physics*, Eds. B. Alder, S. Fernbach, M. Rotenberg, Academic Press, New York, p. 53.
Hummer, D. G., and Rybicki, G. B. 1968, *Ap. J.*, 153, L107.
Jefferies, J. T. 1968, *Spectral Line Formation*, Blaisdel, Waltham, Mass.
Kalkofen, W. 1970, proceedings this colloquium, see page 120.
Kulander, J. L. 1964, Thesis, University of Colorado (unpublished).
Kulander, J. L. 1967, *Ap. J.*, 147, 1063.
Kulander, J. L. 1968, *J. Quantit. Spectrosc. Radiat. Transfer*, 8, 273.
Lyong, L. V. 1967, *Soviet Astron.*, 11, 224.
Magnan, C. 1968, *Astrophys. Letters*, 2, 213.
Mathis, J. 1968, in *Resonance Lines in Astrophysics*, Manuscripts presented at a conference held in Boulder, Colorado 9 - 11 September, 1968, National Center for Atmospheric Research, Boulder, Colorado.

McCrea, W. and Mitra, K. 1936, *Z. Astrophys.*, 11, 359.
Milne, E. A. 1930, *Z. Astrophys.* 1, 98.
Oxenius, J. 1965, *J. Quantit. Spectrosc. Radiat. Transfer*, 5, 771.
Rublev, S. V. 1961, *Sov. Astron.*, 4, 780.
Rublev, S. V. 1964, *Sov. Astron.*, 7, 492.
Rybicki, G. B., and Hummer, D. G. 1967, *Ap. J.*, 150, 607.
Rybicki, G. B. and Hummer, D. G. 1969, *Monthly Notices Roy. Astron. Soc.*, 144, 313.
Sobolev, V. V. 1947, *Moving Envelopes of Stars*, Leningrad State University (in Russian); Transl. By S. Gaposchkin, Harvard University Press, Cambridge, Mass., 1960.
Sobolev, V. V. 1957, *Sov. Astron.*, 1, 678.
Sobolev, V. V. 1958, in *Theoretical Astrophysics*, Ed. V. A. Ambartsumyan, Pergamon Press, New York, Chapter 28.

DISCUSSION

The manuscript of Rybicki arrived very late and consequently it was not possible to prepare a condensed version of the lively discussion following this paper. One aspect of the problem of methods was discussed by C. Magnan who has submitted the following summary of his remarks.

APPLICATION OF MONTE CARLO METHODS IN TRANSFER PROBLEMS

by

C. Magnan

Institut d'Astrophysique
Paris

I have not prepared any formal communication. Nevertheless I would like to mention the types of calculation that are now in progress in Paris.

I am handling transfer problems in moving atmospheres by using Monte Carlo techniques. A two-level atom and an isothermal atmosphere are always assumed. Two types of geometry are considered: a spherical atmosphere with a constant velocity of expansion, or a flat disk with constant velocities of expansion and rotation. Non-coherent scattering (either entirely incoherent or partially coherent) is assumed with respect to the "local frequency" (as seen by the absorbing atoms).

Concerning the "creation" of photons, two problems have been handled: the photons are created via absorption of a continuous spectrum produced by an underlying photosphere (the Schuster problem) or they are created within the envelope via electronic collision or recombination from ionized states.

The most typical results concern the Schuster problem. P Cygni type profiles are very well reproduced with the adopted models; symmetrical emission features on both sides of a central absorption line are found in the case of a rotating disk.

At the present time we are limited to cases where the mean number of scatterings is of the order of twenty. The order of magnitude of this number is given by τ/V (where τ is the optical depth of the envelope and V the macroscopic velocity).

LINE FORMATION IN MOVING ATMOSPHERES

by

W. Kalkofen

Smithsonian Astrophysical Observatory
and
Harvard College Observatory
Cambridge, Massachusetts

ABSTRACT

We discuss an integral equation method that permits the calculation of the line source functions and of the emergent profiles in finite and semi-infinite atmospheres with macroscopic motion normal to the surface. Solutions are presented for a semi-infinite atmosphere with a temperature rise in the outward direction and with a flow that decays with increasing depth. The computed profiles have the form of P Cygni lines.

Key words: line formation, moving atmospheres, line-profile computation.

I. INTRODUCTION

Several authors have obtained numerical solutions of the equations of statistical equilibrium and radiative transfer. Magnan (1968) has employed the Monte Carlo method to determine the source function in a model of a planetary nebula; Hummer and Rybicki (1968) have solved a similar problem by means of differential equations with the Riccati transformation; and Kulander (1968) has used differential equations with the Eddington approximation in the solution of the equation of transfer for atmospheres with simple velocity fields. We describe here an integral equation method and apply it in the calculation of the source function in a model of an extended atmosphere.

The various methods have certain limitations. In the Monte Carlo method the history of many photons is computed. Since the accuracy of the solution increases only slowly with the number of photons considered, the desired accuracy must be balanced against the thickness of the medium. In practice, this method is useful only for media with moderate optical thickness. However, the geometry of the medium and the physical processes taken into account may be quite complicated. Thus, incomplete redistribution of the photons over the line can be treated relatively easily. In the Riccati method the integration steps must be comparable with the shortest photon mean free path. Therefore, this method is also restricted to media with relatively small optical thickness. Kulander's technique permits the calculation of the source function in atmospheres with large optical thickness. But the use of the Eddington approximation in flow problems in which the Doppler shift in the normal direction may be large whereas the horizontal shift is zero can lead to large errors. The method is therefore suitable only for exploratory calculations.

The integral equation method is formulated for the case of a plane-parallel medium that may be finite or semi-finite and that has arbitrary flow along the normal to the surface. Anistropic microturbulence can be taken into account if it can be expressed in terms of normal and horizontal components. Complete frequency and angle redistribution of the photons is assumed so that the line component of the source function is frequency-independent and isotropic.

The conditions that we have imposed in the formulation of the integral equation method will frequently be realized approximately in stellar atmospheres. Thus, for lines we may usually assume that the atmosphere is plane-parallel over regions whose horizontal extent is large compared with the thermalization length. The gas flow will usually be directed along the normal to the surface. Other flow patterns could, in principle, be treated by the same method. But differential motion within horizontal layers could not be dealt with easily. In general, however, the Doppler shift due to horizontal differential velocities that might occur, for example, in a uniform expansion should be small over a thermalization length. One may then compute the source function for a vanishing horizontal velocity gradient but must take its effect into account in the calculation of the emergent flux.

The requirement of complete redistribution will usually be nearly satisfied, as Magnan has shown for a planetary nebula. In this context we note that the case of a semi-infinite stellar atmosphere is less severe than that of a planetary nebula, where the intensity outside the line becomes quite small, whereas in a semi-infinite medium the background radiation sets a limit on the intensity. We may therefore assume that the line source function is virtually frequency-independent and isotropic.

Because of these limitations of the methods, one would solve transfer problems for finite media with a complicated geometry using the Monte Carlo method, with a differential equation technique such as that of Hummer and Rybicki or that of Feautrier (1964), which is described in detail by Cuny (1967), or with the integral equation method of Jones and Skumanich (1968). For finite or semi-infinite media with a plane-parallel geometry, one would use either our integral equation or Feautrier's differential equation method. If the transfer is characterized by incomplete redistribution, one would choose the differential equation; if a large number of frequency and angle points has to be taken into account because of high flow velocities, one would choose the integral equation method. If both complications are present, one could attempt to reformulate the equations in terms of the local frequency variable that has been used by Magnan in the Monte Carlo method. For typical problems arising in extended atmospheres, both Feautrier's technique and our integral equation method could be used successfully, but the latter might give somewhat better results.

2. THE BASIC EQUATIONS

We seek the solution of the simultaneous equations of statistical equilibrium and radiative transfer. Following Thomas (1957), we express the statistical equilibrium equation in the form

$$J - S = \varepsilon(S - \tilde{B}) \quad , \tag{1}$$

where S is the frequency- and angle-independent line component of the source function, J is the mean integrated intensity, ε is the probability of true

absorption, and $\tilde{B}$ is the Planck function that depends, in general, on the electron temperature and on the radiation field exclusive of the line radiation. We write the equation of radiative transfer as

$$J(\tau) - S(\tau) = H(\tau,\tau')S(\tau') + C(\tau) \quad , \qquad (2)$$

where C is the contribution of the background radiation to the line intensity J, and H is an integral operator. In the special case of vanishing background radiation, zero flow velocity, and isotropic Doppler broadening, H is related to the well-known Λ-operator.

In the integral equation method we combine equations (1) and (2) into a single equation for the line component S of the source function. The resulting equation, in matrix form, is solved for S by means of a matrix inversion,

$$S = (\varepsilon - H)^{-1}(\varepsilon \tilde{B} + C) \quad . \qquad (3)$$

This procedure, with perhaps minor alterations, is standard for the integral equation method. For depth- and frequency-dependent but angle-independent absorption profiles, this method was developed by Athay and Skumanich (1967). The new feature that we want to discuss is the calculation of the matrix operator H when the absorption profile of the line depends on depth, frequency, and angle so that the monochromatic Λ-operator cannot be used.

We assume that the gas in the atmosphere is moving with the velocity q along the outward normal of the plane-parallel atmosphere; q is an arbitrary function of the depth. The quantity in the transfer equation that is modified by the flow is the absorption profile. If the line is broadened by the Doppler effect and by damping, the profile is given by the Voigt function,

$$\phi_{\Delta\nu,\mu}(\tau) = \frac{1}{\sqrt{\pi}\ \Delta\ \nu_D}\ \frac{a}{\pi} \int_{-\infty}^{\infty} \frac{e^{-y^2}dy}{a^2 + (v - y)^2} \quad , \qquad (4)$$

where a is the damping parameter, $\Delta\nu_D$ is the Doppler

width due to thermal and random microturbulent motion, and v is given by

$$v = \frac{\Delta\nu - (\nu_o/c)q(\tau)\mu}{\Delta\nu_D(\tau,\mu)} \tag{5}$$

The frequency displacement $\Delta\nu$ is measured in the rest frame of the atom and ν_o is the frequency at the line center. We note that the Doppler width depends on direction when the microturbulence is anisotropic.

An important property of the absorption profile ϕ is its symmetry with respect to the frequency displacement $\Delta\nu$ and the direction cosine μ,

$$\phi_{\Delta\nu,\mu}(\tau) = \phi_{-\Delta\nu,\,-\mu}(\tau) \ . \tag{6}$$

Because of this symmetry in ϕ it is convenient to define an average intensity I:

$$\bar{I}_{\Delta\nu,\mu}(\tau) = \frac{1}{2}\left[I^{+}_{\Delta\nu,\,\mu}(\tau) + I^{-}_{-\Delta\nu,-\mu}(\tau)\right] \ , \quad \mu > 0, \tag{7}$$

in which the intensity in the forward direction along the ray $(\Delta\nu,\mu)$ is combined with the intensity in the opposite direction along the ray $(-\Delta\nu,-\mu)$.

The integral form of the transfer equation for $\bar{I}$ is given by the equation

$$\bar{I}_{\Delta\nu,\mu}(\tau_{\Delta\nu,\mu}) = \int_0^{T_{\Delta\nu,\mu}} dt\ K(\tau_{\Delta\nu,\mu},t)\mathcal{S}_{\Delta\nu,\mu}(t), \tag{8}$$

where $\mathcal{S}$ is the total source function,

$$\mathcal{S}_{\Delta\nu,\mu}(\tau) = \frac{k^L(\tau)\phi_{\Delta\nu,\mu}(\tau)S(\tau)\ k^C(\tau)B(\tau)}{k^L(\tau)\phi_{\Delta\nu,\mu}(\tau) + k^C(\tau)} \ , \tag{9}$$

with k^L and k^C the opacities of the line and of the background continuum, respectively, and B the source

function of the background continuum, and where $\tau_{\Delta\nu,\mu}$ is the specific monochromatic optical distance along the ray $(\Delta\nu,\mu)$; $T_{\Delta\nu,\mu}$ is the corresponding distance between the two boundaries if the medium has finite optical thickness.

The integral kernel K is given by the equation

$$K(\tau,t) = \frac{1}{2} e^{-|\tau-t|} \quad . \tag{10}$$

The kernel has the following asymptotic behavior:

$$K(\tau,t) = \delta(\tau,t)\left\{1 + \frac{d^2}{d\tau^2} + \mathcal{O}(e^{-\tau}) + \mathcal{O}[e^{-(T-\tau)}]\right\} \quad , \tag{11}$$

where δ is the Dirac δ-function. At large distances from the boundaries of the medium, therefore, the kernel K becomes essentially the second-derivative operator. The mean integrated intensity J is defined by the expression

$$J(\tau) = \int_{-\infty}^{\infty} d(\Delta\nu) \int_0^1 d\mu \phi_{\Delta\nu,\mu}(\tau)\ \bar{I}_{\Delta\nu,\mu}(\tau) \quad . \tag{12}$$

In order to solve the equations numerically, we choose a discrete set of depth points and expand the total source function $\mathcal{S}$ in terms of piecewise quadratic segments. Instead of the integral operator involving the kernel K, we obtain for equation (8) the product of a matrix operator and the vector of the total source function $\mathcal{S}$. By combining equations (8), (9), and (12) and regrouping terms, we finally obtain the transfer equation in the form of equation (2).

3. SOLUTIONS

Our aim is to study the influence of macroscopic flow on the line source function and on the emergent monochromatic flux, and hence to investigate the formation of "P Cygni lines." To keep the interpretation relatively simple, we have worked with a single model of a semi-infinite plane-parallel atmos-

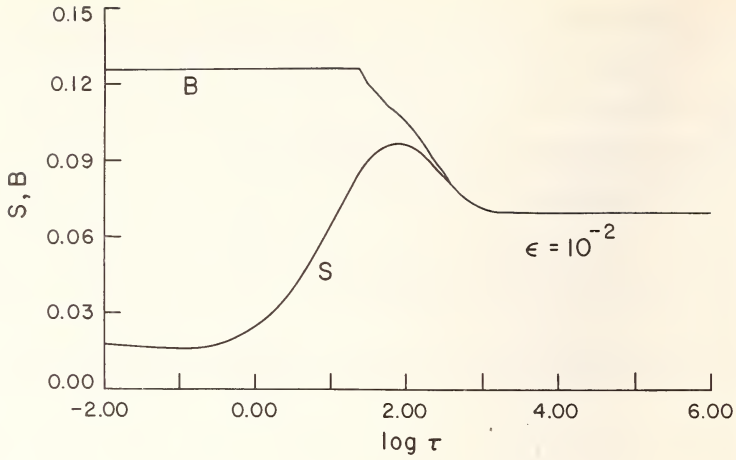

PLANCK FUNCTION AND SOURCE FUNCTION FOR THE VELOCITY $v(\tau) = \frac{2}{1 + \tau/0.1}$

Figure 1.

phere with a temperature rising in the outer layers from 8000°K - 10,000°K. In this medium we compute a line source function with the frequency of the Hα line for $\varepsilon = 10^{-2}$, a = 0, and constant thermal Doppler width. The function $\tilde{B}$ in equation (1) of statistical equilibrium is equal to the source function B of the background continuum. The function $B(\tau)$, divided by $2h\nu^3/c^2$, is plotted in Figures 1 and 3. The ratio of the opacity of the line at the center to that of the background continuum is constant with $k^L/k^C = 10^4$. The velocities $q(\tau)$ are given in units of the constant thermal Doppler width by the equation

$$V(\tau) = \frac{V(0)}{1 + \tau/T} \quad , \tag{13}$$

where

$$V = \frac{\nu_0}{c} \frac{q}{\Delta\nu_D} \quad .$$

The optical depth τ is measured along the local line center.

In a preliminary investigation we have deter-

TABLE 1.

ACCURACY OF THE ANGLE QUADRATURE

Angle approximation	Error (in percent) S (0)	S (0.1)	I (0.3)
7	0.04	0.2	0.06
6	0.1	0.5	0.16
5	0.2	0.9	0.3
4	0.3	1.4	0.6
3	0.5	2.3	1.1
2	1.3	4	2.5
1	1.4	8	9

mined the dependence of the computed source function, the emergent normal intensity, and the emergent monochromatic flux on the angle quadrature. For this purpose we have solved the equations with $V(0) = 2$ and $T = 0.1$. This flow velocity produces a shift of the absorption profile by two Doppler widths at the surface, and the velocity gradient is large only in the outermost layers. The source function has a minimum at a depth of $\tau = 0.1$, and the minimum of the intensity is displaced in the violet direction by 0.3 thermal Doppler width. Table 1 gives the accuracy in percent of the solutions for the first to the seventh angle approximations measured against the solution in the eighth approximation. All solutions were obtained with 63 frequency points in the range (-4,4) of the frequency in Doppler units and 40 points in the depth range $(0,10^6)$. An accuracy of at least one percent in the quantities listed requires at least five discrete angle points. All subsequent solutions were therefore computed with the fifth angle points. All subsequent solutions were therefore computed with the fifth angle approximation. In the calculation of the monochromatic emergent flux, five angles did not give sufficiently accurate results. This quantity was therefore computed in the 24th approximation.

In order to investigate the effects of flow in a moving atmosphere, we have solved the equations for four cases of macroscopic flow and for the static atmosphere. For the flow problems we have chosen

$$V(0) = 10 \quad \text{and} \quad T = 10,\ 10^2,\ 10^3,\ 10^4.$$

Thus the velocity is largest at the surface and decays essentially as τ^{-1}. The gradient is large only near $\tau = T$. The computer plot of these velocities is given in Figure 2.

We note that for $\varepsilon = 10^{-2}$, the "thermalization length" of a Doppler-broadened line is $\tau_0 = 100$. The line that is formed in the atmosphere with the flow parameter $T = 10^4$, therefore, sees only the constant flow velocity corresponding to 10 Doppler widths in the line formation region. Hence the source function should be identical with that of a static atmosphere. This is indeed the case, as can be seen from Figure 3, where the solutions for the stationary medium and for the atmosphere with

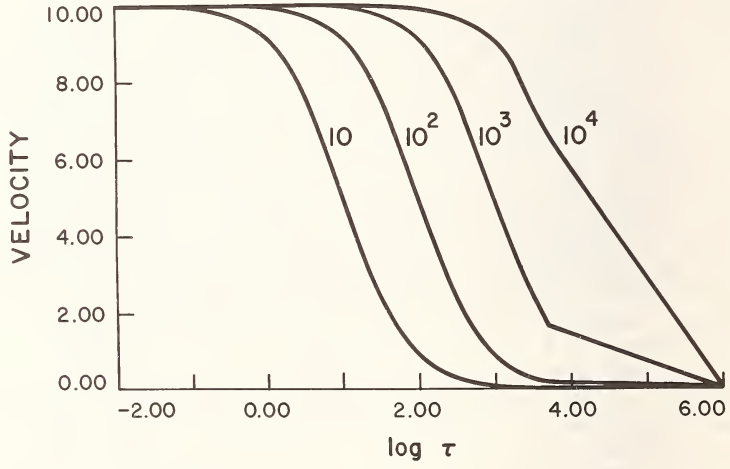

MACROSCOPIC VELOCITIES

$$v(\tau) = \frac{v(0)}{1+\tau/T}\ ,\ v(0)=10\ ,\ T=10\ ,10^2\ ,10^3\ ,10^4$$

Figure 2.

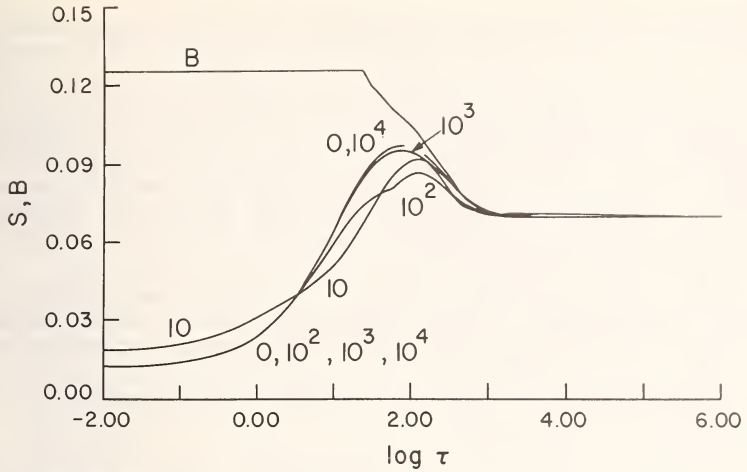

PLANCK FUNCTION AND LINE SOURCE FUNCTIONS FOR $\epsilon = 10^{-2}$ AND $v(\tau) = \frac{10}{1+\tau/T}$, $T = 10, 10^2, 10^3, 10^4$. THE STATIC CASE IS LABELLED BY 0.

Figure 3.

constant expansion velocity in the significant surface layers coincide. For $T = 10^3$, there is already a noticeable gradient in the macroscopic flow in the region of the atmosphere in which the line radiation reaches saturation. Because of the frequency shift of the line opacity, photons emitted near the maximum of S can escape more easily than they can in the static case. The source function maximum is therefore reduced. The surface layers below $\tau = 100$, however, still have a nearly constant flow velocity. The surface value of S is therefore still virtually identical with that of the static solution. The same effects are seen in the source function for $T = 100$, for which the velocity change is large in the relaxation region and small near the surface. Thus the value of the source function at its maximum is further reduced but its surface value is nearly unchanged. For $T = 10$, the velocity gradient is small in the relaxation region and large near the surface. Near the source function maximum, the solution for S, therefore, moves back toward the static solution. But in the surface layers where V is varying rapidly, the line absorption coefficient is now large in a spectral range where the background radiation can exert a stronger

influence on the line radiation. The surface value of S is consequently raised above that of the static case.

If the region in which the velocity gradient is large is pushed sufficiently close to the surface by reducing T further, or if ε is reduced significantly below 10^{-2}, the source function can be forced by the background radiation to rise near the surface. This effect can, indeed, be seen in Figure 1, where $V(0) = 2$ and $T = 0.1$.

The most striking result of these calculations is the similarity in the solutions for a wide range of flows, which indicates that the source functions are not very sensitive to the Doppler shift. The emergent radiation field, however, is strongly influenced by the flow.

The emergent normal intensities are shown in Figure 4. For the static atmosphere the intensity is symmetric. For the flow parameter $T = 10^4$, the intensity is blue-shifted by 10 Doppler widths. The profile is nearly symmetric, only the slight enhancement of the red peak indicating the flow. For smaller values of the flow parameter T, the peaks on the low-frequency side of the line center are more and more shifted to the red, the amplitudes having heights that correspond to the values of the maximum in the source functions. For $T = 10$, the intensity minimum is shifted to $\Delta\nu = 8.75$.

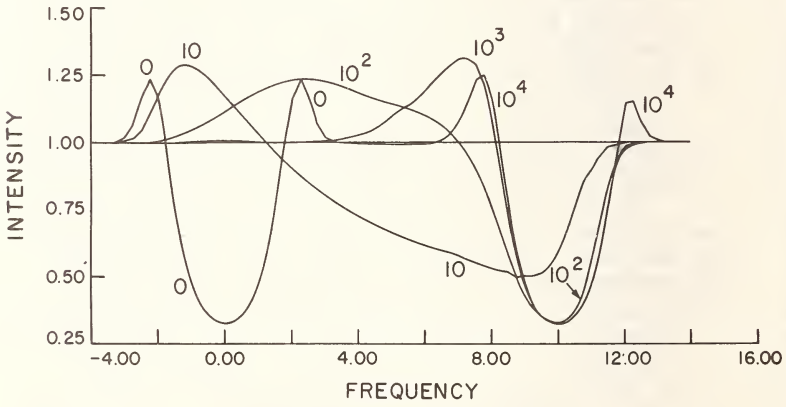

THE NORMAL, EMERGENT INTENSITY FOR $v(\tau) = \frac{v(0)}{1+\tau/T}$ WITH $v(0) = 10$ AND $T = 10, 10^2, 10^3, 10^4$, AND FOR $v(0) = 0$.

Figure 4.

The emergent monochromatic fluxes are plotted in Figure 5. Since the fluxes result from the weighted superposition of intensities for normal emergence, for which the frequency shift amounts to 10 Doppler widths, down to those for grazing emergence, for which the line is centered on $\Delta\nu = 0$, the flux profiles are nonsymmetrical even for the uniform expansion given by the case of $T = 10^4$. Only the static atmosphere produces a symmetrical flux profile. The flux curves for the flows with $T = 10^2$ and $T = 10$ have peaks on the low-frequency side of the line profile. The condition for the appearance of such emission features is that the maximum of the source function fall into a region of the atmosphere for which the flow velocity is sufficiently small.

The minima of the fluxes are blue-shifted by $\Delta\nu = 8.25$ thermal Doppler widths for the flow parameters $T = 10^4$ and 10^3, by $\Delta\nu = 7.75$ for $T = 10^2$, and by $\Delta\nu = 4.5$ for $T = 10$. The two maxima occur at $\Delta\nu = 0.25$ for $T = 10^2$ and at $\Delta\nu = 1.75$ for $T = 10$. The separation of the extrema is therefore $\Delta\nu = 7.5$ Doppler widths for $T = 10^2$ and $\Delta\nu = 6.25$ for $T = 10$. Thus, the blue shift of the central absorption feature is smaller than might have been expected on the basis of a normal velocity displacement of 10^4 Doppler widths, even when the outer layers expand uniformly as, in effect, they do for $T = 10^4$; and the separation of emission and absorption features

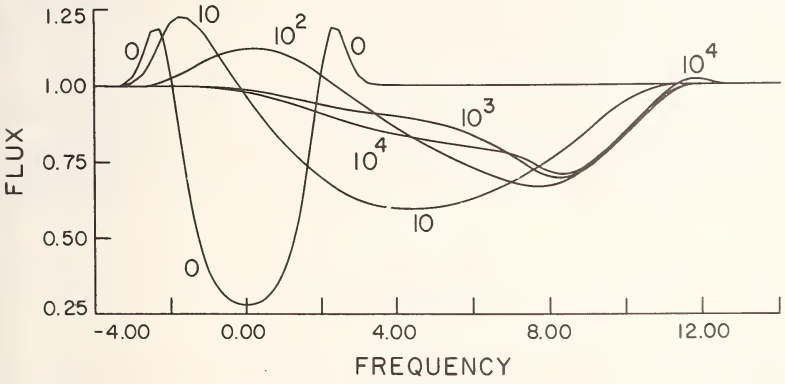

THE EMERGENT MONOCHROMATIC FLUX FOR

$$v(\tau) = \frac{10}{1+\tau/T},\ T = 10, 10^2, 10^3, 10^4,\ \text{AND FOR } v = 0.$$

Figure 5.

is not simply related to the flow velocity in the line formation region. The thermal Doppler width can be easily determined only in the line of the static atmosphere.

4. CONCLUSIONS

The profiles that we have computed have the general appearance of "P Cygni lines," from which they differ mainly in the relatively low emission intensities. The emission can be increased by means of a higher temperature rise in the outer layers of the star. Our model atmosphere was chosen more in accordance with the model calculations of Feautrier (1968) and of Auer and Mihalas (1969), who found temperature increases of 1000° - 2000°K for their models of early-type atmospheres in radiative and statistical equilibrium. Some mechanical mode of energy transport could give a much larger temperature rise as, for example, it does in the Sun. Such a temperature increase has been postulated for the supergiant α Cygni by Groth (1960), who furthermore placed the emission into an inward-falling outer shell at a high temperature. Such an elaborate model atmosphere is clearly not necessary, as our calculations show. The only requirements for the appearance of P Cygni lines are a temperature inversion in the atmosphere or envelope and flow in the outward direction.

It is a pleasure to thank Deane Peterson for discussions of the numerical method, Charles Whitney for useful comments on the interpretation of the results, and Lane Emerson for his help in computing and plotting with the aid of an electronic computer.

REFERENCES

Athay, R. G., and Skumanich, A. 1967, *Ann. d'ap.*, 30, 669.
Auer, L. H., and Mihalas, D. 1969, *Ap. J. (Letters)*, 156, L151.
Cuny, Y. 1967, *Ann. d'ap.*, 30, 143.
Feautrier, P. 1964, *C. R.*, 258, 3189; 1968, *Ann. d'ap.*, 31, 257.
Groth, H. G. 1960, *Z. Astrophys.*, 51, 231.

Hummer, D. G., and Rybicki, G. B. 1968, *Proc. Conf. on Resonance Lines in Astrophys.*, National Center for Atmospheric Research.
Jones, H. P., and Skumanich, A. 1968, *Proc. Conf. on Resonance Lines in Astrophys.*, National Center for Atmospheric Research.
Kuhlander, J. L. 1968, *J.Q.S.R.T.*, 8, 273.
Magnan, C. 1968, *Ap. J. (Letters)*, 2, 213.
Thomas, R. N. 1957, *Ap. J.*, 125, 260.

DISCUSSION

Underhill: How many levels did you include in your calculations?

Kalkofen: We included only two levels to show the principle of the problem.

Underhill: The observations do not show the long tails which you have calculated.

Kalkofen: But there is also an increase in the line core, which is in agreement with the observation. If you apply the theory to the lines in the spectrum of ε Ori the agreement is fairly good.

Underhill: The observations show only very weak P Cyg profiles in Hα.

LASER ACTION IN NON-LTE ATMOSPHERES

by

Donald H. Menzel

Harvard College Observatory
and
Smithsonian Institution Astrophysical Observatory

ABSTRACT

The radiative transfer equation is written in microscopic form, and from some simplifications on the ratio of occupation numbers for upper and lower level, a laser action is suggested.

Key words: radiative transfer, laser action.

I like to write the equation of radiative transfer for line absorption in a plane-parallel atmosphere in the following exact form:

$$\mu \frac{dI}{dr} = - \left(n_1 - n_2 \frac{\tilde{\omega}_1}{\tilde{\omega}_2} \right) I\alpha + \frac{2h\nu^3}{c^2} n_2 \frac{\tilde{\omega}_1}{\tilde{\omega}_2} \alpha , \qquad (1)$$

where I is the specific intensity and α is the atomic absorption coefficient at frequency, ν. The quantities n_1 and n_2 are the atomic populations of the lower and upper levels, whose respective statistical weights are $\tilde{\omega}_1$ and $\tilde{\omega}_2$.

In thermodynamic equilibrium, a single parameter, the absolute temperature T, governs the Boltzmann and Planck formulas, so that

$$\frac{n_2}{n_1} = \frac{\tilde{\omega}_2}{\tilde{\omega}_1} e^{-h\nu/kT} \text{ and } I = \frac{2h\nu^3}{c^2} \frac{1}{e^{h\nu/kT} - 1} . \qquad (2)$$

When these equations are substituted into (1) the right-hand side vanishes, as it must for thermodynamic equilibrium, since the intensity is isotropic and independent of position.

In equation (1), the second term in the parenthesis represents the stimulated emission or, as it should more properly be called, the negative absorption. Too many astrophysicists either combine it with the random emission, the second term on the right-hand side, or neglect it altogether. The true source function takes the form of the second term on the right-hand side of (1), which in no sense resembles a Planck function except when $h\nu >> kT$.

The quantities n_1 and n_2 are to be calculated from the equations of statistical equilibrium, which involve collisional excitation and de-excitation as well as radiational processes.

Many years ago, in problems related to gaseous nebulae, I introduced a dimensionless parameter, b, to indicate the degree of departure of a gas from thermodynamic equilibrium at temperature T of the electron gas. This parameter equalled unity for thermodynamic equilibrium. Thus I could write

$$\frac{n_2}{n_1} = \frac{b_2 \bar{\omega}_2}{b_1 \tilde{\omega}_1} \, e^{-h\nu/kT} \tag{3}$$

with which expression (1) becomes

$$\frac{dI}{dh} \cos\theta = - n_1 \alpha \left[\left(1 - \frac{b_2}{b_1} e^{-h\nu/kt} \right) I + \right.$$
$$\left. + \frac{2h\nu^3}{c^2} \frac{b_2}{b_1} e^{-h\nu/kT} \right] \tag{4}$$

As long as $h\nu/kT >> 1$, we can usually neglect the term representing the stimulated emissions. And, as long as b_2/b_1 does not depart too far from unity, the second term on the right-hand side is approximately equal to the source function.

Many studies have shown that the b's exhibit the following behavior for nebulae and, presumably, also for stars with highly distended atmospheres. First of all, b's for ground or metastable levels

tend to be high. Second, the first excited levels directly above the ground level tend to have b's much less than unity. Third, the b's for still higher levels slowly tend to unity at the series limit.

For all lines except those from the ground or metastable levels, then, b_2/b_1 will exceed unity. And when the temperature is high enough, the stimulated emission may exceed the ordinary absorption so that

$$\frac{dI}{dh} \cos\theta \sim n_1 \alpha \frac{b_2}{b_1} e^{-h\nu/kT}\left(\frac{2h\nu^3}{c^2} + I\right) \quad . \qquad (5)$$

Since this term is essentially positive, the emission line increases in intensity with depth.

This process is truly a laser action, analogous to those responsible for the high-level radio emission of atomic hydrogen. I believe this process can explain many of the anomalies referred to by Miss Underhill as occurring in stars of exceptionally high temperatures.

The process is self-limiting, however, since an increase in the intensity of the incident radiation causes the medium to approach local thermodynamic equilibrium. However, as long as the energy is "diluted," some sort of laser action will occur.

DISCUSSION

Hearn: It is important to know the electron density. In the case of the higher levels you get an equilibrium distribution because of electron collisions. If the electron density is large enough even the lower levels will have a Boltzmann population. For the lower levels the spontaneous emissions are much more important than the induced emissions. In the case of Hα the induced emission is very small. If the electron density is of the order 10^{10} or 10^{12} the lower levels follow the Boltzmann distribution and there is no induced emission at all.

Menzel: There is a cooling effect by forbidden

transitions, which will also cause strong deviations from LTE.

Underhill: In the main part of the atmospheres of WR stars, the electron densities are of the order of 10^{11} to 10^{12} and the electron temperatures are of the order of 30000° to 50000° K. These values are not suitable for efficient laser action, which you have described.

Rybicki: To my knowledge, no non-LTE solutions in multi-level atoms have shown inverted populations for stellar atmospheres extended or not, even when stimulated emissions have been properly included. Of course one should always be aware of this possibility, since, if it occurs, it can be a dominant effect in the formation of the spectrum. It should be noted that any laser action will build up intensities that will tend to destroy the action by returning the population ratios to their normal order. This is particularly true in a strict plane-parallel atmosphere where any negative opacity in a region between two planes would build up infinite intensities, since infinite path lengths exist within the negative opacity region.

LINE FORMATION IN MULTI-DIMENSIONAL MEDIA

by

H. P. Jones and A. Skumanich

High Altitude Observatory and University of Colorado
Boulder, Colorado

ABSTRACT

The flux divergence technique of Athay and Skumanich (1967) is generalized for application to media whose properties vary in more than one spatial dimension. In this method, the flux divergence is viewed as an integro-differential functional of the source function. The source function is then expanded in terms of basis functions along characteristic paths, and, with the help of various interpolations, the flux divergence is converted to an approximate linear algebraic operator on a discrete spatial grid. A large but finite set of linear, inhomogeneous, simultaneous algebraic equations with known matrix coefficients is thus generated and is solved by direct matrix inversion for the source function at each point of the spatial grid.

Some aspects of the accuracy, stability, and computational convenience of the technique are discussed. Sample solutions for depth dependent, axially symmetric variations of temperature are shown.

Key words: radiative transfer in inhomogeneous media, line formation in multi-dimensional media, numerical methods in transfer, matrix methods for integro-differential operators.

I. INTRODUCTION

A casual inspection of a spectroheliogram at almost any wavelength reveals that the radiation field of the solar atmosphere has considerable horizontal structure. The ordinary plane-parallel

idealization is thus at best an average description of the medium, and a more realistic treatment can be provided by model atmospheres whose properties are allowed to vary in two or three dimensions.

The formation of spectrum lines in such media has, until recently, received little attention. Rybicki (1965) has developed Fourier transform techniques suitable for media in which the absorption coefficient is constant with position. Wilson (1968) has published results obtained with a trial and error scheme making use of a three-dimensional equivalent of the Eddington approximation. Avery and House (1968) have adapted the Monte Carlo technique for use in line formation problems and have paid particular attention to spicular geometries.

In the present paper, we will present a new numerical technique for dealing with line formation in multi-dimensional media. The method is a generalization of a one-dimensional technique developed independently by Kuhn (1966) and by Athay and Skumanich (1967). In contrast with the Monte Carlo scheme, it is "deterministic" or non-statistical. The method may be used with variable absorption coefficient and is, in principle, non-iterative for linear problems.

II. BASIC EQUATIONS

We write the time independent transfer equation as

$$\frac{1}{K_\nu(\vec{x})}\,\hat{n}\cdot\vec{\nabla}\,I_\nu(\vec{x},\hat{n}) = S_\nu(\vec{x}) - I_\nu(\vec{x},\hat{n}) \quad . \qquad (1)$$

We have used the following notation: $\vec{x}$ is the position vector of a point in the region of interest; $\hat{n}$ is a unit direction vector; K_ν is the absorption coefficient at frequency ν; S_ν is the source function; I_ν is the specific intensity.

In the one-dimensional case it is customary to use a geometric position variable which increases outward (i.e., away from the region of interest) and an optical depth scale increasing in the opposite sense; this results in the multiplication of the right hand side of (1) by -1. We have not adopted

this convention here. As a result certain sign differences will appear when the following analysis is compared with the equations of Athay and Skumanich (1967).

We define two angular moments of the specific intensity by

$$J_\nu(\vec{x}) = \frac{1}{4\pi} \int I_\nu(\vec{x},\hat{n})\, d\Omega \qquad (2)$$

and

$$\vec{H}_\nu(\vec{x}) = \frac{1}{4\pi} \int \hat{n}\, I_\nu(\vec{x},\hat{n})\, d\Omega \qquad (3)$$

where the integrations are over the full domain of the solid angle Ω. If one integrates Eq. (1) over solid angle, one obtains

$$\frac{1}{K_\nu} \vec{\nabla}\cdot\vec{H}\,(\vec{x}) = S_\nu(\vec{x}) - J_\nu(\vec{x}) \quad . \qquad (4)$$

We wish to consider the equation of transfer at frequencies centered about a spectrum line with maximum absorption coefficient at $\nu = \nu_o$. We split the absorption coefficient into the sum of the part arising from bound-bound processes in the line ($K_L(\nu)$) and the part arising from all other processes occurring at the same frequency ($K_c(\nu)$). Thus, at any point $\vec{x}$, we write

$$K_\nu = K_L(\nu) + K_c(\nu) \quad . \qquad (5)$$

To a good approximation $K_c(\nu)$ is independent of frequency at frequencies where $K_L(\nu)$ is appreciable. Defining $K_c = K_c(\nu_o)$ and $r_\nu = K_c/K_L(\nu)$ we have

$$K_\nu = K_L(\nu)(1 + r_\nu) \quad . \qquad (6)$$

Letting $r_o = r_{\nu_o}$, $K_o = K_L(\nu_o)$, and $\Phi_\nu = \dfrac{K_L(\nu)}{K_o}$ we have

$$K_\nu(\vec{x}) = K_o(\vec{x})(\Phi_\nu(\vec{x}) + r_o(\vec{x})). \quad (7)$$

Separating the emission coefficient in similar fashion and noting that the source function is the ratio of emission to absorption one obtains

$$S_\nu(\vec{x}) = \frac{\phi_\nu(\vec{x}) S_{L,\nu}(\vec{x}) + r_o S_{c,\nu}(\vec{x})}{\Phi_\nu(\vec{x}) + r_o(\vec{x})} \quad (8)$$

where $S_{L\nu}$ and $S_{c\nu}$ are the line and continuum source functions. For this paper, we will take $S_{c,\nu}(\vec{x}) = B_{\nu_o}(T_e(\vec{x})) = B(\vec{x})$; i.e., for frequencies around the line, the continuum source function is the Planck function at frequency ν_o and local electron temperature $T_e(\vec{x})$. If one assumes "complete redistribution" in frequency of scattered radiation in the rest frame of the atom, the line source function is frequency independent. For a two-level atom the statistical equilibrium equation may be written in the form

$$S_L = \frac{\bar{J} + \varepsilon B}{1 + \varepsilon} \quad (9)$$

where

$$\bar{J} = \int_o^\infty \Phi_\nu J_\nu \, d\nu \quad (10)$$

and

$$\varepsilon = \frac{C_{UL}}{A_{UL}} \left(1 - \exp\left\{ - h\nu_o/kT_e \right\}\right) . \quad (11)$$

Here, Φ_ν is the profile coefficient normalized to unity $\left(\Phi_\nu = \phi_\nu / \int_o^\infty \phi_\nu d\nu\right)$, C_{UL} is the collisional rate per atom from the upper to lower levels in the atom, and A_{UL} is the Einstein A coefficient.

To obtain a single equation for the source function, one can use the transfer equation to eliminate $\bar{J}$ from Eq. (9). Operating on (1) with

$$\int_0^\infty d\nu \Phi_\nu ,$$

we have that

$$\int \frac{\Phi_\nu}{K_\nu} \vec{\nabla}\cdot\vec{H}_\nu d\nu = \int \Phi_\nu S_\nu d\nu - \bar{J}. \qquad (12)$$

Substituting (8) and (9) into (12) one has that

$$\int \frac{\Phi_\nu}{K_\nu} \vec{\nabla}\cdot\vec{H}_\nu d\nu = S_L \int \frac{\Phi_\nu \phi_\nu d\nu}{\phi_\nu + r_o} - (1+\varepsilon) S_L + \varepsilon B + B \int \frac{r_o \Phi_\nu d\nu}{\phi_\nu + r_o} \quad . \qquad (13$$

We define

$$\delta = \int \frac{r_o \Phi_\nu d\nu}{\phi_\nu + r_o}$$

and note that since

$$\frac{\phi_\nu}{\phi_\nu + r_o} = 1 - \frac{r_o}{\phi_\nu + r_o}$$

$$\int \frac{\phi_\nu \Phi_\nu d\nu}{\phi_\nu + r_o} = 1 - \delta \ . \qquad (14$$

Putting (14) into (13) and combining terms, one finally has that

$$S_L + \frac{1}{\varepsilon+\delta} \int_0^\infty \frac{\Phi_\nu}{K_\nu} \vec{\nabla}\cdot\vec{H}_\nu d\nu = B \quad . \qquad (15$$

We will use (15) as the basic equation in developing our multi-dimensional technique. It is incomplete, however, until we relate $\vec{\nabla}\cdot\vec{H}_\nu$ to S_L and B i.e., until we express $\vec{H}_\nu$ as a functional of S_L and B. To find the needed relation we must turn to the formal solution of the equation of transfer.

At any point $\vec{x}$ we form characteristics or paths, $p(\vec{x},\hat{n})$, which are straight lines passing through $\vec{x}$ in direction $\hat{n}$. If s represents a geometric length along the path, measured from some arbitrary origin and increasing in direction $\hat{n}$, the vector $\vec{x}^p(s)$ of any point on the path is given by

$$\vec{x}^p(s) = \vec{x} + \hat{n}\ (s-s_o) \qquad (16)$$

where s_o is the distance from $\vec{x}$ to the point at which s = o. Figure 1 illustrates the path geometry.

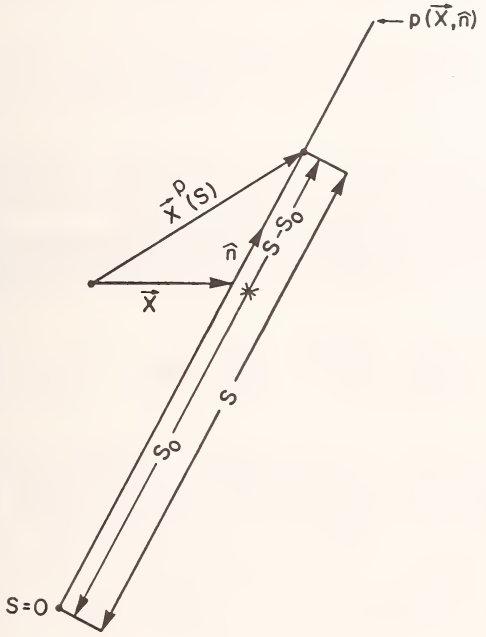

Figure 1. Geometry of a path $p(\vec{x},\hat{n})$ passing through $\vec{x}$ in direction $\hat{n}$. Geometric length s is measured from an arbitrary origin and increases in the same sense as $\hat{n}$. s_o is the length from the origin to $\vec{x}$, and $\vec{x}^p(s)$ is the position vector of an arbitrary point on the path.

We define an optical path length, t_ν, by

$$t_\nu(s) = \int_0^s K_\nu(\vec{x}^p(s'))\, ds' \tag{17}$$

and adopt the following conventions: a quantity evaluated along the path will be denoted by a script letter. If it is regarded as a function of geometric path length, a superscript s will be included, while if no superscript appears, the quantity is understood to be a function of optical path length at frequency ν.
Thus

$$S_\nu(\vec{x}^p(s)) = \mathcal{S}_\nu^s(s) = \mathcal{S}_\nu(t_\nu(s)), \tag{18}$$

$$I_\nu(\vec{x}^p(s)) = \mathcal{I}_\nu^s(s) = \mathcal{I}_\nu(t_\nu(s)), \tag{19}$$

$$K_\nu(\vec{x}^p(s)) = k_\nu^s(s) = k_\nu(t_\nu(s)). \tag{20}$$

It must be remembered that our path notation implies that a script quantity is an implicit function in $\vec{x}$ and $\hat{n}$ and explicit in path length.

With these definitions and conventions, the equation of transfer (1) may be rewritten as

$$\frac{1}{k_\nu(s)} \frac{d\mathcal{I}_\nu^s}{ds} = \frac{d\mathcal{I}_\nu}{dt_\nu} = \mathcal{S}_\nu - \mathcal{I}_\nu . \tag{21}$$

Equation (21) has the well-known solution for $\mathcal{I}_\nu$ in terms of $\mathcal{S}_\nu$

$$\mathcal{I}_\nu(t_\nu) = e^{-t_\nu}\mathcal{I}_\nu(o) + e^{-t_\nu}\int_0^{t_\nu} \mathcal{S}_\nu(t'_\nu) e^{t'_\nu}\, dt'_\nu \quad . \tag{22}$$

We will assume that $\vec{x}^p(s=0)$ is at a boundary and either $\mathcal{I}_\nu(0) = 0$ or is specified by appropriate boundary conditions. Since we shall be considering half-spaces we shall assume that $\mathcal{I}_\nu(0)$ is suffi-

ciently bounded so that $e^{-t_\nu}\mathcal{I}_\nu(0)\to 0$ for $t_\nu\to\infty$.

In Eq. (15) we are interested in the quantity

$$\int_{-\infty}^{\infty} \frac{\Phi_\nu}{k_\nu} \vec{\nabla}\cdot\vec{H}_\nu d\nu \ .$$

We note that

$$\frac{1}{K_\nu} \vec{\nabla}\cdot\vec{H}_\nu = \frac{1}{4\pi} \int \frac{d\mathcal{I}_\nu}{dt_\nu} d\Omega \ . \tag{23}$$

Note that $d\mathcal{I}_\nu/dt_\nu$ depends implicitly on direction and location. Our final functional relation is that

$$\int^{\infty} \frac{\Phi_\nu}{K_\nu} \vec{\nabla}\cdot\vec{H}_\nu d\nu =$$

$$= \frac{1}{4\pi} \int_0^{\infty} \int_\Omega \frac{\Phi_\nu}{K_\nu} \frac{d}{dt_\nu} \left(e^{-t_\nu} \int_0^{t_\nu} \mathcal{I}_\nu(t'_\nu) e^{t'_\nu} \, dt'_\nu \right) d\Omega d\nu . \tag{24}$$

An alternate expression can be obtained by transforming the integration in (24) to a volume integration. For example, one can show (cf. among others, Rybicki 1965) that

$$\vec{H}_\nu(\vec{x}) = \frac{1}{4\pi} \int_V K_\nu(\vec{x}') S_\nu(\vec{x}') e^{-\tau_\nu(\vec{x},\vec{x}')} \frac{(\vec{x}-\vec{x}')}{|\vec{x}-\vec{x}'|^3} d^3\vec{x}' \tag{25}$$

where V is the volume of interest. Here, $\tau_\nu(\vec{x},\vec{x}')$ is the optical path length along the characteristic between the "field point" $\vec{x}$ and the "source point" $\vec{x}'$. In this case, Eq. (24) becomes

$$\int_{-\infty}^{\infty} \frac{\Phi_\nu}{K_\nu} \vec{\nabla}\cdot\vec{H}_\nu d\nu =$$

$$= \frac{1}{4\pi} \int_0^{\infty} \frac{\Phi_\nu}{K_\nu} \vec{\nabla}\cdot \int_V S_\nu(\vec{x}') K_\nu(\vec{x}') e^{-\tau_\nu(\vec{x},\vec{x}')} \frac{(\vec{x}-\vec{x}')}{|\vec{x}-\vec{x}'|^3} d^3\vec{x}' . \tag{26}$$

In either case, we see that the weighted frequency integral of the flux divergence is an integro-differential operator on the total monochromatic source function. We call this operator α_V if (26) is to be used and α_p if (24) is used; more precisely, we write

$$\frac{1}{\varepsilon+\delta}\int_{-\infty}^{\infty}\frac{\Phi_\nu}{K_\nu}\nabla\cdot\vec{H}_\nu d\nu = \alpha_V(S_\nu) = \alpha_p(\mathscr{J}_\nu).$$

Note particularly that α is a linear operator, i.e.,

$$\alpha(a\,S_\nu^1 + b\,S_\nu^2) = a\alpha(S_\nu^1) + b\alpha(S_\nu^2) \qquad (27)$$

where a and b are arbitrary constants, α is α_V or α_p and S_ν^1 and S_ν^2 are arbitrary functions of appropriate arguments. The linearity of α holds only so long as k_ν is independent of S_ν, a condition that is approximately satisfied in some, but by no means all, situations of astrophysical interest. If the operator is non-linear, then iterative techniques must be employed.

In general form, then (15) may be written

$$S_L + \alpha_p\mathscr{J}_\nu = S_L + \alpha_V S_\nu = B. \qquad (28)$$

Using (8) and (27) we have that*

$$S_L + \alpha_V\left(\frac{\phi_\nu S_L}{\phi_\nu + r_o}\right) = B - \alpha_V\left(\frac{r_o B}{\phi_\nu + r_o}\right) = B'. \qquad (29)$$

Letting $\alpha_V^\circ(S_L) = \alpha_V\left(\frac{\phi_\nu S_L}{\phi_\nu + r_o}\right)$ and $\alpha_V'(B) = \alpha_V\left(\frac{r_{oB}}{\phi_\nu + r_o}\right)$,

we have

$$(\underline{1} + \alpha_V^\circ)\,S_L = (\underline{1} - \alpha_V')B = B' \qquad (30)$$

---

* Note that (29) holds even if α is non-linear since it remains linear in the factor S_ν.

where $\underline{1}$ is the unit operator. We regard, ε, δ, and B' as known functions and wish to solve for S_L. Formally,

$$S_L(\vec{x}) = (\underline{1} + \alpha_\nu^\circ)^{-1} B'(\vec{x}) \quad . \tag{31}$$

We now seek an algebraic representation of α. The basic step is to assume that we may represent S_ν in terms of its values on a finite grid of space points $\{\vec{x}_n;\ n = 1,2, \ldots N\}$, i.e., we assume

$$S_\nu(\vec{x}) \simeq \sum_{n'=1}^{N} P_{\nu,n'}(\vec{x}) S_\nu(\vec{x}_{n'}) \tag{32}$$

where the functions $\{P_{\nu,n}(\vec{x});\ n = 1,2, \ldots, N\}$ are presumed known** but are left unspecified for the moment. We let

$$\alpha_n^\circ(\vec{x}) = \alpha_V\left(\frac{\phi_\nu}{\phi_\nu + r_o} P_{\nu,n}\right) = \alpha_p\left(\frac{\phi_\nu}{\phi_\nu + r_o} P_{\nu,n}(\vec{x}^p(t_\nu))\right)$$

and

$$\alpha'_n(\vec{x}) = \alpha_V\left(\frac{r_o}{\phi_\nu + r_o} P_{\nu,n}\right) = \alpha_p\left(\frac{r_o}{\phi_\nu + r_o} P_{\nu,n}(\vec{x}^p(t_\nu))\right) \quad .$$

Then (29) becomes

$$S_L(\vec{x}) + \sum_{n'=1}^{N} \alpha_{n'}^\circ(\vec{x}) S_L(\vec{x}_{n'}) = B'(\vec{x}) \tag{33}$$

with

$$B'(\vec{x}) = B(\vec{x}) - \sum_{n'=1}^{N} \alpha'_{n'}(\vec{x}) B(\vec{x}_{n'}) \quad . \tag{34}$$

** If the $P_{\nu,n}(\vec{x})$ are known in terms of the spectral functions of the operator α, then the truncation error in (32) is, in principle, known.

Setting $B'(x_n) = B'_n$, $S_L(x_n) = S_n$, and evaluating (33) at each of the grid points one obtains the N-fold set of equations

$$S_n + \sum_{n'=1}^{N} \alpha^{\circ}_{n'}(\vec{x}_n) S_{n'} = B'_n \quad , \quad n = 1, \ldots, N. \tag{35}$$

Letting $\alpha^{\circ}_{nn'} = \alpha^{\circ}_{n'}(\vec{x}_n)$, we have

$$\sum_{n'} (\delta_{nn'} + \alpha^{\circ}_{nn'}) S_{n'} = B'_n \tag{36}$$

where $\delta_{nn'}$ is the Kronecker delta. Clearly, (36) is the algebraic analog of (30). Defining $Q_{nn'} = \delta_{nn'} + \alpha^{\circ}_{nn'}$ one finally has

$$\sum_{n'} Q_{nn'} S_{n'} = B'_n \tag{37}$$

We have thus expressed αS at any point of our grid as a linear combination of S's at every other point on the grid; i.e., we have formed a set of N inhomogeneous, simultaneous, linear, algebraic equations with known coefficients (provided we can evaluate $\alpha^{Q}_{n'}(\vec{x}_n)$) which may be cast in matrix-vector form and solved by some suitable standard matrix inversion technique. The method is non-iterative if a direct inversion scheme such as Gauss elimination is used.

The method is limited in practice by the size of the matrices that can be calculated, stored, and inverted. Even a modest grid may produce quite a large matrix; for example, for a 30 × 30 two-dimensional grid, the matrix Q has order of approximately 1,000. If the matrix is full, roughly 10^6 numbers must be calculated and stored and a 1,000 × 1,000 matrix must be inverted. A high speed, large-scale computer is thus a necessity.

In view of the scale of the computations, a desirable characteristic of the method is that it be spatially stable, that is, the solutions should be relatively insensitive to the "fineness" of the discrete grid. One reason for choosing (15) as the basic operator equation is that previous experience in one-dimension (cf. Athay and Skumanich 1967) indicates just this kind of stability.

III. EVALUATION OF THE FLUX DIVERGENCE OPERATOR

The method outlined in the preceding section illustrates the form of the procedure we have used but masks considerable detail. In particular, we have not said how to evaluate $\alpha(P_{\nu,n}(\vec{x}))$; nor have we specified what functions $P_{\nu,n}(\vec{x})$ are suitable for our purposes. We proceed to examine both of these points in more detail.

To evaluate $\alpha(P_{\nu,n})$ for any known function $P_{\nu,n}(\vec{x})$ we may use either (24) or (26). Equation (26) has the more concise analytic form and may appear to be more suitable at first sight. However, useful closed-form expressions for $\alpha_n(\vec{x})$ are difficult to obtain even for simple functions $P_{\nu,n}$ and standard two-dimensional geometries. They are nearly impossible to obtain if one considers a wide class of problems with variable absorption coefficient (possibly given in tabular form, for example). We have tried approximating volume integrals of the form in (25) by certain types of quadrature formulae and have met with some success. However, we have not yet been able to satisfactorily carry out the full set of operations in (26). Further, the methods so far devised have proven extremely inefficient with regard to computing time. Some of the difficulty may be seen in the behavior of the kernel

$$e^{-\tau_\nu(\vec{x},\vec{x}')} \frac{(\vec{x}-\vec{x}')}{|\vec{x}-\vec{x}'|^3}$$

which has a singularity (although integrable) at $\vec{x} = \vec{x}'$ and whose variation differs considerably in different parts of the range of $\vec{x} - \vec{x}'$.

We have found equation (24) to be more suitable for numerical purposes. The operations involved here are fairly simple and are in a form where variable absorption coefficient can be handled more conveniently.

The disadvantage in the use of (24) is that the dependence of the operators on the basic spatial coordinates $\vec{x}$ is now implicit. One must thus be careful to preserve the order of the operations and must be prepared to relate functions evaluated along a path to those evaluated in the basic coordinate system.

Though much of what follows is applicable to general geometries, we now confine our attention to a two-dimensional, axisymmetric medium. The atmosphere is bounded by a plane at $z = 0$ and is semi-infinite in the z-coordinate. We take z to increase into the atmosphere. The axis of symmetry is perpendicular to the boundary, distance from the axis is denoted by r, and $0 \leq r \leq \infty$. Directions $\hat{n}$ at points (r,z) in the medium are specified by two angles, θ and ϕ, such that $\hat{n}\cdot\hat{r} = \sin\theta\cos\phi$ and $\hat{n}\cdot\hat{z} = \cos\theta$, where r and z are local unit vectors in the direction of increasing coordinate.

We assume, as we have indicated before, that we can write along a path

$$\mathscr{I}_\nu(t_\nu) \simeq \sum_{\ell=1}^{N} c_\ell f_\ell(t_\nu) \tag{38}$$

where the f_ℓ are the quadratic basic functions of Avrett and Loeser (1963),

$$\begin{aligned} f_1(t) &= 1 \\ f_\ell(t) &\begin{cases} = (1 - \frac{t}{t_\ell})^2 & 0 \leq t \leq t_\ell \\ = 0 & t > t_\ell \end{cases} \quad \ell = 2,3,\ldots,N-1 \\ f_N(t) &= t. \end{aligned} \tag{39}$$

We choose the constants c_ℓ such that

$$\mathscr{I}_\nu(t_m) = \sum_{\ell=1}^{N} c_\ell\, f_\ell(t_m) \equiv \sum_{\ell=1}^{N} F_{m\ell} c_\ell \quad . \tag{40}$$

Thus

$$c_\ell = \sum_{m=1}^{N} F_{\ell m} \mathscr{I}_\nu(t_m) \tag{41}$$

or

$$\mathscr{I}_\nu(t_\nu) \simeq \sum_{m=1} \left\{ \sum_{\ell=1} f_\ell(t_\nu) F_{\ell m}^{-1} \right\} \mathscr{I}_\nu(t_m). \tag{42}$$

For a given set of t_m, the $F_{\ell m}^{-1}$ are easy to compute (cf. Athay and Skumanich 1967). We shall use the same set of t_m for each frequency. The geometric point along the path corresponding to a given t_m is therefore a function of frequency and we relate $\mathcal{J}_\nu(t_m)$ to $\mathcal{J}_\nu^S(s_k)$ for a fixed set of s_k by an interpolatory transformation due to Kalkofen (1967), i.e.,

$$\mathcal{J}_\nu(t_m) = \sum_k V_{mk}(\nu,\vec{x},\hat{n})\mathcal{J}_\nu^S(s_k) \tag{43}$$

where the transformation depends on the frequency ν and the path $p(\vec{x},\hat{n})$. We note here that any spatial variations in k_ν are introduced via V_{mk}.

Similarly, we transform $\mathcal{J}_\nu^S(s_k)$ to $S_\nu(\vec{x}_{n'})$ by an interpolatory routine such that

$$\mathcal{J}_\nu^S(s_k) = \sum_{n'} T_{kn'}(\vec{x},\hat{n})S_\nu(\vec{x}_{n'}). \tag{44}$$

Thus we have that

$$\mathcal{J}_\nu(t_\nu) \simeq \sum_{\ell,m,k,n'} f_\ell(t_\nu)F_{\ell m}^{-1}V_{mk}T_{kn'}S_\nu(\vec{x}_{n'})$$

$$= \sum_{n'} P_{\nu,n'}(t_\nu)S_\nu(\vec{x}_{n'}) = \sum_{n'} P_{\nu,n'}(\vec{x}^p(t_\nu))S(\vec{x}_{n'}). \tag{45}$$

The elements of V and T will be discussed in a later section. We now proceed to evaluate $\alpha_p(P_{\nu,n'}(t_\nu))$.

According to (24) the first step is to find

$$\mathcal{J}_\nu(t_\nu) = e^{-t_\nu}\int_0^{t_\nu}\mathcal{J}_\nu(t_\nu')e^{t_\nu'}dt_\nu' \quad . \tag{46}$$

To accomodate the semi-infinite geometry more conveniently, we will now restrict our paths to have directions $\hat{n}$ with $0 \leq \theta \leq \pi/2$ and will evaluate $\mathcal{J}_\nu(t_\nu)$ in both the $+\hat{n}$ and $-\hat{n}$ directions. We therefore define

$$\left.\begin{aligned} \mathcal{J}_\nu^+(t_\nu^+) &= \mathcal{J}_\nu(t_\nu)_{(\vec{x},\theta,\phi)} \\ \mathcal{J}_\nu^-(t_\nu^+) &= \mathcal{J}_\nu(t_\nu)_{(\vec{x},\pi-\theta,\phi+\pi)} \end{aligned}\right\} 0 \leq \theta \leq \frac{\pi}{2} \qquad (47)$$

where the subscripts give the arguments defining the path. The origin of geometric and optical path length is taken to be at the intersection of the path and the boundary plane. The notation t_ν^+ implies optical path length measured in the above way and increasing into the medium, while t_ν on the right hand side of (47) implies optical path length increasing in the same sense as $\hat{n}$ implied in the subscripts. Thus

$$\left.\frac{d\mathcal{J}_\nu(t_\nu)}{dt_\nu}\right)_{(x,\pi-\theta,\phi+\pi)} = -\left.\frac{d\mathcal{J}_\nu^-(t_\nu^+)}{dt_\nu^+}\right)_{(\vec{x},\theta,\phi)} .$$

We will henceforth drop the + from t_ν, always understand that our paths are now restricted, and remember that we must use

$$-\frac{d\mathcal{J}_\nu^-}{dt_\nu}$$

in evaluating our operator.

Now Eq. (46) yields

$$\mathcal{J}_\nu^+ = e^{-t_\nu}\int_0^{t_\nu} \mathcal{S}_\nu(t'_\nu)e^{t'_\nu}dt'_\nu \equiv \mathcal{L}_\nu^+(\mathcal{S}_\nu) \qquad (48)$$

and

$$\mathcal{J}_\nu^- = e^{t_\nu}\int_{t_\nu}^{\infty} \mathcal{S}_\nu(t'_\nu)e^{-t_\nu}\,dt'_\nu \equiv \mathcal{L}_\nu^-(\mathcal{S}_\nu) \qquad (49)$$

Letting $\mathcal{G}_\ell^\pm(t_\nu) = \mathcal{L}_\nu^\pm(f_\ell)$, we have that

$$\mathcal{G}^{\pm}_{\nu}(t_\nu) = \sum_{\ell,m,k,n'} \mathcal{G}^{\pm}_{\ell}(t_\nu) F^{-1}_{\ell m} V_{mk} T_{kn'} S_\nu(\vec{x}_{n'}) \qquad (50)$$

where

$$\mathcal{G}^{+}_{1}(t_\nu) = 1 - e^{-t_\nu}$$

$$\mathcal{G}^{+}_{\ell}(t_\nu) =$$

$$= \begin{cases} \left(1 - \frac{t_\nu}{t_\ell}\right)^2 + \frac{2}{t_\ell}\left(1 - \frac{t_\nu}{t_\ell}\right) + \frac{2}{t_\ell^2} - e^{-t_\nu}\left(1 + \frac{2}{t_\ell} + \frac{2}{t_\ell^2}\right); 0 \le t_\nu \le t_\ell \\ \frac{2e^{-(t_\nu - t_\ell}}{t_\ell^2} - e^{-t_\nu}\left(1 + \frac{2}{t_\ell} + \frac{2}{t^2_\ell}\right); \; t_\ell < t_\nu < \infty \end{cases}$$

$\ell = 2,3,\ldots N-1$ (51)

$$\mathcal{G}^{+}_{N}(t_\nu) = e^{-t_\nu} + t_\nu - 1$$

and

$$\mathcal{G}^{-}_{1}(t_\nu) = 1$$

$$\mathcal{G}^{-}_{\ell}(t_\nu) =$$

$$= \begin{cases} \frac{-2e^{-(t_\ell - t_\nu)}}{t_\ell^2} + \left[\left(1 - \frac{t_\nu}{t_\ell}\right)^2 - \frac{2}{t_\ell}\left(1 - \frac{t_\nu}{t_\ell}\right) + \frac{2}{t_\ell^2}\right]; 0 \le t_\nu \le t_\ell \\ 0; \; t_\ell < t_\nu < \infty \end{cases}$$

$\ell = 2,3,\ldots N-1$ (52)

$$\mathcal{G}^{-}_{N}(t_\nu) = 1 + t_\nu \quad .$$

We note that $G^{\pm}$ is the "path" analog of the G-function introduced by Athay and Skumanich (1967).

We can now take the derivative of (50) by differentiating (51) and (52). Note that the f_ℓ in (38) are well suited for this procedure since both the f_ℓ and their first derivatives are continuous over the entire range of the argument. Thus, we have that, letting

$$d\mathcal{G}_\ell^{\pm}(t_\nu)/dt_\nu = \dot{\mathcal{G}}_\ell^{\pm} \quad ,$$

$$\frac{d\mathcal{D}_\nu^{\pm}(t_\nu)}{dt_\nu} = \sum_{\ell,m,k,n'} \dot{\mathcal{G}}_\ell^{\pm}(t_\nu) F_{\ell m}^{-1} V_{mk} T_{kn'} S_\nu(\vec{x}_{n'}) \qquad (53)$$

$$\dot{\mathcal{G}}_1^{+}(t_\nu) = e^{-\tau_\nu} \qquad (54)$$

$$\mathcal{G}_\ell^{+}(t_\nu) = \begin{cases} e^{-t_\nu}\left(1+\frac{2}{t_\ell}+\frac{2}{t_\ell^2}\right)-\frac{2}{t_\ell}\left(1-\frac{t_\nu}{t_\ell}+\frac{1}{t_\ell}\right); 0\leq t_\nu \leq t_\ell \\ e^{-t_\nu}\left(1+\frac{2}{t_\ell}+\frac{2}{t_\ell^2}\right)-\frac{2e^{-(t_\nu-t_\ell)}}{t_\ell^2}; \; t_\ell < t_\nu < \infty \end{cases}$$

$$\ell = 2,3,\ldots N-1$$

$$\dot{\mathcal{G}}_N^{+}(t_\nu) = 1 - e^{-t_\nu}$$

and that

$$\dot{\mathcal{G}}_1^{-}(t_\nu) = 0$$

$$\dot{\mathcal{G}}_\ell^{-}(t_\nu) = \begin{cases} -2\left[\frac{e^{-(t_\ell-t_\nu)}}{t_\ell}-\frac{1}{t_\ell^2}+\frac{1}{t_\ell}\left(1-\frac{t_\nu}{t_\ell}\right)\right]; \; 0 \leq t_\nu \leq t_\ell \\ 0; \; t_\ell < t_\nu < \infty \end{cases}$$

$$\ell = 2,3,\ldots,N-1 \qquad (55)$$

$$\dot{\mathcal{G}}_N^{-}(t_\nu) = 1 \quad .$$

As indicated previously (cf. pg. 151) we have transformed $\mathcal{I}$ defined on an "internal" space of path grid points $t_\nu = \{t_\ell,\ \ell = 1,\ldots,N\}$ to an "external" space $s = \{s_\ell,\ = 1,\ldots N\}$ via $\mathcal{I} = V\mathcal{I}^S$. If we were to proceed in strict analogy to the one-dimensional case, we would evaluate $\mathcal{G}^{\pm}_\ell(t_\nu)$ at each of the internal points $\{t_n,\ n = 1,\ldots,N\}$. Then, letting $(\mathcal{G}^{\pm}F^{-1})_{n,m} = \sum_\ell \mathcal{G}^{\pm}_\ell(t_n)F^{-1}_{\ell m}$, we would transform the vector $(\mathcal{G}^{\pm}F^{-1})V\mathcal{I}^S$, which is defined on the internal grid to a vector on the external grid by some other (inverse) interpolatory scheme represented by a matrix W. In other words,

$$(\mathcal{G}^{\pm}F^{-1})_{ext} = W(\mathcal{G}^{\pm}F^{-1})_{int}V \quad ,$$

(cf. Kalkofen 1968). Because of the simple nature of the dependence of $\mathcal{G}^{\pm}_\ell(t_\nu)$ on t_ν, we have not found this necessary. Instead, we calculate $t_\nu(\vec{x},\hat{n})$ for every ν, $\vec{x}$, and $\hat{n}$ and proceed analytically. This is done conveniently by precalculating the following quantities:

$$h_m = \sum_{\ell=2}^{N-1} F^{-1}_{\ell m}\left(1 + \frac{2}{t_\ell} + \frac{2}{t_\ell^{\,2}}\right)$$

$$U^{+}_{1m} = 0$$

$$U^{+}_{nm} = 2\sum_{\ell=2}^{n} \frac{F^{-1}_{\ell m}\, e^{-(t_\ell - t_{n+1})}}{t_\ell^{\,2}}$$

$$U^{-}_{nm} = 2\sum_{\ell=n+1}^{N-1} \frac{F^{-1}_{\ell m}\, e^{-(t_\ell - t_{n+1})}}{t_\ell^{\,2}}$$

$$V^{+}_{nm} = 2\sum_{\ell=n+1}^{N-1} \frac{F^{-1}_{\ell m}}{t_\ell^{\,2}}$$

$$W^{+}_{nm} = 2 \sum_{\ell=n+1}^{N-1} \frac{F^{-1}_{\ell m}}{t_\ell} \left(1 + \frac{1}{t_\ell}\right)$$

$$W^{-}_{nm} = W^{+}_{nm} - 2V^{+}_{nm}$$

$$U^{-}_{N-1,m} = U^{-}_{N,m} = V^{+}_{N-1,m} = V^{+}_{N,m} = W^{\pm}_{N-1,m} = W^{\pm}_{N,m} = 0 \quad .$$

Using the above quantities, one can show that

$$(\dot{\mathcal{G}}^{+}F^{-1})_{t_\nu,m} = \sum_{\ell=1}^{N} \dot{\mathcal{G}}^{+}_{\ell}(t_\nu)F^{-}_{\ell m} = e^{-t_\nu}\left(h_m + F^{-1}_{1m} - F^{-1}_{Nm}\right)$$
$$-e^{-(t_\nu - t_n)}U^{+}_{nm} + t_\nu V^{+}_{nm}$$
$$-W^{+}_{nm} + F^{-1}_{Nm}$$

and

$$(\dot{\mathcal{G}}^{-}F^{-1})_{t_\nu,m} = \sum_{\ell=1}^{N} \dot{\mathcal{G}}^{-}_{\ell}(t_\nu)F^{-1}_{\ell m} = -e^{-(t_{n+1} - t_\nu)}U^{-}_{nm} + t_\nu V^{+}_{n,m}$$
$$-W^{-}_{n,m} + F^{-1}_{N,m}$$

where $t_n < t_\nu \leq t_{n+1}$. Thus $(\dot{\mathcal{G}}^{\pm}F^{-1})_{t_\nu,m}$ can be evaluated for any t_ν by calculating three exponentials, finding n (i.e., the interval in which t_ν lies), and performing a small number of multiplications and additions.

The remaining operations are integrations over solid angle and frequency. We first consider

$$\frac{1}{K_\nu}\vec{\nabla}\cdot\vec{H}_\nu = \frac{1}{4\pi}\int_0^{2\pi} d\phi \int_0^{\pi} \sin\theta \, d\theta \left(\frac{d\mathcal{D}_\nu}{dt_\nu}\right)_{(\vec{x},\theta,\phi)} \quad . \qquad (56)$$

Noting that a characteristic passes through the same r and z points for both $+\phi$ and $-\phi$, we have

$$\frac{1}{K_\nu}\nabla\cdot\vec{H}_\nu = \frac{1}{2\pi}\int_0^\pi d\phi \int_0^\pi \sin\theta\, d\theta \left(\frac{d\mathcal{J}_\nu}{dt_\nu}\right)_{(\vec{x},\theta,\phi)} . \quad (57)$$

We approximate both integrals by quadrature formulae. Although many schemes are possible, we have used Gauss-Legendre quadrature for the θ - integration and Gauss-Chebyshev quadrature for the ϕ -integration (cf. *Handbook of Mathematical Functions*, AMS 55, 1964). Thus

$$\frac{1}{K_\nu}\nabla\cdot\vec{H} = \frac{1}{2\pi}\sum_{\mu=1}^{M}\sum_{\lambda=1}^{L} W_\mu W_\lambda \left[\left(\frac{d\mathcal{J}_\nu}{dt_\nu}\right)_{(\vec{x},\cos^{-1}(\gamma_\mu),\phi_\lambda)} + \left(\frac{d\mathcal{J}_\nu}{dt_\nu}\right)_{(\vec{x},\cos^{-1}(-\gamma_\nu),\phi_\lambda)}\right] . \quad (58)$$

In (58) 2M is the order of the Legendre quadrature, L is the order of the Chebyshev quadrature, γ_μ are the appropriate roots of Legendre polynomials, and $\cos\phi_\lambda$ are roots of Chebyshev polynomials. Noting that $\cos^{-1}(-\gamma_\mu) = \pi - \cos^{-1}(\gamma_\mu)$, we have

$$\frac{1}{K_\nu}\nabla\cdot\vec{H} = \frac{1}{2\pi}\sum_{\mu=1}^{M}\sum_{\lambda=1}^{L} W_\mu W_\lambda \left[\left(\frac{d\mathcal{J}_\nu^+}{dt_\nu}\right)_{(\vec{x},\cos^{-1}(\gamma_\mu),\phi_\lambda)} - \left(\frac{d\mathcal{J}_\nu^-}{dt_\nu}\right)_{(\vec{x},\cos^{-1}(\gamma_\mu),\pi-\phi_\lambda)}\right] . \quad (59)$$

Recalling that $\frac{d\mathcal{J}_\nu^\pm}{dt_\nu}$ is even in ϕ and noting that $\phi_\lambda = \pi\frac{(2\lambda-1)}{2L}$ we see that $\pi-\phi_\lambda = +\phi_{L+1-\lambda}$. The W_λ are

equal ($W_\lambda = \frac{\pi}{L}$) and since we sum over all λ, (57) becomes

$$\frac{1}{K}\vec{\nabla}\cdot\vec{H} = \frac{1}{2\pi}\sum_{\mu,\lambda} W_\mu W_\lambda \left[\frac{d\mathfrak{N}_\nu^+}{dt_\nu} - \frac{d\mathfrak{N}_\nu^-}{dt_\nu}\right]_{\mu,\lambda}$$

where

$$\left(\frac{d\mathfrak{N}_\nu^\pm}{dt_\nu}\right)_{\mu,\lambda} =$$

$$= \sum_{\ell,m,k,n'} \dot{\mathfrak{G}}_\ell^\pm(t_\nu) F_{\ell m}^{-1} V_{mk}(\nu,\vec{x},\hat{n}_{\mu\lambda}) T_{kn'}(\vec{x}\,\hat{n}_{\mu\lambda}) S_\nu(\vec{x}_{n'}). \tag{60}$$

The frequency integral is reduced to the following quadrature formula

$$\int \phi_y f(y)dy = \sum_{\zeta=1}^{x} c_\zeta f(y_\zeta) + c_{x+1} f_\infty \tag{61}$$

where f_∞ is the asymptotic value of $f(y)$ as $y \to \infty$. The weights c_ζ are computed following a quadrature procedure developed by one of us (Skumanich 1966) in which $f(y)$ is approximated by piecewise linear segments with the subsequent integrals performed analytically. We have simply chosen y_{x+1} to be sufficiently large so that

$$\int \phi_y f(y)dy = \sum_{\zeta=1}^{x+1} c_\zeta f_\zeta \quad . \tag{62}$$

Here

$$y = (\nu-\nu_o)/\Delta\nu_D \quad . \tag{63}$$

Thus

$$\Phi_y = \frac{\phi_y}{\int_\infty^\infty \phi_\nu d\nu} = \frac{\Delta\nu_D \phi_y}{n} \tag{64}$$

where

$$n = \int_{-\infty}^{\infty} \phi_y dy \quad . \tag{65}$$

Then

$$\int_0^{\infty} d\nu \, \frac{\Phi_\nu}{K_\nu} \vec{\nabla}\cdot\vec{H}_\nu = \frac{2}{n} \int_{-\infty}^{\infty} dy \, \frac{\phi_y}{K_y} \vec{\nabla}\cdot\vec{H}_y \simeq \frac{2}{n} \sum_{\zeta=1}^{x+1} \frac{c_\zeta}{K_\zeta} \vec{\nabla}\cdot\vec{H}_{y_\zeta} \, . \tag{66}$$

Recalling the definitions of $\alpha_{n'}^0(\vec{x})$ and $\alpha_{n'}^1(\vec{x})$ we have

$$\alpha_{n'}^0(\vec{x}) = \frac{1}{\pi n(\varepsilon(\vec{x}) + \delta(\vec{x}))} \sum_{\zeta,\mu,\lambda} \sum_{\ell,m,k} c_\zeta(\vec{x}) W_\lambda W_\mu$$

$$\times \left[G_\ell^+(t_\nu(\vec{x},\hat{n}_{\mu\lambda})) - G_\ell^-(t_\nu(\vec{x},\hat{n}_{\mu\lambda})) \right] \tag{67}$$

$$\times \; F_{\ell m}^{-1} \, V_{mk}(\nu,\vec{x},\hat{n}_{\mu\lambda}) T_{kn'}(\vec{x},\hat{n}_{\mu\lambda}) \, \frac{\phi_\zeta(x_{n'})}{\phi_\zeta(\vec{x}_{n'}) + r_o(\vec{x}_{n'})} \quad .$$

Note that $\alpha_{n'}^1(\vec{x})$ is given by the same formula with

$$\frac{\phi_\zeta(\vec{x}_{n'})}{\phi_\zeta(\vec{x}_{n'}) + r_o(\vec{x}_{n'})}$$

replaced by $r_o(\vec{x}_{n'})/(\phi_\zeta(\vec{x}_{n'}) + r_o(\vec{x}_{n'}))$. We then evaluate $\alpha_{n'}^0$ and $\alpha_{n'}^1$ at all points $(\vec{x}_{n'})$ and proceed to form and solve the linear algebraic equations as outlined in §II.

IV. INTERPOLATORY TRANSFORMATIONS

For the transformation of functions of a single variable we have used a subroutine, MAPPAR, written by Kalkofen (1967). The basic step is to suppose that a function in a given domain is well represented by an interpolation function. A "backward" parabola is fitted such that for a function f(x') on the interval $x_j \leq x' < x_{j+1}$

$$f(x') \simeq \frac{(x'-x_j)(x'-x_{j+1})}{(x_{j-1}-x_j)(x_{j-1}-x_{j+1})} f_{j-1} + \frac{(x'-x_{j-1})(x'-x_{j+1})}{(x_j-x_{j-1})(x_j-x_{j+1})} f_j$$

$$+ \frac{(x'-x_{j-1})(x'-x_j)}{(x_{j+1}-x_{j-1})(x_{j+1}-x_j)} f_{j+1} \quad . \tag{68}$$

For x' in the same interval a "forward" parabola is given by

$$f(x') \simeq \frac{(x'-x_{j+1})(x'-x_{j+2})}{(x_j-x_{j+1})(x_j-x_{j+2})} f_j + \frac{(x'-x_j)(x'-x_{j+2})}{(x_{j+1}-x_j)(x_{j+1}-x_{j+2})} f_{j+1}$$

$$+ \frac{(x'-x_j)(x'-x_{j+1})}{(x_{j+2}-x_j)(x_{j+2}-x_{j+1})} f_{j+2} \quad . \tag{69}$$

In MAPPAR, except for the end intervals, a weighted sum of the two is taken; the backward weight is P, the forward Q = 1-P. Then, for $x_j \leq x_i' \leq x_{j+1}$

$$f(x_i') \simeq \sum_{j'=j-1}^{j+2} V_{ij'} f_{j'} \tag{70}$$

where

$$V_{ij-1} = P \frac{(x_i'-x_j)(x_i'-x_{j+1})}{(x_{j-1}-x_j)(x_{j-1}-x_{j+1})} \quad , \tag{71}$$

$$V_{ij} = P\frac{(x_i'-x_{j-1})(x_i'-x_{j+1})}{(x_j-x_{j-1})(x_j-x_{j+1})} + Q\frac{(x_i'-x_{j+1})(x_i-x_{j+2})}{(x_j-x_{j+1})(x_j-x_{j+2})} \quad , \tag{72}$$

$$V_{ij+1} = \tag{73}$$

$$= P \frac{(x_i'-x_{j-1})(x_i'-x_j)}{(x_{j+1}-x_{j-1})(x_{j+1}-x_j)} + Q\frac{(x_i'-x_j)(x_i'-x_{j+2})}{(x_{j+1}-x_j)(x_{j+1}-x_{j+2})} \quad ,$$

and

$$V_{ij+2} = Q \frac{(x_i'-x_j)(x_i'-x_{j+1})}{(x_{j+2}-x_j)(x_{j+2}-x_{j+1})} \quad . \tag{74}$$

Note particularly that the V's can be expressed in matrix form and depend only on the relation of x_i' to x_j and not on the f's. Also, the x_i' and x_j must refer to the same variable so that in our problem, where we wish to find $\mathscr{L}^s(s)$, we must first find either $s(t_\nu)$ or $t_\nu(s)$, where

$$s(t_\nu) = \int_0^{t_\nu} \frac{dt'_\nu}{K_\nu(\vec{x}^p(t'_\nu))} \tag{75}$$

$$t_\nu(s) = \int_0^s K_\nu(\vec{x}^p(s'))ds' \quad . \tag{76}$$

A similar but somewhat simpler formula is used for finding T, the transformation between $\mathscr{L}^s(s)$ and S(r,z). We assume that it is approximately valid to write

$$\mathscr{S}^s(s) = S(r^p(s),z^p(s)) = \frac{(r^p(s)-r_{i+1})(z^p(s)-z_{j+1})}{(r_i-r_{i+1})(z_j-z_{j+1})} S_{i,j}$$

$$+ \frac{(r^p(s)-r_{i+1})(z^p(s)-z_j)}{(r_i-r_{i+1})(z_{j+1}-z_j)} S_{i,j+1}$$

$$+ \frac{(r^p(s)-r_i)(z^p(s)-z_{j+1})}{(r_{i+1}-r_i)(z_j-z_{j+1})} S_{i+1,j}$$

$$+ \frac{(r^p(s)-r_i)(z^p(s)-z_j)}{(r_{i+1}-r_i)(z_{j+1}-z_j)} S_{i+1,j+1} \quad (77)$$

whenever $r_i \leq r^p(s) < r_{i+1} \leq r_I$ and $z_j \leq z^p(s) \leq z_{j+1} \leq z_J$. Letting $n = i + I(j-1)$ we have

$$S(\vec{x}^p(s_k)) = \sum_n T_{kn} S_n \quad (78)$$

where the non-zero elements of T are given from (77).

In the cylindrical geometry which we have chosen

$$r^p(s) =$$

$$\left[r^2+(z \tan \theta - s \sin\theta)^2 - 2r(z \tan \theta - s \sin\theta)\cos\phi\right]^{1/2} \quad (79)$$

and

$$z^p(s) = s \cos\theta \quad (80)$$

where r and z are coordinates through which the path $p(r,z,\theta,\phi)$ passes. To change geometries, one must carefully choose the s = 0 point with respect to the boundary configuration and appropriately alter the $\vec{x}^p(s)$ functions.

Boundary conditions on the present geometry are that $S_L(r,z) \to B_\infty(z)$ as $z \to \infty$, where $B_\infty(z) = \lim_{z\to\infty} B(r,z)$ and is independent of r. Also $S_L(r,z) \to S_L(\infty,z)$ as $r \to \infty$, i.e., for large r the source function reverts to the one-dimensional case. These conditions are used in the mappings by assuming that S_L is linear (as is B) in τ_c for $z \geq z_J$ and $S_L(r_I,z)$ for $r \geq r_I$. Thus we must be sure to make r_I amd z_J sufficiently large.

V. RESULTS AND CONCLUSIONS

Some sample solutions obtained with the above procedure are shown in Figures 2-7. In each case, all parameters except temperature are constant with

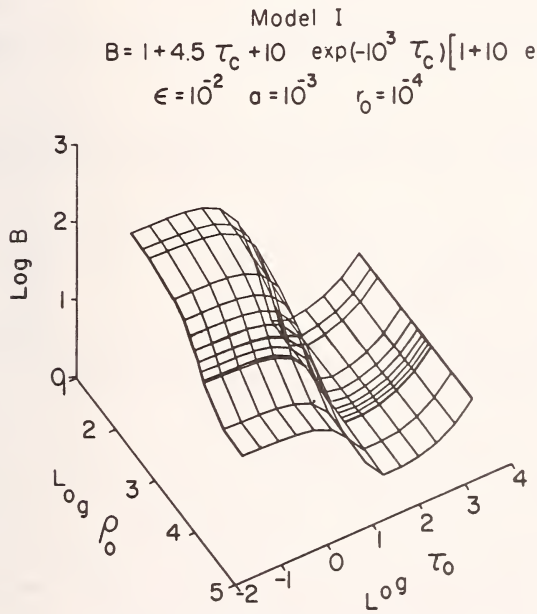

Figure 2. Planck function surface for Model I. Log $B(\rho_o,\tau_o)$ is plotted vs. log ρ_o and log τ_o. τ_o is the total optical depth at line center and ρ_o is the total line center radial optical distance from the axis.

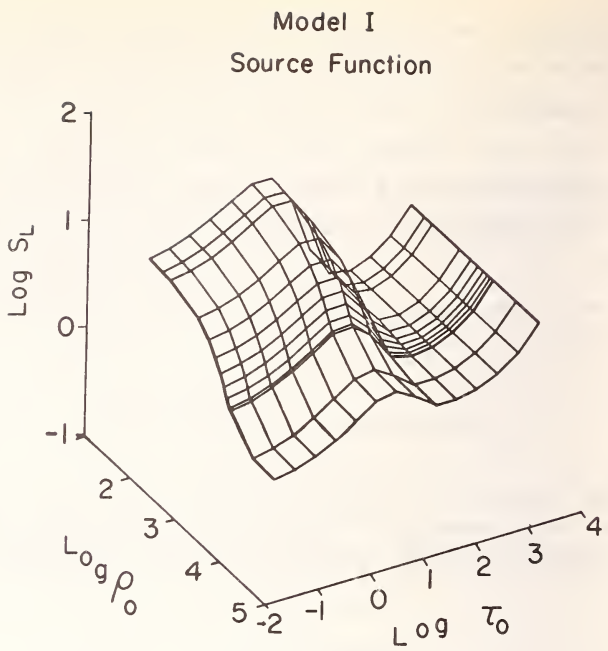

Figure 3. Source function surface, $S_L(\rho_o,\tau_o)$ for Model I.

position. We have arbitrarily chosen $\varepsilon = 10^{-2}$, $a = 10^{-3}$, and $r_o = 10^{-4}$ while the Planck functions has form

$$B(\rho_c,\tau_c) = 1 + Ae^{-c\tau_c}(1 + Be^{-(d\rho_c)^m}) + \beta\tau_c$$

where τ_c is the continuous vertical optical depth and ρ_c is the continuous radial optical depth measured from the axis. The absorption coefficient at line center is assumed to be 1.

We have in mind a temperature structure designed to mimic a hot "chromospheric" column ($\rho_c < 1/d$) imbedded in a cooler ambient "chromosphere" ($\rho_c > 1/d$) and overlying a homogeneous, plane-parallel "photosphere" $\tau_c >> 1/c$ with linear vertical gradient in B. The model is merely for numerical testing, however, and we will not attempt to draw from our results any direct conclusions about lines actually observed in the solar atmosphere. The models are nevertheless not unlike possible choices one might make in attempting to treat certain solar lines.

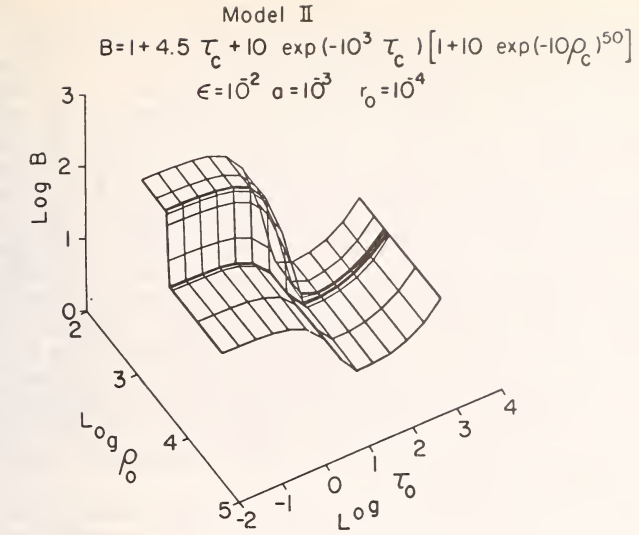

Figure 4. Planck function for Model II.

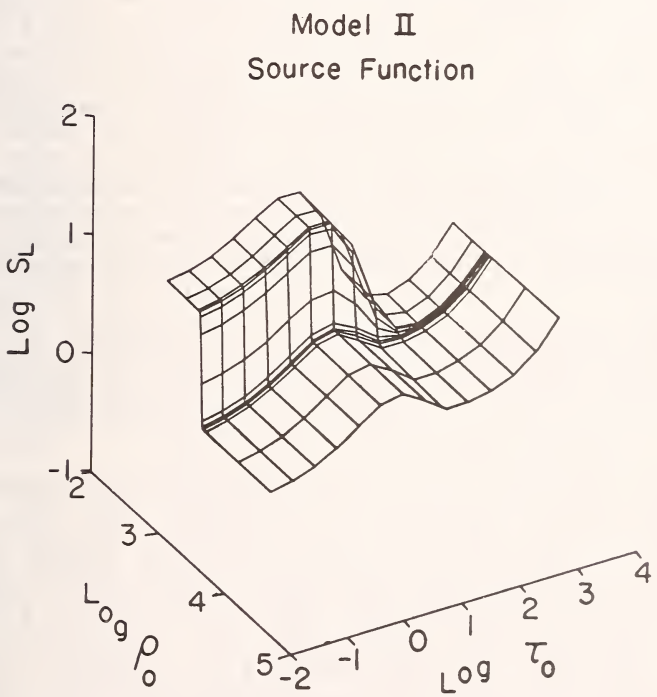

Figure 5. Source function for Model II.

The figures show B and S_L surfaces with the vertical axis being log B (or log S_L) and the horizontal axis being the logarithm of the respective total optical coordinate at line center. In all cases A = B = 10, and c = 10^3 (corresponding to a "chromospheric" optical thickness of about 10 at line center). The parameter d controls the radial thickness of the hot inhomogeneity while m and d control the "edge scale of the radial variation of B.

In the model I solution, the radial thickness is 10^3 at line center and m = 1 so that the edge scale is also of order 10^3. All horizontal scales are thus larger than a thermalization length ($\sim 10^2$). It is not surprising that the two-dimensional solution for any value of ρ is very nearly that which would be obtained from a strictly plane-parallel atmosphere with the vertical behavior of the Planck function the same as at the given radius in the two-dimensional case.

Model II differs from Model I in that m = 50, or the edge scale is ~ 20. Detailed examination of the solution shows that the source function reaches its asymptotic radial behavior at a distance of roughly a thermalization length on either side of the region of rapid radial variation of the Planck function. (This is not evident in Figure 5 due to the large scale of the ρ-axis compared to a thermalization length). Even though the edge scale for B is less than a thermalization length, the radial dependence of S_L is suprisingly similar to that of B. It is possible that the solution is incorrect. However, both the radial thickness and the edge scale are larger than the vertical thickness of the "chromosphere." Since both scales are coupled in the term $\vec{\nabla} \cdot \vec{H}_\nu$, a possible explanation of the result is that the vertical scale still dominates. In terms of photon diffusion, a photon originating at a given radius can escape from the surface of the atmosphere or diffuse to the homogeneous photosphere more readily than it can diffuse to a different radius with noticeably different temperature.

In Model III, m = 1 and the radial thickness is 1. The radial scale should dominate, then, at least at intermediate depths. The solution, however, is unstable in the sense that oscillations appear which have no apparent physical cause. One would also expect the source function near the axis to be less for a radially thin region than for a radially thick one. However, the sharp peak in S_L in Model III at $\tau_o \sim 10$ near the axis is about twice the value of S_L for Model I in the corresponding region.

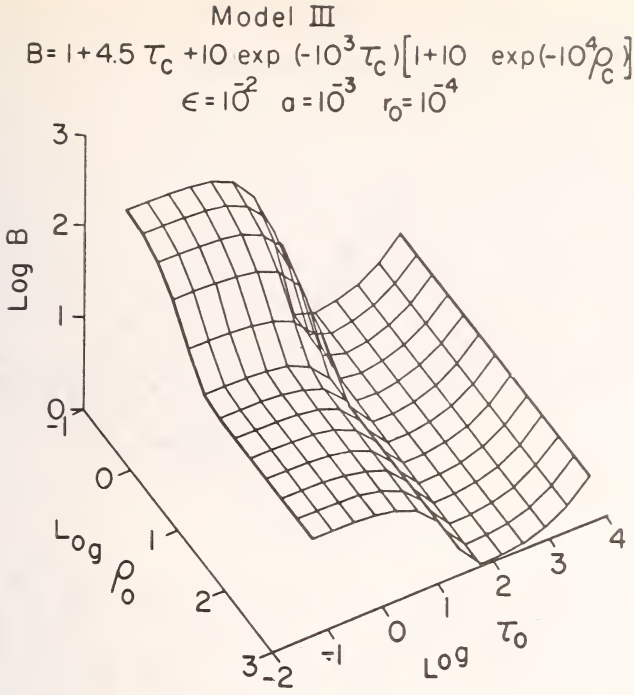

Figure 6. Planck function for Model III.

The source function behavior can be made smoother with some adjustment of grids, but the peak remains. Apparently, then, no physically realistic solution has been obtained for the third model.

Some simple tests of the method have been made. First, we must obtain the correct solution in the plane-parallel case. We have compared our technique with independent plane-parallel calculations for $B = 1 + Ae^{-c\tau_c} + \beta\tau_c$ with $c = 10^3$, $\beta = 4.5$, the same ϵ, a, and r_0 as before, and A = 10, 100, and 1000. The two-dimensional code with a 10 × 10 $\rho \times \tau$ grid agrees to better than 10 percent in all cases with a typical error of less than 4 percent.

For a thick inhomogeneity, the solutions near the axis and at very large radii must also reduce to the corresponding plane-parallel limit. Again, our solutions satisfy this requirement to about the accuracy indicated above.

With the exception that points must be nested

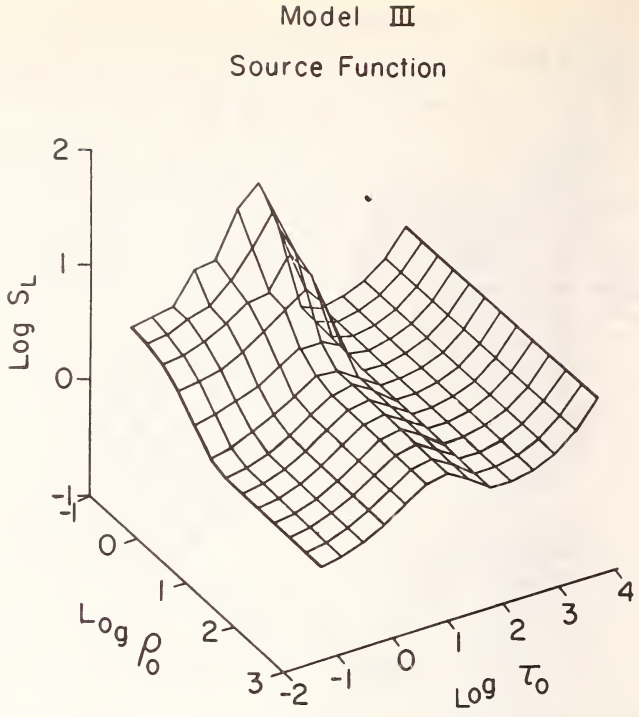

Figure 7. Source function for Model III.

so that a reasonable number lie in regions of Planck function variation, the nesting of the spatial grid has not proven critical. Different types and orders of angular quadratures have been tried and again, do not have much effect on the solution to within the sort of accuracy indicated above.

The selections of the t_ℓ (the path grid) does seem to be important in determining the solution. In every case that has been so far attempted, oscillatory solutions appear at intermediate depths ($\tau_o \gtrsim 2$) whenever the radial behavior of the Planck function is sharp enough to dominate; these are just the solutions which are sensitive to choice of path grid. Numerical experiments to determine more exactly how different choices of path origin and path grid affect the numerical stability of the technique are in progress.

The technique is quite convenient for media with an absorption coefficient which is constant or varies

only with depth. Central processing time for such a problem with a 10 × 10 grid is about 45 seconds on the CDC 6600 and increases linearly with the total number of space points (i.e., to about 90 seconds for a 14 × 14 grid). Fully variable opacity will of course cause an increase in computing time.

In spite of the stability problems encountered to date, we feel the method holds great promise. In principle, it is able to deal with quite arbitrary spatial behavior and boundary configurations and is particularly well-suited for media with very large optical extent.

The authors wish to thank Professor R. D. Richtmyer for valuable discussion in the early stages of this work.

REFERENCES

Athay, R. G., and Skumanich, A. 1967, *Ann. d'Ap.*, 30, 669.
Avery, L. W., and House, L. L. 1968, *Ap. J.*, in press.
Avrett, E. H., and Loeser, R. 1963, *J. Quant. Spect. and Rad. Transf.*, 3, 201.
Davis, P. J., and Polosnky, I. 1964, "Numerical Interpolation, Differentiation, and Integration" in *Handbook of Mathematical Functions*, ed. M. Abramowitz and I. Stegun (Washington, D. C.: U. S. Government Printing Office) p. 875.
Kalkofen, W. 1967, private communication.
Kalkofen, W. 1968, *Boulder Conference on Resonance Lines in Astrophysics*, in press.
Kuhn, W. R. 1966, Thesis, University of Colorado.
Rybicki, G. B. 1965, Thesis, Harvard University.
Skumanich, A. 1966, *Astr. J.* 71, 871.
Wilson, P. R. 1968, *Ap. J.* 151, 1029.

DISCUSSION

Underhill: Did you use depth-dependent functions in your calculations?

Skumanich: We considered only horizontal

changes in the examples shown. But we have also calculated other models, as indicated in the text.

Underhill: Can you include the granulation?

Skumanich: We have thought it best to calculate simple nonstatistical structures initially. The granulation problem, if modeled by periodic structures, can and will be included ultimately.

THE CONTINUOUS SPECTRUM OF HYDROGEN IN A LOW-DENSITY ENVELOPE

by

H. Gerola

Universidad de Buenos Aires, Departamento de Fisica, Facultad de Ciencias Naturales y Exactas, Buenos Aires, Argentina

and

N. Panagia

Laboratorio di Astrofisica, Frascati (Roma), Italy

ABSTRACT

A progress report on theoretical work on the formation of a continuum in low-density stellar envelopes. Preliminary results are given on a comparison between the recombination case and the case for a semi-empirical approach including the effect of collisions from the ground state.

Key words: recombination case, collisional excitation, low-density envelope.

This note is a progress report on the theoretical work concerning the problem of formation of the continuum in low density stellar envelopes excited essentially by collisions. By low density envelope is meant an envelope in which emission lines are formed.

When collisions are important for ionization and excitation essentially two facts must be considered, which may give the following significant differences with respect to the normal radiative recombination theory:

(1) the metastable level of hydrogen, 2s, may be

populated directly from the ground level, which is b far the most populated level in typical nebular conditions. This is the difference with respect to the solely radiative excitation situation, when the 2s level may be reached only from the upper levels;

(2) for the same values of electron temperature and density, the product of the electron density and neutral hydrogen concentration is much higher in the collisional case than in the radiative case.

These facts lead one naturally to consider the effects of two emission processes:

(i) the two-photon continuous emission in the decay of the 2s level;

(ii) the continuous emission in the reaction for the formation of the negative hydrogen ion.

The effect of two-photon emission in the case of pure collisional excitation was studied by the authors in a previous paper (Gerola and Panagia, 1968), with the usual approximation of cases A and B due to Baker and Menzel (1938).

If the degree of ionization is considered, it is found that, for the same values of electron density and electron temperature, the ionization in the collisional case is smaller than in the radiative case. This fact opens the possibility that another process may lead to an important contribution to the continuous spectrum only in the collisional excitation case: this process is the continuous emission in the reaction for the formation of the negative hydrogen ion. The rate of this reaction is proportional to the product of electron density and neutral hydrogen density and this product is larger in envelopes when collisions are responsible for ionization. It is to be expected that the efficiency of this process will be greater at temperatures lower than 10^4°K.

Greenstein and Page (1951) found that H^- emissivity is unimportant for planetary nebulae; it should be remembered that typical planetary nebulae seem to be definitely radiatively excited.

It has been verified that in low density conditions an abundance of H^- ions high enough to give a finite opacity for the continuum of the Balmer and higher series and to modify the neutrality condition is never reached. What is found instead is that the H^- concentration is of the order of $10^{-7}N_e$ and can therefore be neglected.

So the continuum is simply the sum of recombination plus two-photon plus H^- free-bound emission.

To see the problem, let us write the statisti-

cal equilibrium equation for the levels with $n \geq 3$ in the form:

$$\sum_{n''=n+1}^{\infty} F_{n''n} + \int_{\nu}^{\infty} F_{kn}\,d\nu + \mathcal{H}\,\mathcal{F}^{*}_{1n} + F_{1n} = \sum_{n'=1}^{n-1} F_{nn'}$$

where $\sum_{n''=n+1}^{\infty} F_{n''n}$ is the radiative cascade rate from upper levels to level n;

$\int_{\nu_n}^{\infty} F_{kn}\,d\nu$ is the recombination rate from the continuum;

$\mathcal{F}^{*}_{1n}$ is the collisional rate of excitation from ground level for the pure collisional case;

F_{1n} is the radiative rate of excitation from ground level,

and $\sum_{n'=1}^{n-1} F_{nn'}$ is the radiative rate of decay from level n.

Now we shall discuss the $\mathcal{H}$ factor, which was introduced in 1953 by Chamberlain in his first study of the collisional Balmer decrement, where it was pointed out that all intermediate cases between $\mathcal{H} = 0$ and $\mathcal{H} = 1$ are physically possible. This factor assumes the value 0 in the radiative case and 1 in the collisional case and represents the amount of colli-

sional ionization from ground level relative to the total amount of ionization.

In reality a combination of the two excitation mechanisms is possible and the effective value of $\mathcal{H}$ depends not only on the present geometry and the ultraviolet radiation field, but also on the past history of the system nebula plus the exciting star. So, for example, the envelope of a star that has recently flared actually has an energy input due to the present radiation of the star and to the energy

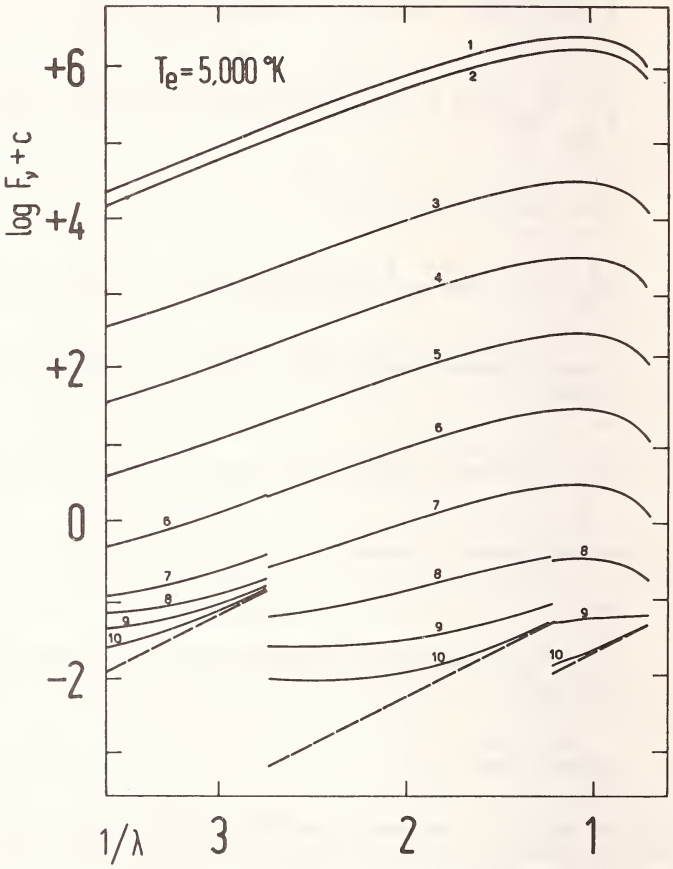

Figure 1. The dashed curve represents the recombination spectrum; for the other continua (solid lines) the number attached to each curve refers to the values of $\mathcal{H}$ which are listed in Table 1. All the continuous spectra were computed for $N_e = 10^4$ cm^{-3} and $R = 10^{16}$ cm.

TABLE 1.

VALUES OF $\mathcal{H}$

Number of the curve	T_e (°K) 5000 (Fig.1)	10000 (Fig.2)	20000 (Fig.3)
1	1.00×10^{0}	1.00×10^{0}	1.00×10^{0}
2	6.67×10^{-1}	6.21×10^{-1}	5.70×10^{-1}
3	1.22×10^{-1}	2.01×10^{-1}	1.26×10^{-1}
4	1.22×10^{-2}	2.01×10^{-2}	1.26×10^{-2}
5	1.22×10^{-3}	2.01×10^{-3}	1.26×10^{-6}
6	1.22×10^{-4}	2.01×10^{-6}	——
7	1.22×10^{-5}	2.01×10^{-10}	——
8	1.22×10^{-6}	——	——
9	1.22×10^{-7}	——	——
10	1.22×10^{-10}	——	——

injected into the envelope by the recent flare of the star. Only a detailed model of the evolution of this system would permit the determination of $\mathcal{H}$ from other physical parameters. We have chosen an empirical approach, being interested here on the actual appearance of the continuum, that is in the spectroscopic problem; so $\mathcal{H}$ was let free to run as an independent parameter, and the computed spectra were compared with observations.

A detailed description of the calculations will be found in a paper that will be published soon.

Figures 1, 2 and 3 represent some computed continua for different values of electron temperature. Dashed curves correspond to the recombination spectrum while the other curves represent the total continuum for the values of $\mathcal{H}$ given in Table 1.

It is to be noted that even with a small value of $\mathcal{H}$ the behaviour of the continuum is very different from the pure recombination spectrum. This is so

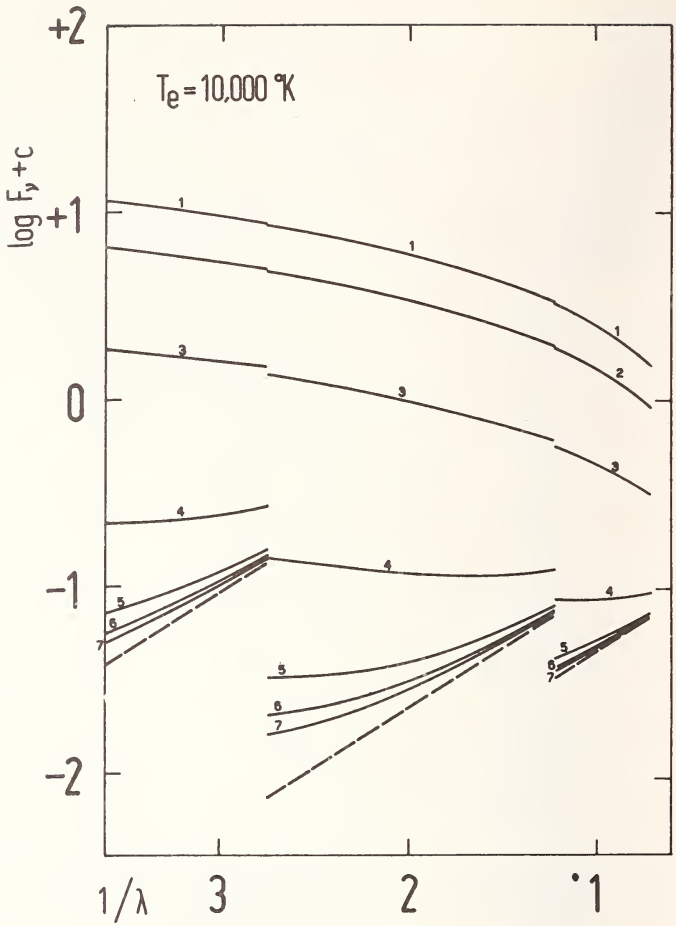

Figure 2. As in Figure 1.

because the ground level is so highly populated that a small collisional contribution is sufficient to affect profoundly the 2s level population, with all the consequences for the continuous spectrum. Clearly for very small values of $\mathcal{H}$, that is, for those values, corresponding to the radiative case, our results are very similar to those obtained by Spitzer and Greenstein (1951) and by Seaton (1960).

Regarding the comparison with observations, Pagel (1969) and Viotti (1969) found that the continuous emission spectrum of the peculiar object η Car and the intensity of the Hα-line can be explained in terms of a collisional case spectrum.

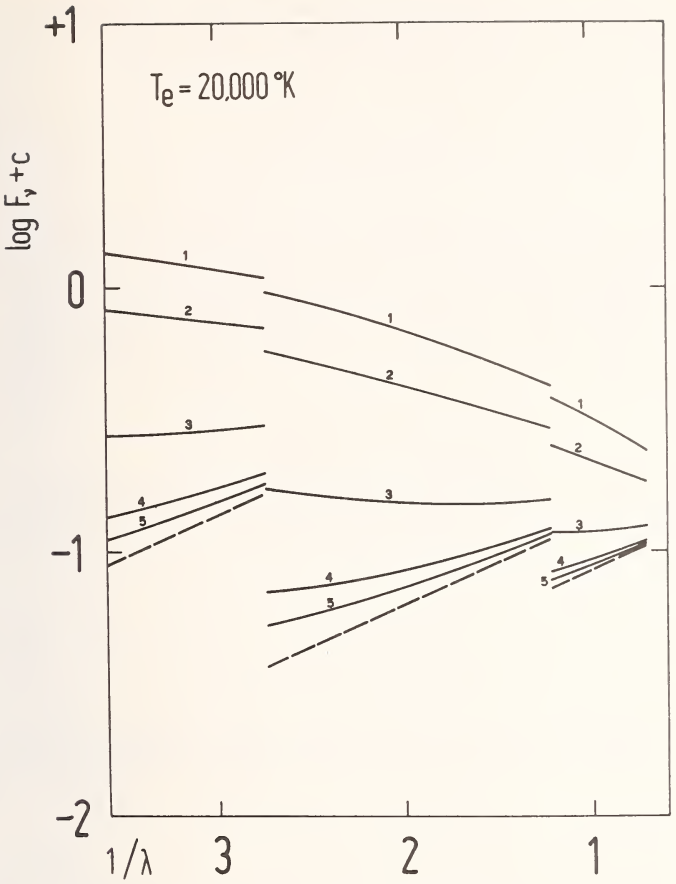

Figure 3. As in Figure 1.

Another object with similar features is MHα 328-116. Up to 1964 its appearance was that of a normal M star with some emission features superimposed on the M spectrum; in 1965 this star abruptly rose in luminosity, changing also the spectral characteristics.

O'Dell's measurements of the continuum (1967) and those independently obtained by Caputo et al. (1969) can be fitted very well with a continuous spectrum corresponding to a mixed case of excitation ($\mathfrak{X} \simeq .6$).

What is to be noted is that these spectra cannot be explained by means of any other emission mechanism.

Studies of the Balmer decrement, taking into account the reabsorption from 2s and 2p levels, in the cases of a mixed excitation, are being considered.

REFERENCES

Baker, J. G., and Menzel, D. H. 1938, *Ap. J.* 88, 52.
Caputo, F., Panagia, N., and Gerola, H. 1969, to be published.
Chamberlain, J. W. 1953, *Ap. J.* 117, 387.
Gerola, H., and Panagia, N. 1968, *Ap. Space Sci.* 2, 285.
Greenstein, J. L., and Page, T. 1951, *Ap. J.* 114, 106.
O'Dell, C. R. 1967, *Ap. J.* 149, 373.
Pagel, B. E. J. 1969, *Nature* 221, 325.
Seaton, M. J. 1960, *Rep. Prog. Phys.* 23, 313.
Sptizer, L., Jr., and Greenstein, J. L. 1951, *Ap. J.* 114, 407.

DISCUSSION

Swings: Collision terms were already introduced in the statistical equilibrium equation by Menzel.

Gerola: The notation I used is due to Chamberlain.

Editorial remark: In the paper by Gerola and Panagia the definition of $\mathcal{H}\,\mathcal{F}^*_{in}$ is not explained in detail although the reason for introducing this term can be seen. Confusion exists about what is meant by the factor $\mathcal{H}$, which was not introduced in precisely this manner by Chamberlain (1953 *Ap. J.* 117, 387) and about what the expression is, for "the collisional rate of excitation from the ground level for the pure collisional case." In the examples presented the parameter $\mathcal{H}$ is used only as an arbitrary multiplying factor. To understand fully the meaning of the results one must know the precise definition of $\mathcal{F}^*_{in}$. It is presumed that this definition will be given in the unpublished work by Gerola and Panagia to which reference is made.

BANDWIDTH REQUIREMENTS IN SPECTRAL LINE TRANSFER CALCULATIONS

by

R. Grant Athay

High Altitude Observatory
National Center for Atmospheric Research
Boulder, Colorado

ABSTRACT

Accurate evaluation of a line source function, S, requires that the frequency bandwidth be sufficiently large to include properly transfer effects in the line wings. The bandwidth required to achieve a given level of accuracy in the evaluation of S can be specified, in units of the Doppler width, in terms of three parameters: the ratio of continuum to line opacity, r_o, the probability for collisional de-excitation, ε, and the Voigt wing parameter $\underline{a}$. Bandwidths required to give S to an accuracy of 2 percent are given for values of ε and r_o from 10^{-2} to 10^{-8} and for values of $\underline{a}$ from 10^{-2} to 10^{-5}.

Key words: line source function, bandwidth requirements.

I. INTRODUCTION

In computing a line source function, S, by numerical techniques, it is generally necessary to discretize the frequency variable and to limit the frequency range to some finite band centered on the line. The accuracy with which S can be evaluated depends upon both the nesting of the frequency points and the total bandwidth considered.

The bandwidth required to achieve a given level of accuracy in S depends upon the extent of the line wings and, in addition, upon departures from local thermodynamic equilibrium, LTE. In LTE one frequency

can be treated independently of any other frequency and the required bandwidth reduces to zero. In non-LTE S depends upon radiation transfer effects over a band of frequencies that, for some lines, may be very broad. Generally, if a line has negligible wings the bandwidth can safely be restricted to the Doppler core and the bandwidth is sufficiently narrow that it presents no particular difficulties. When, however, the line wings are strongly developed the problem of properly treating the entire bandwidth of the line with a set of discrete frequency points may lead to serious difficulties. It is essential to know, therefore, how far into the line wings the bandwidth must extend in order to give an accurate evaluation of S.

The strength and extent of line wings are determined by two parameters: the Voigt parameter a and the ratio of continuum to line opacity, $r_o = d\tau_c/d\tau_o$. If we define the shape factor for the line absorption coefficient to be ϕ_y, where y is a dimensionless frequency measured in units of the Doppler width, i.e., $y = \Delta\nu/\Delta\nu_D$, we may approximate ϕ_y for a Voigt profile by

$$\phi_y = e^{-y^2} \qquad y \leq 1$$

$$\phi_y = e^{-y^2} + \frac{a}{\sqrt{\pi} y^2} \qquad y > 1 \tag{1}$$

An element of opacity at frequency y is then given by

$$d\tau_y = \phi_y \, d\tau_o + d\tau_c$$

$$= (\phi_y + r_o) \, d\tau_o$$

For constant r_o, $\tau_y(\text{line}) = \tau_c$ for a value of y such that $\phi_y = r_o$ and $\tau_y(\text{line}) = 10^{-n} \tau_c$ for $\phi_y = 10^{-n} r_o$. One may reasonably argue that the effects of the wings are adequately included if $\tau_y(\text{line}) = 10^{-2} \tau_c$. Equation (1) gives for this case a limiting y of

$$y_1 = 7.5 \, (a/r_o)^{1/2} \tag{2}$$

In extreme cases such as the H and K lines of Ca II or Lyman-α in the solar spectrum $(a/r_o)^{1/2} \approx 10^4$. Hence, we find $y_1 \approx 10^5$.

To properly treat such large values of y is both difficult and time consuming. Furthermore, it is totally unnecessary in cases where the wings are formed in LTE.

The purpose of the calculations presented here is to evaluate the bandwidth requirements for a range of the relevant parameters. We treat the simple case of a two-level atom, which requires only one parameter in addition to $\underline{a}$ and r_o. The added parameter is the ratio of collisional to radiative de-excitation rates, which we define as $\varepsilon = C_{21}/A_{21}$ where the subscripts designate the upper and lower levels respectively. For a given set of ε, $\underline{a}$ and r_o, we evaluate the minimum value of y for which S is accurate to 2 percent at each depth. The parameters ε, $\underline{a}$ and r_o together with the temperature and Doppler width are held constant with depth.

II. CALCULATIONS AND RESULTS

The line source function is computed using the flux divergence method of Athay and Skumanich (1967). In their formulation for a two-level atom with non-coherent scattering, the frequency independent source function is given by

$$S = B + \frac{2N}{\varepsilon+\delta} \int_0^\infty \frac{\phi_y}{\phi_y+r_o} \frac{dH_y}{d\tau_o} \, dy \quad , \tag{2}$$

where B is the Planck function, H_y is the monochromatic net flux,

$$N = \left(2 \int_0^\infty \phi_y \, dy\right)^{-1} \approx \pi^{-1/2} \quad , \tag{3}$$

and

$$\delta = 2\pi^{-1/2} \, r_o \int_0^\infty \frac{\phi_y}{\phi_y+r_o} \, dy. \tag{4}$$

We note from the form of equation (3) that two general conclusions can be stated about the required bandwidth as follows:

(1) If $\delta > \varepsilon$, y_1 must be sufficiently large to give an accurate value of

$$\frac{1}{\delta} \int_0^{y_1} \frac{\phi_y}{\phi_y + r_o} \frac{dH_y}{d\tau_o} \, dy.$$

This quantity would be independent of y_1 if $dH_y/d\tau_o$ were constant with y, which is true in LTE but not in the general case. In non-LTE the quantity $dH_y/d\tau_o$ is relatively large near line center and decreases to a relatively small, constant value at some point in the line wings.

At the surface $\tau_o = 0$, $S/B \propto \delta^{1/2}$. Thus, if we considered that only δ depended upon y_1 we would require 4 percent accuracy in δ to attain 2 percent accuracy in S.

Also, we note that in the case, $\delta >> \varepsilon$, the required bandwidth is independent of ε.

(2) If $\varepsilon >> \delta$, the bandwidth will depend upon ε. For large ε, the non-LTE effects will be limited to the Doppler core and $y = 3$ will suffice. For small ε, the required bandwidth will extend into the wings, but not so far as in case 1 for a value of δ equal to the ε of case 2.

It is clear from case 1 that an extreme limit on y_1 for 2 percent accuracy in S is given by the condition that δ be accurate to 4 percent. Thus, if we write

$$\delta = 2\pi^{-1/2} r_o \int_0^{y_1} \frac{1}{1 + \frac{\sqrt{\pi} r_o}{a} y^2} \, dy$$

$$= 2\pi^{-3/4} (a\, r_o)^{1/2} \tan^{-1} y_1 \, (\sqrt{\pi} r_o / a)^{1/2} \qquad (5)$$

$$= \pi^{1/4} (a\, r_o)^{1/2} \quad y_1 = \infty \ ,$$

the 4 percent criterion for δ gives

$$y_1 = 11.5\ (a/r_o)^{1/2} \ , \qquad (6)$$

which is about a factor 1.5 greater than the value given by equation (2). The limit on y_1 set by equation (2) corresponds to approximately 6 percent accuracy in δ, or 3 percent accuracy in S if $\delta >> \varepsilon$.

To evaluate y_1 more explicitly for a given combination of ε, r_o and $\underline{a}$, we solve equation (3) for a set of values of y_1. We increase y_1, step-wise, until an increase in y_1 by a factor of ten changes S by less than 2 percent at each optical depth point. We assume that S has converged to a correct solution when this condition is met.

The values of y_1 tested are 3, 4 10^k, 3 $\times$ 10^k, and 10^{k+1} for $k > 1$. The spacings of the y points for $y < 10$ are as follows:

$0 \le y \le 3$	$3 \le y \le 4$	$4 \le y \le 10$
0.25	0.5	3

For $y \ge 10^k$, $k \ge 1$, four points in y are used per decade. These are spaced at 1.5 $\times$ 10^k, 3 $\times$ 10^k, 6.5 $\times$ 10^k and 10^{k+1}. As an example, if $y = 10^3$ the number of points used is:

$0 \le y \le 3$	$3 \le y \le 4$	$4 \le y \le 10$
13	2	2

$10 \le y \le 100$	$100 \le y \le 1000$
4	4

After y_1 is carried far enough to show convergence a minimum value of y_1 is determined that gives S accurate to 2 percent. These minimum values are obtained by interpolation between the tested values of y_1. They should be accurate to at least a factor of two.

It is possible, of course, that our convergence criterion is not strict enough. When both ε and r_o are small and when $\underline{a}$ is large the convergence is very slow. For example, with $\varepsilon = r_o = 10^{-8}$ and $\underline{a} = 10^{-2}$ the 2 percent criterion gives $y_1 \approx 2 \times 10^4$ whereas a 10 percent criterion gives $y_1 \approx 500$. We note, however, that $y_1 = 2 \times 10^4$ is about a factor of two greater than the value given by equation (6). Hence, we conclude that our convergence test is valid in this case, which is the case of slowest convergence treated here. In all other cases, y_1 is less than or equal to the value given by equation (2) and the convergence is reasonably fast.

The greatest likelihood of error in determining y_1 by the method described is in underestimating y_1. Thus, it is more likely that the value of y_1 given for a particular set of values of ε, r_o and $\underline{a}$ is too low, rather than too high.

The convergence of S to its correct solution as y_1 increases occurs differently in different parts of the atmosphere and for different values of the various parameters. The most notable effects are related to the wing parameter $\underline{a}$. For $\tau_o << a^{-1}$, the convergence is from below, i.e., if y_1 is too small S is too small. For $\tau_o >> a^{-1}$, however, the convergence is from above. Also, if $(\varepsilon + r_o) < a \lesssim 10 (\varepsilon + r_o)$ the convergence of S is much more rapid for $\tau_o >> a^{-1}$. These two effects are illustrated in Figure 1.

Values of y_1 for the 2 percent criterion are shown in Figure 2 for different combinations of values of r_o and ε between 10^{-2} and 10^{-8} and for values of $\underline{a}$ between 10^{-2} and 10^{-5}. Computations were made each two decades in ε and r_o (10^{-2}, 10^{-4}, 10^{-6} and 10^{-8}) and each decade in $\underline{a}$ (10^{-2}, 10^{-3}, 10^{-4} and 10^{-5}). The curves shown, therefore, are drawn through four points in each case. We emphasize again that the absolute errors in y_1 may be as large as a factor of two. On the other hand, the curves drawn through the points show a large measure of continuity from one curve to another. Thus, the errors do not appear to be so large as to obscure the nature of the curves.

There are threshold effects around $y_1 = 3$ for $\underline{a} \leq 10^{-3}$ and $y_1 = 15$ for $\underline{a} = 10^{-2}$ that strongly

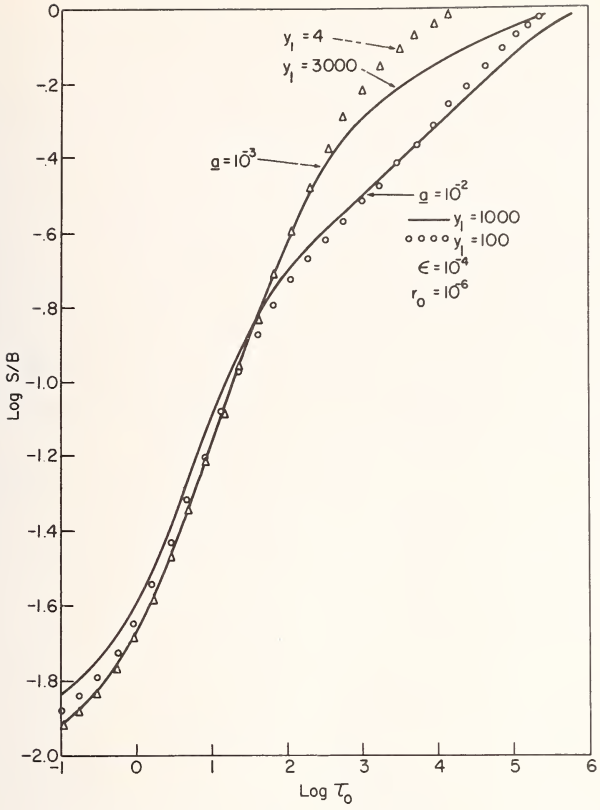

Figure 1. Illustration of approach to proper solution as y_1 is increased for two cases $\underline{a} = 10^{-3}$ and $\underline{a} = 10^{-2}$

influence the shapes of the curves for small values of y_1. However, certain systematic effects are evident in the curves whenever y_1 is large or when either ε or r_o is small.

In the plot of log y_1 versus log δ in Figure 2, it is evident that for $\delta >> \varepsilon$ $y_1 \propto \delta^{-1}$. Within the range of δ and $\underline{a}$ where this is evident, viz., $\delta \leq 10^{-3}$ and $\underline{a} \geq 10^{-3}$ line wings are well developed. Equation (5) shows that, for this case, $\delta \propto r_o^{1/2}$. Thus, we find a region where $y_1 \propto r_o^{-1/2}$ as predicted by equations (2) and (6). The plots of log y_1 versus log r_o exhibit the $r_o^{-1/2}$ dependence for $r_o = 10^{-6}$ and 10^{-8}. Also, when $\delta << \varepsilon$ the results in Figure 2 show y_1 to be independent of δ. The same effect is again evident in the plot of log y_1 versus log r_o for $\varepsilon = 10^{-2}$.

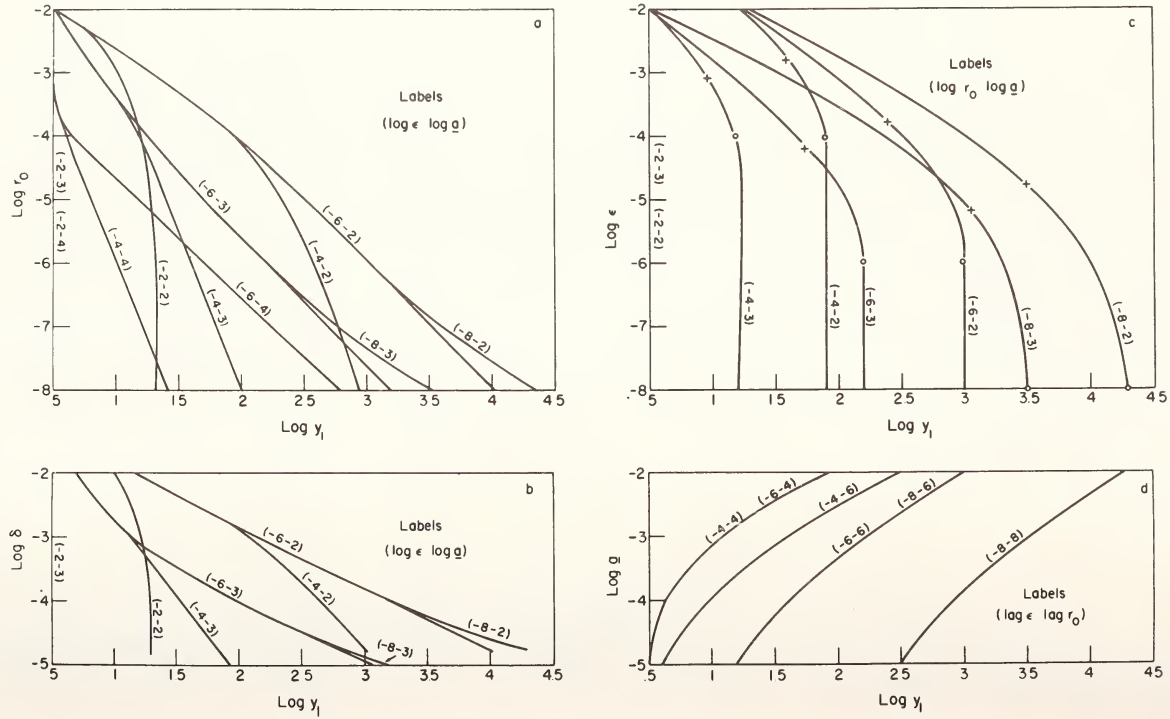

Figure 2. Dependence of y_1 upon a - r_o, b - δ, c - ε and d - g. Note saturation effects for δ << ε in figure b and for ε << δ in figure c.

Similarly, in the plot of log y_1 versus log $\underline{a}$ we find that when $\underline{a} \lesssim 10^{-3}$ and y_1 is well away from its threshold values $y_1 \propto \underline{a}^{1/2}$ as expected. There is a tendency in all four curves of log y_1 versus log $\underline{a}$ to have more nearly $y_1 \propto \underline{a}$ for $\underline{a} > 10^{-3}$. To preserve the $\underline{a}^{1/2}$ dependence it would be necessary to reduce all of the y_1 values for $\underline{a} = 10^{-2}$ by about a factor of two. While this is permissable for individual points it seems unlikely that all of the values of y_1 for $\underline{a} = 10^{-2}$ would be overestimated by the same amount.

On the plots of log y_1 versus log ε in Figure 2 the plus signs indicate the points $\varepsilon = \delta$ and the open circles indicate the points $\varepsilon = r_o$. It is clear that the dependence of y_1 on ε weakens at about the point $\varepsilon = \delta$ and that y_1 becomes essentially independent of ε for $\varepsilon < 10^{-1}\ \delta$. For $\varepsilon > \delta$ and y_1 well away from its threshold values (i.e., on the curves $r_o = 10^{-8}$) it appears that $y_1 \propto \varepsilon^{-1}$.

To an accuracy of about a factor of two and for $y_1 \gtrsim 10$, the results in Figure 2 may be approximated by:

$$y_1 \approx \frac{a^{1/2}}{\varepsilon} , \qquad \varepsilon >> \delta$$

$$y_1 \approx \frac{1}{3}\frac{a^{1/2}}{\varepsilon} , \qquad \varepsilon \approx \delta \tag{7}$$

and

$$y_1 \approx 10(a/r_o)^{1/2} \approx 13\,\frac{a}{\delta} , \qquad \delta >> \varepsilon .$$

The first of these limits on y_1 corresponds to $\tau_y \approx \varepsilon^2\ \tau_o$, or to $\tau_y = 1$ at $\tau_o = \varepsilon^{-2}$, the thermalization length for the pure dispersion case.

It should be remembered that the above values of y_1 are valid for the 2 percent criterion on the accuracy of S. When line wings are well developed and when $\delta >> \varepsilon$ the required values of y_1 for a given accuracy in δ can be estimated from equation (5). For 20 percent accuracy in δ, equation (5) gives values of y_1 a factor of five below those required for 4 percent accuracy and for 2 percent accuracy in δ a factor of two increase in y_1 is required. However, accuracy in δ is not the only criterion for accuracy in S.

Estimates of y_1 for 10 percent accuracy in S were made along with the estimates for 2 percent accuracy. A few checks were made on y_1 for 1 percent accuracy in S. In almost all cases where $\delta >> \varepsilon$ the changes in y_1 indicated in the preceding paragraph give an accuracy in S equal to twice the accuracy in δ, i.e., 20 percent accuracy in δ corresponds to 10 percent accuracy in S. In a few cases much larger changes in y_1 are indicated. For example, with $\underline{a} = 10^{-2}$ and $\varepsilon = r_o = 10^{-8}$ the estimated values of y_1 are 500, 2×10^4 and $> 10^5$ for accuracies in S of 10, 2 and 1 percent, respectively.

In the case of $\varepsilon >> \delta$, 10 percent accuracy in S requires values of y_1 about a factor of five below those given in Figure 2 and 1 percent accuracy in S requires values of y_1 about a factor of two larger than those given in Figure 2.

A few additional calculations were made in which both B and $\Delta\nu_D$ varied with depth. The depth variation of B mimicked the solar atmosphere and $\Delta\nu_D$ was equated to the thermal Doppler width. This did not produce any substantial change in y_1. However, rapid depth variations in any one of the parameters influencing S, viz., B, $\Delta\nu_D$, ε, r_o and $\underline{a}$ may very well lead to significant changes in y_1. It is perhaps wise in using the results in Figure 2 and equation (7) to use the minimum values of ε and r_o and maximum values of $\underline{a}$ for a particular problem.

Although calculations have not been made for multilevel atoms, I see no particular reason why the inclusion of added levels should increase the values of y_1. However, if the added levels increase the effective value of ε the required values of y_1 may be substantially reduced. It would seem entirely safe, therefore, to use the results found here for multilevel problems.

REFERENCE

Athay, R. G., and Skumanich, A. 1967, *Ann. d'Ap.*, 30, 669.

DISCUSSION

Underhill: Have you investigated what happens if you encounter a neighbouring line in your necessary bandwidth y_1 (100 Doppler-widths) for the frequency integration?

Athay: No, I don't know what happens to y_1 in that case.

COMPARISON OF DISCRETE SPACE AND DIFFERENTIAL EQUATION METHODS IN NON-LTE LINE TRANSFER PROBLEMS

by

I. P. Grant and G. E. Hunt

Science Research Council, Atlas Computer Laboratory
Chilton, Didcot, Berkshire, England

ABSTRACT

Numerical methods are essential to the treatment of line formation in inhomogeneous non-LTE atmospheres. The new methods due to Hummer and Rybicki and to Feautrier now make it possible to make such calculations, although these are often quite time-consuming.

We shall describe an alternative approach using discrete space techniques depending on concpets of invariance. The solution algorithm is closely related to the method of Hummer and Rybicki, whose equations are obtained as a limiting case. The stability and errors of our algorithm are susceptible to mathematical analysis, and make it possible to identify the critical parameters in the calculation with precision. The results for a two-level problem will be compared with those from an implementation of the Rybicki-Hummer equations and a comparison will be made of the performance of the two procedures in respect of speed of computation and storage requirements.

Key words: line formation, inhomogeneous non-LTE atmospheres, numerical methods.

1. INTRODUCTION

In this paper, we shall be concerned with computational problems arising in the calculation of the line spectrum of a non-LTE model stellar atmosphere. This field has recently been treated in book form by

Jefferies,[1] and Hummer and Rybicki[2] have reviewed the state of the art of computation as it was at October 1966. At the time that these articles were written, the best methods available for atmospheres in which the parameters vary with depth were the Riccati method[2,3] and that of Feautrier.[2,4,5] Since then, we have developed a theory of radiative transfer, based on principles of invariance, which is particularly suited to computation.[6,7] The equations of this theory have a simple structure which is easy to interpret in physical terms, and their solution is a relatively rapid and simple matter. Their form is sufficiently universal to make generalization easy, and it is possible to make a sufficiently precise analysis of error propagation and stability to give us confidence in the numerical results obtained.

We shall present an application of this general theory to the problem of determining the line profile due to non-coherent scattering in an inhomogeneous plane-parallel atmosphere. We have confined ourselves for the present to problems already treated by the Riccati method,[3] and we have therefore assumed that we are dealing with a model atom with two discrete levels only. One of our objects has been to see if our methods are in any way competitive with others already in the field; astrophysicists will want solutions to more elaborate model problems in the future, and reliable methods promising any economy while maintaining accuracy are highly desirable. We shall therefore make a detailed comparison of our technique with the Riccati method, and, in so doing, deal with some problems that we have encountered in carrying out their implementation.

2. GENERAL PRINCIPLES

Our computational procedures depend upon a conservation principle which may be expressed in the form

$$\begin{aligned} u^+(y) &= t(y,x)u^+(x) + r(x,y)u^-(y) + \Sigma^+(y,x) \\ u^-(x) &= r(y,x)u^+(x) + t(x,y)u^-(y) + \Sigma^-(x,y) \end{aligned} \qquad (1)$$

where x,y are depth co-ordinates in the plane-parallel atmosphere such that $a \leq x < y \leq b$. The quantities $u^+(x)$, $u^-(x)$, $u^+(y)$, $u^-(y)$ are the

specific intensities of radiation at the corresponding levels x, y, the superscripts referring to the sign of the cosine, μ, of the angle between the direction in which the radiation travels and the normal to the layers in the sense of increasing depth, x. In the present case, $u^+(x)$, for example, will take values $u^+(x)(\mu,\xi) \equiv I(\mu,\xi;x)$, where $I(\mu,\xi;x)$ is the specific intensity for some particular value of μ, $0 < \mu \leq 1$, and ξ is a scaled frequency variable, $\xi = (\nu-\nu_o)/\Delta_s$, at depth x. The terms $\Sigma^+(y,x)$, $\Sigma^-(x,y)$ represent the emission of radiative energy within the layer [x,y] in the positive (negative) direction at y(x). Finally, the quantities t(y,x), t(x,y), r(y,x), r(x,y) represent operators that describe the transmission and reflection of radiation by the layer. In line transfer problems they will involve, in general, redistribution of radiant energy both in direction and in frequency. Thus, for example, we may write

$$[r(x,y)u^-(y)](\mu,\xi) \equiv$$

$$\frac{1}{2\mu}\int_0^1 d\mu' \int_{-\infty}^{\infty} d\xi'\ R(x,y|\mu,\xi;-\mu',\xi')[u^-(y)(-\mu',\xi')] \quad (2)$$

for the radiation diffusely reflected from negative directions into the positive direction μ at the surface y of the layer [x,y]. This representation is intractable for computation as it stands, but if, as is common, in practice we use a discrete-ordinate approximation both with regard to μ and to ξ, the intensities $u^+(x)$, $u^-(x)$, and sources $\Sigma^+(y,x)$, $\Sigma^-(x,y)$ can be written as vectors in a finite-dimensional linear vector space, and the quantities t(x,y), t(y,x), r(x,y), r(y,x) become matrix operators mapping this space onto itself. We can then apply familiar computational techniques to deal with equations (1).

Suppose, for the moment, that we know the operators and source vectors for each layer of an arbitrary finite partition of [a,b] into N layers by planes at $x = x_n$, $a = x_1 < x_2 < \ldots < x_{N+1} = b$. Equations (1) then provide a set of 2N equations for the 2N intensity vectors u_n^-, $1 \leq n \leq N$ and u_n^+, $2 \leq n \leq N+1$ in terms of the boundary values $u_1^+ = u^+(a)$, $u_{N+1}^- = u^-(b)$ and internal sources. We may write these equations in the form

$$(\underset{\sim}{I} - \underset{\sim}{L})\ \underset{\sim}{U} = \underset{\sim}{\Sigma} + \underset{\sim}{\Sigma}_s \tag{3}$$

where the vectors $\underset{\sim}{U}$, $\underset{\sim}{\Sigma}$ and $\underset{\sim}{\Sigma}_s$ are defined by

$$\underset{\sim}{U} = \begin{bmatrix} u_2^+ \\ u_1^- \\ u_3^+ \\ u_2^- \\ \cdot \\ \cdot \\ \cdot \\ u_{N+1}^+ \\ u_N^- \end{bmatrix}, \quad \underset{\sim}{\Sigma} = \begin{bmatrix} \Sigma^+(2,1) \\ \Sigma^-(1,2) \\ \Sigma^+(3,2) \\ \Sigma^-(2,3) \\ \cdot \\ \cdot \\ \cdot \\ \Sigma^+(N+1,N) \\ \Sigma^-(N,N+1) \end{bmatrix}, \quad \underset{\sim}{\Sigma}_s = \begin{bmatrix} t(2,1)u_1^+ \\ r(2,1)u_1^+ \\ 0 \\ 0 \\ \cdot \\ \cdot \\ \cdot \\ \cdot \\ r(N,N+1)u_{N+1}^- \\ t(N,N+1)U_{N+1}^- \end{bmatrix} \tag{4}$$

and where the matrix $\underset{\sim}{L}$ has the block form

$$\underset{\sim}{L} = \begin{bmatrix} o & o & o & r(1,2) & & & & \\ o & o & o & t(1,2) & & & & \\ t(3,2) & o & o & o & o & r(2,3) & & \\ r(3,2) & o & o & o & o & t(2,3) & & \\ & & t(4,3) & o & o & o & o & r(3,4) \\ & & r(4,3) & o & o & o & o & t(3,4) \\ & & & & & & r(N+1,N) & o \\ & & & & & & t(N+1,N) & o \end{bmatrix} \tag{5}$$

We recognize that this is a particular form of block-tridiagonal matrix; the method of dealing with equations involving such matrices is well-known, and a good account is given in the text book by Isaacson and Keller.[8] When this process is written out, we get an algorithm which may be set out as follows:

Define $r(1,n+1)$, $V^{+}_{n+1/2}$, $V^{-}_{n+1/2}$, $n = 1,2, \ldots .$, N by the equations

$$r(1,1) = 0,\ r(1,n+1) = r(n,n+1) +$$

$$+ t(n+1,n)r(1,n)[I-r(n+1,n)r(1,n)]t^{-1}(n,n+1) \quad (6)$$

$$V^{+}_{1/2} = u^{+}_{1},\quad V^{+}_{n+1/2} =$$

$$\hat{t}(n+1,n)V^{+}_{n-1/2} + \Sigma^{+}(n+1,n) + R_{n+1/2}\Sigma^{-}(n,n+1) \quad (7)$$

$$V^{-}_{n+1/2} = \hat{r}(n+1,n)V^{+}_{n-1/2} + T_{n+1/2}\Sigma^{-}(n,n+1)$$

where

$$T_{n+1/2} = [I-r(n+1,n)r(1,n)]^{-1} \equiv$$

$$I+r(n+1,n)[I-r(1,n)r(n+1,n)]^{-1}r(1,n)$$

$$\hat{t}(n+1,n) = t(n+1,n)[I-r(1,n)r(n+1,n)]^{-1} \quad (8)$$

$$\hat{r}(n+1,n) = r(n+1,n)[I-r(1,n)r(n+1,n)]^{-1}$$

and

$$R_{n+1/2} = \hat{t}(n+1,n)r(1,n)$$

These equations can be solved for increasing values

of n, and the final solutions u^+_{n+1}, u^-_n can be obtained from

$$u^+_{n+1} = r(1,n+1)u^-_{n+1} + V^+_{n+1/2}$$
$$u^-_n = \hat{t}(n,n+1)u^-_{n+1} + V^-_{n+1/2}\ , \tag{9}$$

starting with the specified boundary value of u^-_{N+1}, for n = N, N-1, ... , 1 in succession. The matrix

$$\hat{t}(n,n+1) = T_{n+1/2}t(n,n+1)$$

may be computed at the same time as those of equations (8). More information about these algorithms and their physical interpretation is contained in our earlier papers.[6,7]

Our strategy is therefore to put the equations of the problem into this canonical form, and thence to solve them by the standard technique outlined above. One way of doing this is to remark that in the limit as y tends to x, equations (1) must converge to the conventional differential equation of radiative transfer. In this way, we may identify the leading terms in an expansion of the matrix operators in terms of the layer thickness (y-x); they can be expressed in terms of the usual known physical quantities point-by-point, such as absorption coefficients, scattering coefficients and so on. The source terms may be identified in the same way. The approximations so defined have rather poor truncation errors, and it is better to start with a difference scheme which is known to have higher accuracy (6). That is the approach that we shall adopt in this paper. Of course, the operators and sources obtained in this way must have expansion in powers of the layer thickness agreeing with those obtained from the simpler procedure through first order terms.

3. DISCRETE EQUATIONS FOR LINE TRANSFER PROBLEMS

The purpose of this section is to write the integro-differential equations of transfer for the

formation of spectrum lines in the required form, using a notation rather similar to that of Hummer and Rybicki.[2,3] For a two-level atom, assuming complete redistribution, they write

$$\mu \frac{d}{d\tau} I_{\xi\mu} = [\beta+\phi(\xi)](S_{\xi\mu}-I_{\xi}) \qquad (10)$$

where $I_{\xi\mu}$ is the specific intensity at a frequency specified by

$$\xi = (\nu-\nu_o)/\Delta_s, \qquad (11)$$

in a direction specified by μ where Δ_s is, as usual, some standard frequency interval. Here $\phi(\xi)$ is the line profile, normalized so that

$$\int_{-\infty}^{\infty} \phi(\xi)d\xi = 1. \qquad (12)$$

The mean optical depth is defined in terms of the geometrical depth z by

$$d\tau = k_L(z)dz \frac{h\nu_o}{4\pi\Delta_s} (N_1B_{12}-N_2B_{21})dz \qquad (13)$$

where $B_{12}(z)$, $B_{21}(z)$ are the Einstein coefficients, and $N_1(z)$,$N_2(z)$ the population densities of the lower and upper states respectively. The quantity β is the ratio k_C/k_L of opacity due to continuous absorption per unit interval Δ_s to that in the line, and in this event

$$S_{\xi}(z) = \frac{\phi(\xi)}{\beta+\phi(\xi)} S_L(z) + \frac{\beta}{\beta+\phi(\xi)} S_c(z) \qquad (14)$$

where $S_c(z)$ is the continuum source function, which, for present purposes, we shall write in the form

$$S_c(z) = \rho(z)\ B(\nu_o,T_e(z)) \qquad (15)$$

where B is the Planck function for frequency ν_o at

electron temperature T_e, and both ρ and B are assumed to be independent specified functions of z. The line source function for complete redistribution, $S_L(z)$, is given by

$$S_L(z) = A_{21}N_2(z)/[B_{12}N_1(z) - B_{21}N_2(z)], \quad (16)$$

and, when combined with the statistical equilibrium equation

$$N_1[B_{12}\int_{-\infty}^{\infty}\phi(\xi)J_\xi d\xi + C_{12}] = N_2[A_{21} + C_{21} + B_{21}\int_{-\infty}^{\infty}\phi(\xi)J_\xi d\xi],$$

it becomes

$$S_L(z) = (1-\varepsilon)\int_{-\infty}^{\infty}\phi(\xi)J_\xi d\xi + \varepsilon B \quad (17)$$

where J_ξ is the mean intensity, B is the Planck function and

$$\varepsilon = \frac{C_{21}}{C_{21}+A_{21}[1-\exp(-h\nu_o/kT_e)]^{-1}} \quad (18)$$

is the probability per scatter that a photon will be destroyed by collisional de-excitation. We are, as usual, interested in cases with $\varepsilon << 1$, and we shall assume that this parameter is specified in advance.

Our computational problem is therefore to solve equation (10) with a source function defined by equations (14), (15), and (17) regarding $\beta(z)$, $\rho(z)$, $\varepsilon(z)$, $\phi(\xi) \equiv \phi(z,\xi)$, and B(z) as specified functions. In addition we need boundary conditions specifying the fluxes incident on the external surfaces. This problem will be solved by a suitable discretization in frequency, direction, and space. For the frequency discretization, we choose division points

$\{\xi_i\}$ and weights $\{a_i\}$ such that

$$\int_{-\infty}^{\infty} \phi(\xi) f(\xi) d\xi \approx \sum_{i=-I}^{I} a_i f(\xi_i) \qquad \sum_{i=-I}^{I} a_i = 1 \tag{19}$$

and for the directional discretization we choose abscissae $\{\mu_j\}$ and weights $\{b_j\}$ such that

$$\int_0^1 f(\mu) d\mu \approx \sum_{j=1}^{m} b_j f(\mu_j), \quad \sum_{j=1}^{m} b_j = 1 \ . \tag{20}$$

We define the mxm matrices

$$\underset{\sim}{b} = [b_i \delta_{ij}] \ , \ \underset{\sim}{M}_m = [\mu_i \delta_{ij}]$$

and the m-vectors

$$\underset{\sim}{h} = \begin{bmatrix} 1 \\ 1 \\ \cdot \\ \cdot \\ \cdot \\ 1 \end{bmatrix} \ , \ u^+_{i,n} = \begin{bmatrix} I(\mu_1, \xi_i; \tau_n) \\ \cdot \\ \cdot \\ \cdot \\ \cdot \\ I(\mu_m, \xi_i; \tau_n) \end{bmatrix}$$

$$u^-_{i,n} = \begin{bmatrix} I(-\mu_1, \xi_i; \tau_n) \\ \cdot \\ \cdot \\ \cdot \\ \cdot \\ I(-\mu_m, \xi_i; \tau_n) \end{bmatrix} \tag{21}$$

Then, if we integrate equation (10) from τ_n to τ_{n+1}, we may write the result as

$$\underset{\sim}{M}_m(u^+_{i,n+1}-u^+_{i,n}) = \tau_{n+1/2}(\rho\beta+\varepsilon\phi_i)_{n+1/2}B_{n+1/2}\underset{\sim}{h}$$

$$+ \frac{1}{2}\tau_{n+1/2}\sigma_{n+1/2}\phi_{i,n+1/2} \times$$

$$\times \sum_{i'=-I}^{I} a_{i',n+1/2}(\underset{\sim}{h}\,\underset{\sim}{h}^T)\underset{\sim}{b}(u^+ + u^-)_{i',n+1/2}$$

$$- \tau_{n+1/2}(\beta+\phi_i)_{n+1/2}u^+_{i,n+1/2} \qquad (22)$$

$$-\underset{\sim}{M}_m(u^-_{i,n+1}-u^-_{i,n}) = \tau_{n+1/2}(\rho\beta+\varepsilon\phi_i)_{u+1/2}B_{n+1/2}\underset{\sim}{h}$$

$$+ \frac{1}{2}\tau_{n+1/2}\sigma_{n+1/2}\phi_{i,n+1/2} \times$$

$$\sum_{i'=-I}^{I} a_{i',n+1/2}(\underset{\sim}{h}\,\underset{\sim}{h}^T)\underset{\sim}{b}(u^+ + u^-)_{i',n+1/2}$$

$$- \tau_{n+1/2}(\beta+\phi_i)_{n+1/2}u^-_{i,n+1/2}$$

Here we have used superscript T to denote transposition, $\tau_{n+1/2} = \tau_{n+1} - \tau_n > 0$, and other subscripts $(n+1/2)$ to denote averages for the layer. Also $\sigma_{n+1/2} = 1-\varepsilon_{n+1/2}$.

Corresponding to each pair of subscripts (i,j), we now define an index k so that

$$(i,j) \equiv k = j + (i-1)m, \quad 1 \le k \le K = mI. \qquad (23)$$

For each value of k, we define coefficients $W_k \equiv W_{k,n+1/2}$ by

$$\phi_k W_k = a_i b_j \quad . \tag{24}$$

Let

$$\underset{\sim}{u}_n^{\pm}(L) = \begin{bmatrix} u_{-1,n}^{\pm} \\ \cdot \\ \cdot \\ \cdot \\ \cdot \\ \cdot \\ u_{-I,n}^{\pm} \end{bmatrix} , \quad \underset{\sim}{u}_n^{+}(R) = \begin{bmatrix} u_{1,n}^{\pm} \\ \cdot \\ \cdot \\ \cdot \\ \cdot \\ \cdot \\ u_{I,n}^{\pm} \end{bmatrix} \tag{25}$$

be K-vectors corresponding to frequencies to left (L) and right (R) of the line center. Let $\underset{\sim}{\phi}_{n+1/2}$ and $\underset{\sim}{g}_{n+1/2}$ be K-vectors, where the elements of $\underset{\sim}{g}_{n+1/2}$ are defined by

$$g_{k,n+1/2} = (\rho\beta+\varepsilon\phi_k)_{n+1/2} B_{n+1/2} \tag{26}$$

and let $\underset{\sim\sim}{\Lambda}$, $\underset{\sim\sim}{W}$ and $\underset{\sim\sim}{M}$ be K × K matrices defined by

$$\underset{\sim\sim}{\Lambda}_{n+1/2} = [\Lambda_{kk'}] =$$

$$[(\beta+\phi_k)_{n+1/2}\delta_{kk'}] \ , \ \underset{\sim\sim}{W}_{n+1/2} = [W_{k,n+1/2}\delta_{kk'}], \tag{27}$$

and

$$\underset{\sim\sim}{M} = \begin{bmatrix} \underset{\sim\sim}{M}_m & & & \\ & \underset{\sim\sim}{M}_m & \bigcirc & \\ & & \ddots & \\ & \bigcirc & & \underset{\sim\sim}{M}_m \end{bmatrix}$$

Then equations (22) reduce to

$$\underset{\sim}{M}[\underset{\sim}{u}^{+}_{n+1}(r)-\underset{\sim}{u}^{+}_{n}(R)] + \tau_{n+1/2}\underset{\sim}{\Lambda}_{n+1/2}\underset{\sim}{u}^{+}_{n+1/2}(R)$$

$$= \frac{\pi}{2}_{n+1/2}\sigma_{n+1/2}(\underset{\sim}{\phi}\ \underset{\sim}{\phi}^{T})_{n+1/2}\underset{\sim}{W}_{n+1/2}[\underset{\sim}{u}^{+}(L) +$$

$$+ \underset{\sim}{u}^{+}(R)+\underset{\sim}{u}^{-}(L)+\underset{\sim}{u}^{-}(R)]_{n+1/2}$$

$$+ \tau_{n+1/2}\underset{\sim}{g}_{n+1/2}(R)$$

and (28)

$$-\underset{\sim}{M}[\underset{\sim}{u}^{-}_{n+1}(R)-\underset{\sim}{u}^{-}_{n}(R)] + \tau_{n+1/2}\underset{\sim}{\Lambda}_{n+1/2}\underset{\sim}{u}^{-}_{n+1/2}(R)$$

$$= \frac{\pi}{2}_{n+1/2}\sigma_{n+1/2}(\underset{\sim}{\phi}\ \underset{\sim}{\phi}^{T})_{n+1/2}\underset{\sim}{W}_{n+1/2}[\underset{\sim}{u}^{+}(L) +$$

$$+ \underset{\sim}{u}^{+}(R)+\underset{\sim}{u}^{-}(L)+\underset{\sim}{u}^{-}(R)]_{n+1/2}$$

$$+ \tau_{n+1/2}\underset{\sim}{g}_{n+1/2}(R)$$

and two similar equations with L and R interchanged everywhere. When the line profile is symmetric, we have $\underset{\sim}{u}^{\pm}(L) = \underset{\sim}{u}^{\pm}(R)$, $\underset{\sim}{g}(L) = \underset{\sim}{g}(R)$, and equations (24) simplify. In either case, the structure of the equations is similar to those of equations (2.10) of our earlier paper,[6] and hence the same procedures may be used to re-write them in the form of equations (1). The details are presented in the Appendix. In the symmetric case, to which we shall confine ourselves in this paper, we find

$$\underset{\sim}{u}^{+}_{n+1} = \underset{\sim}{t}(n+1,n)\underset{\sim}{u}^{+}_{n} + \underset{\sim}{r}(n,n+1)\underset{\sim}{u}^{-}_{n+1} + \underset{\sim}{\Sigma}^{+}(n+1,n)$$

$$\underset{\sim}{u}^{-}_{n} = \underset{\sim}{r}(n+1,n)\underset{\sim}{u}^{+}_{n} + \underset{\sim}{t}(n,n+1)\underset{\sim}{u}^{-}_{n+1} + \underset{\sim}{\Sigma}^{-}(n,n+1) \quad (29)$$

where

$$\underset{\sim}{r}(n,n+1) = \underset{\sim}{r}(n+1,n) \equiv$$

$$\underset{\sim}{r}_{n+1/2} = \gamma_{n+1/2} (\underset{\sim}{C}\ \underset{\sim}{C}^T)_{n+1/2} \underset{\sim}{M}\ \underset{\sim}{W}_{n+1/2} \quad (30)$$

and

$$\underset{\sim}{t}(n,n+1) = \underset{\sim}{t}(n+1,n) = \underset{\sim}{t}_{n+1/2} + \underset{\sim}{r}_{n+1/2} \quad (31)$$

in which the first term is a diagonal matrix,

$$\underset{\sim}{t}_{n+1/2} = [\underset{\sim}{I} - \tfrac{1}{2}\tau_{n+1/2} \underset{\sim}{M}^{-1} \underset{\sim}{\Lambda}_{n+1/2}] [\underset{\sim}{I} + \tfrac{1}{2}\tau_{n+1/2} \underset{\sim}{M}^{-1} \underset{\sim}{\Lambda}_{n+1/2}]^{-1}.$$

In these definitions $\underset{\sim}{I}$ is the K × K identity matrix,

$$\underset{\sim}{C}_{n+1/2} = [\underset{\sim}{I} + \tfrac{1}{2}\tau_{n+1/2} \underset{\sim}{M}^{-1} \underset{\sim}{\Lambda}_{n+1/2}]^{-1} \cdot \underset{\sim}{M}^{-1} \underset{\sim}{\phi}_{n+1/2}, \quad (32)$$

and

$$\gamma_{n+1/2} = \sigma_{n+1/2} \tau_{n+1/2} / [1 - 2\delta_{n+1/2}] \quad (33)$$

where

$$\delta_{n+1/2} = \sigma_{n+1/2} \tau_{n+1/2} \times$$

$$\times \sum_{k=1}^{K} \frac{W_{k,n+1/2} \phi^2_{k,n+1/2}}{2\mu_k + \tau_{n+1/2} \Lambda_{kk,n+1/2}} \quad (34)$$

The following properties of the matrices are easy but important consequences of the definitions:

(i) $\underset{\sim}{t}_{n+1/2}$ is a matrix approximation to $\exp [-\tau_{n+1/2} \underset{\sim}{M}^{-1} \underset{\sim}{\Lambda}_{n+1/2}]$, and so represents the unscattered attenuation in the layer.

(ii) $\underset{\sim}{r}_{n+1/2}$ is unsymmetric, but the matrix $\underset{\sim}{S}_{n+1/2}$ defined by

$$\underset{\sim}{S}_{n+1/2} = \underset{\sim}{W}_{n+1/2}\underset{\sim}{M}\underset{\sim}{r}_{n+1/2} \tag{35}$$

(iii) $\underset{\sim}{r}_{n+1/2}$ has non-negative elements (written $\underset{\sim}{r}_{n+1/2} \geq o$). Indeed, from (34), taking account of (24) and (27), we have

$$\delta_{n+1/2} = \sigma_{n+1/2}\tau_{n+1/2}$$

$$\sum_{i=1}^{I}\sum_{j=1}^{M} \frac{a_j b_j \phi_{i,n+1/2}}{2\mu_j + \tau_{n+1/2}(\beta_{n+1/2} + \phi_{i,n+1/2})}$$

$$< \sigma_{n+1/2} \sum_{i=1}^{I}\sum_{j=1}^{M} a_i b_j = \frac{1}{2}\sigma_{n+1/2}$$

so that

$$o < \gamma_{n+1/2} < \frac{\sigma_{n+1/2}\tau_{n+1/2}}{1-\sigma_{n+1/2}}$$

(iv) A sufficient condition for $t_{n+1/2} \geq o$ is

$$\tau_{n+1/2} < \min_k \frac{2\mu_k}{\Lambda_k} = \frac{2\mu_1}{\beta + \phi(0)_{n+1/2}} = \tau^1,$$

say. This is more stringent than one needs to ensure that t(n,n+1) and t(n+1,n) are non-negative. A better sufficient condition is

$$\tau < \tau^1 \min_{i,j}\left[1 - \frac{2(1-\varepsilon)a_i \phi_{i,n+1/2} b_j}{(\beta+\phi_i)_{n+1/2}}\right]^{-1} = \tau_{crit} \tag{36}$$

(v) Let

$$||\underset{\sim}{u}|| = 2\pi \sum_{i=-I}^{I} a_i \sum_{j=1}^{M} b_j u_j \, |u_i(\mu_j)| \tag{37}$$

$$= 2\pi \sum_{k=1}^{K} \underset{\phi_k}{W_k} \, |u_k|$$

Then $||\underset{\sim}{u}||$ is a vector norm satisfying the usual norm conditions, and a matrix norm, $||\underset{\sim}{A}||$, consistent and subordinate to this norm is[7]

$$||A|| = \max_{k'} \sum_{k} \underset{\phi_k}{W_k} \, |A_{kk'}| \, \underset{\phi_{k'}}{W_{k'}}^{-1} \quad . \tag{38}$$

Now define the cell matrix $\underset{\sim}{\Gamma}(n,n+1)$ associated with the layer under consideration by

$$\underset{\sim}{\Gamma}(n,n+1) = \begin{bmatrix} \underset{\sim}{t}(n+1,n) & \underset{\sim}{r}(n,n+1) \\ \underset{\sim}{r}(n+1,n) & \underset{\sim}{t}(n,n+1) \end{bmatrix}$$

By analogy with (38), and assuming (36) holds,

$$||\underset{\sim}{\Gamma}(n,n+1)|| = \max \{ ||\underset{\sim}{t}(n+1,n) +$$

$$+\underset{\sim}{r}(n+1,n)||, \; ||\underset{\sim}{t}(n,n+1)+\underset{\sim}{r}(n,n+1)|| \}$$

$$= ||\underset{\sim}{t}_{n+1/2} + 2\underset{\sim}{r}_{n+1/2}||$$

$$= 1-\tau_{n+1/2} \min_{k} \frac{\{(\beta+\varepsilon\phi_k)_{n+1/2}\}}{\mu_k} + \tag{40}$$

$$+ O(\tau^2_{n+1/2})$$

$$< 1.$$

We have shown[7] that the conditions set out above are necessary and sufficient to ensure the existence of a unique bounded non-negative solution to our equations.

To complete the specification, we need the source vectors, which are given by

$$\Sigma^{+}(n+1,n) = \underset{\sim}{\Sigma}^{-}(n,n+1) \equiv$$

$$\underset{\sim}{\Sigma}_{n+1/2} = \frac{1}{2}\tau_{n+1/2}[\underset{\sim}{I} + \underset{\sim}{t}_{n+1/2} + 2\underset{\sim}{r}_{n+1/2}]\ \underset{\sim}{M}^{-1}\underset{\sim}{g}_{n+1/2}$$

4. IMPLEMENTATION OF THE PROCEDURES FOR LINE TRANSFER

The structure of equations (30) and (31), which represents the reflection operators for a thin layer as a Kronecker product, allows a great simplification of the algorithm. We suppose that we require only to determine the source function and the emergent intensity vector, so that we shall set down only those equations which are directly relevant to the computation in this section. The remaining equations not needed for this part of the computation are set out in the Appendix.

We write

$$\underset{\sim}{S}_{n+1/2} = \underset{\sim}{M}\ \underset{\sim}{W}_{n+1/2}\underset{\sim}{r}(1,n)\ , \tag{42}$$

and define the scalars

$$\lambda_{n+1/2} = \underset{\sim}{C}^{T}_{n+1/2}\underset{\sim}{S}_{n+1/2}\underset{\sim}{C}_{n+1/2}$$

and

$$A_{n+1/2} = \frac{\gamma_{n+1/2}}{1-\gamma_{n+1/2}\lambda_{n+1/2}} \tag{43}$$

Then equations (6) become

$$\underset{\sim}{S}_{n+3/2} =$$

$$\underset{\sim}{W}^{-1}_{n+1/2}\underset{\sim}{W}_{n+3/2}[\underset{\sim}{t}_{n+1/2}\underset{\sim}{S}_{n+1/2}\underset{\sim}{t}_{n+1/2} + A_{n+1/2}\underset{\sim}{X}_{n+1/2}\tilde{\underset{\sim}{X}}_{n+1/2}], \tag{44}$$

to be evaluated recursively for n = 1,2, ··· , N, starting with $\underset{\sim}{S}_{3/2} = 0$, where the K-vectors $\underset{\sim}{X}_{n+1/2}$ and $\tilde{\underset{\sim}{X}}_{n+1/2}$ are defined by

$$\underset{\sim}{X}_{n+1/2} = (\underset{\sim}{M}\, W_{n+1/2} + t_{n+1/2}\underset{\sim}{S}_{n+1/2})\underset{\sim}{C}_{n+1/2}$$

$$\tilde{\underset{\sim}{X}}_{n+1/2} = \underset{\sim}{C}^{T}_{n+1/2}(S_{n+1/2}\underset{\sim}{t}_{n+1/2} + \underset{\sim}{M}\, \underset{\sim}{W}_{n+1/2}).$$

Notice that $\tilde{\underset{\sim}{X}}_{n+1/2}$ will equal $\underset{\sim}{X}^{T}_{n+1/2}$ if $S_{n+1/2}$ is symmetric. This is only the case if $\underset{\sim}{W}_{n+1/2}$ is independent of depth, that is to say if (a_i/ϕ_k) is independent of n. This depends on the choice of quadrature forumla; $\underset{\sim}{W}_{n+1/2}$ is independent of n for most choices.

We also define

$$\tilde{\underset{\sim}{V}}_{n+1/2} = \underset{\sim}{M}\, \underset{\sim}{W}_{n+1/2}\underset{\sim}{V}^{+}_{n+1/2} \tag{45}$$

and the K-vector

$$\underset{\sim}{Y}_{n+1/2} = \underset{\sim}{W}^{-1}_{n-1/2}\underset{\sim}{W}_{n+1/2}\tilde{\underset{\sim}{V}}_{n-1/2} + \underset{\sim}{S}_{n+1/2}\underset{\sim}{\Sigma}_{n+1/2} \quad . \tag{46}$$

Then the first of equations (7) becomes

$$\tilde{\underset{\sim}{V}}_{n+1/2} = \underset{\sim}{t}_{n+1/2}\underset{\sim}{Y}_{n+1/2} + B_{n+1/2}\underset{\sim}{X}_{n+1/2} + \underset{\sim}{M}\, \underset{\sim}{W}_{n+1/2}\underset{\sim}{\Sigma}_{n+1/2}, \tag{47}$$

to be evaluated recursively for n = 1,2, ··· ,N, starting with

$\tilde{\underset{\sim}{V}}_{1/2} = \underset{\sim}{M}\, \underset{\sim}{W}_{1/2}\underset{\sim}{u}^{+}_{1}$ ($\underset{\sim}{W}_{1/2} = \underset{\sim}{W}_{3/2}$ being assumed), where

$$B_{n+1/2} = A_{n+1/2}\underset{\sim}{C}^{T}_{n+1/2}\underset{\sim}{Y}_{n+1/2} \quad . \tag{48}$$

Then, given $\underset{\sim}{u}^{-}_{N+1}$, we can evaluate for n=N, N-1, ...,1 the equation

$$\underset{\sim}{u}^{-}_{n} = \underset{\sim}{t}_{n+1/2}\underset{\sim}{u}^{-}_{n+1} +$$

$$+ [B_{n+1/2} + A_{n+1/2}(\tilde{\underset{\sim}{X}}_{n+1/2}\underset{\sim}{u}^{-}_{n+1})]\,\underset{\sim}{C}_{n+1/2} + \underset{\sim}{\Sigma}_{n+1/2} \qquad (49)$$

to give the upward directed intensities at each interface. The line source function, defined by (17), requires the calculation of

$$\bar{J}_n = \int_{-\infty}^{\infty} \phi(\xi)\, J_{\xi,n}\, d\xi$$

$$\approx \left[\underset{\sim}{\phi}^{T}_{n-1/2}\underset{\sim}{W}_{n-1/2}\underset{\sim}{u}^{+}_{n} + \underset{\sim}{\phi}^{T}_{n+1/2}\underset{\sim}{W}_{n+1/2}\underset{\sim}{u}^{-}_{n}\right] \qquad (50)$$

$$= \underset{\sim}{Z}^{T}_{n}\underset{\sim}{u}^{-}_{n} + \underset{\sim}{\phi}^{T}_{n-1/2}\underset{\sim}{M}^{-1}\tilde{\underset{\sim}{V}}_{n-1/2} \quad ,$$

where

$$\underset{\sim}{Z}^{T}_{n} = \underset{\sim}{\phi}^{T}_{n=1/2}\underset{\sim}{M}^{-1}(\underset{\sim}{W}^{-1}_{n+1/2}\underset{\sim}{W}_{n-1/2}\underset{\sim}{S}_{n+1/2}) + \underset{\sim}{\phi}^{T}_{n+1/2}\underset{\sim}{W}_{n+1/2} \qquad (51)$$

may be computed along with $\underset{\sim}{X}_{n+1/2}$, $\tilde{\underset{\sim}{X}}_{n+1/2}$ and $\underset{\sim}{Y}_{n+1/2}$. Notice that if $\underset{\sim}{u}^{-}_{1}$ and the line source function are all that we require, it is unnecessary to compute $\underset{\sim}{u}^{+}_{n}$ directly.

We may also wish to compute the emission in some other direction μ than that prescribed by the rule for angular quadrature. Now that we have the line-source function this is straightforward. Writing the required frequency distribution as an I-vector, $\underset{\sim}{u}^{-}_{1}(\mu)$, we see that

$$\underset{\sim}{u}^{-}_{1}(\mu) = \int_{0}^{\tau_{N+1}} e^{-\tau\underset{\sim}{\Lambda}(\tau)/\mu}[(1-\varepsilon(\tau))\underset{\sim}{\phi}_{\mu}(\tau)\bar{J}(\tau)+\underset{\sim}{g}_{\mu}(\tau)]d\tau \qquad (52$$

where $\underset{\sim}{\Lambda}(\tau)$ is an I × I diagonal matrix, and $\underset{\sim}{\phi}_\mu(\tau)$, $\underset{\sim}{g}_\mu(\tau)$ are I-vectors defined for the single value of μ as in equations (27) and (26) respectively. The discrete representation of (52) may be written

$$\underset{\sim}{u}_1^-(\mu) \approx \sum_{n=1}^{N} \underset{\sim}{t}(1,n+\tfrac{1}{2})\left[(1-\varepsilon_{n+1/2})\bar{J}_{n+1/2}\underset{\sim}{\phi}_{n+1/2} + \underset{\sim}{g}_{n+1/2}\right]\tau_{n+1/2} \tag{53}$$

The choice of $\bar{J}_{n+1/2}$ and of $\underset{\sim}{t}(1,n+\frac{1}{2})$ is slightly arbitrary. We have used

$$\underset{\sim}{\bar{t}}(1,n+\tfrac{1}{2}) = \tfrac{1}{2}[\underset{\sim}{\bar{t}}(1,n) + \underset{\sim}{\bar{t}}(1,n+1)]$$

where

$$\underset{\sim}{\bar{t}}(1,n) = \prod_{k=1}^{n-1} \underset{\sim}{t}_{n+1/2}(\mu) \ , \tag{54}$$

with

$$\underset{\sim}{t}_{n+1/2}(\mu) = \left[\delta_{ii'}\,\frac{1 - \frac{1}{2}\tau_{n+1/2}\Lambda_i/\mu}{1 + \frac{1}{2}\tau_{n+1/2}\Lambda_i/\mu}\right] ,$$

and

$$\bar{J}_{n+1/2} = \tfrac{1}{2}(\bar{J}_{n+1} + \bar{J}_n) \quad . \tag{55}$$

It would be possible to use more accurate formulae, but we have not found it necessary to do so.

5. THE RICCATI METHOD

If we pass to the limit as $\tau_{n+1/2} \to 0$, our equations reduce to a set equivalent to those of the

Riccati method of Rybicki and Hummer.[2,3] Equation (44) becomes

$$\frac{d\underset{\sim}{S}(t)}{d\tau} = \underset{\sim}{W}^{-1}(\tau)\ \frac{d\underset{\sim}{W}(\tau)}{d\tau}\ \underset{\sim}{S}(\tau) - \underset{\sim}{M}^{-1}\underset{\sim}{\Lambda}(\tau)\underset{\sim}{S}(\tau) +$$

$$- \underset{\sim}{S}(\tau)\underset{\sim}{M}^{-1}\underset{\sim}{\Lambda}(\tau) + \sigma(\tau)\underset{\sim}{X}(\tau)\tilde{\underset{\sim}{X}}(\tau) \qquad (56)$$

with initial condition $\underset{\sim}{S}(o) = 0$,

$$\underset{\sim}{X}(\tau) = [\underset{\sim}{W}(\tau) + \underset{\sim}{S}(\tau)\underset{\sim}{M}^{-1}]\ \underset{\sim}{\phi}(\tau)$$

$$\tilde{\underset{\sim}{X}}(\tau) = \underset{\sim}{\phi}^{T}(\tau)\ [\underset{\sim}{M}^{-1}\underset{\sim}{S}(\tau) + \underset{\sim}{W}(\tau)]\ .$$

also

$$\frac{d\tilde{\underset{\sim}{V}}(\tau)}{d\tau} = \underset{\sim}{W}^{-1}(\tau)\ \frac{d\underset{\sim}{W}(\tau)}{d\tau}\ \tilde{\underset{\sim}{V}}(\tau) - [\underset{\sim}{\Lambda}(\tau) + \qquad (57)$$

$$- \sigma(\tau)\underset{\sim}{X}(\tau)\underset{\sim}{\phi}^{T}(\tau)]\underset{\sim}{M}^{-1}\tilde{\underset{\sim}{V}}(\tau) + (\underset{\sim}{W}(\tau) + \underset{\sim}{S}(\tau)\underset{\sim}{M}^{-1})\underset{\sim}{g}(\tau)$$

corresponding to (47), with $\tilde{V}(o) = MW(o)\ u^{+}(o)$, and

$$\frac{d\underset{\sim}{u}^{-}(\tau)}{d\tau} = \underset{\sim}{M}^{-1}[\underset{\sim}{\Lambda}(\tau) - \sigma(\tau)\underset{\sim}{\phi}(\tau)\underset{\sim}{X}(\tau)]\ \underset{\sim}{u}^{-}(\tau) +$$

$$- \sigma(\tau)\underset{\sim}{M}^{-1}\underset{\sim}{\phi}(\tau)\underset{\sim}{\phi}^{T}(\tau)\underset{\sim}{M}^{-1}\tilde{\underset{\sim}{V}}(\tau) - \underset{\sim}{M}^{-1}\underset{\sim}{g}(\tau) \qquad (58)$$

while (50) and (51) give

$$\bar{J}(\tau) = \tilde{\underset{\sim}{X}}(\tau)\ \underset{\sim}{u}^{-}(\tau) + \underset{\sim}{\phi}^{T}(\tau)\underset{\sim}{M}^{-1}\tilde{\underset{\sim}{V}}(\tau). \qquad (59)$$

Apart from superficial differences arising from a difference of notation, the set (56) - (59) differ from those of Rybicki and Hummer by terms involving $\underset{\sim}{W}^{-1}\ \frac{d\underset{\sim}{W}}{d\tau}$. The matrix $\underset{\sim}{W}$ is defined by (24). In most applications, the weights for the frequency integra-

tion, a_i, have been chosen proportional to the corresponding value of ϕ. Thus the element

$$W_k = \frac{a_i b_j}{\phi_k}$$

in such cases is independent of τ, and the terms involving $\underset{\sim}{W}^{-1} \frac{d\underset{\sim}{W}}{d\tau}$ disappear. This has a number of useful consequences both for the discrete and the Riccati methods; in particular the operator $\underset{\sim}{S}$ becomes symmetric, a fact which can be used to reduce both the work and the storage required. Other aspects of the choice of quadrature formulae will be discussed in the following section.

We can also solve equations similar to (52) to determine the emissions in directions other than those used in the quadrature formula. This may be conveniently incorporated in the procedure by way of differential equations which can be integrated along with equation (58).

6. COMPUTATIONAL ASPECTS

We have generated solutions of the two-level model using both techniques on the ICT Atlas computer at the S.R.C.'s Chilton Laboratory. The discrete method involves extensive use of a matrix multiplication routine which computes scalar products of two vectors double length and rounds the result correctly to single length. In the Riccati method, we use Merson's version of the fourth-order Runge-Kutta method, which provides an estimate of error that can be used to control the step-length. It is also necessary in the Riccati method to interpolate in tables of $\underset{\sim}{X}_n$ and $\Psi_n = \underset{\sim}{\phi}_n^T \underset{\sim}{M}^{-1} \underset{\sim}{Y}_n$ generated on the forward sweep to provide the necessary intermediate values for Runge-Kutta integration in the reverse direction. We have done this by constructing the coefficients of a Newton interpolation polynomial for a given set of nodes for each interval in turn. The coefficients may be preserved, and used to evaluate the interpolation polynomial for each of the required intermediate points. The coefficients are changed only when the nodes change, and this enables us to deal very simply with the end intervals.

6.1 Storage Allocation

Both programs require basic data to generate the following information in the general inhomogeneous case:

$$\underset{\sim}{M}, \underset{\sim}{W}, \tau_n, \varepsilon_{n+1/2}, \gamma_{n+1/2}, \underset{\sim}{g}_{n+1/2}, \underset{\sim}{\Lambda}_{n+1/2}, \underset{\sim}{\phi}_{n+1/2}$$

Total: $3(K+1)N + 2K+1$ cells.

The discrete method requires storage of

$$A_{n+1/2}, B_{n+1/2}, \underset{\sim}{t}_{n+1/2}, \underset{\sim}{X}_{n+1/2}, \underset{\sim}{C}_{n+1/2}, \varepsilon_{n+1/2}, \underset{\sim}{\tilde{V}}_{n+1/2}, \underset{\sim}{Z}_n$$

on the forward sweep, and of $\bar{J}_n$ on the reverse sweep.

Total: $(6K+3)N+1$ cells.

The Riccati method requires storage of

$$\Psi_n, \underset{\sim}{X}_n$$

on the forward sweep, and of $\bar{J}_n$ on the reverse sweep.

Total: $(K+2)N$ cells.

These requirements must be added to the storage needed for program and system routines and for working space. For a typical problem with I = 10, m = 2 (giving K = 20) and N = 50, the additional storage required by the discrete method is about 8 blocks of 512 words, less than 20% of the total. It would be possible, with small modifications of the discrete method, to reduce this excess considerably.

6.2 Timing

We have estimated the amount of computing time required by counting multiplications and divisions needed in both methods. This does not allow for storage references and other operations, but it is reasonable to assume that they are roughly proportional to the number of multiplications and divisions in a problem of this type, and we have found no evidence to contradict the assumption. On this basis, the discrete calculation uses $\{5K^2 + 28K + 4\}$

operations per layer, and the Riccati method $\{\frac{55K^2}{2} + \frac{125K}{2} + \frac{1}{2}p(p+11)(K+1)\}$ operations per layer, where p is the order of interpolation required on the reverse sweep. For practical values of K of about 20, this means that the discrete method is between 5 and 6 times faster than the Riccati method per layer. We have found that it is often necessary in the Riccati method to subdivide the layers in order to maintain accuracy, particularly near the boundaries. This is, of course, done automatically by the step controller. There is no such problem in the discrete method for which we only need to satisfy the inequality (36), so that the practical increase in speed is often larger, although book-keeping overheads diminish the effect. For example in a typical problem with constant Doppler width, having $\tau = 50$, $\beta = 0$, $\varepsilon = 10^{-6}$, $K = 30$, the discrete method completed the computation in 30 seconds, whereas the Riccati method took over 6 minutes.

6.3 Angular Quadrature

There are few problems involved here; we have found that the line profiles and source functions are insensitive to our choice. We have usually employed the abscissae and weights for Gauss quadrature of order m = 2 over [0,1], using an additional integration to compute the normal emergent line profile. We have also used Radau quadrature of order 3 with an abscissa specified at $\mu = 1$. This simplifies the program, but, in addition to increasing the storage requirement, it is rather expensive in computing time, firstly because it increases K by 50%, and secondly because the smallest cosine, μ_1, is nearer to zero than with the Gauss rule. This causes a decrease in the critical step size in the discrete method.

6.4 Frequency Quadrature

The choice of frequency quadrature presents a more difficult problem. For pure Doppler broadening, we can employ the finite bandwidth approximation used by Avrett and Hummer.[9] In our implementation, we have truncated the frequency interval to become $-\alpha \leq \xi \leq \alpha$, and used Gauss quadrature over this finite range. The accuracy depends on the number of

points, and on the value of α, and we have selected a value of I such that the normalization condition (19) is satisfied to prescribed accuracy. For example, choosing $\alpha = 4$, we require I = 10, so that the error in normalization may be less than one part in 10^6. We renormalize the integral to ensure that (19) is satisfied to within the round-off accuracy of the computer, about 11 decimal digits. It is important to do this so as not to introduce spurious sources and sinks in the calculation.[7]

Hummer and Rybicki have pointed out[2,3] that this finite bandwidth approximation is unsatisfactory for Voigt profiles, for the bandwidth α has to be increased substantially, particularly when $\beta > o$. They have discussed methods of overcoming this difficulty which involve splitting the range of integration and renormalizing each segment separately. While it certainly eliminates difficulties arising from lack of normalization, there is an arbitrariness about the procedure which is a little unsatisfactory, and it is not clear what effect changes in the method of splitting have on the final results. The difficulty will be more acute in variable property media, and it seems clear that this problem needs further investigation.

7. NUMERICAL RESULTS

Our main effort has been directed towards the comparison of the discrete and Riccati methods in a few idealized situations. We have computed the line source function $S_L(\tau)$ at a selected set of optical depths in slabs of various thicknesses together with the normal emergent intensity for Doppler broadened lines.

In the case of a homogeneous slab, the results from the two programs are closely similar, as Figures 1 and 2 indicate. However, there are small differences which are best demonstrated by an examination of Table 1.

(a) *Symmetry of $S_L(\tau)$ About the Mid-Plane.* The discrete solution is symmetric to the number of decimal places printed out. The Riccati solution is asymmetric by up to 5% in the worst case of linear interpolation, and up to 2% when cubic or quintic polynomial interpolation is used on the backward sweep.

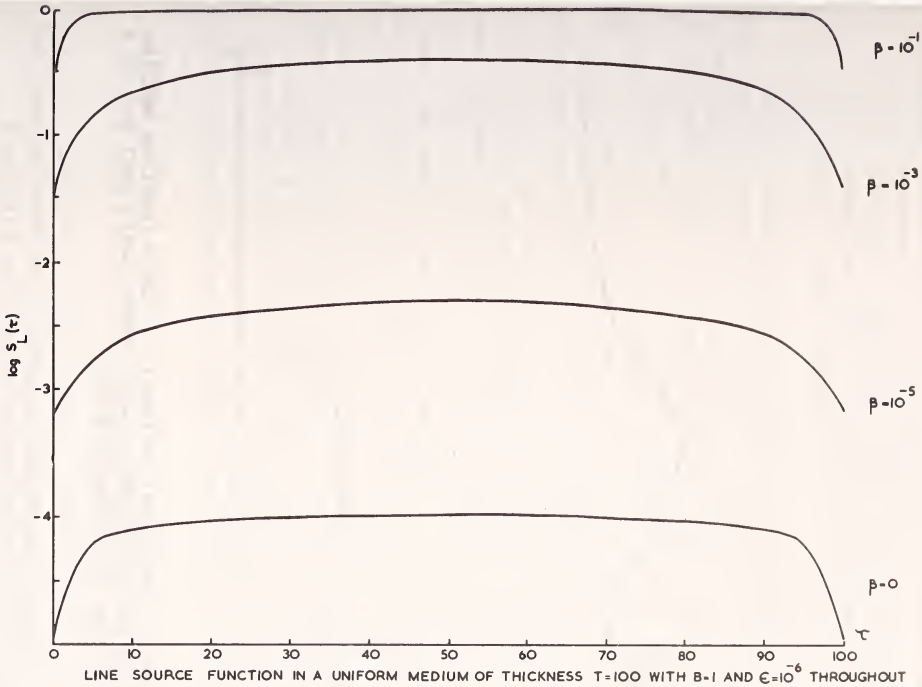

Figure 1. Line source function in a uniform medium, $\tau = 100$, with $B = 1$, $\rho = 1$, and $\varepsilon = 10^{-6}$. Discrete and Riccati solutions are not resolved.

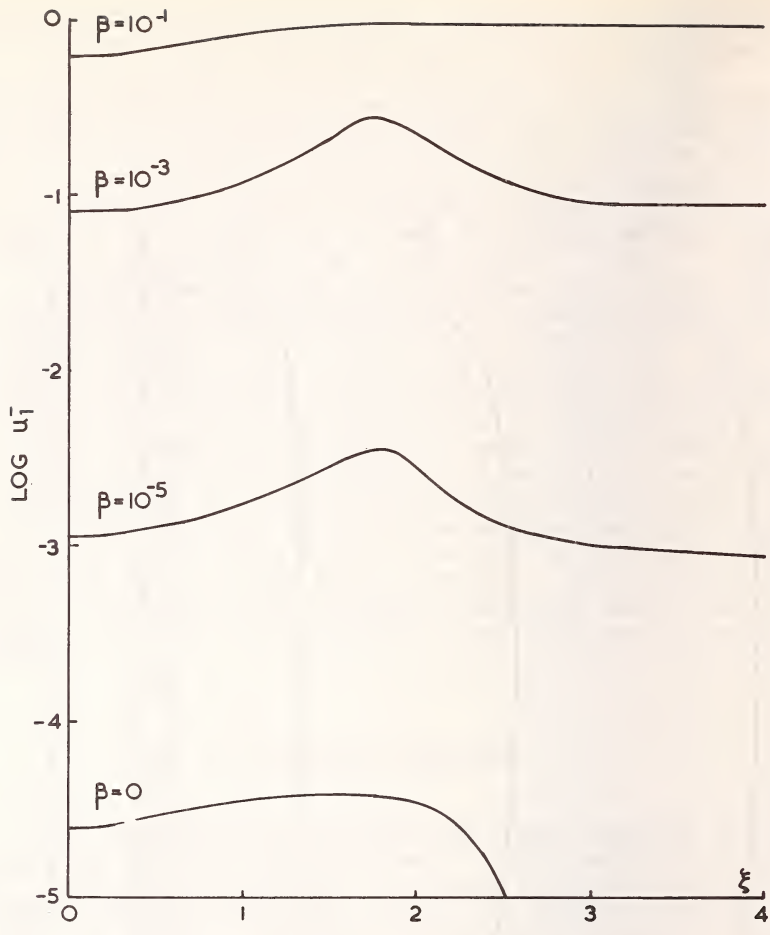

NORMAL EMERGENT INTENSITY FROM A UNIFORM MEDIUM OF OPTICAL THICKNESS T=100, WITH $\epsilon=10^{-6}$ AND B=1, AS A FUNCTION OF DOPPLER WIDTH.

Figure 2. Normal emergent intensities corresponding to the line source functions shown in Figure 1. Discrete and Riccati solutions are not resolved.

(b) *Choice of Angular Quadrature.* The results are insensitive to this choice. Comparing Gauss and Radau solutions, we see that the greatest difference is in the fourth significant figure, both for the line source function and for the normal emergent intensity.

(c) *Variation of Step Length.* The layer thicknesses are presented in the discrete method. We have done some experiments to examine the truncation errors involved, which are summarized in Table 2.

It is clear that we can be confident of reducing the discretization error from this source to a reasonable level if we take $\tau<\tau_{crit}$. Further work to be published elsewhere shows that this error, for the operator approximations we have used, is proportional to the square of the layer thickness. This is verified by the results of Table 2.

In the Riccati method we have asked for an absolute accuracy of 10^{-4} in the S-integration, and a relative accuracy of 10^{-4} in the $\tilde{V}$ and u^- integrations. The program chooses its own step length to meet these criteria. This is always reduced most near the boundaries at the start of a sweep, sometimes as small as 0.03δ (where δ is the Doppler width) though for the most part it is close to the value of 0.7δ quoted as the stability limit by Rybicki and Hummer.[3] The very small step size needed near the boundaries is almost certainly associated with the fact that the source function has a logarithmically infinite slope there,[9] so that the Taylor expansion about $\tau = 0$, on which the Runge-Kutta process is based does not exist in the first interval.

(d) *Effect of Order of Interpolation in the Riccati Method.* Table 2 shows that the biggest improvement comes from replacing linear by cubic interpolation. The use of a fifth-order polynomial produces a less marked effect, and it is clear that there is little point in going further than third-order with step sizes of the order used in this problem.

(e) *The Line Profile.* The most marked discrepancy between the two calculations is at the line center, which is formed in the outermost layers of the slab. There is a deficiency at $\xi = 0$ of about 6% in the Riccati

TABLE 1

This table gives typical solutions for the line source functions S_L and the normal emergent intensity for a plane parallel layer of thickness $\tau = 50$, with $\beta = 0$, $B = 1$. The frequency quadrature used a bandwidth $\alpha = 4$, and a 10-point Gauss rule.

(a) $\varepsilon = 10^{-}$

$\tau_{crit} = 1.0035$ (Gauss), 0.636 (Radau)

Source Function $S_L(\tau)$

	Discrete		Riccati with Radau quadrature		
τ	Gauss	Radau	p=1	p=3	p=5
0	0.3075426	0.3076172	0.2939989	0.3011204	0.3024015
2.5	0.5778	0.5770	0.5732	0.5792	0.5774
5.0	0.6940	0.6941	0.6922	0.6941	0.6934
10.0	0.8066	0.8067	0.8061	0.8067	0.8066
25.0	0.8817	0.8818	0.8817	0.8818	0.8818
40.0	0.8066	0.8067	0.8066	0.8067	0.8067
45.0	0.6940	0.6941	0.6938	0.6939	0.6939
47.5	0.5778	0.5770	0.5766	0.5766	0.5766
50.0	0.3075426	0.3076172	0.3076162	0.3076162	0.3076162

Normal Emergent Intensity*

ξ					
0.3061	5.031 (-1)	5.036 (-1)	4.730 (-1)	4.919 (01)	4.941 (-1)
0.9111	5.941 (-1)	5.943 (-1)	5.741 (-1)	5.881 (-1)	5.888 (-1)
1.4948	7.079 (-1)	7.079 (-1)	7.012 (-1)	7.065 (-1)	7. 064(-1)
2.0435	2.736 (-1)	2.736 (-1)	2.726 (-1)	2.735 (-1)	2.734 (-1)
2.5442	3.321 (-2)	3.321 (-2)	3.310 (-2)	3.319 (-2)	3.319 (-2)
2.9853	2.955 (-3)	2.955 (-3)	2.945 (-3)	2.953 (-3)	2.953 (-3)
3.3565	2.812 (-4)	2.812 (-4)	2.803 (-4)	2.811 (-4)	2.811 (-4)
3.6489	3.625 (-5)	3.625 (-5)	3.614 (-5)	3.623 (-5)	3.623 (-5)
3.8559	7.671 (-6)	7.671 (-6)	7.646 (-5)	7.667 (-6)	7.666 (-6)
3.9725	3.078 (-6)	3.078 (-6)	3.069 (-6)	3.077 (-6)	3.077 (-6)

(b) $\varepsilon = 10^{-6}$

τ_{crit} = 1.0392 (Gauss), 0.7094 (Radau)

Source Function $S_L(\tau) \times 10^5$

	Discrete		Riccati with Radau quadrature		
τ	Gauss	Radau	p=1	p=3	p=5
0	0.8966753	0.8977293	0.8362320	0.8724352	0.8767388
2.5	2.069	2.068	2.048	2.081	2.071
5.0	2.794	2.796	2.784	2.797	2.792
10.0	3.788	3.789	3.784	3.789	3.789
25.0	4.852	4.850	4.848	4.849	4.849
40.0	3.788	3.789	3.789	3.789	3.789
45.0	2.794	2.796	2.795	2.795	2.795
47.5	2.069	2.068	2.066	2.066	2.067
50.0	0.8966753	0.8977293	0.8977239	0.8977239	0.8977239

Normal Emergent Intensity*

ξ					
0.3061	1.763 (-5)	1.766 (-5)	1.649 (-5)	1.726 (-5)	1.731 (-5)
0.9111	2.318 (-5)	2.320 (-5)	2.242 (-5)	2.300 (-5)	2.300 (-5)
1.4908	3.307 (-5)	3.308 (-5)	3.281 (-5)	3.303 (-5)	3.302 (-5)
2.0435	1.324 (-5)	1.324 (-5)	1.320 (-5)	1.324 (-5)	1.323 (-5)
2.5442	1.608 (-6)	1.608 (-6)	1.604 (-6)	1.608 (-6)	1.608 (-6)
2.9853	1.431 (-7)	1.431 (-7)	1.427 (-7)	1.431 (-7)	1.431 (-7)
3.3565	1.362 (-8)	1.362 (-8)	1.358 (-8)	1.362 (-8)	1.362 (-8)
3.6489	1.756 (-9)	1.756 (-9)	1.751 (-9)	1.755 (-9)	1.755 (-9)
3.8559	3.715 (-10)	3.715 (-10)	3.705 (-10)	3.714 (-10)	3.714 (-10)
3.9725	1.491 (-10)	1.491 (-10)	1.487 (-10)	1.491 (-10)	1.490 (-10)

*The representation a(-b) is used for a x 10^{-b}.

TABLE 2

Dependence of Line Source Function and Normal Emergent Intensity on step size in solution by the Discrete method Case (a) of Table 1, $\tau_{crit} = 1.0035$ (Gauss quadrature).

	Percentage changes	
$k = \Delta\tau/\tau_{crit}$	$\lvert S_L(0)_k - S_L(0)_{k=1}\rvert / S_L(0)_{k=1}$	$\lvert \bar{u}(0)_k - \bar{u}(0)_{k=1}\rvert / \bar{u}(0)_{k=1}$
2.0	4	10
0.5	1	2
0.25	0.25	0.3

Note: The maximum change always occurs at the boundary.

solution with linear interpolation falling to 2% if cubic interpolation is used. This difference decreases towards the wings of the line as may be expected.

We have also computed some results with variable line-profile. The results, shown in Figures 3 and 4 are closely similar to those of the corresponding Figures 6 and 7 of Rybicki and Hummer's paper.[3]

8. CONCLUSIONS

The discrete method has a number of advantages compared with the Riccati method which may be summarised as follows:

1. Much greater speed - an order of magnitude.
2. Better control of discretization and round-off errors.
3. Ease and simplicity of programming.

Its greatest disadvantage is that it requires more storage, at least in the current version. It might be possible to circumvent this by reprogramming so that it is unnecessary to retain data for all depths other than certain specified ones. This may be done by computing $\underset{\sim}{Z}_n$ and the scalar product $\phi^T_{n-1/2}\underset{\approx}{M}^{-1}\tilde{\underset{\sim}{V}}_{n-1/2}$ required for (49) for selected points $n = n_1, n_2, \ldots$ on the forward sweep, together with vectors $\underset{\sim}{\Sigma}^-(n_\ell, n_{\ell+1})$ and matrices $\underset{\approx}{t}(n_\ell, n_{\ell+1})$ required to solve the equation

$$\underset{\sim}{u}^-_{n_\ell} = \hat{\underset{\approx}{t}}(n_\ell, n_{\ell+1})\underset{\sim}{u}^-_{n_{\ell+1}} + \underset{\sim}{V}^-(n_\ell, n_{\ell+1})$$

These vectors and matrices are obtained by simple recurrence forumlae derivable from equation (49).

A similar dodge has been used to limit the storage requirement in our version of the Riccati method, but the larger the intervals chosen, the more strain is thrown on the interpolation polynomial in the backward sweep. There is no such constraint in the discrete method. The accumulation of round-off error in calculating scalar products in the Riccati method also needs some investigation, but it could largely be eliminated at the cost of a little inconvenience.

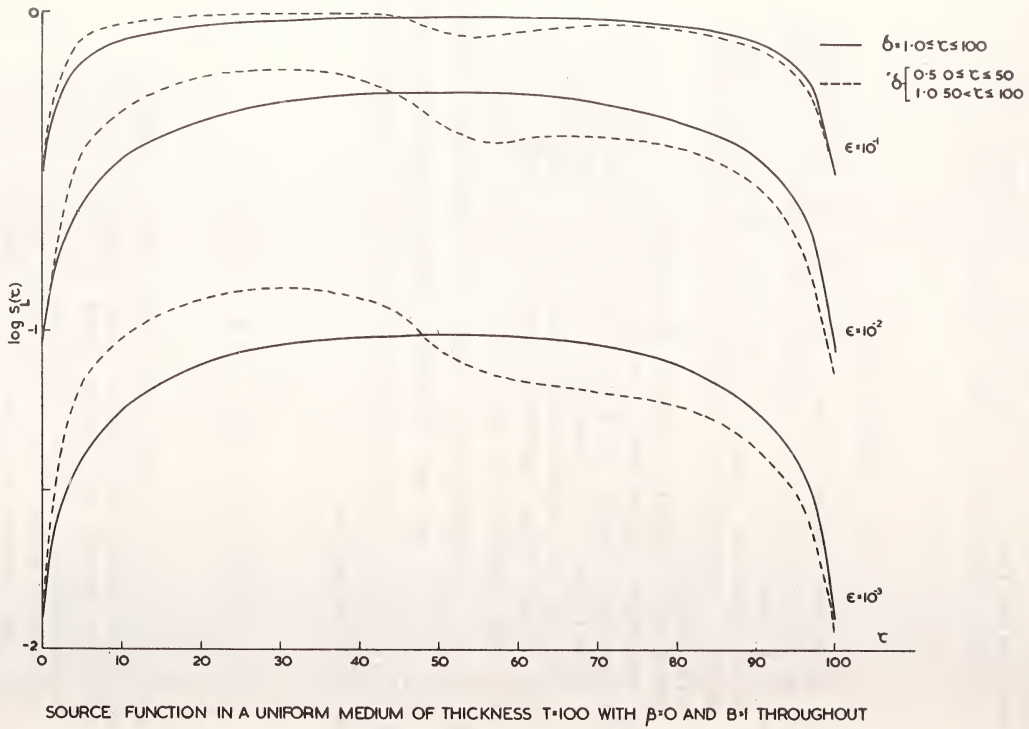

Figure 3. Line source function in a medium of thickness $\tau = 100$ with $\beta = 0$, $B = 1$ throughout, and ε independent of depth. The Doppler width $\delta = 0.5$ for $0 \leq \tau < 50$, and $\delta = 1.0$ for $50 < \tau \leq 100$.

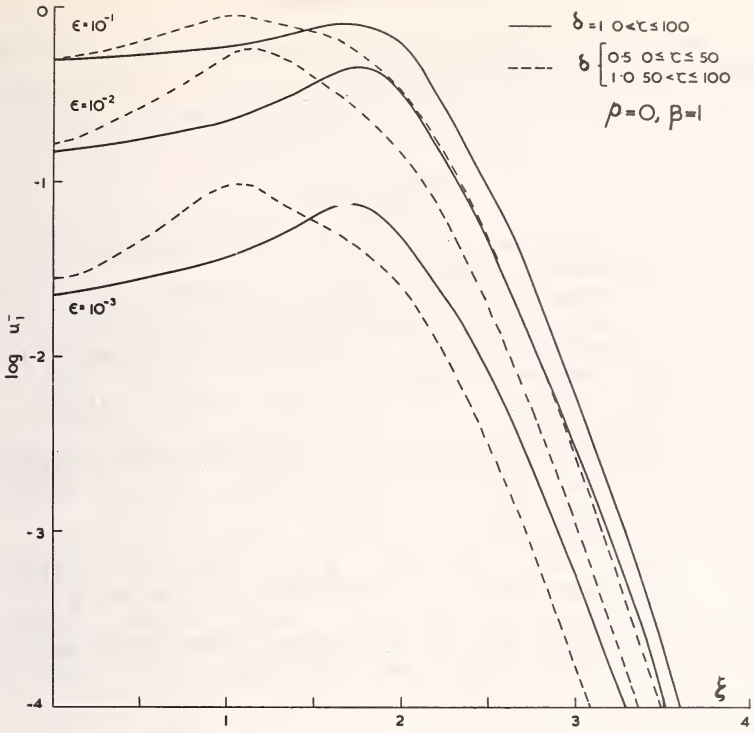

NORMAL EMERGENT INTENSITIES FROM A UNIFORM MEDIUM OF OPTICAL THICKNESS T=100, AS A FUNCTION OF DOPPLER WIDTH

Figure 4. Normal emergent intensities at $\tau = 0$ corresponding to the line source functions shown in Figure 3.

We have not attempted any solutions for semi-infinite media so far, but it would not be difficult to do so using the Asymptotic theory as described by Rybicki and Hummer.[3] Alternatively, since the asymptotic region is of necessity assumed to be homogeneous, the doubling method could be applied.[6,7]

Finally, we may remark that Feautrier's method leads to a set of matrix equations which, like our own equations (3), have a block tridiagonal form and can be solved using the same algorithm.[8] We have tried to see if it is possible to interpret the Feautrier algorithm in terms of our theory. We have not been able to do so because the way in which the positive and negative intensities are combined by Feautrier makes it impossible to disentangle the operators. We have therefore been unable to make any fair comparison of his method and our own.

ACKNOWLEDGMENT

We are indebted to Mrs. Elizabeth Gill for her assistance with the programs.

REFERENCES

1. J. T. Jefferies, *Spectral Line Formation*, Blaisdell (1968).
2. D. G. Hummer and G. Rybicki, *Methods of Computational Physics* 7, 53-127 (1967).
3. G. B. Rybicki and D. G. Hummer, *Astrophys. J.* 150, 607-635 (1967).
4. P. Feautrier, *C. R. Acad. Sci. Paris*, 258, 3189 (1964).
5. D. Mihalas, *Astrophys. J.* 150, 909-925 (1967).
6. I. P. Grant and G. E. Hunt, *Mon. Not. R. Astr. Soc.* 141, 27-42 (1968).
7. I. P. Grant and G. E. Hunt, *Proc. Roy. Soc.* A313, 183-198; ibid. A313, 199-216, (1969).
8. E. Isaacson and H. B. Keller, *Analysis of Numerical Methods*, pp. 58-62. Wiley (1966).
9. E. H. Avrett and D. G. Hummer, *Mon. Not. R. Astr. Soc.* 130, 295-331 (1965).

APPENDIX

A. The results of Sections 3 and 4 depend heavily on the following Lemma. Let $\underset{\sim}{X}$ and $\underset{\sim}{Y}$ be any two K-vectors and let

$$z = \underset{\sim}{Y}^T \underset{\sim}{X}.$$

Then if $|z| < |a|$,

$$[a\underset{\sim}{I} - \underset{\sim}{X}.\underset{\sim}{Y}^T]^{-1} = a^{-1}[\underset{\sim}{I} + (a-z)^{-1}\underset{\sim}{X}.\underset{\sim}{Y}^T].$$

Proof. By the binomial expansion, the result follows directly.

B. Thin Layer Operators and Sources

The approximations given in our paper (6) for thin-layer operators make use of matrices

$$\underset{\sim}{Z} = \underset{\sim}{\Lambda} - \sigma\underset{\sim}{\phi}\underset{\sim}{\phi}^T \underset{\sim}{W}, \quad \underset{\sim}{Y} = \sigma\underset{\sim}{\phi}\underset{\sim}{\phi}^T \underset{\sim}{W} \tag{B1}$$

and

$$\underset{\sim}{\Delta} = [\underset{\sim}{M} + \tfrac{1}{2}\tau\ \underset{\sim}{Z}]^{-1}. \tag{B2}$$

If the "diamond" weights are taken to minimize the local truncation error, equations (A.7) and (A.8) of reference 6 may be written for the present problem in the form

$$\underset{\sim}{r} = \underset{\sim}{\rho}(\underset{\sim}{I} - \underset{\sim}{\rho}^2)^{-1}\underset{\sim}{\theta}, \quad \underset{\sim}{t} = 2(\underset{\sim}{I} - \underset{\sim}{\rho}^2)^{-1}\underset{\sim}{\theta} - \underset{\sim}{I} \tag{B3}$$

where

$$\underset{\sim}{\rho} = \tfrac{1}{2}\tau\ \underset{\sim}{\Delta}\ \underset{\sim}{Y}, \quad \underset{\sim}{\theta} = \underset{\sim}{I} - \tfrac{1}{2}\tau\ \underset{\sim}{\Delta}\ \underset{\sim}{Z} \tag{B4}$$

From (B2) and (B1)

$$\underset{\sim}{\Delta} = [\underset{\sim}{M} + \frac{1}{2}\tau\ \underset{\sim}{\Lambda} - \frac{1}{2}\sigma\tau\underset{\sim}{\phi}\underset{\sim}{\phi}^T\underset{\sim}{W}]^{-1}$$

$$= (\underset{\sim}{M} + \frac{1}{2}\tau\underset{\sim}{\Lambda})^{-1}\ [\underset{\sim}{I} - \underset{\sim}{\phi}\underset{\sim}{\phi}^T\underset{\sim}{D}]^{-1}$$

where

$$\underset{\sim}{D} = \frac{1}{2}\tau\underset{\sim}{W}\ (\underset{\sim}{M} + \frac{1}{2}\tau\underset{\sim}{\Lambda})^{-1}$$

is a diagonal matrix. Applying the lemma, we get

$$\underset{\sim}{\Delta} = (\underset{\sim}{M} + \frac{1}{2}\tau\underset{\sim}{\Lambda})^{-1}[\underset{\sim}{I} + \frac{1}{1-\delta}\ \underset{\sim}{\phi}\underset{\sim}{\phi}^T\underset{\sim}{D}] \qquad \text{(B5)}$$

where

$$\delta = \underset{\sim}{\phi}^T\underset{\sim}{D}\underset{\sim}{\phi}$$

is the quantity written out in equation (34). Thus

$$\underset{\sim}{\rho} = \frac{1}{1-\delta}\ (\underset{\sim}{M} + \frac{1}{2}\tau\underset{\sim}{\Lambda})^{-1}\underset{\sim}{\phi}\underset{\sim}{\phi}^T(\frac{1}{2}\sigma\tau\underset{\sim}{W})$$

and an additional application of the lemma gives

$$(\underset{\sim}{I} - \underset{\sim}{\rho}^2)^{-1} = \underset{\sim}{I} + \frac{\delta}{1-2\delta}\ (\underset{\sim}{M} + \frac{1}{2}\tau\underset{\sim}{\Lambda})^{-1}\underset{\sim}{\phi}\underset{\sim}{\phi}^T(\frac{1}{2}\sigma\tau\underset{\sim}{W}) \qquad \text{(B6)}$$

Equations (30) to (33) now follow in a straightforward manner.

C. Discrete Equations which are not used in the present problem

We first list the local operators that we do not use explicitly:

$$\underset{\sim}{T}_{n+1/2} = \underset{\sim}{I} + A_{n+1/2}\underset{\sim}{C}_{n+1/2}\underset{\sim}{C}^T_{n+1/2}\underset{\sim}{S}_{n+1/2}$$

$$\hat{\underset{\sim}{t}}(n+1,n) = \underset{\sim}{t}_{n+1/2} + A_{n+1/2}\underset{\sim}{M}^{-1}\underset{\sim}{W}^{-1}_{n+1/2}\underset{\sim}{X}_{n+1/2}\underset{\sim}{C}^{T}_{n+1/2}\underset{\sim}{MW}_{n+1/2}$$

$$\hat{\underset{\sim}{r}}(n+1,n) = A_{n+1/2}\underset{\sim}{C}_{n+1/2}\underset{\sim}{C}^{T}_{n+1/2}\underset{\sim}{M}\ \underset{\sim}{W}_{n+1/2} \qquad \text{(C1)}$$

$$\underset{\sim}{R}_{n+1/2} = \underset{\sim}{M}^{-1}\underset{\sim}{W}^{-1}_{n+1/2}\{\underset{\sim}{t}_{n+1/2} + A_{n+1/2}\underset{\sim}{X}_{n+1/2}\underset{\sim}{C}^{T}_{n+1/2}\}\underset{\sim}{S}_{n+1/2}$$

$$\hat{\underset{\sim}{t}}(n,n+1) = \underset{\sim}{t}_{n+1/2} + A_{n+1/2}\underset{\sim}{C}_{n+1/2}\tilde{\underset{\sim}{X}}_{n+1/2}$$

The equation that is not used explicitly on the forward sweep is

$$\underset{\sim}{V}^{-}_{n+1/2} = \underset{\sim}{\Sigma}_{n+1/2} + B_{n+1/2}\underset{\sim}{C}_{n+1/2}\ , \qquad \text{(C2)}$$

and that which is not used explicitly on the backward sweep is

$$\underset{\sim}{u}^{+}_{n+1} = \underset{\sim}{M}^{-1}\underset{\sim}{W}^{-1}_{n+3/2}\underset{\sim}{S}_{n+3/2}\underset{\sim}{u}^{-}_{n+1} + \underset{\sim}{M}^{-1}\underset{\sim}{W}^{-1}_{n+1/2}\tilde{\underset{\sim}{V}}_{n+1/2}\ . \qquad \text{(C3)}$$

COHERENT LINE FORMATION WITH DEPTH-DEPENDENT PARAMETERS

by

T. R. Carson

University Observatory
St. Andrews, U.K.

ABSTRACT

A discrete ordinate method is developed for solving the equation of coherent line formation, for arbitrary given variations with depth in an atmosphere of the temperature (or Planck function, assuming local thermodynamic equilibrium) and the line absorption and scattering coefficients. The direct solution thus obtained can then be used as the starting point of an iterative procedure. Results obtained for an exactly soluble case indicate the utility of the method.

Key words: numerical methods, coherent line formation.

INTRODUCTION

The equation of coherent line formation can be solved exactly only in a number of special cases where certain restrictions are put upon the problem (see references). Such restrictions may include the imposition of simplifying boundary conditions and/or assuming particular variations with optical depth of parameters such as the temperature and the coefficient of absorption and scattering in the line. When these restrictions are invalid, or otherwise unacceptable, a rigorous solution may still be obtained by numerical iteration from an initially guessed

trial solution, but this method converges very slowly when the scattering coefficient is large compared with the absorption coefficient. In the method of the present paper none of the above mentioned simplifications is assumed. The equation of transfer is written in the form of an integral equation for the source function for which a solution is obtained directly by reduction of the integral equation to a set of simultaneous linear equations. Iteration from the direct solution then leads to more accurate results, as indicated by applying the method to a known soluble case.

THE EQUATION OF TRANSFER

The equation of radiative transfer, including line absorption, in plane parallel geometry may be written

$$\mu \frac{dI_\nu(x,\mu)}{\rho dx} = -(k_\nu + \ell_\nu) I_\nu(x,\mu) +$$

$$+ (1-\varepsilon)\ell_\nu J_\nu(x) + (k_\nu + \ell_\nu) B_\nu(T(x))$$

where ν is the frequency, x is the geometrical depth measured in the direction of the outward normal to the atmosphere, μ is the cosine of the angle between the direction of transfer and the outward normal, and ρ is the mass density. $I_\nu(x,\mu)$ is the specific intensity of radiation, $J_\nu(x)$ the mean intensity, $B_\nu(T)$ the Planck function for temperature T, k_ν and ℓ_ν are the continuous and line mass absorption coeficient and $(1-\varepsilon)$ is the fraction of radiation absorbed which is scattered. Introducing an optical depth τ_ν defined in terms of some absorption coefficient k_ν by the relation

$$d\tau_\nu = -k_\nu \rho dx$$

the equation of transfer takes the form

$$\mu \frac{dI_\nu(\tau_\nu,\mu)}{d\tau_\nu} = \alpha_\nu(\tau_\nu) I_\nu(\tau_\nu,\mu) +$$

$$- \beta_\nu(\tau_\nu) J_\nu(\tau_\nu) - \gamma_\nu(\tau_\nu) B_\nu(\tau_\nu)$$

$$\alpha_\nu = \frac{k_\nu + \ell_\nu}{\kappa_\nu}$$

$$\beta_\nu = \frac{(1 - \varepsilon)\ell_\nu}{\kappa_\nu}$$

$$\gamma_\nu = \frac{k_\nu + \ell_\nu}{\kappa_\nu}$$

Defining the source function

$$S_\nu(\tau_\nu) = \beta_\nu(\tau_\nu) J_\nu(\tau_\nu) + \gamma_\nu(\tau_\nu) B_\nu(\tau_\nu)$$

the equation of transfer becomes

$$\mu \frac{dI_\nu(\tau_\nu,\mu)}{d\tau_\nu} = \alpha_\nu(\tau_\nu) I_\nu(\tau_\nu,\mu) - S_\nu(\tau_\nu)$$

for which the solution may be formally written down

$$I_\nu(\tau_\nu,-\mu) = \int_0^{\tau_\nu} \exp - \int_{\tau'_\nu}^{\tau_\nu} \alpha_\nu(\tau''_\nu) \frac{d\tau''_\nu}{\mu} S_\nu(\tau'_\nu) \frac{d\tau'_\nu}{\mu}$$

$$I_\nu(\tau_\nu,+\mu) = \int_{\tau_\nu}^{\infty} \exp \left\{ - \int_{\tau_\nu}^{\tau'_\nu} \alpha_\nu(\tau''_\nu) \frac{d\tau''_\nu}{\mu} \right\} S_\nu(\tau'_\nu) \frac{\alpha\tau'_\nu}{\mu}$$

Using the relations

$$J_\nu(\tau_\nu) = \tfrac{1}{2}\int_{-1}^{+1} I_\nu(\tau_\nu,\mu)\,d\mu$$

$$= \tfrac{1}{2}\int_0^\infty S_\nu(\tau'_\nu)\; E_1\left\{\left|\int_{\tau'_\nu}^{\tau_\nu} \alpha_\nu(\tau''_\nu)\,d\tau''_\nu\right|\right\}\, d\tau'_\nu \quad ,$$

where $E_n(x)$ is the exponential integral of index n defined by

$$E_n(x) = \int_1^\infty e^{-xt} t^{-n}\,dt = \int_0^1 e^{-xs}\, s^{n-2}\,ds$$

the source function $S_\nu(\tau_\nu)$ then satisfies the integral equation

$$S_\nu(\tau_\nu) = \frac{\beta_\nu(\tau_\nu)}{2}\left[\int_0^\infty S_\nu(\tau'_\nu) E_1\left\{\left|\int_{\tau'_\nu}^{\tau_\nu}\alpha_\nu(\tau''_\nu)\,d\tau''_\nu\right|\right\} d\tau'_\nu\right] +$$

$$+ \gamma_\nu(\tau_\nu) B_\nu(\tau_\nu)$$

SOLUTION FOR THE SOURCE FUNCTION

Suppressing the indicated frequency dependence of all quantities, the integral equation for the source function may be written

$$S(\tau) = \frac{\beta}{2}\left[\int_0^\infty S(\tau')\; E_1\left\{f(\tau,\tau')\right\} d\tau'\right] + \gamma B(\tau)$$

where

$$f(\tau,\tau') = \left|\int_\tau^{\tau'} \alpha(\tau'')\,d\tau''\right|$$

Choosing a set of points of subdivision τ_i with appropriate weights a_i, the integral over τ' may be replaced by a summation, thus transforming the integral equation into a set of simultaneous linear equations

$$S_i = \frac{\beta_i}{2} \left[\sum_j a_i E_1\{f_{ij}\} \; S_{j,} \right] + \gamma_i B_i$$

where the indices i,j denote that the quantities are evaluated for τ_i, τ_j. The calculation of the coefficient matrix elements is straightforward as long as the range of integration does not include an interval or subdivision one end of which corresponds to $j = i$. For $j = i$, f_{ij} vanishes and hence $E_1\{f_{ij}\}$ is infinite. We must therefore find an alternative expression for the integral over those ranges of integration that include the singularity viz.,

$$\int_{\tau_{i-1}}^{\tau_i} E_1 \left\{ f(\tau_i, \tau') \right\} S(\tau') d\tau'$$

and

$$\int_{\tau_i}^{\tau_{i+1}} E_1 \left\{ f(\tau_i, \tau') \right\} S(\tau') d\tau'$$

Since as $f \to o$

$$E_1(f) \to -\gamma - \sum_1^{\infty} \frac{(-1)^n f^n}{n.n!} - \ell nf = E_1'(f) - \ell nf$$

where $\gamma = 0.577215665....$ we may isolate the singularity in the ℓnf term and write

$$\int E_1 \left\{ f(\tau') \right\} S(\tau') d\tau' = \int E_1 \left\{ f(\tau') \right\} S(\tau') d\tau' +$$

$$- \int \ell nf(\tau') S(\tau') d\tau'$$

The integrand of the first term on the right-hand side is now everywhere finite and so the integral may be represented by a quadrature formula in the usual way, as a weighted sum of the values of the integrand at the points of subdivision. The second integral may also be so represented provided we make some assumptions about the variation of the integrand. Thus expanding $\phi(\tau")$ about $\tau" = \tau_i$

$$\alpha(\tau") = \alpha_i + \alpha_i'(\tau" - \tau_i) + \ldots\ldots$$

where $\alpha_i' = (d\alpha(\tau")/d\tau")_{\tau_i}$ we have up to the terms indicated

$$\alpha_i(\tau_i - \tau') - \frac{\alpha_i'}{2}(\tau' - \tau_i)^2, \quad \tau' \leq \tau_i$$

$f(\tau') =$

$$\alpha_i(\tau' - \tau_i) + \frac{\alpha_i'}{2}(\tau' - \tau_i)^2, \quad \tau' \geq \tau_i$$

and

$$\ell n\alpha_i + \ell n(\tau_i - \tau') + \ell n\left\{1 - \frac{\alpha_i'}{2\alpha_i}(\tau_i - \tau')\right\}, \quad \tau' \leq \tau_i$$

$\ell nf(\tau') =$

$$\ell n\alpha_i + \ell n(\tau' - \tau_i) + \ell n\left\{1 + \frac{\alpha_i'}{2\alpha_i}(\tau' - \tau_i)\right\}, \quad \tau' \geq \tau_i .$$

Putting $S(\tau') = S(\tau_i) = S_i$ and taking it outside the integral sign we have

$$\int_{\tau_{i-1}}^{\tau_i} \ell nf(\tau')S(\tau')d\tau' = S_i\left[(\ell n\alpha_i)t + \right.$$

$$+ F_1(t) + F_2(t, -b)\Big], \quad t = \tau_i - \tau_{i-1}$$

$$\int_{\tau_i}^{\tau_{i+1}} \ell n f(\tau')S(\tau')d\tau' = S_i\Big[(\ell n\alpha_i)t +$$

$$+ F_1(t) + F_2(t, +b)\Big], \quad t = \tau_{i+1} - \tau_i$$

where $b = \alpha_i'/2\alpha_i$ and

$$F_1(t) = \int_0^t \ell nx dx = \Big[x(\ell nx - 1)\Big]_0^t = t(\ell nt - 1)$$

$$F_2(t,b) = \int_0^t \ell n(1+bx)dx = \Big[\frac{1}{b}(1+bx)\Big\{\ell n(1+bx)-1\Big\}\Big]_0^t =$$

$$= \frac{1}{b}\Big[(1+bt)\Big\{\ell n(1+bt)-1\ -1\Big\}\ .$$

Now replacing the derivative α_i' by the divided differences

$$\alpha_i' = (\alpha_i - \alpha_{i-1})/(\tau_i - \tau_{i-1}), \quad \tau_{i-1} < \tau' < \tau_i$$

$$\alpha_i' = (\alpha_{i+1} - \alpha_i)/(\tau_{i+1} - \tau_i), \quad \tau_i < \tau' < \tau_{i+1}$$

we obtain an expression for the integral through the singularity at τ_i in terms of S_i, thus completing the reduction of the integral equation to a set of simultaneous linear equations.

THE EMERGENT INTENSITY

Given the source function, the specific intensity at any depth and in any direction may then be

obtained. To facilitate the quadrature we write

$$f(\tau') = f_i + f'(\tau' - \tau_i)$$

$$S(\tau') = S_i + S'(\tau' - \tau_i)$$

where f is as defined, $f_i = f(\tau_i)$, $S_i = S(\tau_i)$ and the primes denote derivatives. The contribution to I_ν due to the source function in any interval (τ_1, τ_2) is then

$$\Delta_{12} I_\nu = \frac{1}{\mu} \int_{\tau_1}^{\tau_2} \exp\left[-\left\{ f(\tau') \right\} / \mu \right] S(\tau') d\tau'$$

$$= \frac{1}{\mu} e^{-a} \left[\left(\frac{1}{b} S_1 + \frac{1}{b^2} S'_{12} \right)(1 - e^{-bt}) - \frac{1}{b} S'_{12} t e^{-bt} \right] ,$$

where $t = \tau_2 - \tau_1$, $a = f_1/\mu$, $b = f'_{12}/\mu$, $f'_{12} = (f_2 - f_1)/t$ $S'_{12} = (S_2 - S_1)/t$. The intensity emergent from the atmosphere in the direction corresponding to μ is simply $I_\nu(o,\mu)$ from which the equivalent width of a line in wavelength units is given by

$$W_\lambda(\mu) = \int \left\{ 1 - R_\lambda(o,\mu) \right\} d\lambda \quad ,$$

where the residual intensity

$$R_\lambda(o,\mu) = \frac{I_\lambda(o,\mu)}{I^c_\lambda(o,\mu)}$$

and $I^c_\lambda(o,\mu)$ is the background or continuous emergent intensity in the absence of line absorption. When the integrated width, and not the variation with the angle of emergence, is required we have instead

$$W_\lambda = \int \left\{ 1 - R_\lambda(o) \right\} d\lambda$$

with

$$R_\lambda(o) = \frac{\int_o^1 \mu I_\lambda(o,\mu)\,d\mu}{\int_o^1 \mu I_\lambda^c(o,\mu)\,d\mu}$$

NUMERICAL CALCULATIONS

To test the feasibility of our method we apply it to a situation where the solution is already accurately known. For $\kappa_\nu = k_\nu$ (so that τ_ν is now the optical depth in the continuum) and with $\eta = \ell_\nu/k_\nu$ constant with depth, $\varepsilon = o$ and a temperature distribution such that $B_\nu(\tau_\nu) = B_o(1 + 3/2\ \tau_\nu)$ the exact solution has been given by Chandrasekhar (1947) in the form

$$R(o,\mu) = H(\mu)\left[\frac{2}{3} + \mu\delta + \frac{1}{2}\,\delta^{1/2}(1-\delta)\alpha_1\right]\delta^{1/2}/(\mu + \frac{2}{3})$$

$$R(o) = 3\left[\frac{1}{2}\,\delta\alpha_2 + \frac{1}{3}\,\alpha_1 + \frac{1}{4}\,\delta^{1/2}(1-\delta)\alpha_1^{1/2}\right]\delta^{1/2}$$

where $\delta = 1/(1+\eta)$ and

$$\alpha_n = \int_o^1 \mu^n H(\mu)\,d\mu$$

$H(\mu)$ being the solution of the integral equation

$$H(\mu) = 1 + \frac{1}{2}\,(1-\delta)\,\mu H(\mu)\int_o^1 \frac{H(\mu')\,d\mu'}{\mu+\mu'}$$

In applying the method of solution developed in the present paper, the number and distribution of the points of subdivision in optical depth have to be specified. It seemed desirable to have a distribution with zero optical depth as one end point and for which the points of subdivision were closer together at small optical depth than at large optical

depth. The points of subdivision were therefore chosen according to the formula

$$\tau_n = A(n-1)^2 \quad , n = 1, \ldots\ldots N$$

with A and N as variable parameters. Because of the unequal intervals the trapezoidal rule was used in performing the relevant quadratures.

Calculations were carried out for N = 25 and with A taking the values 0.01, 0.02 and 0.04. The results for $R_\lambda(o)$ for various values of $1/(1+\eta)$ obtained from both the direct and iterated solutions, are shown in Table 1 together with the exact results. It may be seen that the direct solution is very good for small η but can be considerably in error for large η. However iteration of the solution leads to a very marked improvement, but for any value of η the best direct solution does not necessarily lead to the best iterated solution. Thus while A = 0.02 gives the best iterated solution for small η, that for large η is obtained with A = 0.01, indicating that small optical depths are more important for strong lines than for weak lines. The results have also been used to calculate the equivalent width W_λ of a line, for various values of the Voigt profile parameter a which is the ratio of the Lorentz width to the Gaussian width and for various values of η_o, the value of η at the line centre. Table 2 gives the values of log (W_λ/λ). It will be observed that both the direct and iterated solutions give good agreement with the exact results. In particular the iterated solution for A = 0.02 gives results which are indistinguishable from the exact results for all values of the parameters considered. This convergence of the calculated values of the equivalent width must be due to the fact that the important contributions come from regions of the line where η is small, for which values both the direct and iterated solutions are most accurate.

ACKNOWLEDGMENT

The author wishes to express his thanks to Professor D. W. N. Stibbs for initiating and sustaining his interest in this problem. Most of the work described in this paper was carried out during the author's tenure of a 1967-1968 Visiting Fellow-

TABLE 1.

$R_\lambda(o)$

$\frac{1}{1+\eta}$	Exact	$\tau_n = 0.01(n-1)^2$		$\tau_n = 0.02(n-1)^2$		$\tau_n = 0.04(n-1)^2$	
		Direct	Iterated	Direct	Iterated	Direct	Iterated
1.000	1.0000	1.0000	1.0000	1.0000	1.0000	1.0000	1.0000
0.900	0.9481	0.9609	0.9500	0.9491	0.9481	0.9593	0.9476
0.800	0.8939	0.9207	0.8965	0.9185	0.8939	0.9180	0.8938
0.700	0.8369	0.8798	0.8397	0.8771	0.8367	0.8760	0.8362
0.600	0.7762	0.8381	0.7791	0.8352	0.7759	0.8329	0.7752
0.500	0.7109	0.7962	0.7128	0.7928	0.7101	0.7882	0.7084
0.400	0.6391	0.7548	0.6418	0.7496	0.6381	0.7400	0.6356
0.300	0.5580	0.7156	0.5585	0.7045	0.5557	0.6797	0.5522
0.200	0.4616	0.6819	0.4619	0.6442	0.4558	0.5674	0.4408
0.150	0.4036	0.6625	0.4014	0.5809	0.3921	0.4496	0.3857
0.100	0.3340	0.6009	0.3250	0.4309	0.2994	0.2679	0.3084
0.075	0.2919	0.5017	0.2724	0.2991	0.2268	0.1627	0.2586
0.050	0.2412	0.3056	0.1898	0.1517	0.2123	0.0678	0.1969
0.025	0.1735	0.0820	0.1444	0.0335	0.1302	0.0165	0.1144
0.000	0.0000	0.0000	0.0000	0.0000	0.0000	0.0000	0.0000

TABLE 2.

$\text{Log}(W_\lambda/\lambda)$

log a	log η_o	Exact	$\tau_n = 0.01(n-1)^2$		$\tau_n = 0.02(n-1)^2$		$\tau_n = 0.04(n-1)^2$	
			Direct	Iterated	Direct	Iterated	Direct	Iterated
-2	-2	-7.255	-7.378	-7.271	-7.264	-7.255	-7.361	-7.251
	-1	-6.282	-6.405	-6.298	-6.290	-6.282	-6.387	-6.278
	0	-5.470	-5.593	-5.486	-5.478	-5.470	-5.575	-5.466
	1	-5.048	-5.171	-5.064	-5.056	-5.048	-5.154	-5.044
	2	-4.859	-4.982	-4.875	-4.867	-4.859	-4.964	-4.854
-1	-2	-7.248	-7.371	-7.264	-7.256	-7.248	-7.353	-7.243
	-1	-6.273	-6.396	-6.289	-6.282	-6.273	-6.379	-6.269
	0	-5.456	-5.579	-5.473	-5.465	-5.456	-5.562	-5.452
	1	-4.997	-5.120	-5.013	-5.006	-4.997	-5.103	-4.993
	2	-4.509	-4.632	-4.525	-4.517	-4.509	-4.614	-4.505
0	-2	-7.167	-7.290	-7.184	-7.176	-7.167	-7.273	-7.162
	-1	-6.189	-6.132	-6.205	-6.197	-6.189	-6.294	-6.185
	0	-5.338	-5.461	-5.355	-5.347	-5.338	-5.444	-5.334
	1	-4.760	-4.883	-4.776	-4.769	-4.760	-4.866	-4.756
	2	-4.303	-4.426	-4.319	-4.311	-4.303	-4.409	-4.299
1	-2	-7.103	-7.226	-7.119	-7.111	-7.103	-7.209	-7.099
	-1	-6.122	-6.245	-6.138	-6.130	-6.122	-6.227	-6.118
	0	-5.255	-5.378	-5.271	-5.263	-5.255	-5.360	-5.250
	1	-4.635	-4.758	-4.651	-4.643	-4.635	-4.740	-4.631
	2	-4.139	-4.262	-4.155	-4.147	-4.139	-4.244	-4.135

ship at the Joint Institute for Laboratory Astrophysics of the National Bureau of Standards and the University of Colorado

REFERENCES

Chandrasekhar, S. 1947, *Ap. J.*, 106, 145. Also *Radiative Transfer* (Oxford: Clarendon Press, 1950), §84.
Eddington, A. S. 1929, *M.N.R.A.S.*, 89, 620.
Hulme, H. R. 1939, *M.N.R.A.S.*, 99, 730.
Krook, M. 1938, *M.N.R.A.S.*, 98, 477.
Siewert, C. E., and McCormack, N.J. 1967, *Ap. J.*, 149, 649.
Spitzer, L., Jr. 1938, *Ap. J.*, 87, 1.
Swings, P., and Dor, L. 1938, *Ap. J.*, 88, 516.

DISCUSSION

Kalkofen to Grant: Can you apply your method to semi-infinite media?

Grant: We did not try that, but it may be possible to handle these cases.

Pecker: As we conclude today's session I would like to remind you once more that many phenomena that can be observed very clearly on the solar disk are practically invisible in stellar spectra or can be found only in the far UV. This means that many of the important phenomena that occur in extended atmospheres give only very small observable effects.

PART C

CHROMOSPHERES AND CORONAE OF STARS

Chairmen: J. C. Pecker, D. G. Hummer

WHAT DO WE KNOW THROUGH SPECTRAL INFORMATION ON STELLAR CHROMOSPHERES AND CORONAS?

by

Françoise Praderie

Observatoire de Paris
Section d'Astrophysique de Meudon

ABSTRACT

Four problems in interpreting spectra to infer chromospheres-coronas are summarized. (1) The a priori difficulties in interpreting spectra lie in uncertainty on the range of possible models, coming from uncertainty as to which conservation equations may be applied, and from lack of an exhaustive list of spectral indicators that may be used for uniqueness tests. (2) As spectral indicators we consider: emission lines, self-reversed emission cores, the presence of He I lines in stars not of early type, coronal-type high ionization, excess continuum emission in the rocket UV and the far infrared. (3) To determine what we can infer from observations, we summarize information: inferred by comparison of models to data, on velocity fields, and on spectral variability which might suggest chromospheric activity. (4) We summarize the evidence for chromospheres in A stars, as being those where convection-induced acoustic heating is marginal.

Key words: chromosphere, corona, spectral indicators, conservation equations.

In the framework R. N. Thomas proposed at this colloquium* for approaching the problem of extended atmospheres, stellar chromospheres and coronas come both under case 3 and case 4.

Case 3: Spectral features that disagree with

---

* See pp. 38-45.

classical atmosphere (CA) predictions appear in stellar spectra. For a few stars, eclipse observations are possible; for many others even non-eclipse observations imply the existence of a chromosphere or corona. At this point, the last sentence says no more than: "CA assumptions are insufficient." However it leads to a first definition of a stellar chromosphere.

Taking account of the very common occurrence of H and K reversals in stars later than F0, one can give a symptomatic definition of one type of stellar chromosphere: an outer layer giving rise to emission in the H and K lines of ionized calcium. This definition applies to otherwise "normal" and rather cool stars even if they are variable in light, and suggests an analogy with the sun. But exceptions to this statement appear immediately. Stars with a majority of emission lines, like Wolf-Rayet stars, or with a certain number of emission lines, recurrent novae, P Cyg or Be, or peculiar systems like β Lyr, are not included in such an empirically based, and necessarily limited, definition. However some of these stars show certain chromospheric or coronal indications like the He I λ 10830 line (β Lyr, P Cyg). On the other hand, the only coronal lines of highly ionized atoms observable in stars appear in repeating novae like T CrB, in variable stars like CI Cyg, AG Peg, RX Pup, or in stars like Z And. Thus, the symptomatic definition, based only on the K line (or on other lines, whatever they are), is not satisfactory.

Case 4 is the logical consequence of case 3; it stresses the search for the physical causes that act to violate the CA assumptions so as to produce peculiar spectral features attributable to an extended atmosphere. A causal definition of a chromosphere or corona is then more satisfying: chromosphere and corona are hot (relative to the photosphere), tenuous extended parts of the atmosphere, transparent in all but a few wavelengths, produced by the dissipation of mechanical energy waves; Cayrel's mechanism (1963) appeals to a purely radiative source, and may be efficient in the lowest chromospheric layers as a subsidiary cause for the increase of electron temperature. One must admit that the heating mechanisms can act even if no striking observational consequences appear at first sight. They produce a rise of the electron temperature T_e, after some minimum obtained in the low photospheric layers. As a result, the excitation and ionization conditions in the chromosphere (or corona)

and the spectroscopic state of the gas cannot be described by a simple LTE theory, or even a non-LTE theory that imposes radiative equilibrium.

The plan of this talk will be:

I. Introduction: What are the difficulties in interpreting spectral information about stellar chromospheres and coronas?
II. Spectral indicators of chromospheres and coronas.
III. Interpretation of chromospheric (and coronal) spectral features.
IV. Do the A stars have chromospheres?

Neither the heating mechanisms nor the generation process of a stellar wind will be reviewed, and I will completely exclude the solar case, only referring to it as a powerful guide toward the study of the outer layers of stars.

I. INTRODUCTION

a. Model Problem

The basic problem in interpreting spectral information in chromospheres and coronas is not essentially different from what it is in any atmosphere: one wants to deduce the complete physical state of the gas from the observed distribution of radiation intensity with the frequency ν, and from the shape of spectral lines. That is what Jefferies (1968) calls the analytical problem in interpreting the observations.

The main difficulty in that problem has often been underlined by Thomas and Jefferies and by others: to solve this analytical problem, one has to go first through a preliminary and unavoidable synthetic approach; namely, the theoretical computation of the radiation emitted by a gas specified by the distribution of density, kinetic temperature, and chemical composition. So one needs a good theory of line and continuum formation.

Moreover, and this distinguishes the chromospheric and coronal situation from the classical photospheric case, the equation of energy conservation includes a mechanical contribution in addition to the radiative one. The energy is transported and dissipated under several qualitatively well-

known forms, and eventually the whole heated material of the corona expands hydrodynamically, as first suggested by Parker (1963). Delache has shown (1967) that the equation of momentum conservation must include a wave-radiation pressure term, which at least in the transition region between the solar chromosphere and corona prevents the hydrostatic equation from being a good approximation. Therefore the a priori models that are built as a preliminary step to compute, even by a good theory, the emergent spectrum from a chromosphere or corona are not complete.

It makes no sense to infer the physical conditions in the chromospheric or coronal gas from the spectral information unless one checks that the conservation laws are not violated at each height. Omitting this check would imply that the transport and dissipation phenomena are completely known and that one knows where the mechanical energy is generated (Lighthill 1967), which is far from true. Thus the conservation laws can at best be used to put boundary conditions on the run of T_e and N_e.

Finally, the very few models that have been computed in the stellar case are stationary and assume that the material is homogeneous. The last assumption is known to be far from reality in the solar case.

b. Uniqueness of the Models

Due to these theoretical limitations and to the scarcity of easily accessible spectral features (i.e., in the near UV or visible part of the spectrum) in stars other than the sun, one cannot be sure, at the present time of being able to derive unique interpretations from the chromospheric and coronal observations. Each observed characteristic in the spectrum, especially in the line spectrum, depends on the model via several parameters, which are all depth dependent. As an example, let us quote the systematic study of the H and K lines by Athay and Skumanich (1968b). For stars not too different from the sun, they show the dependence of the intensity I_2 and of the width w_2 of the K_2 emission with (1) the Doppler width and its gradient through the atmosphere, (2) parameters describing the run of $B_\nu(T_e)$, the Planck function, with τ_c, the continuous optical depth, and (3) characteristics of the line such as $\varepsilon = C_{21}/A_{21}$, the optical depth τ_o at the line center, the damping constant a, each

depending on N_e, T_e. We adopt

$$B_\nu(T_e) = 1 + \beta\tau_c + A\, e^{-(C\tau_c)^x} - \alpha\, e^{-(300\,\tau_c)^{1/2}} ,$$

$$D = \frac{\Delta\lambda_D(\tau_c)}{\Delta\lambda_D(\tau_c=1)} = 1 + \zeta\, e^{-(d\tau_c)^z} ,$$

$$r_o = \frac{d\tau_c}{d\tau_o} = r_{o,1}\,\tau_o^{1/3} + 10^{-10}$$

With several restrictions on a, $r_{o,1}$, and C, Athay and Skumanich give the following expressions for I_2 and W_2:

$$I_2 \sim \frac{A\varepsilon}{(r_{o,1}Ca^2)^{1/4}} \cdot \frac{1}{(1+\zeta)^{1/2}} ,$$

$$w_2 \sim \left(\frac{a^2}{r_{o,1}^2 C}\right)^{1/4} (1+\zeta) .$$

Of course, all these parameters cannot be left free a priori if one has at one's disposal only the observed profile of the K line, i.e., essentially 3 measurable quantities: I_2, w_2, and their product, which varies like the energy loss in the chromosphere.

Therefore it is urgent both to search for more observable chromospheric and coronal spectral indicators and to improve the model theories.

II. THE KNOWN CHROMOSPHERIC AND CORONAL INDICATORS

Normal stars as well as variable stars show strong observational evidence of the presence of chromospheres and coronas. One often speaks of chromospheric "activity," even for normal stars, because of the variation in the structure of the H and K lines from night to night.

I will list the spectral features that indicate the presence of a chromosphere or a corona and in which stars they appear; I will omit the peculiar case of eclipsing systems, which are reviewed in Groth's paper.

a. Line Spectrum

Prominent chromospheric stellar lines lie in the visible, ultraviolet, and near infrared spectral regions. A self-reversed emission core in a strong resonance line is often a signature of a chromosphere because it reflects a map of the source function with depth, showing a maximum for small values of τ_{5000}*. But the cores of all strong lines are formed in the low part of the chromosphere and even in absorption they give insight to the properties of the corresponding layers.

(1) H and K reversals are observed in numerous G, K, M giants and supergiants and in many main-sequence stars (Wilson and Bappu 1957). The K_2 intensity, I_2, takes very different values for stars of the same luminosity and spectral type. For main-sequence stars, the brighter the emission, the closer the position of the star to the lower boundary of the zero-age main sequence (Wilson and Skumanich 1964). The width of the emission, w, is correlated with the visual luminosity (Wilson-Bappu effect, $w \sim L_V^{1/6}$) independently of I_2 and of the spectral type. This relation does not apply to cepheids (Kraft 1957) nor to T Tauri stars (Kuhi 1965).

For stars of earlier spectral type than the sun, the spectral type in which the H-K emission ceases seems to be a matter of dispersion of the spectrograms, as long as the photospheric brightness is not too high. With a dispersion of 10 Å/mm, no emission is found for b-y < 0.30 (type F5), but weak emission appears on high dispersion spectra of α CMi, F5 IV (Kraft and Edmonds 1959, 3.2 and 4.8 Å/mm) α Car F0 Ib (Warner 1966, 6.8 Å/mm and γ Vir B, F0 V (Warner 1968, 4.7 Å/mm).

(2) Traces of variable chromospheric activity have been searched for in 139 stars by Wilson (1968), who observed the flux at the center of the H and K lines with a two-channel photometer over one year. The results are not clearly in favour of a variability. Deutsch (1967) found large changes of K_2

* See R. N. Thomas, pp. 38-45.

emission in two K giants: α Tau (K5 III) and γ Aql (K3 II).

H-K emission is the only chromospheric emission feature observable in the visible spectrum of a great majority of the stars studied by Wilson. In T Tauri stars, however, the near infrared triplet of Ca II seems to be characteristic (Herbig, quoted by McConnell, 1967). Due to the presence of many other emission lines in the spectrum of T Tauri stars, to their irregular variability, and to the peculiarities of their UV spectrum, one cannot safely compare their chromospheric problem to that of normal stars, even if one can be sure that there is one.

Hα is often observed in absorption in stars with H and K reversals. Suspecting that its central part is formed in the same region as the K_2 emission, Kraft, Preston, and Wolff (1964) tried to correlate the width of the core with the luminosity of stars. The relation between this width and the absolute ultraviolet magnitude is not as good as the relation discovered by Wilson and Bappu.

He I λ 10830 was first observed in emission in P Cyg and in carbon Wolf-Rayet stars (Miller 1954), with IZ emulsion and a very low dispersion (1300 Å/mm at 1μ); then Kuhi (1966) made photoelectric scans around the helium line in Wolf-Rayet stars, and observed it in emission in all Wolf-Rayet stars. The development of image tubes and the Lallemand camera now allows one to observe the helium line in absorption and in late type stars. Vaughan and Zirin (196 (1968) looked for this line at 8.4 Å/mm in 86 stars, the majority being of G and K type. About 30 of them show the He line in absorption; in 5 others the line appears in emission. Among the 12 B, A, and F stars of the sample, only β Ori (B8 Ia) and α CMi (F5 IV) show the line, in absorption. For 2 stars an activity is detected by variations of the helium line with time. In several cases, the line shows a structure.

Although it does not constitute a simple case of a star with a chromosphere, β Lyr presents a broad emission feature at λ 10830 (observation by Knappenberger and Fredrick, 1968, with a mica window image tube, 58 Å/mm.

In the ultraviolet spectrum of stars, the resonance doublet of Mg II at 2800 Å has been reported (Heinze et al. 1967) in absorption in the spectrum of αCMa. One would think it would be observed, with an emission, in all stars where H and K emission exists, since in the sun the emission in Mg II is stronger than that in Ca II (Dumont 1967, Kandel 1967, Athay and Skumanich 1968a).

Ly α observed in six Orion hot stars by Morton et al. (1968) is probably of interstellar origin only. The same difficulty in separating the stellar Lyman lines from the interstellar ones is quoted by Smith (1969) in a paper on rocket observations of α Vir Bl V).

Anway, it seems preferable to search for Ly α in late type stars, where the maximum of the photospheric flux is very far from the spectral range of the Lyman lines and where ultraviolet emission, if it exists at all, can only be of chromospheric origin. Predictions have been made by Oster and Patterson (1968), who conclude that chromospheric Ly α could be detectable with a 10 cm reflector for very near cold stars (distance less than 3 parsec).

Coronal line observations in stellar spectra are rare. Coronal lines were discovered by Adams and Joy (1933) in RS Oph, a repeating nova, but were not identified until 1945. Other repeating novae show lines of highly ionized atoms: T Pyx, T CrB. For this last star, Bachonko and Malville (1968) measured the equivalent widths of the following lines: λ 5303 [Fe XIV]; λ 6374 [Fe X]; λ 5536 [A X], on spectra obtained during the 1946 outburst of the star, and analyzed the green coronal line, from which they deduced a relation between the radius of the corona and the density necessary to produce the observable green line: $N_e = 3\text{-}5 \cdot 10^7 cm^{-3}$, T_e is assumed to be 10^6 °K.

Other coronal lines have been observed in CI Cyg and AG Peg (lines of [Fe X]), in RX Pup (lines of [Ca VII]), in Z And (lines of [Fe VII]). Sahade (1960) has discussed these peculiar emission-line stars, and further work is due, among others, to Bloch (1964), Boyarchuk (1966), and Boyarchuk et al. (1964, 1967).

Coronal ions could be observed in ultraviolet spectra, but severe limitations exist. (1) Below 912 Å, all stellar flux is absorbed by interstellar hydrogen even for the nearest stars. (2) The total light flux emitted by the solar corona is several powers of ten lower than the visible flux. A stellar corona would have to be much more powerful than the solar one to be detected with the available space equipment, except for very hot stars.

b. Continuous Spectrum

For the same reason as in the sun, it is possible to see the low chromospheric layers of a star by observation of the continuous spectrum in the ultra-

violet and infrared regions, where $\tau_\lambda = 1$ corresponds to very small values of τ_{5000} (Noyes et al. 1966). But the lack of angular resolution in the observations is a very strong limitation, and the derivation of semi-empirical models by inversion of limb-darkening curves is excluded thus far.

Nevertheless, absolute intensities in the ultraviolet spectrum below 2000 Å, especially in A and F stars where the opacity due to metals (Mg, Si, Al) and to carbon dominates that of hydrogen (H I and H^-) and is very strong, will help to check the validity of theoretical model atmospheres in the very superficial layers. But it seems impossible to expect that these observations will be of as much help in determining stellar chromospheric models as those coming from the study of the cores of strong lines.

Towards the longer wavelengths, observation of an intense infrared emission near 10μ has been reported first in 1965 for 3 late-type stars: α Ori, α Tau, and μ Cep (Low 1965). Gillett et al. (1968) have confirmed this feature for 4 cool stars (α Ori, μ Cep, o Cet, χ Cyg), but nothing appears for a hot star like α CMa; they suggest two interpretations, one implying a chromospheric temperature, the other an emission by circumstellar matter around the star. Other authors now favour the last item, on the basis of the general appearance of such circumstellar envelopes around several types of cool stars (Stein et al. 1969), and of the resemblance of the emission to that of solid particles (see Wolf and Ney, 1969).

The evidence of a stellar wind in α Ori (Deutsch 1959, Weymann 1962) led Weymann and Chapman (1965) to compute the theoretically predicted free-free emission of a hydrodynamic hot flow emitted by α Ori. They concluded that between 1 mm and 3 cm the absolute flux is just at the limit of detectability for radio astronomers. Kellermann and Pauliny-Toth (1966) searched for that emission at $\lambda = 1.9$ cm, but could not detect it.

All in all, there is very little indirect evidence for chromospheres and coronas in the stellar case. The only exception consists of the K-line emission, which has been detected for more than a hundred stars.

III. WHAT IS INFERRED FROM THE OBSERVATIONS?

The observed quantities are essentially (1) relative continuous intensities, and (2) line para-

meters: central intensity I_o, emission width, half-width $\Delta\lambda_{1/2}$, equivalent width W, and in rare cases, structure of the whole profile.

Due to the significant results obtained in recent years on the solution of the transfer problem (Cuny, Dumont) which allow one to consider the "synthetic problem" in line formation to be fairly well solved, I will focus my attention on three main fields where physical information has been gained from stellar chromospheric observations.

a. Construction of Models (i.e. Jefferies' "analytical problem")

Given my restricted definition of stellar chromospheres, I will review only the work done by Kandel on late-type emission dwarfs. Groth will report on chromospheres in K giants belonging to eclipsing binaries. In the first case, deduction of the model from the observations is mainly based on the Ca II K line. Other chromospheric indicators have not yet been intensively used for the purpose of models; we will consider them later.

(1) Kandel (1967) constructed chromospheric models to interpret the strong K line emission observed in K and M dwarfs that showed no Hα emission. He specifies the chromosphere by a temperature profile $T_e(N)$, electron temperature versus the number of hydrogen nuclei, N, in a column of 1 cm^2 above a reference level corresponding to the surface of a photospheric model; the parameters are the temperature T_c and the mass N_c of a large plateau, and the gradient $C = -d(\log T_c)/d(\log N)$ of the temperature law just under the plateau. Other basic assumptions in Kandel's computation are hydrostatic equilibrium and LTE ionization balance. They are questionable, but are adopted for simplicity.

A series of such a priori chromospheric models was put at the top of convenient photospheric models that were built to reproduce the visible absorption spectrum. Kandel computed the Ca II emission equivalent width, E_k, by using the non-LTE theory of Dumont (1967) and traced iso-E curves in a (N_c, T_c) diagram. Computing then the radiative energy loss by these theoretical chromospheres, Kandel eliminated those models that are thermally unstable and those that should produce emission in Hα. A very limited region remains acceptable, with $T_c < 10{,}000°K$.

Despite its evident limitations, Kandel's approach is a physically well-grounded one. One can

suspect his photospheric models, as he does himself, because of the importance of convection; the mechanical flux he pumps in the convection zone to heat the chromosphere is as uncertain as the application of Lighthill's theory to stars. But, given the present set of developed theories, he tries to derive the most complete model. If one remains unsatisfied by all the approximations involved in such an exercise, one must return to the problem of improving the energy generation and transport theories.

(2) Rough indications about chromospheric conditions have been derived from other lines. The He I λ 10830 line has been shown by Athay (1963) to be very sensitive to the temperature between 10^4 and $2 \cdot 10^4$ °K. When it is observed, the He I absorption line indicates a hot chromosphere or more explicitly, a chromosphere hotter than that of stars with only K reversal ($T > 20,000$°K). Let us recall that λ 10830 appears in emission in three supergiants, including ε Ori (BO Ia) (Vaughan and Zirin 1968); its presence in absorption in β Ori might be used as a test of Underhill's hypothesis on helium overabundance in B supergiants if the non-LTE problem is solved uniquely.

The Hα core has been suggested by Cuny (1968) to be a test for low chromospheric solar models. She computed the non-LTE Hα profile with two solar models, HAO1 and the interspicular model of Athay and Thomas. With the latter the residual intensity is larger than observed; with the former, smaller. Collisions have a greater contribution to the source function in the interspicular model, which is denser, so she proposed that the central part of the Hα line could be used, by comparison with observations at high spectral resolution, at least to check plausible chromospheric models, if not to establish them.

In a rather similar way, Kandel has used the absence of Hα emission in 61 Cyg B to limit the possible range of his chromospheric parameters for that star.

The Ly α and Ly β lines, if they can be ever observed in cool stars, will be an excellent tool for studying stellar chromospheres.

(3) Purely theoretical non-grey, radiative-equilibrium atmosphere-models were computed by Feautrier (1968). Taking account of H^- departures from LTE, Feautrier's models present a rise of temperature above the purely photospheric layers; these models constitute a good set of a priori models to be used in studying chromospheric conditions from spectral features in stars hotter than the sun.

b. Velocity Fields

Although this subject is not completely separate from the model problem, because of coupling between dynamical phenomena, transfer, and physical structure of the atmosphere, one can only be very short and restrict one's attention to qualitative or first approximation theory results. The whole theoretical problem lies indeed in a premature state. Velocity fields are however deduced from two types of observations.

(1) Line displacements. Stellar chromospheric lines often show an absorption component displaced towards the violet, the emission component being shifted longward. The case of the K line in cepheids is typical, but the phenomenon is more general. For instance, He I λ10830 in the most luminous stars observed by Vaughan and Zirin presents the same feature. P Cygni type profiles are observed also in extended atmospheres which may not be chromospheres in the restricted sense given above. In the expanding envelopes discovered by Morton (1967) for 3 supergiants, the absorption components of the strong resonance lines of Si IV, C IV, N V, and Si III indicate velocities in excess of the estimated escape velocity. A P Cygni profile is characteristic of the He I λ10830 line in β Lyr (Knappenberger and Fredrick 1968).

(2) Line asymmetries. As in the sun, where both the Ca II and Mg II resonance lines show asymmetry in the reversed part of the core, large asymmetries are observed in stellar K_2 components (Wilson and Bappu 1957, Deutsch 1969), which vary with time, so that it seems difficult to think of any interpretation of the K-line profile that would ignore motions and inhomogeneities in the atmosphere of those stars.* The most prominent feature of chromospheric line profiles is broadness, so that their halfwidth cannot be interpreted as being due to a purely thermal Doppler effect. Large turbulent motions are present in chromospheric layers. Several authors have argued that these motions are macroturbulent ones, arising from large mass motions. Moreover, there seems to be a correlation between K-line emission and photospheric turbulence: (1) In cepheids, Kraft (1967) reported that the turbulence increases after minimum light, at the same time as the K emis-

*I am indebted to Dr. A. J. Deutsch for having stressed this point to me.

sion appears. (2) Bonsack and Culver (1965), on the other hand, have produced evidence that the K-line emission width w is correlated with the halfwidth $\Delta\lambda_{1/2}$ of photospheric V I lines in a sample of G, K, and M stars. The correlation being less clear between w and the curve-of-growth velocity, they concluded that macroturbulent motions exist in the photosphere of the stars studied, and stressed a possible common origin of the K reversal width and broadening of photospheric lines.

c. Activity

One gets a very qualitative insight to chromospheric activity from the following facts:

(1) Emission in the K line has been found to be variable in cool giants, first by Griffin (1963) and later by Deutsch (1967) and Liller (1968).

(2) The K-line reversal seems to be associated with magnetic field in the hottest star in which it has been found (Warner 1968).

(3) The λ10830 He I line shows intensity variations which recall the increase of intensity of that line in solar plages and prominences.

Wilson (1963) suggested that the existence of a chromosphere and the strength of the K-line emission are correlated with the presence of magnetic activity and that they decline with time as do the magnetic fields.

A very special case is that of the transitory character of the K-line emission in cepheid atmospheres; the appearance and disappearance of the emission is connected with the phase of the pulsation, and may be interpreted by periodic modifications of the excitation in the atmosphere, which are probably not of the same nature as those which appear, periodically or not, in the above quoted examples. Indeed, the change in excitation is generally associated with the passage of a shock wave through the atmosphere.

To end this paragraph, I would only mention the problem of correlation of chromospheric properties with general properties of the stars. The fundamental explanation of the Wilson-Bappu effect seems to be still unknown; on the other hand, stars like the cepheids or T Tauri stars do not obey the Wilson-Bappu relation, supporting the idea that the K emission may have a different origin in stars where the chromosphere is heated by different mechanisms. If one tentatively accepts the idea that the type of

variability that gives rise to light variation in cepheids or in T Tauri stars, and that probably differs between both types of stars, generates mechanical energy in the outer layers of these stars, one is prepared to admit that the Wilson-Bappu effect is relevant only to stars in a certain stage of their evolution, which stage is characterized by a certain kind of heating. As pointed out by Athay and Skumanich (1968), "W_2 reflects on the nature of the energy conversion mechanism." Of course the interpretation of chromospheric observations in stars can be considered as being directed towards discovering the mechanical energies at work in a star.

IV. DO A STARS HAVE A CHROMOSPHERE?

In A stars, no chromosphere has been identified with confidence; on theoretical grounds, it is usually thought that since ionization convection zones become thin for stars hotter than spectral F_0- F_5, no strong acoustic energy may be generated. Thus the conditions for a strong chromosphere are not present. But Wilson (1966) has claimed that he sees no good reason why chromospheres should cease towards the uper edge of main-sequence stars. Leaving for the moment the question of B stars, and by close continuity with the observations already available, I will give some arguments in favour of chromospheres in A stars.

(1) There are favorable observational indices for chromospheres in these stars, although at this time they do not constitute indicators:

(a) K reversal in γ Vir B (F0 V), which is a magnetic star. Many A stars are magnetic stars.

(b) Variability in the K line. Henry (1967) observed 4 Ap stars already known to be variable in the K line, confirmed their variability, and discovered 4 others. Baglin et al. (1968) discovered a large variation of that type in γ Boo (A7 III), which is a δ Scuti variable. The variation seems to have nothing to do with the light curve period. This is under further study.

(c) The A stars show a large microturbulent parameter (6.9 km/s) and this feature is not limited to Am stars, as was established by Baschek and Reimers (1969).

(2) What else should one look at to detect chromospheres in A stars?

(a) The core of the K and of the Hα line. If the K line, collision dominated, presents even a small reversal, this will imply a chromospheric temperature gradient. The Lallemand camera is the best detector to use for such a study of the cores of very strong lines because of its lack of threshold at low fluxes and the linearity of its response.

(b) O I, C I, Si II, Al II, Mg II resonance lines in the ultraviolet spectrum.

(c) There is almost no chance of detecting Ly α, even if its emission in an A star would be the same fraction as in the sun of the acoustic flux heating the chromosphere.

An estimate made for a typical A star with $T_{eff} = 8000°$, log g = 3.9 indicates a flux at the ground of 5.10^{-4} photons $cm^{-2}s^{-1}$, to compare with the value of 6 for the sun.

(3) How could one heat a chromosphere in A type stars?

A model study of an Am star (Praderie 1967) shows that if the observed microturbulent parameter ξ_t is not due to other physical effects (such as NLTE effects of the source function for lines on the plateau of the curve of growth), the atmosphere must be very convective to produce the value of ξ_t derived from the curve of growth. But an adequate convective model fails to reproduce the wings of strong lines, which, for A stars, are formed in the convectively unstable layers of the photosphere.

With the help of Lighthill's theory of generation of acoustic noise from convective turbulence, and a convection efficiency compatible with line-wing observations, the acoustic flux produced in the convection zone may be estimated. For a star of $T_{eff} = 8000°K$, log g = 3.9, it turns out to be one-tenth of the solar value (assumed to be 10^8 ergs $cm^{-2}s^{-1}$). Thus it seems doubtful that one could heat, in that star, a chromosphere as hot as the solar chromosphere.

But the problem of the high ξ_t parameter remains. The acoustic flux produced in the convection can be increased by enhancing the helium abundance and then the depth of the He I and He II parts of the ionization convection zone (Mariai 1969). However, in Am stars, no He I line is observable. In some silicon Ap stars, work by Searle and Sargent (1964) and by Hyland (1967) gave observational

evidence for helium depletion in the atmosphere. So no conclusions can be drawn about helium abundance; but significant progress will arise from the search for He I λ10830 in Ap stars with strong magnetic fields, both to decide if a temperature of 20,000°K can be obtained in a possible chromosphere for these stars and to see if the helium abundance distribution in these stars is uniform with depth. In some of those stars, Zirin (1968) has already found evidence of the presence of He^3.

To conclude, I stress that several factors that might have a strong relation to the presence of chromospheres in stars have not been reviewed here. The role of a companion in enhancing the chromospheric spectral features has often been mentioned. The problem of generation of stellar winds was out of the scope of the colloquium, but its importance should not be minimized.

ACKNOWLEDGMENTS

I am indebted to R. N. Thomas and J. C. Pecker for useful discussions, and to A. J. Deutsch and L. V. Kuhi who made me aware of several references that I would have missed otherwise.

REFERENCES

Adams, W. S., and Joy, A. H. 1933, *PASP*, 45, 301.
Athay, R. G. 1963, *Ap. J.* 137, 931.
Athay, R. G., and Skumanich, A. 1968b, *Ap. J.* 152, 141.
Athay, R. G., and Skumanich, A. 1968a, *Solar Phys.* 3, 181.
Baglin, A., Praderie, F., and Perrin, M. N. 1968, Comm. presented at the Budapest Symposium on Non-Periodic Phenomena in Variable Stars.
Baschek, B., and Reimers, D. 1969, *Astr. and Astrophys.* 2, 240.
Bloch, M. 1964, *Ann. Astr.* 27, 292.
Bochonko, D. R., and Malville, J. 1968, *PASP*, 80, 177.
Bonsack, W. K., and Culver, R. B. 1966, *Ap. J.* 145, 767.

Boyarchuk, A. A. 1964, *Variable Stars*, 15, 48.
Boyarchuk, A. A. 1966, *Astrofisika*, 2, 101.
Boyarchuk, A. A. 1967, *Izv. Krim. Astr. Obs.* 37.
Cayrel, R. 1963, *C. R. A. S.* 257, 3309.
Cuny, Y. 1968, *Sol. Phys.* 3, 204.
Delache, P. 1967, *Ann. Astr.* 30, 827.
Deutsch, A. J. 1959, *Ap. J.* 129, 570.
Deutsch, A. J. 1967, *PASP*, 79, 431.
Deutsch, A. J. 1969, Comm. presented at the Lunteren Symposium.
Dumont, S. 1967, *Ann. Astr.* 30, 421.
Feautrier, P. 1968, *Ann. Astr.* 31, 257.
Gillet, F. G., Low, F. J., and Stein, W. A. 1968, *Ap. J.* 154, 677.
Griffin, R. F. 1963, *Observatory*, 83, 255.
Henize, K. G., Wackerling, L. R., O'Callaghan, F. G. 1967, *Science*, 155, 1407.
Henry, R. C. 1967, Princeton University, Thesis.
Hyland, A. R. 1967, Canberra University, Thesis.
Jefferies, J. T. 1968, *Spectral Line Formation*, Blaisdell Publishing Co., New York.
Kandel, R. S. 1967, *Ann. Astr.* 30, 999.
Kellerman, K. I., and Pauliny-Toth, I. I. K. 1966, *Ap. J.* 145, 953.
Knappenberger, P. H., and Fredrick, L. W. 1968, *PASP*, 80, 96.
Kraft, R. P., and Edmonds, F. N. 1959, *Ap. J.* 129, 522.
Kraft, R. P., Preston, G. W., and Wolff, S. C. 1964, *Ap. J.* 140, 235.
Kraft, R. P. 1967, *5th Symposium on Cosmical Gas Dynamics*, ed. R. N. Thomas, Academic Press, New York, p. 229.
Kuhi, L. V. 1965, *Ap. J.* 145, 715.
Lighthill, M. J. 1967, *5th Symposium on Cosmical Gas Dynamics*, ed. R. N. Thomas, Academic Press, New York, p. 429.
Liller, W. 1968, *Ap. J.* 151, 589.
Low, F. J. 1965, IAU Circ. No. 1884-85.
McConnell, J. 1967, *PASP*, 79, 66
Miller, F. D. 1954, *A. J.* 58, 222.
Morton, D. C. 1967, *Ap. J.*, 147, 1017; 1967, *Ap. J.* 150, 535.
Morton, D. C., Jenkins, E. B., and Bohlin, R. C. 1968, *Ap. J.* 154, 661.
Nariai, K. 1968, preprint.
Noyes, R. W., Gingerich, O., and Goldberg, L. 1966, *Ap. J.* 145, 344.
Oster, L., and Patterson, N. P. 1968, *J.Q.R.S.T.* 8, 305.

Parker, E. N. 1963, *Interplanetary Dynamical Processes*, Interscience Publishers, New York.
Praderie, F. 1967, *Ann. Astr.* 30, 773.
Sahade, J. 1960, *Stars and Stellar Systems*, vol. 6, 494.
Searle, L., and Sargent, W. L. W. *Ap. J.* 139, 799.
Smith, A. M. 1969, *Ap. J.* 156, 93.
Stein, W. A., Gaustad, J. E., Gillett, F. C., and Knacke, R. F. 1969, *Ap. J.* 155, L3.
Vaughan, A. H., and Zirin, H. 1968, *Ap. J.* 152, 123.
Warner, B. 1966, *Observatory*, 86, 82.
Warner, B. 1968, *Observatory*, 88, 217.
Weymann, R. 1962, *Ap. J.* 136, 844.
Weymann, R., and Chapman, G. 1965, *Ap. J.* 142, 1268.
Wilson, O. C., and Bappu, M. K. V. 1957, *Ap. J.* 125, 661.
Wilson, O. C. 1963, *Ap. J.* 138, 832.
Wilson, O. C., and Skumanich, A. 1964, *Ap. J.* 140, 1401.
Wilson, O. C. 1966, *Ap. J.* 144, 695.
Wilson, O. C. 1968, *Ap. J.* 153, 221.
Woolf, N. J., and Ney, E. P. 1969, *Ap. J.* 155, L181.
Zirin, H. 1968, *Ap. J.* 152, L177.

WHAT SHOULD WE DO TO KNOW MORE ABOUT CHROMOSPHERES AND CORONAE OF STARS?

by

Richard N. Thomas

*Joint Institute for Laboratory Astrophysics**
Boulder, Colorado

ABSTRACT

Chromospheres-coronas satisfy the last two of the proposed classification schemes: inadequacy of the classical atmosphere (CA) model to represent observations and a priori rejection of the CA model. So we survey the question of what is required for more knowledge from the standpoint of asking what conceptual modifications will increase knowledge and what new observations are required. We stress that continued progress requires a continual interchange of ideas between the solar situation and the range of stellar situations.

Key words: chromospheres, coronas, classical atmosphere model.

The general subject of today's discussion is: "What do we know about chromospheres and coronae of stars?" Thus, as Françoise Praderie emphasized in the preceding summary paper, we restrict attention today to a particular kind of extended stellar atmosphere, one which can fall into either classification 3 or 4 of the alternatives I proposed the first day of this conference. I would like to emphasize to you that we are, at least implicitly, making a much stronger restriction of the kind of stellar configuration to be discussed than we would have, with the same literal title, in a discussion of extended stellar atmospheres 25, or even 15, years ago. The

---

* Of the National Bureau of Standards and the University of Colorado.

fact that it is a stronger restriction means, of course, that we think we know more today about chromospheres and coronae than we did 25, or even 15, years ago. I think we all generally understand that by "chromosphere" and "corona" in today's thinking, we mean an extended stellar atmosphere that arises as a consequence of a departure from strictly radiative or convective equilibrium because of a local dissipation of mechanical energy. In the chromosphere and corona, we have a reversal of the photospheric temperature gradient: $dT_e/dh > 0$. Overall, the evolution of thought during the last 25 years has centered on how deep in the atmosphere this region $dT_e/dh > 0$ can be pushed, and how many phenomena arise because of this outward rise in T_e. In this symposium where we ask what the problems of extended stellar atmospheres are, the important thing is not just the fact that we know more about this particular kind of extended stellar atmosphere, but also the way in which that knowledge has evolved. The path has not been simply one of acquiring new data, but also one of more critical analysis of old data and old concepts. So as we explore my topic today--What should we do to know more about chromospheres and coronae?--we might follow the same path: examining concepts as well as data.

Even 40 years ago, most astronomers would have said that stellar chromospheres and coronae satisfied classification 3 of extended stellar atmospheres--inadequacy of the CA model to represent observations--even though neither observations nor the idea of the CA model were as clear as they are today. Twenty-five or even 15 years ago, most astronomers would have admitted that a stellar chromosphere probably satisfied the category 4 criterion: a priori rejection of the CA model. But the conceptual basis for rejecting the CA model 40 and 25 years ago differed considerably from that which has evolved over the last 25 years. At that time, the admission of inadequacy rested upon the ad hoc construction of a phenomenon outside either our laboratory experience or conceptual understanding--the "turbulent" models of 40, 25, 15 and even more recent years ago--and the inability to see how it could arise from the CA model because we didn't understand what it was. So the chromosphere probably departed from the CA conditions, but probably because HE was invalid, while RE and LTE probably remained valid. Today, however, we profess to a very explicit physical understanding of why the atmosphere is extended, relative to the physical picture underlying the CA model. We have

simply dropped the notions that either RE or CE provide all the energy transport in the atmosphere, and that LTE under the RE distribution of T_e describes the state of the gas. We have admitted the possibility that various kinds of instabilities arising even in the CA model may amplify, producing a local dissipation of mechanical energy, and that excitation conditions may differ from the CA strictures. By loosening the strictures placed on the diagnostic framework, we permit a tightening on the physical picture of the model.

The dropping of LTE--which has loomed large, sometimes almost irrelevantly so--in the discussions this week has a different kind of significance than that of RE. The RE, HE questions relate to the aerodynamical phenomena and give us the extended or non-extended configuration of the atmosphere; they tell us how the configuration occurs. Dropping LTE simply lets us state, unbiasedly and correctly, what the configuration and state of the gas is.

So we restrict attention to a kind of extended stellar atmosphere, whose general physical cause we think we understand. But when we ask what we know about chromospheres and coronae, it is the details of the phenomenon and the variation in details from spectral type to spectral type that we must investigate. In this connection, I have stressed the points in the preceding paragraphs for two reasons.

First, we have reached the stage of being willing to accept the above implications on what we mean by stellar chromospheres and coronae through a combination of two kinds of investigation: on the one hand, an analysis of physical self-consistency of atmospheric model and of spectroscopic diagnostics; on the other hand, an application of this analysis to solar observations and models. To this, we have added also observationally-less-detailed, exploratory investigations of other stellar atmospheres. But by and large, the situation is as I said: a compound of general theory and solar interpretive-observational work. Then, we have generalized and extrapolated to various stellar cases--testing, substantiating, modifying as we have been able.

Second, Françoise Praderie has given us a very complete summary of what we know about chromospheres and coronae of stars. In addition, in the process of asking what the spectral indicators of the presence of chromospheres and coronae are, she has gone a long way toward answering the question of what we must do to learn more: How do we extend the observation of these spectral indicators. It would be

pointless for me, here, to follow her discussion by simply commenting on the various indicators she has summarized.

So, in considering this path of evolution of our knowledge, to answer the question of what we must do to learn more about chromospheres and coronae, I lean heavily on the evolution of thinking about the solar case. And, in the context of the specific features discussed by Françoise, we continue this extrapolation-generalization from the solar case.

I would stress that we must adopt a conceptual generalization from solar considerations, not necessarily a literal one. In such a literal approach, we would assume that all chromospheres must originate from the detailed causes underlying the solar chromosphere, and must have the detailed structure of the solar chromosphere. Such a literal approach, for example, is found in the 1955 IAU *Joint Discussion on Turbulence in Stellar Atmospheres*, held at Dublin. On the other hand, my own thinking has always centered around the notion that the common feature of chromospheres and coronae is simply a mechanical energy supply, which may arise in many different ways in many different spectral classes. I have repeatedly cited the sun and the Wolf-Rayet stars as probably lying near the two extremes of the kind of steady-state atmospheres produced by aerodynamical effects. In the sun, we consider only departures from RE; in the WR stars, departures from both RE and He. I consider to be most misleading the kinds of arguments cited that expect chromospheres-coronae only in stars of spectral class FO and later, based on the notion of acoustic waves from an atmospheric convection zone as the source of chromospheres-coronae. Such arguments confuse the existence of sources of mechanical instability with the details of one such source. I have stressed this point in the first paper of the series: Superthermic Phenomena in Stellar Atmospheres (Thomas 1948) and in the introduction to our survey of the physics underlying the solar chromosphere (Thomas and Athay 1961). Parker makes the same point in the concluding chapter of his monograph on the solar wind (Parker 1963). The two symposia on cosmical gas dynamics devoted to aerodynamical phenomena in stellar atmospheres developed this outlook (Thomas 1961, 1967). The symposium on Wolf-Rayet stars held in 1968 brought together much material that strengthened the case for considering the line-forming region of the WR atmosphere simply as an extended chromosphere (Gebbie and Thomas 1968). So what I would stress to you

here, when we ask what we should do to know more about stellar chromospheres and coronae, is that it is not only a matter of getting more and better observations of known indicators. It is equally a matter of becoming very clear about the kind of evolution in our thinking that led us to focus on the true nature of the chromosphere-coronal phenomenon, hence the kind of parameters that might tell us more about them.

Tables I and II summarize the evolution of our thinking on the solar chromosphere-corona. Table I concentrates on the "classical" problem, referring to the concepts of 40 and 25 years ago that I stressed above. Points 1 and 2 of Table II [corresponding to points 1 and 2 of Table I] refer to the resolution of these problems.

The dilemma and resolution summarized in the tables in points 1 and 2 require little discussion. In essence, the "classical" dilemma of the extended solar atmosphere comes from looking at an apparent gross anomaly--the atmospheric extent--which is significant enough to vitiate the CA model, through a set of glasses tinted with the CA predictions: the excitation state of the outer atmosphere must not exceed that of the photosphere, and the outer atmosphere must be so thin as to be transparent, certainly in its effect on the disk spectrum, likely in considering the eclipse line spectrum. Given these observations, and given these strictures on interpretation, the only resolution was to "invent" a new kind of phenomenon, "astronomical turbulence," whose physical properties were constructed explicitly to (1) satisfy the observations as interpreted within the diagnostic strictures, and (2) beg the question of physical consistency by postulating unknown physical interactions. (1) refers to the requirement that emission gradient be interpreted as density gradient. (2) refers to the requirement that "astronomical turbulence," with characteristic random velocity exceeding the thermal velocity of the medium, somehow have any mechanical energy dissipation suppressed. The "secondary" classical dilemma, that associated with the symbiotic behavior of excitation state, was relegated to secondary status mainly because we retained the CA-tinted glasses, even in studying this non-CA phenomenon. The final resolution of these two aspects of the dilemma came when the diagnostic approach was freed from all a priori imposition of the strictures of the CA model, under the principle that no one of the CA assumptions should be more sacred than any other, when it became

TABLE I. SCHEMATIC EVOLUTION

How Astronomers Viewed the Solar

Original Observational Problem	Original Interpretation
1. Anomalous extent of atmosphere:	"Turbulent" momentum support.
a. Apparent scale-height of order 1000 km.	No energy dissipation by such turbulence
(i) Differential scale-heights from different lines, and continua	
b. Isothermal scale-height of order 100 km.	
2. Symbiotic excitation phenomena	
a. Presence of He I, He II	UV excess in sun
b. T_{ex} as low as 3000° for some metals	Line-blanketing depression of T [boundary]
c. Excitation increases outward	
(i) Spectral lines of "coronium"	

necessary to relax any one of them. Lifting the restriction on excitation state and opacity of the atmosphere permitted the density gradient to depart from the emission gradient, and a distribution of T_e to be sought which made the observations coherent. It is interesting to note that the path of resolution was not really so logical as stated, but came as a shocked necessity to permit $dT_e/dh > 0$ from the

OF THINKING ON SOLAR CHROMOSPHERE

Chromospheric Problem 25 Years Ago

Original Physical Problem	Perturbing Questions
Physical model of such "turbulence"	How to tell T_e, T_k from V_{turb} How to avoid mechanical energy dissipation, hence rise in T_k, T_e
Origin of such excess	Why should excitation increase outward in such a model?
Self-consistent calculation	Why such different values from different lines?

identification of the coronal lines. But it took some time to admit this situation to the region where the dilemma was quantitatively the most evident--the chromosphere--and to recognize that these regions could have an effect on the disk spectrum.

Points 3-5 of Table II refer to observational details that arose later, somewhat after the classi-

TABLE II, SCHEMATIC EVOLUTION OF

Change in "Observational" View

Original Observational Problem	Refined Observation
1. Anomalous extent of atmosphere:	"True" scale-heights differ from observed
a. Apparent scale-height of order 1000 km.	Differs from line to line
(i) Differential scale-heights from different lines, and continua	
b. Isothermal scale-height of order 100 km.	Atmosphere not isothermal, but HE not bad approximation up to 1000 km. Any turbulence definitely subsonic
2. Symbiotic excitation phenomena	Symbiotic appearance exists
a. Presence of He I, He II	Same
b. T_{ex} as low as 3000° for some metals	Same
c. Excitation increases outward	Same; identification of "coronium" lines
(i) Spectral lines of "coronium"	
3. Emission lines in rocket UV, on disk	Same form as Ca^+ cores
4. Correlation between H and K lines and magnetic field	Profile changes over disk
5. Non-spherically symmetric emission	Same

THINKING ON SOLAR CHROMOSPHERE

of Solar Chromosphere Today

Physical Interpretation	Questions Remaining
Compound of outward increase in excitation, coming from $dT_e/dh > 0$, and of self-absorption, non-LTE Above	Refined observation still needed
Mechanical energy supply; $dT_e/dh > 0$ Non-LTE ionization equilibrium	Source, and interpretation, of any turbulence
Compound of $dT_e/dh > 0$ and non-LTE coming from boundary	Better observations More detailed non-LTE calculations for complex ions
$dT_e/dh > 0$; collisions + radiative excitation	Influence of inhomogeneous atmosphere
Non-LTE coming from boundary Line-blanketing effect small on non-LTE theory	Detailed calculation More refined observation
Consequence of $dT_e/dh > 0$	Detailed model
Consequence of $dT_e/dh > 0$	Detailed calculation Questions of line-broadening
Non-uniform mechanical dissipation under influence of magnetic field	Detailed mechanism and model
Inhomogeneous mechanical heating; inhomogeneous mechanical structure	Detailed observation Detailed model

cal dilemma represented by points 1 and 2 was well on the way toward resolution. But had the observational material underlying these points 3-5 been available 25, possibly even 15 years ago, we must be honest and realistic enough to admit that the same CA-tinted glasses would probably have inhibited their correct interpretation. This suggests that a useful way to compare the path of evolution of thinking on the solar chromosphere-corona to that on the stellar, would be to compare the full range of "anomalous" phenomena for each, using always as reference the CA model. After all, when we discuss "extended stellar atmospheres," we do so relative to the "non-extended" CA model atmosphere.

If we adopt this approach, we recognize that we can group the apparent anomalies under three headings: "apparent" macroscopic structural anomalies; symbiotic excitation anomalies, usually microscopic, at least in implication; and basic conceptual anomalies. Consider these, specifically.

THE OUTER SOLAR ATMOSPHERE

A. "Apparent" Structural Anomalies

1. Overall extent of the atmosphere:
   Emission scale-heights large relative to the scale-height of an isothermal atmosphere, using a temperature derived from either a CA theory or a CA-interpreted observation.
   Differing emission scale-heights from different lines and differing elements.
2. Gross structural inhomogeneities:
   Mainly apparent in those observations capable of resolving small fractions of the solar disk.
3. Differential brightness correlated with differential values of local magnetic fields:
   Again, mainly apparent in those observations capable of resolving small fractions of the solar disk.
4. Differential macroscopic velocity fields:
   Two kinds of measures exist; those depending on resolving small fractions of the solar disk, and those not so depending.
   a. Non-dependent on disk resolution:
      Inferences of differential macroscopic fields from conclusions on line-broadening

mechanisms; either for a line-profile, or a total energy lying in the line.
Inferences based on asymmetries of line profile, which are interpreted in terms of differential motions.

b. Dependent on disk-resolution:
Indirect inferences in the Doppler cores of spectral lines based on limb-darkening data.
Direct measures based on line-shifts on different parts of the disk.

I have grouped items 3 and 4 in this heading of "structural" anomalies because of the evident temptation to associate structural behavior with kinematic behavior of the atmosphere, on the one hand; and the problem of separating thermal motion from other velocity fields, on the other hand. Uncertainty on thermal motions introduces uncertainty in what the extent of the atmosphere should be, even in HE.

B. Symbiotic Excitation Anomalies

1. Low-excitation indicators:
   a. The low residual intensities, or low values of T_{ex}, in most strong lines of the disk spectrum; values much below the CA-derived boundary values for T_e.
   b. The persistence to great heights of a significant population of the second quantum level of hydrogen.
2. High-excitation indicators:
   a. The presence of HE I 10830 in the disk spectrum, and of lines of He I and He II in the eclipse spectrum as low as 1300 km above the limb.
   b. The intensity in the continuum, on the disk, in the rocket UV and in the radio regions.
   c. The presence of highly-ionized elements in the eclipse spectrum, and in the rocket UV spectrum of disk and limb.
3. Mixed:
   The self-reversed emission cores of Ca^+ and Mg^+ in the disk spectrum coupled with the low values of T_{ex}; the absence of such emission cores in hydrogen Balmer lines and in other strong lines; self-reversed emission lines for hydrogen Lyman [and possibly

other strong] lines in rocket UV disk spectrum.

C. Basic Conceptual Anomalies

1. The presence of a wide variety of emission lines in the solar rocket UV disk spectrum.
2. Evidence for a continuous outward mass flow from the sun.

REMARKS

I have deliberately omitted features of the "non-quiet" sun, and associated high-energy phenomena, to remain in keeping with the "steady-state" restriction of this meeting. Such an attitude may well be as subject to the same criticism that has been directed to the attitude that holds too strongly to an attempt to retain the CA model, which I have criticized here. But, I adopt it.

At first sight, some items in the categories A-C might equally well, or even better, be placed in another. For example: emission lines is placed in C rather than in B; the magnetic-correlation item (A3) is in A rather than in B. But consider the logic of the categories.

In category A, I tried to group those features bearing directly--either diagnostically or causally--with the atmospheric extent. Thus all material relating to velocity fields comes there, regardless of whether the velocity field is implied to extend the atmosphere by a momentum action, as in a flow field or "turbulence," or whether it might be, or might produce, a thermal field. I include item A3 here because, although there have been suggestions in the literature that the magnetic field somehow directly modifies the source function, it seems much more likely that it affects the velocity fields present--either macroscopic or thermal--and the energy dissipation from them.

In category B, I tried to group those features giving direct empirical evidence on the excitation--when properly intepreted, of course. The point of using the term "symbiotic" is that it describes very aptly what we have in such an atmosphere. There is a competition between the processes controlled by radiative effects--the photospheric radiation field corresponding to RE and the radiative transfer effects of the boundary--and those processes introduced by the mechanical dissipation of energy.

In category C, I have placed those features which, when present in stellar spectra, immediately suggest the presence of chromospheres and coronae, simply by their presence. The inference is not completely certain; some further criteria are required. But their presence stands as a stimulating and embarrassing beacon into our inquiry as to the adequacy of the CA model for any particular star. Embarrassing, because on a literal CA model, they cannot exist; stimulating, because of the attempts to see how little of the CA structure can be changed to accomodate them.

In a broad sense, we have now two questions to answer. (1) What can we say about the broad array of data, suggesting anomalies, that exists for stellar chromospheres-coronae? (2) In what ways are we trying to make these data more coherent for the solar case, in order to make the solar picture more quantitatively detailed; and how is this applicable to the stellar situation, again in the broad sense? Consider these in turn; my remarks on the first need only be a summary, drawing on the material already presented by Francoise Praderie.

THE EXTENDED STELLAR ATMOSPHERE

A. "Apparent" Structural Anomalies

1. Overall extent of the atmosphere:
   Apparent density gradient inferred from transmission characteristics of the eclipsing atmosphere in binaries.
   "Cool" atmospheres such as ζ Aur, 31 Cyg.
   "Hot" atmospheres such as V444 Cyg.
   Differential size of continuum-emitting, and line-emitting, atmosphere, from interferometric studies.
2. Macroscopic velocity fields:
   a. Curve-of-growth studies:
      Large "turbulent" velocities, some superthermic, from data on supergiants.
      Superthermic relative to a temperature derived from CA-theory or CA-interpretation.
      "Turbulent" velocities from curve-of-growth eclipse studies.
   b. Line-profile studies:
      Large "turbulence" values necessary to match line-profiles.

c. Evidence on systematic flow fields from line-displacements, either from element to element, or between emission and absorption components. Visual and rocket UV.

B. Symbiotic Excitation Anomalies

1. Low-excitation indicators:
   a. Low residual intensities, or low values of T_{ex}, in strong spectral lines, relative to T_e inferred from continuum.
   b. Apparent indications of anomalously high number of second-quantum level population of hydrogen.
2. High-excitation indicators:
   a. Presence of λ10830 of He I in cool stars.
   b. UV and IR excesses in certain spectral classes, especially in supergiants.
   c. The Russell-Adams effect.
   d. A higher ionization and excitation level in the line spectrum than in the continuum.
3. Mixed:
   a. All the features of the "standard" symbiotic stars.
   b. The self-reversed emission cores of Ca^+ H and K; in addition, there are other lines that seem to show such self-reversal.
   c. The appearance of He I emission lines in the carbon, cool star R Cor Bor.

C. Basic Conceptual Anomalies

1. The presence of emission lines generally, both in the visual and in the rocket UV.
2. Evidence, in some stars, of a continuous outward mass flow.

When we compare the two tabulations for the solar and the stellar cases, we are struck by the similarities of "anomalous phenomena." When we discuss interpretations, we are struck by the repetition of the "inertia" encountered in the early days of solar work now in the stellar case. Consider the kinds of attempts being made to clarify the above anomalies, with respect to these two points of similarity. Again, I would stress that all these considerations are based on similarity of general problem--the evidence that a mechanical dissipation of energy produces an outward rise in

T_e--not on any required identity of details of mechanical energy supply.

RESOLUTION AND INTERPRETATION OF ANOMALOUS FEATURES

1. Distribution of T_e

We have remarked, at the outset, the generally accepted interpretation of a chromosphere-corona today is an outer extended atmosphere arising because of an outward increase in T_e, coming from a mechanical dissipation of energy. So, a primary problem is to establish, for any given star, whether T_e does indeed increase outward, and the details of its distribution.

a. Empirical

For the sun, we still do not have a complete specification of the value of T_e [min] and the details of its behavior in this region. A great deal of effort is being devoted to the problem. Some aspects can be duplicated in the stellar case.

From the Continuum. In those spectral regions where τ_ν does not reach 1 near T_e [min], limb-darkening studies are required for precise work. Eclipse studies are required, generally, to go far into the atmosphere, except in those spectral regions of great opacity, such as the rocket UV and the radio region. For intermediate regions, where $\tau_\nu \sim 1$ does correspond to T_e [min], such as is--apparently--the case in the submm region and that near $\lambda \sim 1200$A, unresolved disk studies can be used in a scheme of successive approximation. All these procedures can be followed in the solar case; presently the most fruitful lines of further effort appear to lie in higher geometrical resolution studies. In most stellar cases, we are confined to integrated-disk results. So, one is forced to use $F[\lambda]$ rather than $I_\lambda[\mu]$, and an iterative scheme. But indications of stars having both UV and IR excesses already suggest, as in the solar case, the presence of an outward rise in T_e as the simplest explanation. Extending observations to the rocket UV, and farther into the mm and radio regions, increases the supply of data. For two classes of stars, we gain additional information, of the limb-darkening type. One class is the eclipsing binaries, for which change in spectral features during ingress and egress can be studied. A second class consists of those stars for which the new refinements in interferometry can be applied (e.g., Hanbury Brown 1968).

From the lines. The interpretation of such lines as Ca^+ H and K, the Mg^+ lines, the Balmer lines of hydrogen, the Lyman lines of hydrogen, and the NaD lines are more and more discussed in the literature. Difficulties still appear to exist equally in obtaining very high resolution profiles for the stellar case, and being absolutely sure of the details of the theory for both solar and stellar cases. Here, the solar case--where good spectral resolution exists--provides absolutely invaluable "calibration" of the theory against a solar model coming from the continuum. The self-reversed emission core of, e.g., Ca^+ now seems universally accepted as an indicator of the presence of a chromosphere--for, say, the period of the last 12 years. It is however not quite so clear how we interpret the details of the K_2 and H_2 regions outside the emission cores in terms of T_e [min]. In addition to those complications arising because the observed profiles represent the integral over sizeable portions of the disk, more problems arise in the theory: the accuracy of the assumption of complete redistribution for scattering, the problem of line broadening (which couples this problem of the T_e distribution to that of velocity fields), and the question of interlocking with other levels. All these are theoretical problems, but their solution clearly underlies the empirical analysis. And equally clearly, they are the same problem for sun and stars, so that solar and stellar investigations can hardly be separated.

b. Theoretical

We have already remarked on those theoretical aspects underlying the diagnostic spectroscopy here; consider those aspects dealing with theoretical model atmospheres.

One aspect is the problem placed into focus by Cayrel (1963) for the sun, but of long-standing for the planetary nebulae: the balance between quantity and quality of radiation in fixing T_e, and the question of getting some nontrivial outward rise in T_e due to it alone. Clearly, such a rise could introduce confusion in deciding on the presence of a chromosphere. So, the problem must be completely clarified; it is not so, at present (cf. Jordan 1969a, 1969b).

A second aspect is the T_e-distribution arising from the mechanical heating. I do not propose here to summarize all the aspects of the problem, aerodynamical and astronomical. One recent summary for the solar case lies in Jordan's thesis. The papers

by Lighthill and Moore in the 1965 Cosmical Gas Dynamics Symposium focus attention on the problem of whether the particular acoustic heating in the sun arises in the convective, or in the overshoot, region of the solar atmosphere--a most important concept in extending solar thinking to the stellar case.

Again, I hope it is clear to you that the solar case can be utilized as a guide to stellar problems. More often than not, we are trying to extend to the astronomical environment, or develop completely afresh, physical ideas for which the theory is complex and for which we have only little intuition. The solar case provides a useful testing ground because of the wealth of geometrical and spectral resolution.

2. Velocity Fields

We have four main interrelated questions we need to answer on velocity fields. (a) How to separate thermal from macroscopic velocity fields? (b) How to separate the effects of increased kinetic temperature, and of momentum input causing departure from HE, on the atmospheric extent? (c) How to separate the required velocity field from radiation transfer effects in line-broadening mechanisms? (d) What is the origin and aerodynamic behavior of velocity fields?

Questions (a) and (c) overlap in their concern with specifying just what random, macroscopic velocity field must be introduced in addition to the thermal field. If we already knew the thermal field--as is the a priori assumption in the CA approach, or as we might possibly learn if we could get a complete atmospheric model from the preceding point (1)--it would be easier to infer the macroscopic field. Also, in principle, the separation of thermal and random macroscopic fields should be straightforward because of the differential mass dependence. Unfortunately there are two severely complicating factors: radiation transfer effects, and the effects of atmospheric inhomogeneities. Examples of each of these, for the sun, lie in Redman's [1942] attempts to use eclipse profiles of hydrogen, helium, and metals to infer T_e; and early attempts to identify the yellow coronal line by comparison of its width with that of known coronal iron lines (cf., the summary by Billings 1966). We have already commented on the coupling between un-

certainties in line-formation theory and derived velocities, even under the non-LTE approach. The LTE approach gives too shallow lines, hence interpretation of observed line profiles or equivalent widths by an LTE diagnostics gives spurious microturbulent velocities. So we need to pay careful attention to comparison between theory and observation in a known atmosphere before we can be certain of results on an unknown atmosphere. We note that certain stellar eclipsing binaries provide line profiles and equivalent widths that change during the course of the eclipse, and so can presumably be used in a way similar to solar studies. Groth will be reviewing one aspect of this, at this symposium. Kuhi has summarized the situation for the WR stars (1968). So we can advance our knowledge of stellar chromospheres in this respect, by obtaining better observations, and devoting attention to the interpretive problems I have just summarized.

Items (a) and (b) overlap in their concern with what fixes the density gradient of the atmosphere. The problem couples closely to that of specifying the excitation state of the atmosphere, as a function of height. Again, the solar studies provide a useful guide.

Item (d) is almost wholly a theoretical problem at the present time, using as a boundary condition the mechanical energy and momentum supply required to satisfy the results of aspect (1) and (a)-(c) above. Although considerable work has been done on solar-type chromosphere-coronal aerodynamics, much more remains to be done. And the field is essentially virgin on most other chromosphere-coronal types. For example, although much has been done on the aerodynamics of the nonatmospheric regions of cepheids, the atmosphere has thus far been treated in only cursory detail. Possibly Hillendahl's remarks later in the session will cause this comment to be revised.

3. Inhomogeneities, With and Without Magnetic Fields

I do not intend to comment in any way on this most important point, except to say that the only direct information we have, comes from solar studies based on resolution of the disk. Possibly stellar eclipse studies can somehow be interpreted to give indirect information; certainly, we have evidence that the atmospheres are not spherically symmetric.

So what we need are ingenious ideas for empirical inference; or theoretical generalization from experience with the solar case.

4. Excitation Anomalies

There is a temptation to spend a great deal of time on this subject; indeed, I would like to see several days devoted to it. Clearly, to map out excitation stratification effects we need a detailed study of line profiles, studies of lines of different regions of origin in the atmosphere, and stellar eclipse studies. Again, I refer you to the evolution of our thinking on the solar chromosphere as the best example of how an apparently complex situation can be untangled (even though I would be the last to claim that we have done so, in detail, as yet). And I refer you to the WR atmosphere, as the best example of a situation where we cannot yet agree completely on the direction of change of excitation with height in the atmosphere, in more than an overall way. So I think it best to simply say: Consider the excitation problem, in all its aspects, observational and theoretical, when we ask what we can do to know more about stellar chromospheres and coronae. And I would emphasize very heavily any stellar spectrum that shows symbiotic effects as a strong candidate for having a chromosphere-corona.

5. Basic Conceptual Anomalies

In a discussion of a number of points above, we emphasized how to pin down the details of the chromosphere-corona. At the present time, in the great majority of the stellar situations, our first problem is simply to identify which star falls into the extended-atmosphere class, and then of these, which have chromospheres-coronae. Thus, we would like to develop some criteria, based on outstanding features that would help this identification. In the last sentence of (4) above, I suggested that symbiotic spectral features might well be one such criterion. This is a conjecture. Certainly, stars with chromospheres-coronae exhibit some symbiotic features; it is not clear that the converse is true, that all symbiotic stars have chromospheres-coronae. The problem remains to be investigated.

In just this category fall those features that I have labelled basic conceptual anomalies. We know

that stars with chromospheres-coronae exhibit emission lines, and probably exhibit a steady-state mass-loss. The basic properties of each of these two phenomena are directly tied to a high-temperature outer atmosphere. The question is, can we apply the converse, and use these two phenomena as indicators of chromospheres-coronae.

Consider the emission lines. We must distinguish between intrinsic emission lines, and those arising wholly from a geometrical effect--a situation where the opacity in the lines so greatly exceeds that in the continuum over a much larger disk that an emission line results. Then we would first need a method to distinguish an intrinsic emission line from a geometrically induced one. Next, we would need to determine whether intrinsic emission lines come only from a reversal of a T_e-gradient, a chromosphere-corona. We know that in certain situations, fluorescence processes can produce emission; Anne Underhill has discussed examples of these. So we would need a means for discarding such fluorescent-produced lines. Then we are left with the Schuster mechanism which, in the literature, seems to be the favored mechanism, especially among those trying to retain the CA model. Katharine Gebbie and I think we have shown this mechanism can be rejected, in all but exceptionally unlikely cases, in stellar atmospheres (1968). So, we are left to devise methods for distinguishing between intrinsic and "geometrical" emission lines. One approach to this has been described by us some years ago (C. Pecker-Wimel and Thomas 1963); the group under Rense at the University of Colorado has been testing its utility in the solar rocket UV spectrum. Mrs. Gebbie and I are continuing with this problem of trying to decide the use of emission lines as an a priori chromosphere indicator. You have heard from Rybicki of the work by him and Hummer on investigations of the properties of intrinsic emission lines, which can be adapted to chromospheric situations. A number of people in JILA have been working on these problems including, beside Hummer, Mrs. Gebbie, and myself, Castor, Paczynski, Lindsey Smith, van Blerkom. By the time this symposium is over, you will have heard from, or about, a number of other workers elsewhere. Again, reference should be made to Françoise Praderie's summary.

Consider the steady-state mass loss. The physics of the problem are summarized in Parker's book (1963). Again, we see the utility of the solar-stellar comparison. The recent observations of

supergiants (Morton 1967; Stecher and West 1968) exhibiting evidence of expansion in the rocket UV but not in the visual--thus implying stratification of velocity field--coupled with the observed suggestion of UV and IR excesses in the continuum present the kind of observational situation we face. Clearly, the point is to try to put all these observations together into a coherent picture, in the same kind of way Delache has tried for the sun. Again, we come together with Françoise Praderie's summary.

I hope, therefore, I have made clear to you why I believe the best answer to the question: What can we do to know more about stellar chromospheres and coronae lies in continuing this parallel investigation of stellar and solar situation--depending upon the solar studies for high resolution of detail in one specific situation, and upon stellar studies for extrapolating and expanding the varieties of possible causes and configurations of chromospheres-coronae.

REFERENCES

Billings, D. E. 1966, *A Guide to the Solar Corona*, Academic Press.

Cayrel, R. 1963, *Cr. Ac. Sci. Paris*, 257, 3309.

Gebbie, K. B. and Thomas, R. N. 1968, *Ap. J.* 154, 285.

Gebbie, K. B. and Thomas, R. N. 1968, *Proceedings of the Symposium on Wolf-Rayet Stars*, National Bureau of Standards Special Publication 307.

Hanbury Brown, R. 1968, in Gebbie, K. B. and Thomas, R. N., *Proceedings of the Symposium on Wolf-Rayet Stars*, National Bureau of Standards Special Publication 307, p. 79.

IAU, 1957, *Joint Discussion on Turbulence in STellar Atmospheres*, Transactions of the IAU, 1955, IX, 727, Cambridge University Press.

Jordan, S. D. 1969a, in press, *Ap. J.*, 1969b, in press, *Ap. J.*, 1968, Thesis, University of Colorado.

Kuhi, L. V. 1968, in Gebbie, K. B. and Thomas, R. N., *Proceedings of the Symposium on Wolf-Rayet Stars*, National Bureau of Standards Special Publication 307, p. 103.

Morton, D. C. 1967, *Ap. J.* 147, 1017.

Parker, E. N. 1963, *Interplanetary Dynamical Processes*, Interscience Publishers.

Pecker-Wimel, C. and Thomas, R. N. 1963, *Ap. J.* 137, 967.
Redman, R. O. 1942, *MNRAS* 102, 134.
Stecher, T. P. and West, D. K. 1968, in Gebbie, K. B. and Thomas, R. N., *Proceedings of the Symposium on Wolf-Rayet Stars*, National Bureau of Standards Special Publication 307, p. 65.
Thomas, R. N. 1948, *Ap. J.* 108, 130.
Thomas, R. N. 1961, *Proceedings of the Fourth Symposium on Cosmical Gas Dynamics*, Supp. to Nuovo Cimento XXII.
Thomas, R. N. and Athay, R. G. 1961, *Physics of the Solar Chromsophere*, Interscience Publishers.
Thomas, R. N. 1967, *Proceedings of the Fifth Symposium on Cosmical Gas Dynamics*, Academic Press.

DISCUSSION

Hillendahl: For γ Boo (period 6^h) one would expect the K line emission to change with a "period" of about 1^h. This will be explained in my talk later.

Praderie: We observed this star with an exposure time of 3^m at intervals of half an hour. With this high time resolution we found that the Ca II changes sometimes, but not periodically.

Underhill: Can we find from the spectral lines available for analysis in stars of type A and earlier clear indications for an increase of temperature by a significant factor, that is 1.5 times or larger? I doubt it. Consequently it seems to me we have no need for the early type stars to think in terms of chromospheres with a large difference between temperature in the photosphere and the chromosphere.

You have mentioned the often quoted remark that the velocity of outward motion is larger for ions of higher ionization potential in P Cygni stars. This remark is without sound observational basis. In a study of P Cygni to appear in BAN Vol. 20 M. de Groot shows that the clearest monotonic relation is obtained by plotting the expansion velocity versus (IP + EP). The meaning of this empirical relationship cannot be deduced satisfactorily by any simple theoretical considerations.

Thomas: I would like to call your attention to the proceedings of a symposium of Wolf-Rayet stars held at Boulder in 1968 (NBS Special Publication 307, 1968). One of its aims was to consider that the atmospheres of these stars are simply chromospheres.

Praderie: The observation of P Cygni profiles in the UV spectrum of early type stars does show a dependence of expansion velocity on ionization potential.

Underhill: The UV observations are not sufficient to permit such a general conclusion.

Hearn: In the solar spectrum or in the spectrum of late type stars, the observation of He I λ10830 in absorption is a clear indication of a chromosphere. But for early type stars special conditions are indicated only if this line appears in emission.

Athay: It is important in discussing stellar chromospheres to remember that a chromosphere represents some type of equilibrium between a mechanical energy input and an energy output, most probably radiative. The temperature structure of a chromosphere will depend on both input and output. The temperature of the solar chromosphere is determined largely by the fact that hydrogen is an efficient radiator at temperatures a few thousand degrees above the photospheric temperature. In early type stars hydrogen is highly ionized and no longer an efficient radiator. Thus a given mechanical energy input will produce a chromosphere that differs greatly in its general properties from the solar chromosphere. It is possible that even small amounts of mechanical energy could produce important chromospheric phenomena in such stars.

Osterbrock: Observations in the near UV have contributed much to our knowledge of the solar chromosphere. I would like to call attention to the OAO UV measurements made by the University of Wisconsin group. They now have results extending down to about 1500A for over 100 stars, including several late type stars, and though the resolution is low it seems likely, that these observations will be very useful in trying to understand stellar chromospheres.

Skumanich: Observations show a change of the Ca II emission line of 61 Cyg in an interval of 5 years.

Meyer: In the case of the sun a combination of magnetic fields and shock waves is a sufficient mechanism to produce the heating of the chromosphere and corona. If there are similar magnetic fields

in stars this mechanism could be applied.

Hillendahl: There is a thesis by D. M. Pyper on magnetic A-type stars. She gets indications for shock waves.

Hearn: Are there serious arguments against the hypothesis that all stars or most stars have chromospheres?

Thomas: We do know that the sun has a chromosphere, which is produced by the mechanical energy of the convection zone. We further know that all late type stars do have convection zones. Heating of chromospheres by mechanical energy is the only known process. We don't know a specific heating mechanism for early type stars, but that doesn't mean one doesn't exist. Personally, I have pushed studies of aerodynamic phenomena in all stellar atmospheres simply to try to identify such mechanical heating mechanisms; I have always argued that we must be prepared for chromospheres in all stars--but we must find the specific source of their energy supply.

OBSERVATIONS OF ζ AURIGAE STARS AND THEIR INTERPRETATION

by

H. G. Groth

Universitäts-Sternwarte Munchen
Institut für Astronomie und Astrophysik

ABSTRACT

A summary of information on the extended atmosphere of the K component coming from three eclipsing binaries consisting of a K supergiant and a main sequence B star. Various anomalies exist: (1) Discrepancy between electron density and metallic density inferred from observations, noting that the electrons should come from the metals. This suggests a cloud structure in the atmosphere. (2) Anomalous excitation temperatures and populations of the second quantum level of hydrogen suggests a solar-chromosphere type behavior for these K atmospheres. (3) Significant changes in the profiles of the Ca^+ lines from one eclipse to another. The necessity to distinguish between effects coming from radiation of the B star on the K atmosphere and chromospheric-like effects is emphasized.

Key words: chromosphere, super-excitation, Russell-Adams effect, chromospheric clouds.

It is very difficult to get direct information about the outermost layers of stars other than the sun. The information comes mainly from spectral pecularities and the absorption or emission in the centers of strong lines. But there is a group of stars that permits us to make detailed analysis of the extended outer atmospheres of a few late type supergiants. These are the eclipsing and spectroscopic binaries with long period (972^d - 3800^d). I shall discuss three of them: ζ Aur, 31 Cyg, and

32 Cyg. Each system consists of a K type supergiant (K3 - K5 Ib) and a main sequence B star (B3-B8 V). The diameter of the B type component is small compared with the dimensions of the extended atmospheres of the K supergiants. Both components show equal intensity near λ 4000, so that outside eclipse the spectrum is the sum of a K and a B type spectrum. Some time before or after the total eclipse of the B star by the K star, the light of the B star is absorbed in the chromosphere (the outer layers of the atmosphere) of the K supergiant. These additional absorption lines have been observed and analysed by several authors at different heights above the "limb" of the star, giving valuable information of the physical state of these layers (see, i.e., O. C. Wilson 1960).

But in spite of a long series of observational results and great effort in the analysis of the observations in the last thirty years, there is no satisfactory interpretation.

At a first glance the problem seems to be quite simple. There is a light source and some absorbing material, a nearly ideal situation for spectroscopic analysis. But unfortunately a B star is a very hot light source and the separation of the two components is not very large. For ζ Aur the mean separation of the K star and the B star is only three times the radius of the K component. As a consequence we must expect an influence of the B radiation on the K atmosphere, and so we get into trouble.

What information can we get from the observations? If we measure the chromospheric part of the absorption, we can derive the number of atoms and its gradient for different elements in a column across the chromosphere by using the curve-of-growth method for pure absorption. By assuming spherical symmetry it is easy to calculate the number density from the solution of an Abel-type integral equation. If the assumption of spherical symmetry is correct, we have the number of atoms per cm^3 and its dependence on height, that is on the distance from the limb of the K star, for some atoms: Hydrogen (Balmer quanta), Ca II, Ca I, (Fe II), Fe I, Ti II, Ti I, and others. From the curve-of-growth analysis we have in addition excitation temperatures, which are of the order of 4000 to 4500°K. Some authors have deduced an increasing temperature with increasing height. The microturbulence comes out to be 10-20 km/sec.

If we employ normal abundance ratios of the metals to hydrogen, we get a total hydrogen density of 10^{10} atoms/cm^3 at a height of 4×10^6 km above

the limb for ζ Aur. The decrease of density can be described by an exponential law.

$$N = N_o \cdot e^{-\alpha h}$$

with α of the order of a few times $10^{-7}km^{-1}$.

All authors agree (for all three stars) that the radiation of the B star is not able to ionize hydrogen in the K chromosphere. Some detailed calculations by Mr. Pöllitsch of our Institute have shown for the system ζ Aur that the Strömgren limit would be in the atmosphere of the B component. We should expect to have only neutral hydrogen in the K type atmosphere and as a consequence all electrons would come from the metals. In the case of the first ionisation of the metals (5-8 eV) we can neglect the optical dilution and take only pure geometrical dilution of the B radiation (the dilution factor is of the order of 10^{-6} to 10^{-7}). We can use a modified Saha equation and calculate the electron density assuming an appropriate temperature for the B star. We find that the local temperature calculated from the diluted B radiation is approximately the same as the excitation temperature derived by the curve-of-growth method.

Using the Saha equation for the metallic ionisation, we are surprised to find a very large electron density of 10^9-10^{10} per cm^3, the number of metallic atoms being of the order of 10^6 per cm^3. With the hydrogen completely neutral we must come to the conclusion that the material in the chromosphere of the K star must be concentrated in clouds that have a density 10^3-10^4 times larger than we calculated for a smooth density distribution. The number of clouds in the line of sight must be large enough to produce rather small density fluctuations. There are observations that show some fluctuations especially in the K line of Ca II. It seems that we can explain the ionisation of metals by the radiation of the B star, if we propose a cloudy structure for the K atmosphere. In this connection, there is only a problem with the second ionisation of calcium which has an ionisation potential of 11.8 eV. A larger number of Ca III atoms could be formed than has been considered, but this is of minor importance here.

The main question and, in my opinion, the key for the whole problem is the excitation of the Balmer lines.

From the observed number of metallic atoms, assuming normal abundances, we get the total number of hydrogen atoms. We observe the Balmer lines in absorption and get the number of atoms in the second state. Using the normal Boltzmann equation, we find in any case a temperature of 6000-7000°K for the excitation of hydrogen, which is considerably higher than the excitation temperature of the metals. The Lyα radiation is responsible for the population of the second state of hydrogen. To get enough Lyα quanta for the observed Balmer lines we have to consider several possibilities:

1. Direct Lyα radiation from the B star.
   a. If the Lyα line is an absorption feature, the number of Lyα quanta is too small unless the star has a temperature of the order of 100,000°K.
   b. If Lyα shows up in emission, there could be enough quanta coming from the B star itself, but we do not know how strong the Lyα radiation of a main sequence B star can be.
2. Lyα quanta coming from the H II zone around the B star. It is very difficult to calculate the Lyα radiation field in this geometrically very complicated case. If the H II zone ends up in the B atmosphere we have case 1b.
3. Increase of temperature in the K chromosphere, that means a transition from chromosphere to corona as in the case of the sun.

The most favourable possibilities are cases 2 and 3. If we have an H II zone around the B star, there would be a transfer of Ly continuum radiation to Lyα radiation in a manner similar to the cascade processes which occur in diffuse nebulae. Any Ly continuum quantum can end up as a Lyα quantum, so these quanta can be available in a considerable number for the excitation of the second state in the chromosphere.

But when considering this process we must remember:

1. the ionisation is going on during the whole orbital period.
2. long wavelength quanta are also produced which should be observed as emission components in the Balmer lines, especially Hα.

In this connection it is important to mention that the orbits of all stars are very eccentric. For ζ Aur the eccentricity is 0.4. If there was a considerable amount of emission from the H II zone

around the B star, this emission should show a periodic change, because the density of the material must change with the orbital period. It would be very interesting to observe Hα and other Balmer lines during the whole orbital period and to look for intensity fluctuations with this period. The amplitude of these intensity changes may be very small, so that I am not quite sure whether the changes would be observable or not.

As mentioned earlier, the high excitation of the second state of hydrogen could be produced in the K chromosphere itself. Wellmann and I tried to calculate this effect which we called "super-excitation," in the case of ζ Aur (P. Wellmann 1939; H. G. Groth 1957). The result was that there must be an increase of temperature with increasing excitation or ionisation potential. For hydrogen excitation and ionisation we found a temperature of approximately 6000°K. The chromosphere of the K supergiant would be in a similar state as the solar chromosphere.

There are three observational effects in favor of this last hypothesis. The first one is the long known Adams-Russell phenomenon which is the fact that the hydrogen lines in all late type supergiants are too strong for the spectral types. This effect can be explained by the superexcitation. For the system of ζ Aur I could show that one-half of all hydrogen atoms that contribute to the formation of the Balmer lines in the K spectrum will be excited in the chromospheric layers.

The second observation is by Odgers and Wright (1964). They showed that far outside eclipse there are considerable changes in the emission and absorption profile of the Ca II K line.

These changes are very similar to the changes of the K line on the solar disk, but the scale must be much larger. I would be quite surprised if these changes could be explained as an effect of B star radiation.

The third effect that shows changes in the K chromosphere is the different extent of the chromosphere. The height at which the first trace of chromospheric absorption of the K line has been observed changes by nearly a factor 3. For ζ Aur this normally happens 10-12^d before the beginning or after the end of total eclipse. Sometimes the first trace of a Ca II line was observed 40^d from second or third contact, sometimes the beginning was between these extremes. The chromosphere is not necessarily symmetrical: the extent can be different

at ingress and egress. A relation of these changes with the period of the system has not been found.

Summarising I can say there are some effects that show that the outermost atmosphere of the K supergiants can have a structure similar to that of the solar chromosphere and perhaps the solar corona. The influence of the ultraviolet radiation of the B star cannot be completely neglected.

In my opinion two independent studies are necessary. The first is for the theoreticans, namely to study the ionisation effects of the diluted B radiation in detail and in addition to study the non-LTE effects in the atmospheres of K supergiants.

The second task is the spectroscopic observation of Balmer lines and the Ca II K line during the whole period and further observations of chromospheric eclipses with high dispersion.

REFERENCES

Groth, H. G. 1957, *Z. f. Astroph.* 43, 185.

Odgers, G. J., and Wright, K. O. 1964, *DAO Victoria Contr.* 89.

Wellmann, P. 1939, *Veröffentl. d. Universitäts-Sternwarte Babelsberg XII*, 4.

Wilson, O. C. 1960, *Stars and Stellar Systems*, 6, 436 (Compilation of all papers known to 1960).

DISCUSSION

Pecker: Is the apastron close to the eclipse or not? This could be important for effects that depend on the distances.

Groth: For all three stars the total eclipse is very near to the periastron.

Hillendahl: Does the magnitude of the K star change?

Groth: Observations during total eclipse show irregular changes up to $0^m.1$ in the blue.

Hillendahl: Did you use a velocity distribution in the chromosphere or only turbulent velocities?

Groth: I have used only turbulent velocities.

Wellmann: I have tried to represent the observed curve of growth introducing a velocity gradient. But the calculations show that only a very small gradient might be possible. A larger

gradient would change the curve of growth completely.

Thomas: The large turbulence shows that the dissipation of mechanical energy is sufficient to heat the chromosphere. If this works, you are not forced to postulate clouds of high densities.

Groth: If you assume that the source for the high excitation is in the K atmosphere, it is not necessary to have clouds at all. That was already shown by Wellmann (1939) and in my paper (Groth 1957).

Underhill: There exist fluctuations of the intensity of the Ca II K line. I tried to find fluctuations of the intensities of the Fe I lines, but without success.

Groth: The fluctuations of the Ca II intensities are found mainly in the highest layers. These fluctuations may be due to inhomogeneities in the chromosphere of the K type star. The Fe I lines can be observed only near the limb of the K star, where the density fluctuations are very small.

Magnan: Another idea that can be put into the discussion is the possibility of a mechanical heating of the chromosphere of the K star. This could explain the ionisation equilibrium without the assumption of a cloudy atmosphere (Magnan, 1965, *Ann. d'Astrophys.* 28, 512.

Groth: In the paper by P. Wellmann (Veröffentl. d. Universitäts-Sternwarte Babelsberg XII, 4, 1939) it was already shown that the dissipation of the mechanical energy is sufficient to explain the "superexcitation" of the chromosphere of the K type star.

Hillendahl: There is no source for the mechanical energy and no mechanism to transport it to the chromosphere.

Wellmann: The mechanical energy is supported and transported by convection. The large turbulence velocity shows that it can reach the higher layers.

IONIZATION IN NOVA ATMOSPHERES

by

P. Wellmann

Universitäts-Sternwarte München
Institut für Astronomie und Astrophysik

ABSTRACT

Calculations on the expansion of novae shells are presented, from which the degree of ionization is obtained using a simplified form of a non-LTE ionization equation. From this, estimates of the time of vanishing of the Balmer absorption spectrum can be made.

Key words: novae shell, ionization, expansion.

Atmospheres of novae are strictly speaking not in a steady state. However, relaxation effects are not observed before the later nebular stage. Therefore the development of a nova shell may be understood as a sequence of different extended atmospheres of the type discussed in this colloquium.

The nova phenomenon varies considerably in amplitude, time scale, and light curve details, but it is possible to reduce the data to an average nova by using the time t_3 (the interval between maximum brightness and $m_{max} + 3^m.0$) as a time unit. A nova that followed the average rather closely, and which is appropriate for an investigation because the absolute intensities of emission lines were measured, is DK Lac 1950. It will be used here as an example.

During the first phases from 0.1 t_3 to about 6 t_3 the magnitude m of this star was strongly correlated to T_s (radiation temperature) as well as to the spectral type (intensities of absorption and emission lines). Hence it was possible to eliminate the effects of light and temperature fluctuations and of secondary eruptions. We disregard here the dif-

ferent components of the diffuse enhanced spectra and the Orion spectrum because they belong to the secondary processes or originate in masses of gas, which are negligible compared with the main shell.

The principal spectrum showed an increase of radial velocity from about 800 to 1300 km/sec during the absorption line stage and a nearly constant value in the later development. An estimate shows that the observed RV changes cannot be interpreted as accelerations. Instead we have to assume that velocities between certain limits were present all the time, and that the measured line shift is due to a motion of the effective layer of absorption. Each substantial atmospheric element had a constant outward velocity between v_{min} and v_{max}.

The basic model is a shell with radius and geometrical depth increasing linearly with time. Hence the density of each substantial element decreases with r^{-3}, and the velocity field is

$$v(r,t) = r/t-t_o \ ,$$

t_o being the time of the initial magnitude rise.

During the stages with forbidden lines, N_e, the electron density, can be found from the intensities of these lines. According to a well-known theory, we have, for instance, for [O III],

$$\frac{\text{intensity } (N_1 + N_2)}{\text{intensity } (\lambda\ 4363)} = f(N_e, T_e)$$

with a given function f. Unfortunately f has a form that forbids the solution for N_e and T_e of two such equations for different ions, with a reasonable accuracy. However, because of the "thermostatic" action of the forbidden transitions, an electron temperature of about 10000°K during the whole period can be accepted. The corresponding N_e, proportional to N (total density) is well defined and changes as $(t-t_o)^{-3}$. Using the hydrodynamic force equation,

$$\frac{\partial v}{\partial t} + v\,\frac{\partial v}{\partial r} = k \approx 0 \ ,$$

and the equation of continuity,

$$\frac{\partial N}{\partial t} + \frac{1}{r^2}\,\frac{\partial (N\ v\ r^2)}{\partial r} = 0,$$

it is very easy to verify that the observed relations

agree and that the density field is given by

$$N(r,t) = \frac{N_o}{(t-t_o)^2 r} \quad .$$

The principal shell crossed a radius R during an interval of time,

$$\Delta t = R\left(\frac{1}{v_{min}} - \frac{1}{v_{max}}\right)$$

and that gives Δt in the range of 10^1 to 10^2 min, if R is of the order of the solar radius. The corresponding density is of the order of 10^{20} atoms/cm^3. The nova phenomenon started with a short time "explosion" of a layer not very far below the original photosphere.

We return to the problem of the formation of the spectra of different excitation. The computation of the population of atomic or ionic levels from the steady state equations

$$\frac{d\, N(\chi_i)}{d\, t} = 0$$

is rather complicated. So we use the first approximation for the equation of ionization under non-LTE conditions

$$\frac{N^{(n)} N_e}{N^{(n-1)}} = \frac{2\, B^{(n)}}{B^{(n-1)}}\, K\, W\, T_s (T_e)^{1/2} e^{-\chi_n/kT_s} \quad .$$

The dilution factor is $W \sim (R_*/2r)^2 e^{-\tau}$ where τ is the optical depth between the photosphere and a point at distance r. This is to be combined with the definition of $d\tau$

$$d\tau = (1-x)\varepsilon N(r)\, \bar{a}\, dr,$$

where

$$x = N^{(n)}/\Sigma N^{(n)}_n \quad .$$

Here $\bar{a}$ is the absorption coefficient averaged over ν from the series limit to infinity. It is convenient to write $\bar{a} = 0.5\, a(\text{series limit})$, which can be

verified a posteriori. ε is the abundance of the element investigated. This differential equation has been solved numerically for $\tau(r)$ and $x(r)$, using arbitrary $N(r)$. Of course, the Strömgren theory of ionization zones is the special case N = const, $\varepsilon = 1$.

Under certain conditions, which are fulfilled in many cases, x changes rapidly from 1 to 0 at a distance, r_S. These "Strömgren radii," if of finite size, are very sensitive to T_S: a small change in temperature makes r_S jump through the whole main shell and then causes a very quick spectral change with $m(T_S)$. The motion of r_S for hydrogen through the shell explains the width and the radial velocities of the Balmer lines. At first, the whole shell belongs to the H I region, and the lines are very wide (width corresponding to $v_{max} - v_{min}$), with RV $\sim 0.5 (v_{max} + v_{min})$. Since r_S increases faster than r_{max}, the effective center of the absorptions moves to v_{max}, the width becoming normal. When $r_S = r_{max}$, the whole of the shell belongs to the H II region and the Balmer apsorptions vanish from the spectrum. Using T_S from different observations (spectrophotometry of continuum and Zanstra methods) and adjusting the parameter N_O to give the correct absolute intensities of the hydrogen emissions, it was possible to predict the times of disappearance of the He I, O I, N II, [N II] and [O III] emissions sometimes within a few days. The main source of uncertainty is the still inadequate information on T_S.

It can be shown that the condition for a change of spectral type, r_S equal to the average shell radius, is fulfilled for specific T_S, independently of time, if the degree of ionization follows the temperature without delay. Only in the later nebular stage, when the electron density is below the predicted limiting value of $N_e = 10^{7.6}$, a delay of one day or more between temperature changes and the appearance and disappearance of the nebular lines $N_{1,2}$ has been observed.

REFERENCES

Hiller, I. 1965, Thesis, Hamburg.
Wellmann, P. 1951, Zs. f. Ap., 29, 112.

Osterbrock: Are the time-dependent effects of the finite rate of emission of ionizing radiation by the nova important to your problems?

Wellmann: The retardation of the ionization changes did not occur before $4.t_3$, that is in the later nebular stage, and was observed mainly in [O III].

Nussbaumer: I want to give two warnings: (1) Atomic data: Seaton's group has recalculated some of the [O III] collision cross sections. Changes in some of these are important. For all interpretational work where cross sections or oscillator strengths are used it is worthwhile to make sure that you have the latest calculations. (2) Line widths: Combined effects of radial velocities and temperature gradients may influence the line widths considerably. Suppose a radial expansion but unique temperature, then you have the normal Doppler broadening. Now suppose a radial drop in temperature sets in and increases the abundance of your ion. The displaced line component will then be more intense than the undisplaced component. Thus the radial drop in temperature produces a line width that makes you believe in a temperature increase.

Wellmann: Every time Seaton's group has published new values of the cross sections, we have repeated our calculations for the forbidden lines. Fortunately the fundamental result has not changed very much. But there is another difficulty. The relations between N_e and T_e for different forbidden lines should give a unique solution for electron density N_e and electron temperature T_e. But we don't find such a solution. It may be that this effect is due to inaccurate cross sections.

CIRCUMSTELLAR CA II K LINES IN G, K AND M GIANTS AND SUPERGIANTS

by

A. H. Vaughan, Jr., and A. Skumanich

Mt. Wilson and Palomar Observatories
California Institute of Technology and
Carnegie Institute of Washington
Pasadena, California

and

High Altitude Observatory
*National Center for Atmospheric Research**
Boulder, Colorado

ABSTRACT

Tentative evidence, based on photoelectric observations of the Ca^+ emission core, is presented for the existence of circumstellar envelopes in several G and K type "giants." A significant emission asymmetry in α Tau may imply a chromospheric rather than a circumstellar source.

Key words: Ca^+ emission core, circumstellar absorption lines, late-type giants.

We present here a preliminary report of photoelectric scans of the cores of the CaII K line in several giant and supergiant stars. As Deutsch (1960) has pointed out, M "giants" - this term includes supergiants - have K emission cores on which are superimposed circumstellar (CS) lines. These are distinguishable from the K_3 chromospheric core

---

*The National Center for Atmospheric Research is sponsored by the National Science Foundation.

by "their very low central intensities ... and sometimes by their radial velocities as well." We believe that we have evidence for such CS lines in G and K "giants."

In Figures 1, 2, and 3 we present uncorrected scans averaged over several nights' observations of five "giants." We have plotted photon number (for a given count in the neighboring continuum) versus wavelength in arbitrary units (220 units = 1 Å). The instrumental resolution, instrumental half-width at half-maximum, was 0.14 Å (30 units).

The K emission profile is seen to be asymetric in both giants and supergiants. However, only in the supergiants does one find intensities for the "central" absorption feature which fall below the K_1 value. If one reflects the emission core about its bisector (i.e., if one "symmetrizes" the emission core) one obtains the dashed line indicated in the figures.**

The ratio of the observed intensity to that defined by the dashed line yields a measure of the strength of what we interpret as the CS line. These "absorption" depths are indicated in the top of the diagrams. Table 1 summarizes the equivalent width and wavelength shift for these CS lines.

The tabulated equivalent widths agree in magnitude and show the same increase with luminosity

TABLE 1

Star	Sp	W(Å)	-V km/sec	-V(W+B) km/sec
α Tau	K5 III	0.15	20	4
β And	MO III	0.20	21	16
β Peg	M2 II-III	0.31	4	6
ε Gem	G 8 I b	0.65	17	10
ε Peg	K 2 I b	0.47	26	28

** In the case of ε Gem and β Peg the circumstellar line was also symmetrized to obtain the complete dashed curve.

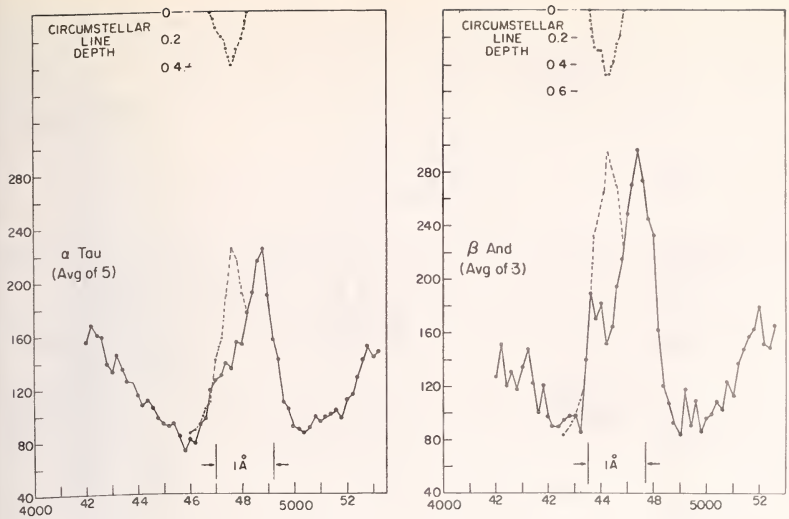

Figure 1. Averaged photoelectric scan of the K emission core (uncorrected for instrumental broadening). Photon count (for a given count in the neighboring continuum) versus scanner setting is represented. Wavelength increases to the right.

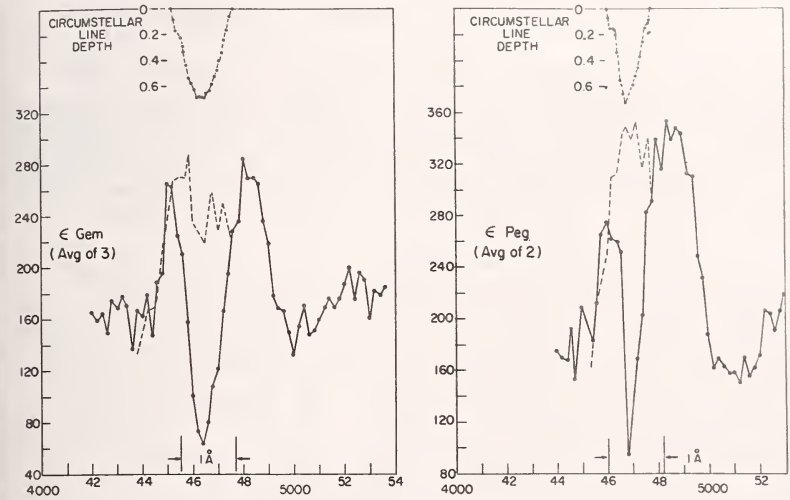

Figure 2. Data similar to Figure 1.

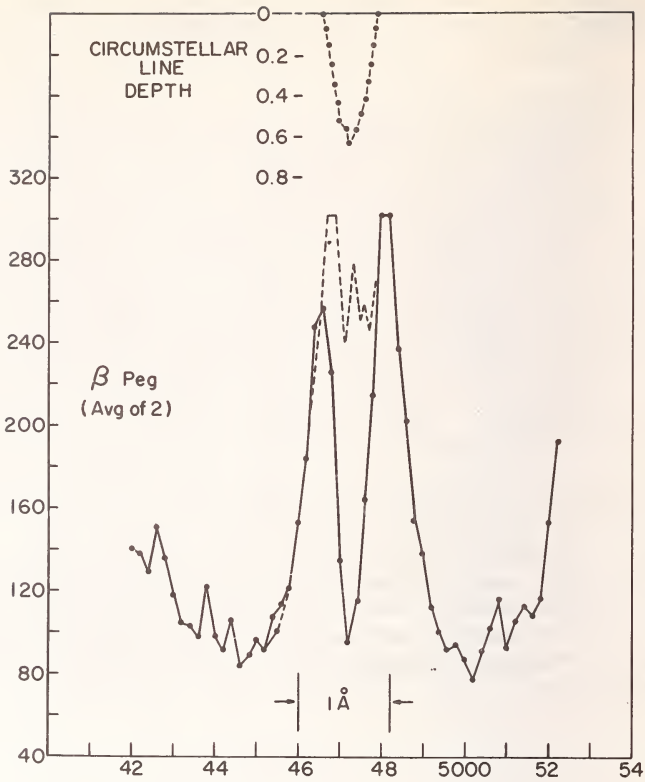

Figure 3. Data similar to Figure 1.

as in the later-type stars, Deutsch (1960). The wavelength shifts (relative to the emission bisector) indicate a nearly constant expansion of ≃ 20 km/sec except for β Peg. For comparison, we have given the shifts measured from spectral plates by Wilson and Bappu (1957). The agreement, except for α Tau, is fairly good.

An alternative explanation for the α Tau profile would be to allow an appreciable velocity gradient through the emission forming layers, cf. Weyman (1963). Such a gradient introduces an asymetry with one side of the K_2 peak reduced (or eliminated) relative to the other, cf. Vaughan (1968) and Hummer and Rybicki (1968). Such an explanation would satisfy the statistical results (based on wavelength shifts) of Wilson (1960) which indicate no mass loss in class III stars earlier than MO. A complicating feature here is the evidence in the individual scans of α Tau of multiple weak dips in the

depressed violet side. This raises the question of the significance of a mean profile. Thus, our results on α Tau should be viewed as tentative and may be changed by the more detailed investigation in progress.

REFERENCES

Deutsch, A. J. 1960, *Stellar Atmospheres: Stars and Stellar Systems, VI*, ed. J. L., Greenstein (Chicago: Univ. of Chicago Press), p. 543.
Hummer, D. G., and Rybicki, G. B. 1968, *Ap. J.*, 153, L107.
Vaughan, A. H., Jr. 1968, *Ap. J.*, 154, 87.
Weyman, R. 1963, *Ann. Rev. Astr. and Ap.*, 1, 97.
Wilson, O. C., and Bappu, M. K. V. 1957, *Ap. J.*, 125, 661.
Wilson, O. C. 1960, *Ap. J.*, 132, 136.

DISCUSSION

Pecker: Is it possible to distinguish between the effects of a chromosphere and those of circumstellar envelopes?

Skumanich: I would prefer an explanation by circumstellar envelopes. This is much simpler and will give a better fit of the line profile. This has already been shown by Deutsch.

Underhill: Have you observed the Na I D-lines by the same technique? If your interpretation of the absorption dips as circumstellar lines is correct, similar dips should be found in Na I, without the additional complication of emission components.

Skumanich: A slight doubling of the Na I D-lines is observed in the spectrum of α Ori; it can be interpreted as a circumstellar effect. In the spectra we have observed the effect is probably too small because the mass of the shell is not large enough. We have not tried to observe the effect.

Wellman: Several years ago I could show that the line doubling in α Ori is due to chromospheric effects.

Skumanich: The doubling of the Na I D-lines should be interpreted by circumstellar clouds. Chromospheric effects tend to wipe out the structure as Hummer has shown.

A PHYSICAL MECHANISM FOR THE GENERATION OF EXTENDED STELLAR ATMOSPHERES*

by

R. W. Hillendahl†

Department of Astronomy
University of California at Berkeley

and

Lockheed Palo Alto Research Laboratory
3251 Hanover Street
Palo Alto, California

ABSTRACT

A physical mechanism that can result in the generation of extended expanding atmospheres is discussed. The process involves the unloading of stellar material following the arrival of a shock wave at the edge of the star. The basic principles are developed from a discussion of a simplified case that has been studied in the laboratory; they are then applied to the atmosphere of a star. A radiation-hydrodynamics computation of a model cepheid is then used to obtain quantitative atmospheric profiles. The computed continuum and spectral lines during the unloading process are then examined. A discussion of the possibility that the unloading process occurs in stars other than cepheids suggests the existence of a shock visibility factor associated with ionization or dissociation in the region behind the shock front and leads to a possible alternate interpretation of the variable star instability strips in the H-R diagram.

Key words: extended atmospheres, shock waves, hydrodynamics, cepheids.

---

*This work was made possible by a grant of computer time made available by the Berkeley Astronomy Department and by a Lockheed Independent Research Grant.

†Now at Lockheed Palo Alto Research Laboratory, 3251 Hanover Street, Palo Alto, California 93404.

INTRODUCTION

Many stars in the upper part of the Hertzsprung-Russell Diagram appear to have extended atmospheres in which an outwardly directed flow of matter is observed. While a number of probable physical causes of this phenomenon have been studied (cf. Weymann[1]), it is clear that our present understanding is far from satisfactory. In the course of a recent study[2] of atmospheric phenomena in classical cepheids, a mechanism was encountered that can cause atmospheric characteristics similar in many respects to those ascribed to some types of these "steady-state extended atmospheres."

It is the purpose of this presentation to discuss the basic concepts associated with this extension mechanism as studied both theoretically and in the laboratory, and then to apply these concepts to stellar atmospheres. Specific results are then given for a model classical cepheid. Finally, it is suggested that the mechanism may not be confined to cepheid atmospheres, but may be of more general applicability. Some of the consequences of this suggestion are then explored.

THE BASIC PHENOMENA

The phenomena to be discussed are associated with the processes that occur when a shock wave progressing through a gaseous medium arrives at an interface between the material and a vacuum. Previous theoretical studies of these phenomena (cf. Bird[3], Sakurai[4]) as they apply to stars have either employed simplifying assumptions or have failed to establish the relationship between the theoretical results and the associated observable characteristics. Recently however, Zel'dovich and Raizer[5] have reviewed both theoretical and laboratory studies of a much simpler configuration, which provide us with a clearer understanding of the dominant processes that occur.

Their studies concern the emergence of a plane-parallel shock front from a solid, for the case in which the strength of the shock wave is sufficient to cause a conversion of the solid into a gaseous state as the shock front advances through the material. As the shock front arrives in the surface layer, the momentum associated with the shock wave causes the surface layer to "blow-off" into the

vacuum. The rapid expansion of this layer of material lowers the pressure in the surface layer and gives rise to an outwardly directed pressure gradient between the surface layer and the next interior layer of material. This newly created pressure gradient then causes the outflow of additional material. This "unloading" process continues into the deeper layers in the form of a rarefaction wave progressing backward into the material, while the unloaded matter itself is accelerated outward in the direction of the initial motion of the shock wave.

The unloading (rarefaction) wave travels backward into the material with the speed of sound that corresponds to the thermodynamic state behind the shock front. Its velocity is directed opposite to and is smaller in magnitude than that of the shock front. If the original extent of material is large, the unloading process can continue for an extended period of time. The duration of this process can therefore be much greater than the time interval associated with the passage of the shock front through the photosphere. Under suitable circumstances, it can resemble a steady state process.

The unloaded material flows outward with a relatively large velocity which is the result of the outward acceleration experienced by the matter in crossing the shock wave and the additional outward acceleration caused by the pressure gradient in the rarefaction wave. The terminal velocity of a given particle after it unloads to (essentially) zero pressure can be calculated by noting that its terminal kinetic energy is equal to the sum of its kinetic and thermal energy prior to its engulfment by the rarefaction wave. For the simplified case of a nearly weak shock emerging from a material having no pressure gradient prior to arrival of the shock, Zel'dovich and Razier[3] obtain the "velocity doubling law," i.e., the terminal velocity of an unloaded particle is twice the velocity imparted to it by acceleration in the shock front. This result is indicative of the importance of the acceleration in the rarefaction wave, but it apparently represents only a special case. The equations for the general case do not limit the velocity increase to a factor of two, and suggest in fact that much larger increases in velocity may occur if ionization or dissociation is occurring within the rarefaction wave.

The passage of the shock front sets the entire mass of material into motion in the direction in which the shock travels. Thus, while the rarefaction

wave moves "inward" in terms of the mass of the material, it and all parts of the material move "outward" with respect to the laboratory frame of reference.

APPLICATION TO STELLAR ATMOSPHERES

While the situation is much more complicated at the edge of a star due to the presence of the pre-existing motion and/or pressure gradients, the basic physical laws that apply to the laboratory situation should still be operative. Thus, when a shock front arrives at the surface of the star, the unloading of stellar material is to be anticipated. It is further to be expected that the unloading process lasts longer and has therefore a higher probability of observation than the passage of the shock through the photospheric layer. This follows because the unloading process involves the motion of a sonic disturbance into an essentially infinite supply of material, while the shock emergence involves the motion of a supersonic disturbance through a relatively narrow photospheric layer.

Neither the outward flow of the unloaded material nor the inward progress of the rarefaction wave can continue indefinitely in a star. The outward moving particles are accelerated to a finite terminal velocity and are subject to the star's gravitational field. Should the terminal velocity exceed the escape velocity, continued outward motion and mass loss could occur. Particles achieving a lesser than escape velocity will reach a maximum altitude and then be accelerated downward. Differential motion should then occur, which under favorable circumstances, might be observable in terms of the shifting and/or asymmetrical contours of spectral lines. Were the material returning under gravitational acceleration to collide with unloading material still in the process of moving outward, a temperature inversion could occur which would result in emission lines.

An interesting phenomenon can also occur in the rarefaction wave as it moves inward in terms of the mass of the star. As has been noted above, the terminal velocity achieved by a given particle in the unloading process is the sum of the velocity achieved due to passage through the shock front and the velocity achieved due to acceleration in the pressure gradient of the rarefaction wave. This

latter acceleration depends primarily upon the thermal energy of the particle prior to the arrival of the rarefaction wave. As this wave progresses deeper into the mass of the star, the temperature and hence the thermal energy increases. Particles in the deeper layers will thus undergo a greater outward acceleration than the particles in layers initially at larger radii. If these particles from successively deeper layers overtake the particles already unloaded, conditions may be favorable for the formation of a secondary shock wave. When the head of the rarefaction wave passes through a region where ionization or dissociation is occurring, a very rapid increase in particle velocity takes place. Conditions for the formation of a secondary shock are therefore most favorable in such regions of the star.

Such a secondary or "blow-off" shock wave would then progress outward through the star in a manner similar to the original shock wave; the blow-off shock should itself be followed by an inward rarefaction wave similar to that which follows the original shock. Thus a shock wave emerging from a stellar atmosphere should be followed by a series of additional shock waves, reasonably well separated in time, until the process becomes the victim of a damping mechanism or is interrupted by the gravitational return of previously unloaded material.

These secondary shock waves provide a possible explanation[2] for multiple and irregular periods that are well known in variable stars (cf. Arp[6], Abt[7]). The frequency with which the secondary shocks might be anticipated would appear to depend upon the instantaneous atmospheric structure of the star, which in turn must ultimately depend upon the structure of the deep interior. However, it is not clear that there exists any direct connection between the interior structure and the periodicity of the secondary shocks, such as, for example, the relationship that defines the fundamental periodicity of a cepheid. Thus, at the present state of our understanding, one cannot assume that the secondary shocks are strictly periodic or that their period is related to the fundamental period of the star.

It should also be noted that the secondary shocks need not be associated with a pulsating star, but may occur in a localized region of any star so long as the diameter of the region from which a shock wave emerges is large compared to the scale height of the atmosphere. For example, the multiple outward waves seen in certain solar disturbances[8] may be related to the secondary shock process, however, it

is not clear in this instance whether or not the magnetic field merely contributes to or actually causes the observed effect.

If spectral absorption lines originate in layers of a star where unloading of material is occurring, the spectroscopic gravity deduced from the analysis of these lines may be significantly lower than the dynamic gravity derived from the mass and radius of the star. This effect results from the lower pressure gradient that occurs everywhere in a rarefaction wave except in the immediate vicinity of the leading edge of the wave, where the pressure gradient is very steep. The unloading process may therefore offer a possible explanation for the low values of spectroscopic gravity associated with stars of the higher luminosity classes. This mechanism can far outweigh the effects of radiation pressure.

THE CLASSICAL CEPHEID AS AN EXAMPLE

The phenomena discussed above are all governed by a well-defined set of physical equations and can therefore be studied in detail. The relevant equations are the familiar equations of stellar structure, but without the restrictive assumption of hydrostatic equilibrium normally used in stellar evolution computations. As is the case for static stellar structure, analytic solutions are made possible by simplifying assumptions, particularly with regard to the equation of state and the opacity. One can deduce general properties from such solutions, but it is difficult to obtain quantitative models for comparison with observation. One therefore resorts to numerical methods, thereby allowing the inclusion of virtually any desired amount of detail in expressing the thermodynamic and optical properties of the gas.

For the present application, a radiation-hydrodynamics code[9,10] written especially for cepheid computations was employed[2]. The code is a one-dimensional, spherical, lagrangian, LTE, transport code employing an augmented[9] gray absorption coefficient. Convection and stellar rotation are not taken into account. The methods used are a generalization of and are patterned directly after the methods of Henyey, et al.[11]

The final results are independent of the choice of the initial configuration so long as the computations are carried far enough in time so as to be-

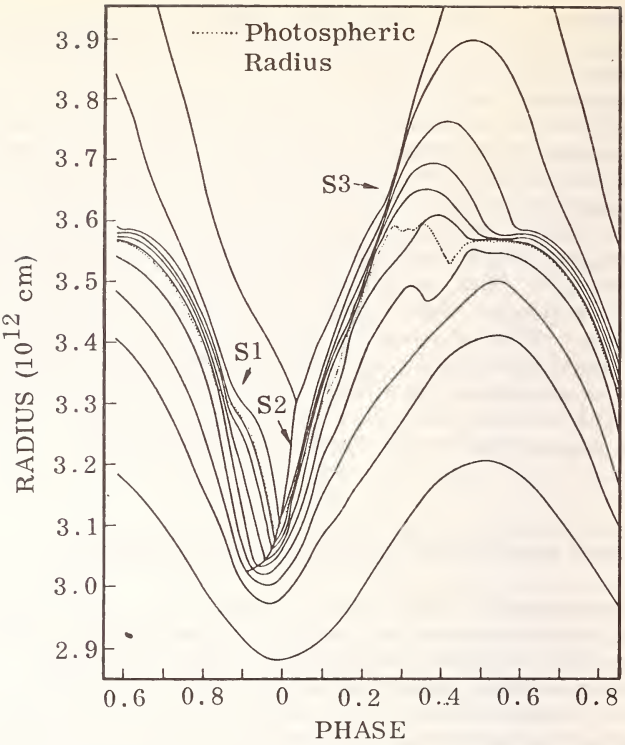

Figure 1. Radius vs time history in the atmosphere layers of a model cepheid.

come reasonably repetitive. The cepheid is therefore an ideal choice for exploratory computations both because the model is relatively free from arbitrary assumptions and because the wealth of available observational data permits a detailed verification of the results. The initial configuration used in present computations consisted of an augmented[2] version of a 7.6-day cepheid model supplied by Christy[12].

In the present context we are interested in the dynamic and optical properties primarily during those phases of the pulsation when unloading occurs. However, for purposes of orientation, Fig. 1 shows the radius versus time history over the entire cycle for every fifth mass point in the computed results. The dotted line represents the photospheric radius. S1 indicates the location of a shock originating in the hydrogen ionization zone which travels inward in terms of radius, but outward in terms of the mass

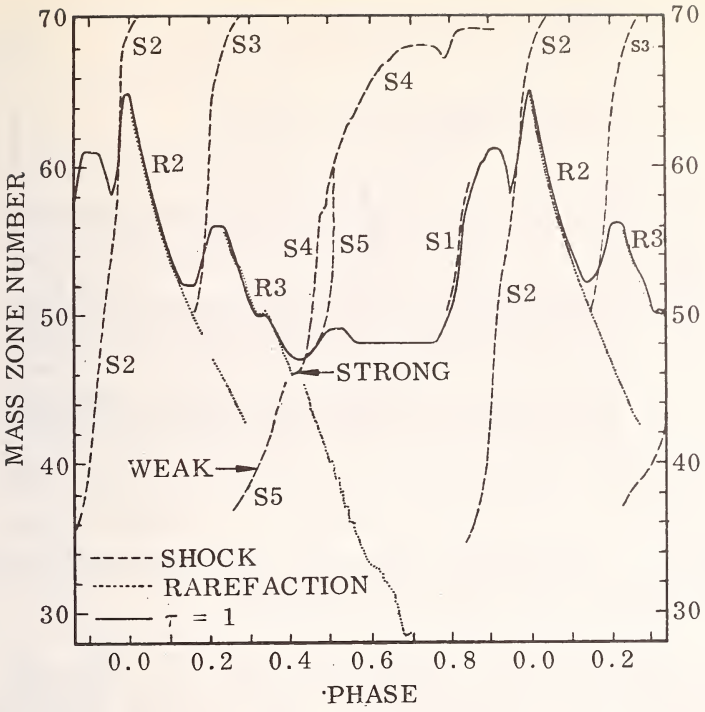

Figure 2. Atmospheric phenomena in a model cepheid.

of the star. This shock causes the bump in the light output during the rise to maximum light, but it is not important to the unloading process. S2 is the primary shock originating in the He II ionization zone which is responsible for the pulsation of the star. It reaches the edge of the star just after maximum light and initiates the unloading process which lasts until a blow-off shock occurs at about phase 0.2.

These events are shown more clearly in Fig. 2 in which the solid line shows the motion of the photosphere throughout the cycle. The short time required for the principal shock S2 to traverse the photosphere, compared to the rarefaction-unloading phase R2, is clearly evident. The process repeats itself as the first blow-off shock S3 traverses the photosphere near phase 0.2 and the resultant rarefaction R3 follows. At about phase 0.35, a bump in the rarefaction R3 can be seen in Fig. 2. This can be identified in Fig. 1 with the reversal of direction

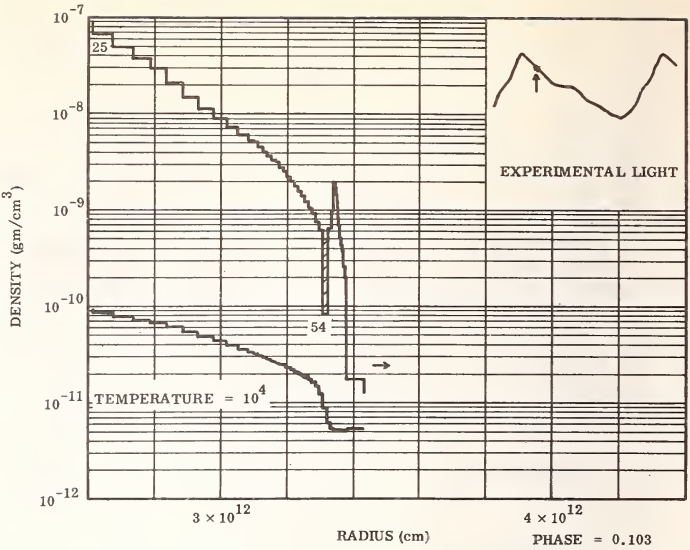

Figure 3. Atmospheric density and temperature profiles during the unloading process.

of the photospheric layers as they reach maximum altitude, and corresponds to the observed secondary maximum in the light output. A second blow-off shock, S4, occurs at phase 0.4, which is soon joined by a reflection S5 of the primary shock off the center of the star. Following this, the atmosphere is characterized by a gravitational collapse. The properties of the model during the rarefaction phase R2 are of primary interest. Fig. 3 shows representative density and temperature profiles during this process. The shaded area serves to locate the photosphere, which occurs at mass zone 54 at this phase. The strange looking density spike is not a shock wave, but is a result of the rarefaction process. As the shock approached the edge of the atmosphere, the rarefaction process had already been initiated in the region behind the shock front. This causes the outward acceleration of material which then overtakes material at larger radii causing a density build-up. The net result is an extended transparent region of relatively high density. The corresponding temperature profile, which has been superposed below the density profile in Fig. 3, shows an extremely steep gradient in the photospheric region, and an extended temperature plateau in the outer atmosphere. The geometrical thickness of this region is approximately

one solar radius at this phase, but becomes almost a factor of 10 larger during the pulsation cycle.

The type of atmospheric profile shown in Fig. 3 results in the emission of a continuum and spectral lines which are different from those which are observed for a hydrostatic atmosphere. Oke[13] has published detailed spectral scanner measurements of the continuum at the appropriate phase (0.1) for the 7.2 day cepheid Eta Aquilae. Six color measurements have also been published by Stebbins, Kron, and Smith[14]. Attempts to match these observations by hydrostatic model atmosphere continua[13,15] have shown that such models cannot be made to fit accurately at both the red and violet extremes of the spectrum.

Using the method of dynamic atmospheres, the author[2] was able to obtain improved correspondence with the observed continuum. This method utilizes a model consisting of a black body source screened by a semi-transparent layer having a given density, temperature, and thickness. The dynamic model fitted to the observations at phase 0.1 consisted of an 8400°K black body screened by a layer of density 10^{-9} gm cm^{-3}, temperature 5500°K, and thickness 1.25×10^{11} cm. The detailed composition of the layer is given in Table 1. The profiles in Fig. 3, from the photospheric layer (zone 54) outward show a close resemblance to this model.

As compared with a hydrostatic atmosphere, the unloading atmosphere has a lower flux in the ultraviolet but has an excess spectral flux near 10,000 A. The extended layer has maximum opacity in the UV and most of the observed radiation is emitted in this layer, while at 10,000 Å the layer is more transparent and most of the radiation originates in the higher temperature photospheric region. The actual spectral continuum computed from the atmospheric profiles given in Fig. 3 agrees qualitatively with the observations, and can be made to agree quantitatively if the temperature in the plateau region is raised about 250°K. The continuum is especially sensitive to this temperature as it determines the population of the Balmer ground state upon which the spectral absorption coefficient is critically dependent.

The absorption lines formed in the atmosphere during the unloading process also show properties that are of interest. Both the unusual temperature and density profiles and the differential motion within the plateau region influence the character of the lines. For a velocity distribution that can be represented analytically, Underhill[16] has demon-

TABLE 1.

DETAILED COMPOSITION AND THERMODYNAMIC PROPERTIES OF DYNAMIC MODEL LAYER FOR ETA AQUILAE AT PHASE 0.1

Total Number Density	4.30×10^{14} /cm^3
Electron Density	3.80×10^{11} /cm^3
HI	3.77×10^{14} /cm^3
HII	3.39×10^{11} /cm^3
H^-	1.76×10^{5} /cm^3
H_2^+	2.44×10^{5} /cm^3
H_2	9.28×10^{8} /cm^3
HeI	5.28×10^{13} /cm^3
HeII	1.63×10^{1} /cm^3
HeIII	———
Metals Composition	GMA
Metals to Hydrogen Ratio	2.0×10^{-3}
Helium to Hydrogen Ratio	0.167
Temperature	5500 °K
Total Pressure	3.289×10^{2} dynes/cm^2
Radiation Pressure	2.3 dynes/cm^2
Gas Pressure	3.266×10^{2} dynes/cm^3
Electron Pressure	0.289 dynes/cm^3
Molecular Weight	1.404 gm/mol
Density	10^{-9} gm/cm^3

strated that a uniformly expanding atmosphere causes the spectral lines to become shallower and broader.

For the present application, a general program was written to accept an arbitrary velocity distribution in the atmosphere. Specific results for selected spectral lines are discussed below. The primary purpose of these calculations is to show the manner in which the dynamic properties of the atmosphere influence the shapes of the spectral lines. No attempt has been made to determine the extent to which these lines agree quantatively with observation.

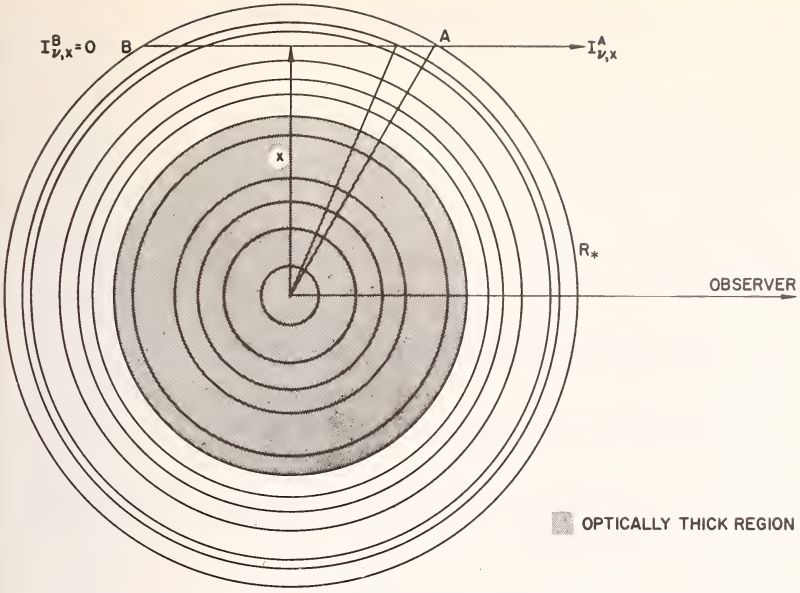

Figure 4. Geometry used in line profile calculations.

Figure 4 shows schematically the instantaneously fixed geometry of a model star consisting of spherical shells of material (70 in the model used here) whose radii, temperatures, densities, and velocities are known from the radiation - hydrodynamics computation. Assuming LTE and a GMA chemical composition, the thermodynamic properties of each shell, including the concentrations of all species, follow from the equation-of-state. The continuum[2] and line absorption[17] coefficients can then be computed directly from the atomic and molecular properties. The Voigt function was evaluated using a routine due to Rybicki[18] while Stark broadening was evaluated using the method of Edmonds, Schulter, and Wells[19].

To obtain the emergent intensity $I^A_{\nu,x}$ for a given radiation frequency, an integration is carried out along a ray path through the star defined by the impact parameter x. Values of x are selected so as to cause the path of integration to bisect each spherical shell as indicated in Fig. 4. The observed flux is then given by

$$F_\nu = 2\,\pi \int_0^{R_*} I^A_{\nu,x}\; x\,dx$$

while the emergent intensity is given by

$$I^{A}_{\nu,x} = \int_{A}^{B} B_{\nu}(\mu z)\, e^{-\mu z}\, d(\mu z)$$

where $\mu = \mu_l + \mu_c$

μ_c = continuum absorption coefficent

μ_l = line absorption coefficient

z = geometrical distance measured along the ray path

B_ν = Planck function.

Since the model results from a radiation-hydrodynamics computation, one is not free to choose the zoning structure so as to maintain a small optical thickness for all of the individual shells of material. The source function is therefore interpolated in optical space[9] to achieve greater accuracy. The radial motion of each shell is reduced to a velocity along the ray path in the evaluation of the line absorption coefficient.

The λ 4508 Å line of Fe II was used as a test line to study the effects of the atmospheric motion upon the line shape. Two computed profiles for this line are shown in Fig. 5. The narrow line with steep sides and flat bottom was produced by arbitrarily setting all of the shell velocities to zero. The broadened line results from the velocity distribution given by the radiation-hydrodynamics computation. It is clear from a comparison of these results that the motion of the atmospheric layers broadens the line and increases its equivalent width. The central flux is increased slightly.

Further numerical experimentation, in which the entire atmosphere was assigned a uniform expansion velocity revealed that both the uniform expansion and the differential expansion make significant

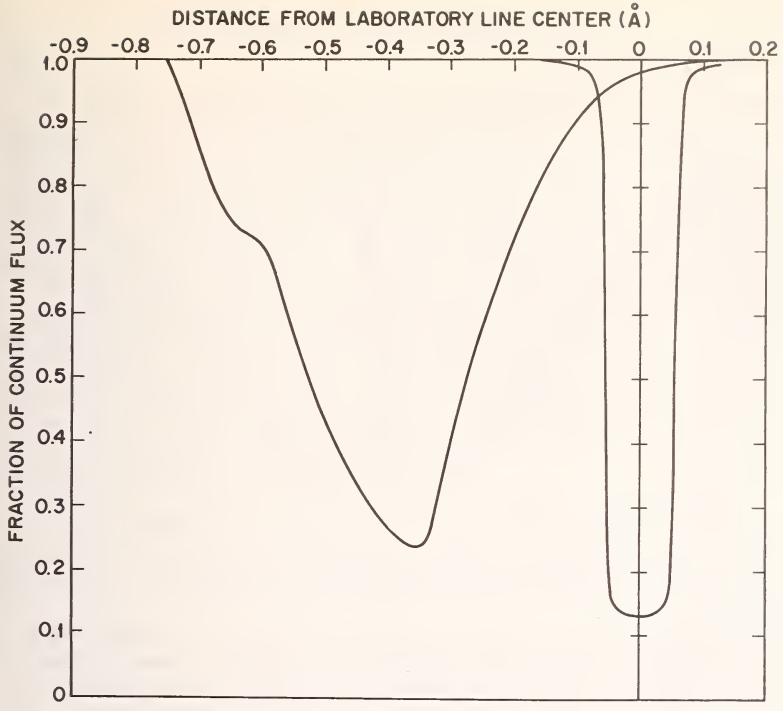

Figure 5. Computed profiles for λ4508Å line of Fe II.

contributions to the line shape. The differential expansion causes an appreciable increase in the equivalent width of the line. The feature on the violet side of the profile is caused by a region of abnormally high outward velocity occurring near the head of the rarefaction wave. The asymmetry of the line appears to be consistent with the analytical results of Van Hoof and Deurinck[20].

The broadened contour of the computed λ 4508 line is similar to the shape for the cepheid SV Vul as observed by Kraft[21], et al. However, in the present computation, neither stellar rotation nor a "turbulent velocity" were assumed in order to produce the line broadening.

The profiles of the first four Balmer lines were also computed. The H_β profile is shown in Fig. 6. The computed profiles for the four lines are all similar, but show a lower central flux and broader wings with increasing principal quantum number. The depression of the continuum over a

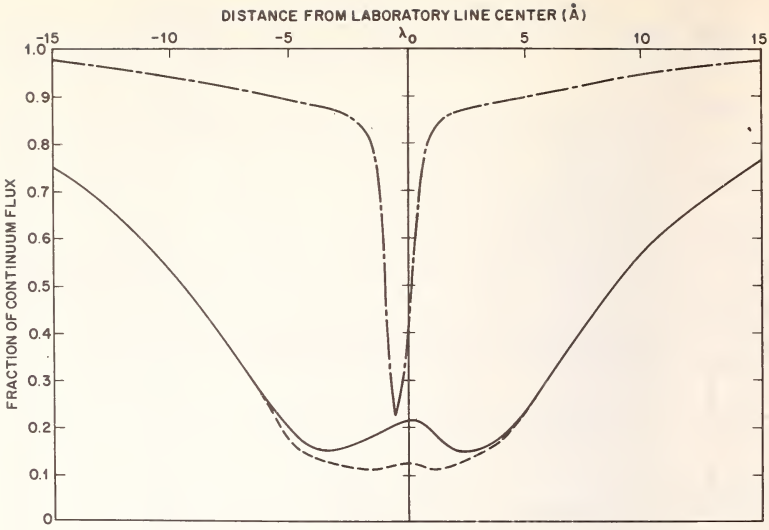

Figure 6. Computed profiles for Hβ and Ca II K lines.

wide region of the spectrum is to be anticipated on the basis of strong wings of these lines. The effect should be particularly evident near the series limit where the wings of the higher members of the Balmer series should overlap and effectively extend the Balmer continuum well to the red of the series limit.

The computed profile for the Ca II K line is also shown in Fig. 6. The line is quite broad and has a weak red shifted emission core. This emission core results from a slight temperature inversion in the outermost shells of the cepheid model as shown in Fig. 3. The dashed line in Fig. 6 shows the change in the K line contour when the outer shell of the cepheid model is arbitrarily removed during the line profile computation. It is interesting to note that the emission core is red shifted, while the absorption profile is blue shifted, even though all parts of the atmosphere are moving outward and might therefore be expected to produce a blue shift. While the reason for this effect has not been positively identified, it apparently is confirmed by the observations of Jacobsen[22].

While the computed profiles have not as yet been quantitatively compared with densitometer profiles, it is clear that the unloading process is capable of producing spectral line characteristics similar to those observed in stars of high luminosity.

GENERALIZATION TO OTHER STARS

A number of lines of evidence indicate the possibility that the unloading mechanism might be operating in stars other than cepheids. Kraft[23], in his extensive discussion of the spectra of supergiants and cepheids, concludes that, "the classical cepheids have spectra that, in detail, are virtually identical with those of the non-variable supergiants at all phases of the variation." Abt[7], in his study of the variability of supergiants, finds that "probably all stars in the H-R diagram above $M_V = +1$ and to the right of the main sequence are variable in light and radial velocity." In addition, he notes that many of the supergiants show a multiple or irregular periodicity in velocity that suggests that secondary shocks might be present.

Taken at face value, these lines of evidence raise the interesting possibility that all luminous stars above the main sequence could actually be variable stars. However, since the stars we normally refer to as "variables" seem to occur in well defined "instability strips" in the H-R diagram, such an interpretation would require that a selection process be operative. Such a selection process could hardly be observational, and would have to have a physical basis.

Historically, the various classes of variable stars have been identified by their relatively large light variations rather than their velocity variations. Abt[7] found that the "non-variable" supergiants have light amplitudes of 0.05 - 0.10 mag., whereas the "variable" stars have light amplitudes on the order of 10 times this amount. The velocities of the "non-variables" have not been studied in sufficient detail to establish any correlation with these light variations. Thus, while it is clear that the existence of instability strips must ultimately be associated with the interior structure of the star, the manner in which this structure manifests itself in terms of observables is not well understood.

A possible cause for the selection phenomenon can be deduced from an analysis of the model cepheid computation discussed earlier. The author[2] found that the large increase in light amplitude in the cepheid resulted from an abrupt spatial density decrease on the back side of the shock front. After shock transparency, this rapid density decrease causes the photosphere to move rapidly inward into

the star, thereby producing a rapid temperature increase in the photospheric region.

It was further found that in the cepheid the steep density decrease behind the shock results from thermal ionization of hydrogen in these layers. If one follows the progress of a given shock from the deep interior of the star to the surface, one finds that the density profile just behind the shock front changes rapidly. Whenever ionization (or dissociation) is occurring behind the shock, a deep density minimum occurs in this region. The density at this minimum may be as low as a factor of 10 below the shock front value. However, when no ionization occurs, the minimum density is rarely more than 30% below the shock front value.

This suggests that the production of a large light amplitude requires that ionization or dissociation occur just behind a shock front during the relatively short time interval when the shock traverses the photosphere. It also implies that the passage of a shock front through the photosphere of a star does not produce large observable effects unless ionization or dissociation is in progress just behind the shock front. This "shock visibility factor" might well be the cause of the apparent instability strips in the H-R diagram.

If one compares the emergence of the primary shock and secondary shocks in the cepheid computation, one finds support for the above interpretation. The shock velocities are nearly equal, but the secondary shocks are followed by only a shallow density minimum. The increase in the computed light output is about 1 mag. for the primary shock emergence, but only about 0.1 mag. for the secondary shock emergence.

There is some observational evidence from variable stars to support this computed result. Bernheimer[24] observed a light increase in Eta Aquilae of 0.15 mag. in 40 minutes. Preston[25] has observed similar rapid low amplitude light variations in RR Lyrae which occur at phases where the emergence of shocks are expected from the radiation-hydrodynamics computations.

A further test of the hypothesis can be made by plotting the traces in the H-R diagram where various ionization and dissociation processes are 50% complete. This can be accomplished by using the data[26] to convert M_V values to log P_e values, and the equation of state. The temperature values associated with these traces are the temperatures in the region behind the shock front. The effective temperature

of the reversing layer just prior to the shock emergence should be lower than this temperature, and systematically related to it. If the major classes of variable stars are superposed on this H-R diagram, it is found that their reversing layer temperatures are about 2/3 of the temperatures where He I ionization, H ionization, and H_2 dissociation are 50% complete. However, this result should be considered as suggestive, rather than conclusive, since the variables occupy rather broad strips in the H-R diagram and it is difficult to establish the $M_V - P_e$ relationship in some parts of the diagram due to the lack of stars. In any event, the unloading process appears to be interesting and should receive further study.

In conclusion, I would like to thank Drs. L. Henyey, R. K. M. Landshoff, R. E. Meyerott, and M. Walt IV for their continued support and encouragement.

REFERENCES

1. R. Weymann, *Astrophys. J.*, 136, 476 (1962).
2. R. W. Hillendahl, Dissertation, Univ. of California at Berkeley (1968).
3. Ya. B. Zeldovich and Yu. P. Raizer, *Physics of Shock Waves and High-Temperature Hydrodynamic Phenomena*, Academic Press, New York and London (1966), pp. 101, 716, 762.
4. G. A. Bird, *Astrophys. J.*, 139, 675 (1964).
5. A. Sakurai, *J. Fluid Mech.*, 1, 436 (1956).
6. H. C. Arp, *Astronomical J.*, 60, 1 (1955).
7. H. A. Abt, *Astrophys. J.*, 126, 138 (1957).
8. G. E. Moreton, *Sky and Telescope*, 21, 145 (1961).
9. R. W. Hillendahl, "Approximation Techniques for Radiation-Hydrodynamics Computations," Defense Atomic Support Agency Report 1522 (1964).
10. R. W. Hillendahl, *Proceedings of the Workshop on the Interdisciplinary Aspects of Radiative Transfer*, ed. R. Goulard Joint Institute for Laboratory Astrophysics, Boulder, Colorado (1965).
11. L. G. Henyey, R. LeLevier, R. D. Levee, K. H. Bohm, and L. Willets, *Astrophys. J.*, 129, 628 (1959).
12. R. H. Christy, California Institute of Technology, private communication (1968).

13. J. B. Oke, *Astrophys. J.*, 133, 90 (1961).
14. J. Stebbins, G. F. Kron, and J. L. Smith, *Astrophys. J.*, 115, 292 (1952).
15. C. Whitney, Dissertation, Harvard University (1955).
16. Anne B. Underhill, *Astrophys. J.*, 106, 128 (1948).
17. L. H. Aller, *Astrophysics*, Ronald Press, New York (1953).
18. G. B. Rybicki, "Routine for Evaluation of the Voigt Function," forwarded by D. G. Hummer.
19. F. N. Edmonds, Jr., F. M. Schluter, and D. C. Wells, III, *Memoirs, Roy. St. Soc.* 71, 271 (1967).
20. A. Van Hoof and R. Deurinck, *Astrophys. J.*, 115, 166 (1952).
21. R. P. Kraft, D. C. Camp, J. D. Fernie, C. Fujita, and W. T. Hughes, *Astrophys. J.*, 129, 50 (1959).
22. T. S. Jacobsen, *Pub. Dominion Ast. Obs. X*, No. 6, 145 (1956).
23. R. P. Kraft, in *Stellar Atmospheres*, ed. J. Greenstein, Univ. of Chicago Press (1960).
24. W. E. Bernheimer, *Lund Medd.*, Ser. II, 61, 11 (1930).
25. G. W. Preston, *Astrophys. J.*, 134, 633 (1961).
26. C. W. Allen, *Astrophysical Quantities*, Univ. of London, Athlone Press (1963), pp. 201, 208.

DISCUSSION

Wellmann: If you extrapolate a nova outburst backward, you will find that a large fraction of the mass has been thrown out during a very short time. This is like the unloading of a shock front. There are also secondary outbursts. Can these be explained by your secondary shock waves? Would your model give the right densities and time scale?

Hillendahl: My model contains many possibilities. It can probably also explain a nova outburst. The production of secondary shock waves by a first shock is a very common physical phenomenon. It is not limited to cepheids, but it is observed in the solar atmosphere as well as in the laboratory; it is also observed with supersonic airplanes and during the re-entry of Gemini space-vehicles.

Lamers: Can your mechanism explain the standing waves in P Cygni type stars, which exist according to a thesis by de Groot?

Hillendahl: Perhaps.

Underhill: It is pleasing to see that your predicted profile for Fe II λ4508 resembles more closely the observed profiles than is the case for outward and inward moving layers. In particular note the difference in asymmetry between the profile from the model with the computed velocity distribution and the profile formed for layers moving with a constant velocity.

Stibbs: I should like to ask, what is the basic physical reason why the proposed shock mechanism leads to a violation of Wesselink's method?

Hillendahl: If you consider the difference between the motion of the masses and the motion of the photospheres you will find a radius that differs by 20 percent from the radius found by Wesselink's method. I think my method is a modified Wesselink-method.

Praderie: Are your results contradictory to Kippenhahn's calculation?

Hillendahl: I didn't say anything about the exciting processes.

Praderie: But how are the shocks produced?

Hillendahl: They are produced by the mechanism given by Christie.

PART D

SUMMARY

CONCLUDING REMARKS

by

J. C. Pecker

Observatoire de Meudon, France

We have seen from the talks of A. B. Underhill and R. N. Thomas how the viewpoints of the many kinds of astronomers who came to this meeting differ, not only with respect to what they mean by "extended atmospheres" but also concerning methods for studying extended atmospheres.

For a long time spectroscopists and theoreticians of stellar atmospheres have not moved exactly in the same universe. This conference is an attempt to fill the gap, we all have seen that it is not easy, but progress has been made. I shall try to summarize the progress starting from the general conceptual approach and trying to come back to the particular cases that puzzle observers.

I. THE CONCEPTS

The problem, as I said, is that for a long time it was found to be very difficult to build models of the good classical type, that is in RE (radiative equilibrium), HE (hydrostatic equilibrium), LTE (local thermodynamic equilibrium), which might represent the most honest stars that theoreticians might be tempted to like. Most of the theoreticians were sufficiently aware of this fact not to give more than very qualitative suggestions on how to explain monsters. On the other hand, however, observers, i.e., spectroscopists, have had a tendency to concentrate on stranger and stranger objects, to have more fun, probably, and they seemed to have been satisfied with zero-order-approximation interpretations--often being so crude as to assume LTE! In a way they were like the entomologists or zoologists of the eighteenth century (thus proving that, contrary to a widely distributed opinion, physical

sciences might follow in their development the biological sciences). Clearly it is no longer possible to be satisfied by this state of affairs. The age of computers has finally come and theoreticians are now able to challenge the analytical or numerical difficulties that one meets when trying to understand nonclassical situations.

In this theoretical approach there are two phases: (a) The first problem to solve, as usual, is that of diagnostics. This is essentially what we have tried to do during these three short days. We have tried to interpret the observed features in terms of models, in the broader sense of this word. I shall come back to this point.

(b) The second problem is the physical interpretation or understanding of models that fit the observations better. We barely touched this problem and we hardly mentioned the physical choice among the variety of models that can represent a given set of observed features. Clearly this approach is linked with stellar evolution, for stellar evolution might affect more rapidly the nondense external layers than it does the general structure of a star. It is only after we shall be able to enter this second phase of the theoretical approach that we may be able to put some unity, or at least some logic, into the description and understanding of our zoological garden.

I shall come back to this point at the end of these final remarks. In a general sense, we should keep in mind the few questions asked a long time ago by Otto Struve, and of which Anne Underhill has very wisely reminded us. We should remember they are still basically unsolved, and are still the essential questions. Slightly reformulating the first ones, one has to reply to the questions: Why have some stars extended atmospheres--whatever meaning each of us gives to the words--and some other stars, otherwise apparently identical, have none? What, in the stars with extended atmospheres, is the cause of the departures from RE, HE, and LTE that one needs to introduce in order to interpret the observations?

It seems that to the last question at least we have a partial reply, which we all seem to agree upon, and about which Anne Underhill and several other speakers have been insisting very much and very rightly. It seems indeed that we do know why there are departures from LTE in a given configuration--or to say it better, why we should not expect LTE to apply. For instance, as stressed by

Anne Underhill, we know that in low density atmospheres we should not expect enough collisions to maintain the extreme situation of LTE. That this is indeed true for all atmospheres has been stressed by R. N. Thomas. This is clear, and I will not come back to this point.

But why are there departures from RE or HE? What heating mechanisms can possibly alter the electron temperature distribution of a classical atmosphere? What is sustaining or pushing the atmosphere in such a way as to produce low effective gravities in the outer layers? We do not know! Our ideas are too vague to allow us to compute these effects in a stellar atmosphere defined by a few observable parameters such as its location in a color-magnitude diagram, or even for a stellar atmosphere much better defined, such as that of the sun.

One can hope that our improvements in the non-LTE atrophysics will enable us to describe in a better way the observations, one cause of the indeterminacy being thus taken away. Figure 1 describes the logic of the methods in use.

In addition, the kind of wrong and artificial determinations that might have been given to the problem by the use of LTE astrophysics and that might have led in some cases to wrong conclusions about the geometry or the velocities, should be now easily avoided. We know that LTE is an assumption that one cannot make a priori, that one cannot use this assumption unless it has been unambiguously proved in a given particular case, that it may, indeed, be used. We know that this is very rarely the case, especially for stars with extended atmospheres.

How to include non-LTE in the transfer equations and how to do it without neglecting curvature terms or velocity terms, or even inhomogeneities has been discussed here at length and in a very clear way by George Rybicki, and after him by Kalkofen, Magnan, Grant, and Skumanich. However, the theory has still a long way to go. Even in cases with simple velocity fields, we have seen that it is difficult, sometimes, to take into account the proper depth variation of the physical parameters. We have also seen with Nussbaumer that severe doubts still exist concerning the physical data needed for the astrophysical theory. Precise physical data is obviously a serious need of non-LTE astrophysics.

But we have seen also that the theory is sometimes satisfying. The range of possible models not only has decreased but some absurd ones cannot be considered anymore. We have seen that the continuum

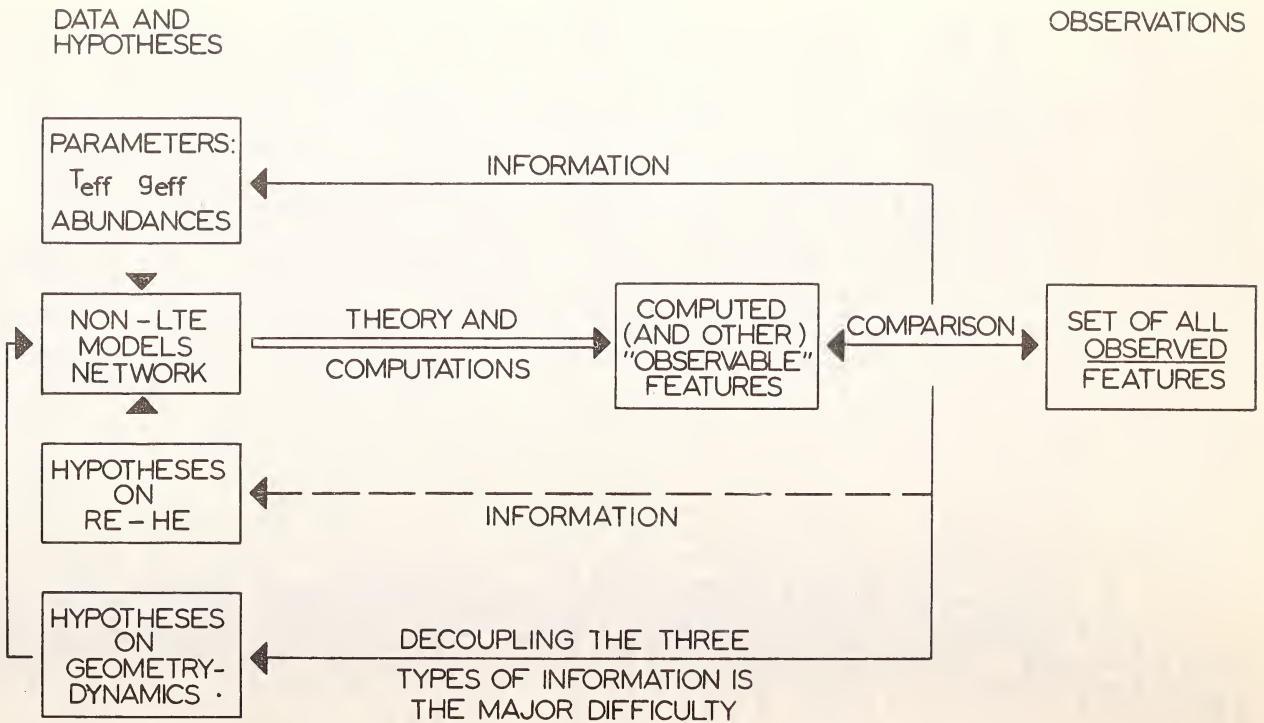

Figure 1. Logic of our scheme of analysis.

spectrum of a star like Eta Carinae is well represented by the nonclassical continuum proposed by Gerola. We have seen, in Kalkofen's paper for example, good (but possibly still not unique) representations for P Cygni lines; Rybicki gave us some examples of profiles of which the asymmetry computed was comparable to those of actual supergiants. Magnan has succeeded in mimicking the Be stars reasonably well; the analysis of WR lines with some non-LTE profiles in plausible geometrical dynamical situations has been noted several times. We have also seen that chromospheric spectral features might be described by some reasonable models, such as those of Kandel, reported this morning by Françoise Praderie. We have seen also the notable progress described by Groth on the chromosphere of the K type component of Zeta Aurigae. Even in the peculiar case of novae, we are coming to a better understanding of the spectrum by making a careful discussion of the ionization, as shown by Wellman.

Certainly even when the crude approximations sometimes made are taken away, a unique description is not yet reached. This has been shown this morning by Groth, but was clear also from several examples given by F. Praderie, and quite clear from Skumanich's interpretation of the K-line reversal in a few red giants.

Coming to this last controversy, we must understand the indeterminacy. A given line is indeed an image, through some convolution, of the trend of the source function with the optical depth. To go from that law to the distribution of physical quantities, we need a model. The critical relation in it might be $\tau(h)$, the relation between the opacity and the altitude in the atmosphere. Eclipses can lead us to guesses about $\tau(h)$ but in other cases we are left without much indication of this behaviour. The relation $\tau(h)$ is strongly coupled with the set of temperatures or densities as a function of the altitude which are coherent, through non-LTE theory, with the source function itself.

This difficulty, I believe, is the chief difficulty we shall meet in the stellar cases, the very origin of the indeterminacy mentioned above. Possibly only careful solution of the simultaneous problem of several different lines can help us. The profile of a line is an indication about $S(\tau)$, but the profile is not dependent on one function only but upon relations such as $T_e(h)$ and $n_e(h)$. How then to solve for this uncertainty of the diagnostics, an uncertainty which is quite general?

In given cases we get a set of possible behaviours of $T_e(\tau)$, $\tau(h)$ and $v(h)$ that depart more or less strongly from the radiative equilibrium temperatures, from the hydrostatic equilibrium relation between τ and h, and from the non-moving atmosphere. The choice is to be determined by the physical plausibility of the models. However we know very little about how to make this choice--as has been said many times during these three days!

II. APPLICATIONS

The methodology being thus clear, but still insufficient, let us see if we can describe in some slightly coherent way the various phenomena we have been talking about. We have considered several types of extended atmospheres following more or less Thomas' classification scheme. It is somewhat difficult or even meaningless to locate some of the types of object we are considering on a color-magnitude diagram, but let us attempt it (see Figure 2).

(1) We have talked about stars in which the extended character is rather severe (WR stars, supergiants, Be stars). These stars are generally highly luminous, in rapid evolution, and some of them are relatively young. It is remarkable, as in the case of the nuclei of planetary nebulae, to see that they are located in the HR diagram near the instability limit set up by the radiation-pressure negative gravity. In other words, the physical phenomenon that appears important is essentially a mechanical support of the outer layers. Clearly the difference between objects with and without an extended atmosphere (everything else being alike) might be a difference of age--a difference that can be indeed linked also with really circumstellar phenomena such as dust clouds. The kind of theory brilliantly developed today by Hillendahl could be compared to this case. Through shock waves reaching the surface, a low effective gravity atmosphere is created--even relatively far from the above quoted instability limit.

(2) Later we turned our attention to more moderate examples, for which we suspect that phenomena similar to those shown in an embryonic way in the sun are also present, possibly more conspicuously. This subject was extensively discussed by F. Praderie.

Different mechanisms that act in different ways can be invoked. In the sun and similar stars, the

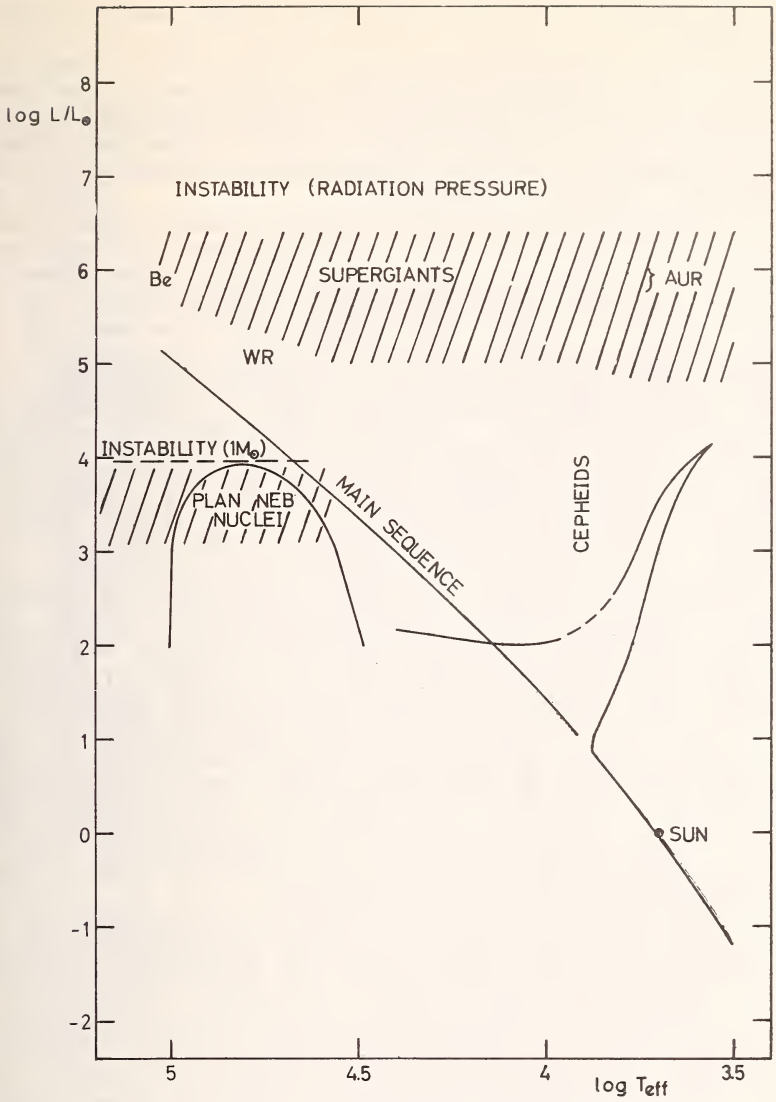

Figure 2. Location of stars with extended atmospheres in the HR diagram.

heating (due to what?) is probably more important than the mechanical support. But in active younger stars, such as T Tauri, very active phenomena integrated over the stellar disk might appear to give strong chromospheric-like phenomena. The heating there is closely linked with the magnetic properties

of the stars--as it may also be in the case of some A stars.

Thomas has shown how the study, not of the sun itself, but of the evolution of thinking in the case of the sun could be mimicked, mutatis mutandi, in stellar cases, account being taken of the fact that the phenomena might be physically different or of a different order of magnitude.

I would like at this point to repeat what Thomas said about the fact that the measurement of continua in UV or IR would be very useful to get the location in the atmosphere of the minimum temperature. To his comments I would like to add that the mass of matter that is above (or outside) the location of the minimum temperature is a parameter which may vary within very large limits; and it might be an essential parameter. Having this remark in mind, one can understand why the UV solar spectrum looks like the visible spectrum of some of the monster-stars; just because the mass of the extended atmosphere--or call it chromosphere if you like--is bigger, much bigger, than that of the sun quite irrespective of what the physical process is which keeps supporting the extended atmosphere. This really explains why the discussion of some features of the UV spectrum of the sun (O I lines) by Athay fitted into the program better on Monday together with the discussion of the chromospheric phenomena.

If we limit ourselves to the observation of the visible integrated light of a star, the chromospheric phenomena in objects that might be low in the HR diagram can be observed, as has been told by F. Praderie, only in the center of some very strong lines. This is naturally a severe difficulty.

When dealing with this kind of very fine and difficult spectroscopy one cannot be satisfied with the kind of rough theory that was described yesterday. It became clear today, at several moments in the discussion, that we should improve the theory greatly to take into account inhomogeneities and to introduce wavelength-dependent source functions, i.e., better frequency redistribution in lines than is generally assumed. Clearly a lot of progress has yet to be made along these lines.

III. CONCLUSION

Clearly observers should observe and theoreticians theorize, and they should incubate together!

We now have a better idea which lines are sensitive to what and what theories are likely to be applicable in a particular case. Let us all remember the philosophy of two famous thinkers: "Things are not what they seem" (Thomas) and "I was pleased--and then I started reading" (A. B. Underhill). In no better way can the need for controversy and for colloquia be expressed.

IV. ACKNOWLEDGMENTS

Yesterday, when Dr. Wellmann was replying to the expression of our gratitude that had been given by Anne Underhill, he said that it might be too early, the meeting being not yet over. I may say today that, the meeting being over, we know perfectly well that Anne Underhill was completely right; it is a great pleasure for me to again thank very heartily Dr. Wellmann and Dr. Groth for all that they have done in order to allow us to take the utmost benefit out these three days, not only through scientific discussions, but through our contacts with our German friends. I would like, Dr. Wellmann, to ask you, also, to convey our thanks to the secretarial staff, which has been so helpful for all of us, and also to your colleagues and students who have been helping so much in many ways, and especially by recording the whole of this conference, and by taking accurate notes during it.

It is customary to limit the thanks to the local organisers, but I think we should also express our gratitude to Anne Underhill, who has been so active in organizing this meeting, and who, fortunately, let it be sufficiently unplanned. It was indeed an excellent thing that this meeting was unplanned, because it gave us the opportunity of extensive discussions about the various points raised by the speakers. I thank also all those who have contributed to the discussion, especially (for different reasons) the younger ones, and our old friend Dick Thomas.

I have said earlier that we are able, now, to express our gratitude to Dr. Wellmann and Dr. Groth, the meeting being finished. Actually, we should possibly wait a little bit, because they have still an enormous amount of work to do with the proceedings of the conference! This is an enormous task, but judging by what I have seen these days, I think it

is quite safe that we can express our gratitude in advance to Dr. Wellmann, Dr. Groth, and their colleagues, for what they will do for us in the near future.

The meeting is adjourned.

☆ U. S. GOVERNMENT PRINTING OFFICE : 1970 O - 401-476